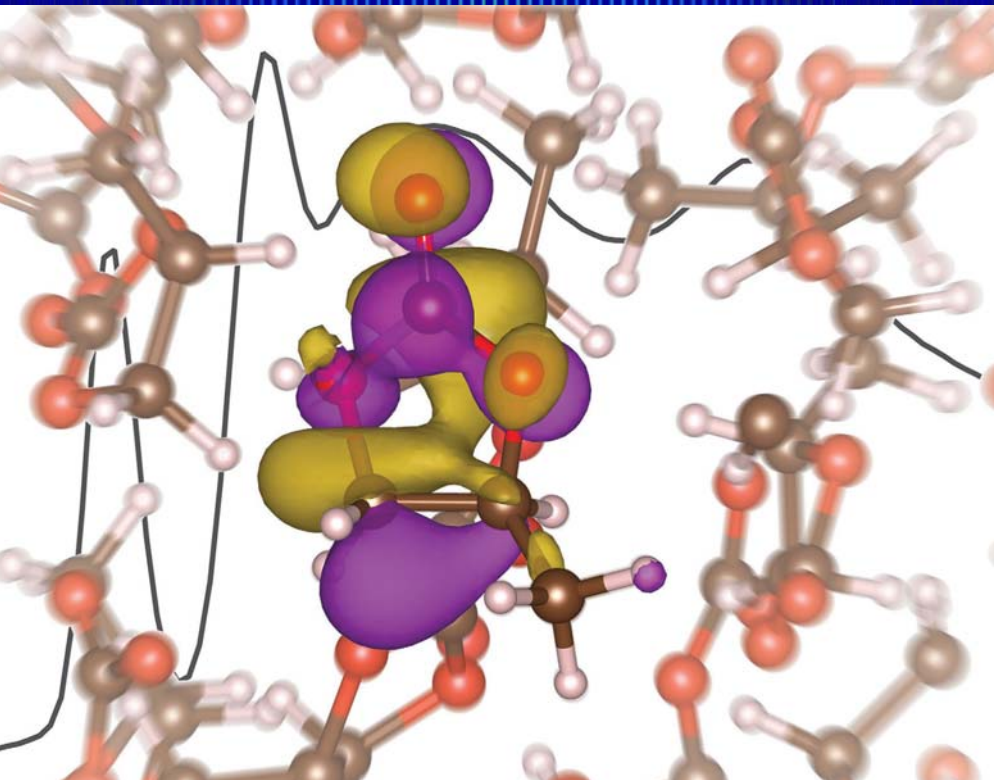




Delay Time



# CPIMS 11

Eleventh Condensed Phase and Interfacial Molecular Science (CPIMS) Research Meeting

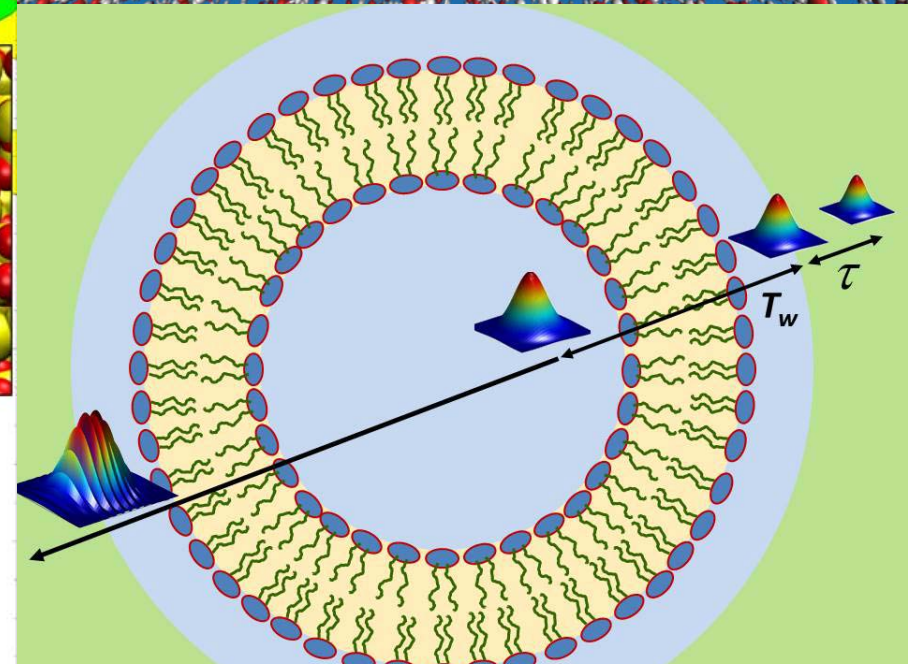
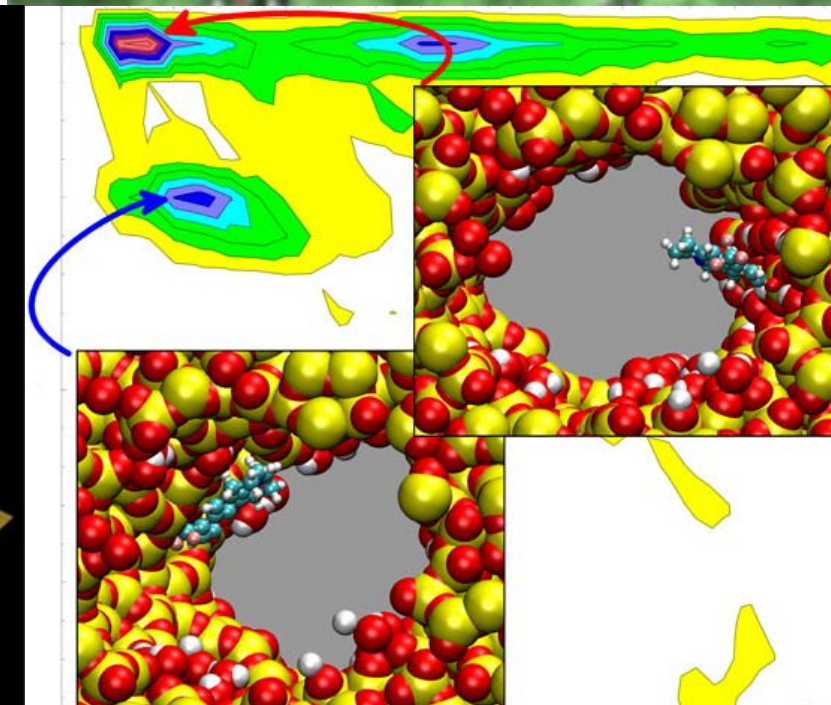
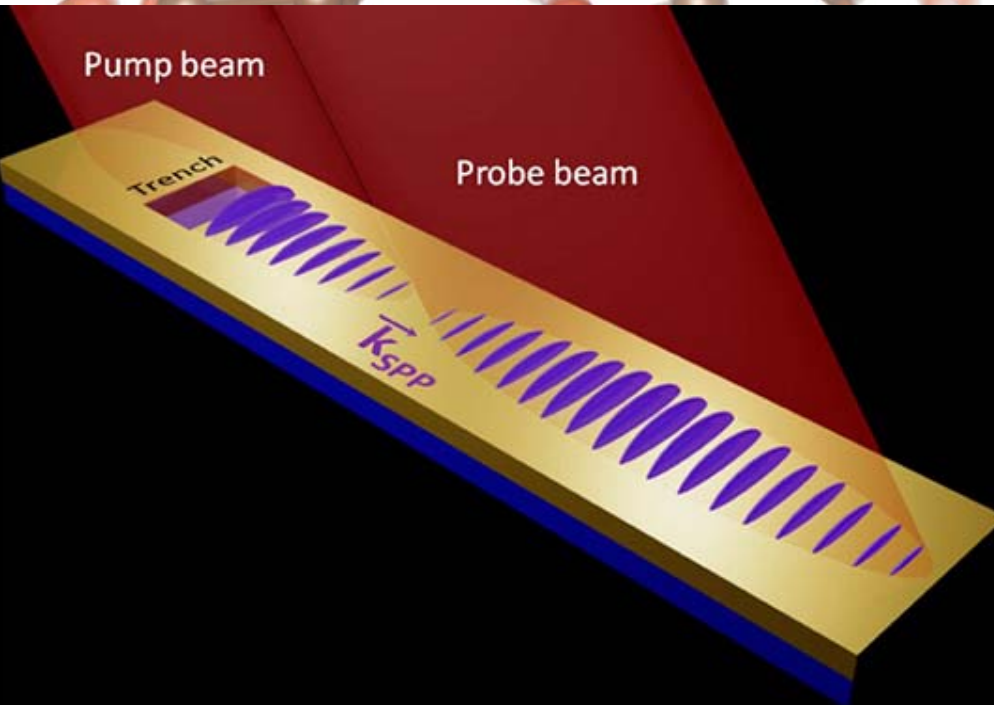
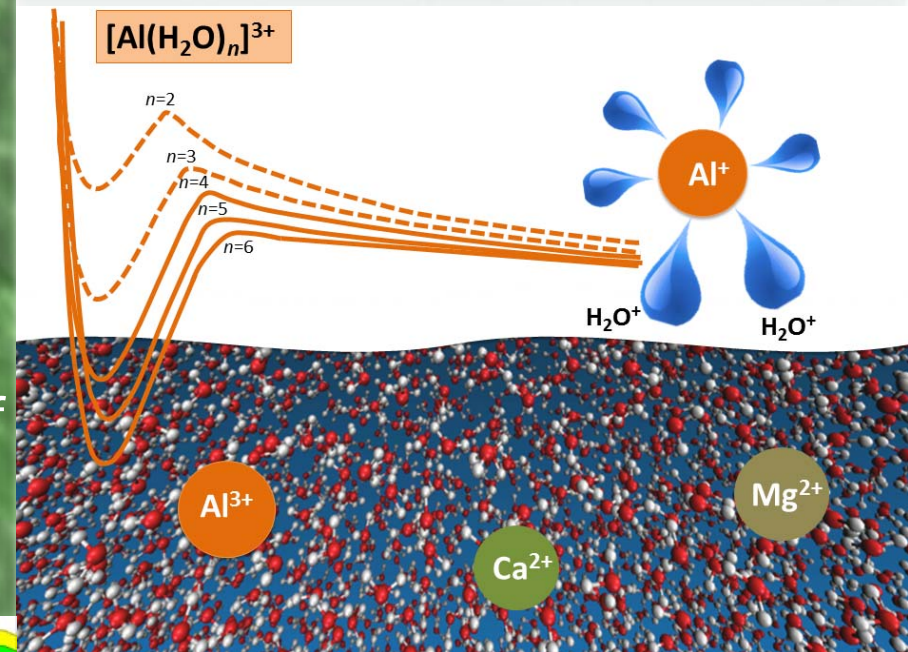
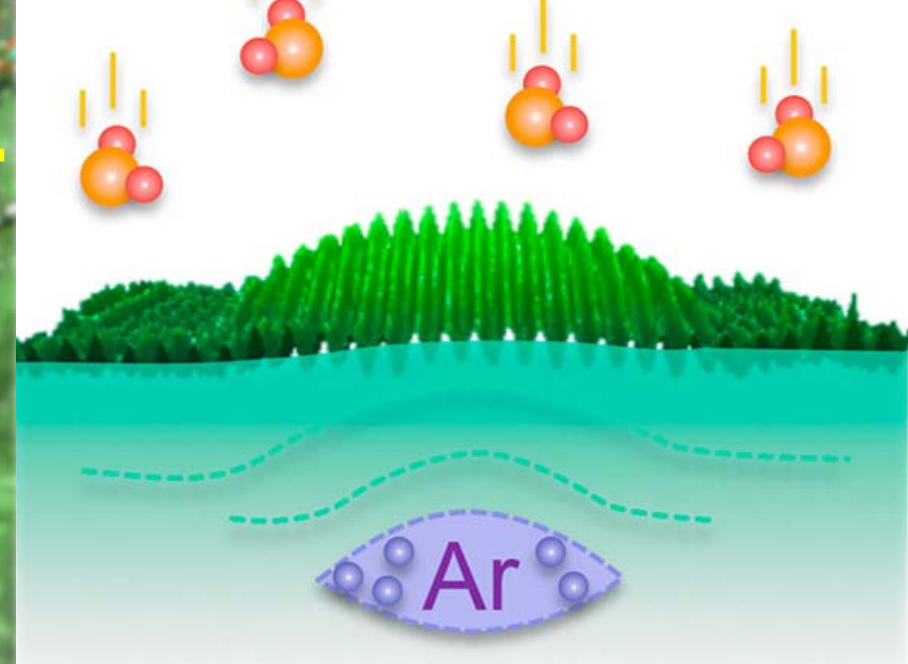
Gaithersburg Marriott Washingtonian Center  
Gaithersburg, MD  
November 1- 4, 2015



U.S. DEPARTMENT OF **ENERGY**

Office of Science

Office of Basic Energy Sciences  
Chemical Sciences, Geosciences & Biosciences Division



# CPIMS 11

## About the Cover Graphics

Transient excitons have been observed in metals for the first time. Here, the surface electrons of silver crystals can maintain the excitonic state more than 100 times longer than for the bulk metal, enabling the excitons to be experimentally visualized by a newly developed, multidimensional coherent spectroscopic technique.

X. Cui, C. Wang, A. Argondizzo, S. Garrett-Roe, B. Gumhalter, H. Petek, *Nature Physics* (2014), DOI: 10.1038/nphys2981

**Submitted by Hrvoje Petek (University of Pittsburgh)**

X-ray absorption spectroscopy was used to investigate the solvation structure of the lithium ion in propylene carbonate, a system similar to the liquid electrolyte within a lithium ion battery. Theoretical calculations indicate that the lithium ion has a solvation number of 4.5, which is larger than expected based on the generally accepted tetrahedral coordination structure.

J. W. Smith, R. K. Lam, A. T. Sheardy, O. Shih, A. M. Rizzuto, O. Borodin, S. J. Harris, D. Prendergast, and R. J. Saykally, *Phys. Chem. Chem. Phys.* (2014), DOI: 10.1039/C4CP03240C

**Submitted by Richard J. Saykally (Lawrence Berkeley National Laboratory)**

Time-resolved, nonlinear photoemission electron microscopy (PEEM) images of propagating surface plasmons (PSPs), launched from a lithographically patterned rectangular trench on a flat gold surface, have been recorded. Power-dependent PEEM images provide experimental evidence for a sequential coherent nonlinear photoemission process, in which one laser source launches a PSP through a linear interaction, and the second subsequently probes the PSP via two-photon photoemission. PEEM images reveal that the launched PSP may be detected at least 250 microns away from the coupling trench structure.

Y. Gong, A.G. Joly, D. Hu, P.Z. El-Khoury, and W.P. Hess, *Nano Letters* (2015), DOI: 10.1021/acs.nanolett.5b00803

**Submitted by Wayne P. Hess (Pacific Northwest National Laboratory)**

Molecular modeling simulations were used to study the adsorption behavior of 1,1,1,3,3-pentafluoropropane (R-245fa) in mesoporous MIL-101 metal organic frameworks (MOFs) at various temperatures. Our simulations indicate that chromium sites are preferential binding sites for adsorption. Computed free energy profiles indicate that, in both the cases, the MOF particles are more attractive in R-245fa compared to water, which implies that nanofluids with these MOF particles will form a more stable suspension in water than in R-245fa.

H. V. R. Annapureddy, S. K. Nune, R. K. Motkuri, B. P. McGrail, and L. X. Dang, *J. Phys. Chem. B* (2015) DOI: 10.1021/jp5079086

**Submitted by Liem X. Dang (Pacific Northwest National Laboratory)**

Replica exchange molecular dynamics simulations of a dye molecule dissolved in ethanol, confined within a 2.4 nm hydrophilic amorphous silica pore, are presented. The dye position and orientation distributions provide insight into time-dependent fluorescence measurements in nanoconfined solvents as well as general features of chemistry in mesoporous materials.

J. A. Harvey and W. H. Thompson, *J. Phys. Chem. B* (2015), DOI: 10.1021/jp509051n

**Submitted by Ward H. Thompson (University of Kansas)**

An array of intense, locally varying strain fields on a TiO<sub>2</sub> (110) surface was created by introducing highly pressurized argon nanoclusters at 6-20 monolayers under the surface. Our results provide direct evidence of the influence of strain on atomic-scale surface chemical properties, and such effects may help guide future research in catalysis materials design.

Z. Li, D. V. Potapenko, and R. M. Osgood, *ACS Nano* (2015), DOI: 10.1021/nn506150m

**Submitted by Richard M. Osgood (Columbia University)**

Replacing lithium with other metals with multiple charges could greatly increase battery capacity. But first researchers need to understand how to keep multiply charged ions stable. The paths that lead to either the hydrolysis of water or the creation of stable metal ion clusters, peacefully surrounded by water, have been determined. It comes down to the pH of the solution, the number of water molecules nearby, and the ionization potential.

E. Miliordos and S. S. Xantheas *Phys. Chem. Chem. Phys.* (2014), DOI: 10.1039/C3CP53636J

**Submitted by Sotiris S. Xantheas (Pacific Northwest National Laboratory)**

2D IR vibrational echo spectroscopy was performed on the antisymmetric CO stretch of vibrational probe molecules, which are located in the interior alkyl regions of phospholipid bilayers. The measurements show that the bilayer interior alkyl region dynamics occur on time scales ranging from a few to many tens of picoseconds. The results suggest that at least a significant fraction of the bilayers' structural dynamics arise from density fluctuations.

O. Kel, A. Tamimi, and M. D. Fayer, *J. Phys. Chem. B* (2015), DOI: 10.1021/jp503940k

**Submitted by Michael D. Fayer (Stanford University)**

Program and Abstracts for

# CPIMS 11

Eleventh Research Meeting of the Condensed  
Phase and Interfacial Molecular Science  
(CPIMS) Program

Gaithersburg Marriott Washingtonian Center  
Gaithersburg, Maryland  
November 1-4, 2015



U.S. DEPARTMENT OF  
**ENERGY**

Office of  
Science

Office of Basic Energy Sciences  
Chemical Sciences, Geosciences & Biosciences Division

The research grants and contracts described in this document are supported by the U.S. DOE Office of Science, Office of Basic Energy Sciences, Chemical Sciences, Geosciences and Biosciences Division.

## FOREWORD

This volume summarizes the scientific content of the Eleventh Research Meeting on Condensed Phase and Interfacial Molecular Science (CPIMS) sponsored by the U. S. Department of Energy (DOE), Office of Basic Energy Sciences (BES). The research meeting is held for the DOE laboratory and university principal investigators within the BES CPIMS Program to facilitate scientific interchange among the PIs and to promote a sense of program awareness and identity.

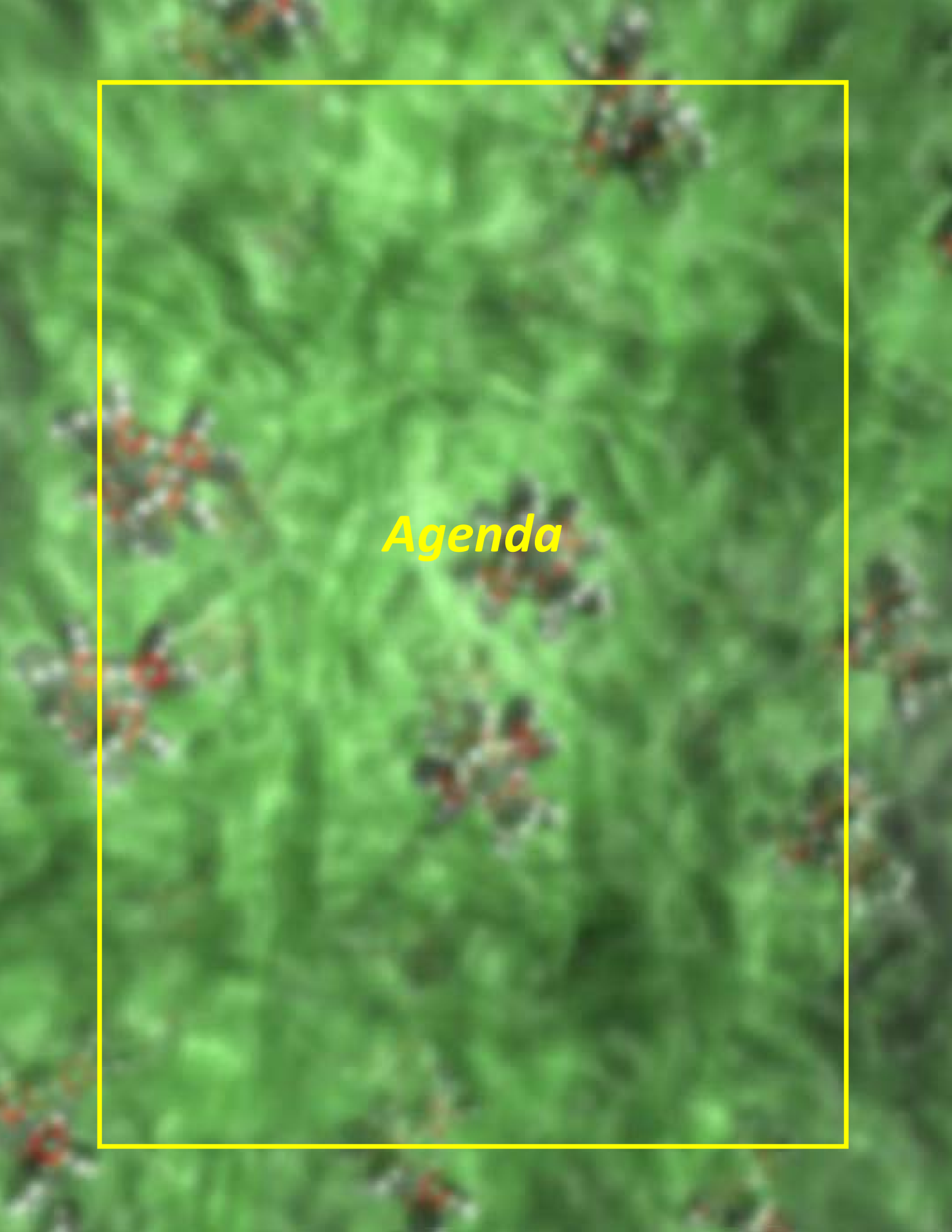
This year's speakers are gratefully acknowledged for their investment of time and for their willingness to share their ideas with the meeting participants.

The abstracts in this book represent progress reports for each of the projects that receive support from the CPIMS program. Therefore, the book represents a snapshot in time of the scope of CPIMS-supported research. A recent tradition is the use of the cover of this book to display research highlights from CPIMS investigators. This year, we have included eight research highlights on the cover. These images were selected from highlights submitted by CPIMS investigators during the past two years. We thank the investigators for allowing us to place their images on the cover of this book, and we thank all CPIMS investigators who submitted research highlights. CPIMS Investigators are encouraged to submit highlight of their results; we will continue to receive these stories of success with great pride. We thank Joshua Haines for his creative advice during assembly of this volume, and his tireless efforts in assembling and editing highlights for the program.

We are deeply indebted to the members of the scientific community who have contributed valuable time toward the review of proposals and programs. These thorough and thoughtful reviews are central to the continued vitality of the CPIMS Program. We appreciate the privilege of serving in the management of this research program. In carrying out these tasks, we learn from the achievements and share the excitement of the research of the many sponsored scientists and students whose work is summarized in the abstracts published on the following pages.

Special thanks are reserved for the staff of the Oak Ridge Institute for Science and Education, in particular, Connie Lansdon and Tim Ledford. We also thank Diane Marceau and Michaelene Kyler-Leon in the Chemical Sciences, Biosciences, and Geosciences Division for their indispensable behind-the-scenes efforts in support of the CPIMS program.

Gregory J. Fiechtner, Mark R. Pederson, and Jeffrey L. Krause  
Chemical Sciences, Geosciences and Biosciences Division  
Office of Basic Energy Sciences

An aerial photograph of a green field with a grid pattern, possibly a golf course or agricultural field. Small red structures are scattered across the field. The word "Agenda" is written in yellow, italicized font in the center.

# *Agenda*

# CPIMS 11



U.S. DEPARTMENT OF

**ENERGY**

Office of  
Science

Office of Basic Energy Sciences

Chemical Sciences, Geosciences & Biosciences Division

## Eleventh Condensed Phase and Interfacial Molecular Science (CPIMS) Research Meeting Gaithersburg Marriott Washingtonian Center, Gaithersburg, Maryland

---

### Sunday, November 1

3:00-6:00 pm \*\*\*\* Registration \*\*\*\*  
6:00 pm \*\*\*\* Reception (No Host, Lobby Lounge) \*\*\*\*  
6:30 pm \*\*\*\* Dinner (Salon E) \*\*\*\*

### Monday, November 2

7:30 am \*\*\*\* Breakfast (Salon E) \*\*\*\*

#### All Presentations Held in Salon F-G

8:30 am *Introductory Remarks and Program Update*  
**Gregory J. Fiechtner**, DOE Basic Energy Sciences

**Session I** Chair: **Bruce Garrett**, Pacific Northwest National Laboratory

9:00 am *Exact Factorization of the Nonadiabatic Electron-Nuclear Wavefunction*  
**John Tully**, Yale University

9:30 am *Towards a Self-Consistent Picture of Local Interactions and Collective Response*  
**Christopher Mundy** Pacific Northwest National Laboratory

10:00 am \*\*\*\* Break \*\*\*\*

**Session II** Chair: **Alex Harris**, Brookhaven National Laboratory

10:30 am *Imaging of CO<sub>2</sub> capture by metal-organic chains supported on Au surfaces*  
**Hrvoje Petek**, University of Pittsburgh

11:00 am *Chemical Kinetics and Dynamics in Nanoscale Water Films I: Transport and Crystallization in Amorphous Solid and Deeply Supercooled Liquid Water*  
**Bruce Kay**, Pacific Northwest National Laboratory

11:30 am *Chemical Kinetics and Dynamics in Nanoscale Water Films II: Nanosecond Laser Induced Melting and Wetting/Dewetting of Crystalline Ice*  
**Greg Kimmel**, Pacific Northwest National Laboratory

12:00 noon *Interfacial Electronic Structure of Supported Metal Oxide Clusters*  
**Michael White**, Brookhaven National Laboratory

12:30 pm \*\*\*\* Lunch (Salon E) \*\*\*\*

1:30 pm-4:00 pm Free/Discussion Time

- Session III**      Chair: **Musahid Ahmed**, Lawrence Berkeley National Laboratory
- 4:00 pm      *How Chaotrope and Kosmotrope Anions Guide the Local Solvation Structure of Water: Insights from Cluster Model Studies*  
**Xue-Bin Wang**, Pacific Northwest National Laboratory
- 4:30 pm      *New Insights into the Catalytic Chemistry of Transition Metal Oxides and Sulfides Part I. Experimental Studies on the Interactions of Suboxide Clusters with H<sub>2</sub>O, ROH*  
**Caroline Chick Jarrold**, Indiana University
- 5:00 pm      *New Insights into the Catalytic Chemistry of Transition Metal Oxides and Sulfides Part II. Computational Studies on the Reactions of Oxides and Sulfides and Theoretical Insights*  
**Krishnan Raghavachari**, Indiana University
- 5:30 pm      \*\*\*\* Reception (No Host, Lobby Lounge) \*\*\*\*
- 6:00 pm      \*\*\*\* Dinner (Salon E) \*\*\*\*

## Tuesday, November 3

- 7:30 am      \*\*\*\* Breakfast (Salon E) \*\*\*\*

- Session IV**      Chair: **Thomas E. Markland**, Stanford University
- 8:30 am      *Understanding the Rates and Molecular Mechanism of Water-Exchange around Aqueous Ions using Molecular Simulations*  
**Liem X. Dang**, Pacific Northwest National Laboratory
- 9:00 am      *Fluctuating Organization in Heterogeneous Aqueous Systems: Rough Surfaces in Space and in Time*  
**Phillip Geissler**, Lawrence Berkeley National Laboratory
- 9:30 am      *Molecular dynamics of complex systems: phase transitions, pre-transition effects and interfaces*  
**Kranthi K. Mandadapu**, Lawrence Berkeley National Laboratory
- 10:00 am      \*\*\*\* Break \*\*\*\*
- 10:30 am      *Atomistic and Coarse-Grained Models and Methods for Electrostatics*  
**Teresa Head-Gordon**, Lawrence Berkeley National Laboratory
- 11:00 am      *Condensed Phase and Interfacial Electric Fields*  
**Shawn M. Kathmann**, Pacific Northwest National Laboratory
- 11:30 am      \*\*\*\* Lunch (Salon E) \*\*\*\*
- 12:30 pm–3:30 pm      Free/Discussion Time

- Session V** Chair: **Richard Osgood**, Columbia University
- 3:30 pm *Stimulated Second Harmonic Generation for High-Speed Interfacial Spectroscopy and Imaging*  
**William A. Tisdale**, Massachusetts Institute of Technology
- 4:00 pm *Coverage-Dependent Ultrafast Desorption Dynamics in Molecular Adlayers*  
**Nick Camillone**, Brookhaven National Laboratory
- 4:30 pm *Heterogeneous Chemistry of Liquid Interfaces*  
**Hendrik Bluhm**, Lawrence Berkeley National Laboratory
- 5:00 pm *Competition for Bonding Sites in Nanoporous Thin Films*  
**Mary K. Gilles**, Lawrence Berkeley National Laboratory
- 5:30 pm \*\*\*\*\* Reception (No Host, Lobby Lounge) \*\*\*\*\*
- 6:00 pm \*\*\*\*\* Dinner (Salon E) \*\*\*\*\*

## Wednesday, November 4

- 7:30 am \*\*\*\*\* Breakfast (Salon E) \*\*\*\*\*

- Session VI** Chair: **Geraldine L. Richmond**, University of Oregon
- 8:30 am *The Dynamics of Protons in Liquid Water Viewed through Ultrafast IR Spectroscopy*  
**Andrei Tokmakoff**, University of Chicago
- 9:00 am *A Simple ab initio Model of the Hydrated Electron that Agrees with Experiment*  
**David Bartels**, Notre Dame Radiation Laboratory
- 9:30 am *Time-Resolved Resonance Raman Studies of Reaction Intermediates in Aqueous Media*  
**Irek Janik**, Radiation Laboratory and Department of Physics, University of Notre Dame
- 10:00 am \*\*\*\*\* Break \*\*\*\*\*
- 10:30 am *Structure, Dynamics, and Spectroscopy of Liquids Confined within Mesoporous Silica*  
**Ward H. Thompson**, Brookhaven National Laboratory
- 11:00 am *Development of Statistical Mechanical Techniques for Complex Condensed-Phase Systems.*  
**Gregory K. Schenter**, Pacific Northwest National Laboratory
- 11:30 am *Closing Remarks*  
**Gregory J. Fiechtner**, DOE Basic Energy Sciences
- 12:00 noon \*\*\*\*\* Meeting Adjourns \*\*\*\*\*

An aerial photograph of a green field with a grid pattern of trees, possibly a plantation or agricultural field. The trees are arranged in a regular grid, and the field is surrounded by a yellow border. The text "Table of Contents" is centered in the field.

# *Table of Contents*

# TABLE OF CONTENTS

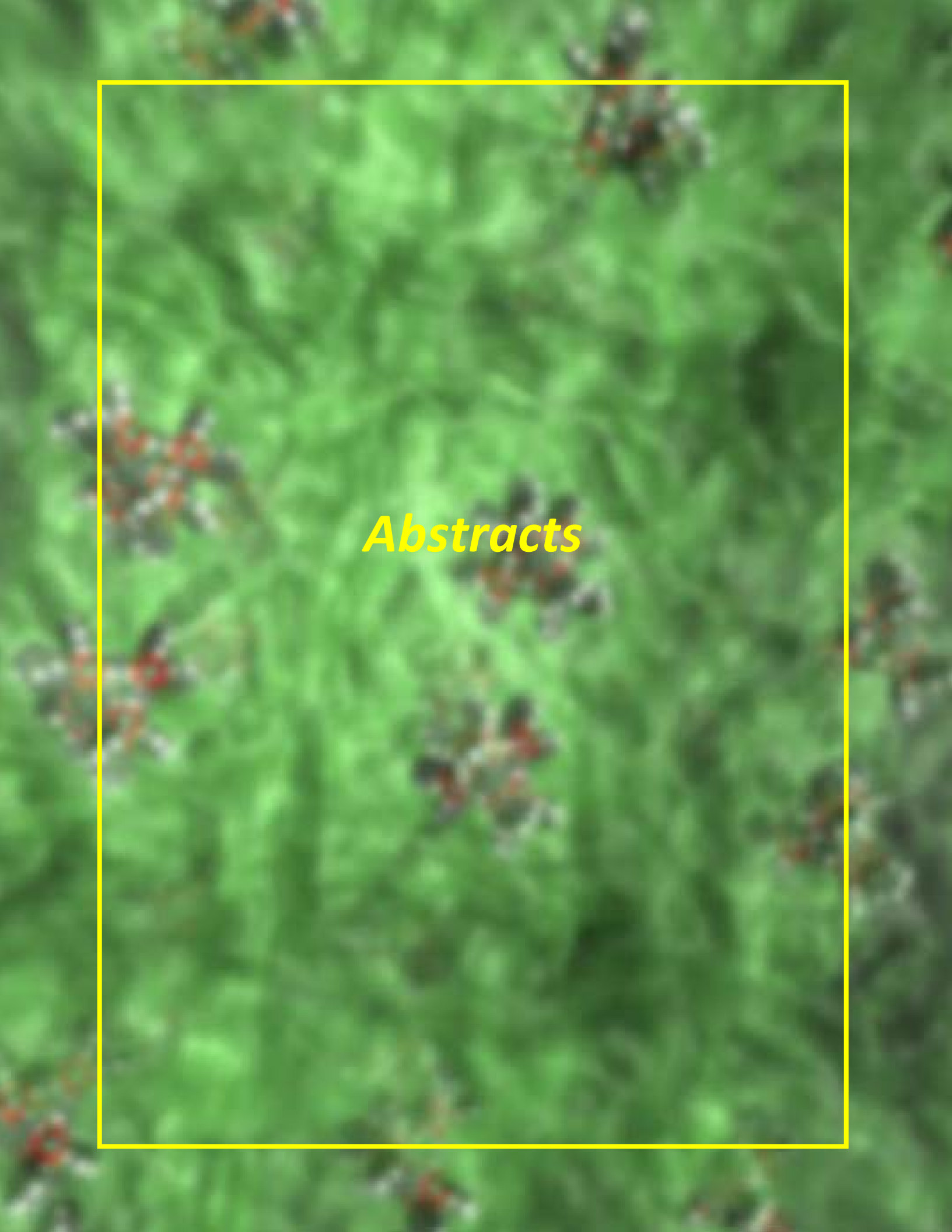
<b>FOREWORD</b> .....	ii
<b>AGENDA</b> .....	iii
<b>TABLE OF CONTENTS</b> .....	vi
<b>ABSTRACTS</b> .....	1
<b><u>CPIMS Principal Investigator Abstracts</u></b>	
<i>Probing Ion Solvation and Charge Transfer at Electrochemical Interfaces Using Nonlinear Soft X Ray Spectroscopy</i> L. Robert Baker (The Ohio State University).....	1
<i>Fundamental Advances in Radiation Chemistry</i> David M. Bartels, Ian Carmichael, Ireneusz Janik, Jay A. LaVerne, and Sylwia Ptasińska (Notre Dame Radiation Laboratory) .....	5
<i>Soft X-ray Spectroscopy and Microscopy of Interfaces Under in situ Conditions</i> Hendrik Bluhm, Mary K. Gilles, David K. Shuh, Musahid Ahmed (Lawrence Berkeley National Laboratory) .....	9
<i>Surface Chemical Dynamics</i> Nicholas Camillone III and Michael G. White (Brookhaven National Laboratory) .....	13
<i>Exceptionally Rapid Solute Radical Cation Formation Following Pulse Radiolysis</i> Andrew R. Cook and John R. Miller (Brookhaven National Laboratory) .....	17
<i>Charge and Molecular Dynamics at Heterogeneous Interfaces</i> Tanja Cuk, Charles Harris, and David Chandler (Lawrence Berkeley National Laboratory) .....	21
<i>Stability of Nano Fluids, Solvent-Exchange Mechanism and Nuclear Quantum Effects. Recent Progress and Future Plans</i> Liem X. Dang (Pacific Northwest National Laboratory) .....	25
<i>Transition Metal-Molecular Interactions Studied with Cluster Ion Infrared Spectroscopy</i> Michael A. Duncan (University of Georgia) .....	29
<i>Confinement, Interfaces, and Ions: Dynamics and Interactions in Water, Proton Transfer, and Room Temperature Ionic Liquid Systems</i> Michael D. Fayer (Stanford University).....	33
<i>Fundamentals of Solvation under Extreme Conditions</i> John L. Fulton (Pacific Northwest National Laboratory).....	37

<i>Probing Chromophore Energetics and Couplings for Singlet Fission in Solar Cell Applications</i> Etienne Garand (University of Wisconsin) .....	41
 <i>Reactions and Transformations</i>	
Phillip L. Geissler, Musahid Ahmed , David Chandler, Rich Saykally (Lawrence Berkeley National Laboratory) .....	45
 <i>Laser Induced Reactions in Solids and at Surfaces</i>	
Wayne P. Hess, Alan G. Joly and Kenneth Beck (Pacific Northwest National Laboratory) .....	49
 <i>Spectroscopic Imaging of Molecular Functions at Surfaces</i>	
Wilson Ho (University of California, Irvine) .....	53
 <i>Development of Approaches to Model Excited State Charge and Energy Transfer in Solution</i>	
Christine Isborn (University of California Merced), Aurora Clark (Washington State University) and Thomas Markland (Stanford University).....	57
 <i>Theory of the Reaction Dynamics of Small Molecules on Metal Surfaces</i>	
Bret E. Jackson (University of Massachusetts Amherst).....	59
 <i>Probing Catalytic Activity in Defect Sites in Transition Metal Oxides and Sulfides using Cluster Models: A Combined Experimental and Theoretical Approach</i>	
Caroline Chick Jarrold and Krishnan Raghavachari (Indiana University) .....	63
 <i>Critical Evaluation of Theoretical Models for Aqueous Chemistry and CO<sub>2</sub> Activation in the Temperature-Controlled Cluster Regime</i>	
Kenneth D. Jordan (University of Pittsburgh) and Mark A. Johnson (Yale University) .....	67
 <i>Nucleation Chemical Physics</i>	
Shawn M. Kathmann (Pacific Northwest National Laboratory) .....	71
 <i>Structure and Reactivity of Ices, Oxides, and Amorphous Materials</i>	
Bruce D. Kay, R. Scott Smith, and Zdenek Dohnálek (Pacific Northwest National Laboratory) .....	75
 <i>Probing Ultrafast Electron (De)localization Dynamics in Mixed Valence Complexes Using Femtosecond X-ray Spectroscopy</i>	
Munira Khalil (University of Washington, Seattle), Niranjan Govind (Pacific Northwest National Laboratory), Shaul Mukamel (University of California, Irvine) and Robert Schoenlein (Lawrence Berkeley National Laboratory) .....	79
 <i>Non-Thermal Reactions at Surfaces and Interfaces</i>	
Greg A. Kimmel and Nikolay G. Petrik (Pacific Northwest National Laboratory) .....	83

*Interfacial Radiation Sciences*

Jay A. LaVerne, David M. Bartels, Daniel M. Chipman, and Sylwia Ptasinska (Notre Dame Radiation Laboratory) .....	87
<i>Single-Molecule Interfacial Electron Transfer</i>	
H. Peter Lu (Bowling Green State University) .....	91
<i>Solution Reactivity and Mechanisms through Pulse Radiolysis</i>	
Sergei V. Lymar (Brookhaven National Laboratory) .....	95
<i>Ab Initio Approach to Interfacial Processes in Hydrogen Bonded Fluids</i>	
Christopher J. Mundy (Pacific Northwest National Laboratory) .....	99
<i>Dynamic Studies of Photo- and Electron-Induced Reactions on Nanostructured Surfaces</i>	
Richard Osgood (Columbia University) .....	103
<i>Studies of Surface Adsorbate Electronic Structure and Femtochemistry at the Fundamental Length and Time Scales</i>	
Hrvoje Petek (University of Pittsburgh) .....	107
<i>Molecular Structure, Bonding and Assembly at Nanoemulsion and Liposome Surfaces</i>	
Geraldine Richmond (University of Oregon) .....	111
<i>Solvation</i>	
Richard Saykally, Musahid Ahmed, Phillip L. Geissler and Charles Harris (Lawrence Berkeley National Laboratory) .....	115
<i>Development of Statistical Mechanical Techniques for Complex Condensed-Phase Systems</i>	
Gregory K. Schenter (Pacific Northwest National Laboratory) .....	119
<i>An Atomic-scale Approach for Understanding and Controlling Chemical Reactivity and Selectivity on Metal Alloys</i>	
E. Charles H. Sykes (Tufts University) .....	122
<i>Solvation Dynamics in Nanoconfined and Interfacial Liquids</i>	
Ward H. Thompson (University of Kansas) .....	126
<i>Imaging Interfacial Electric Fields on Ultrafast Timescales</i>	
William A. Tisdale (Massachusetts Institute of Technology) .....	130
<i>Structural Dynamics in Complex Liquids Studied with Multidimensional Vibrational Spectroscopy</i>	
Andrei Tokmakoff (University of Chicago) .....	133
<i>The Role of Electronic Excitations on Chemical Reaction Dynamics at Metal, Semiconductor and Nanoparticle Surfaces</i>	
John C. Tully (Yale University) .....	136
<i>Reactive Processes in Aqueous Environment</i>	
Marat Valiev (Pacific Northwest National Laboratory) .....	140
<i>Cluster Model Investigation of Condensed Phase Phenomena</i>	
Xue-Bin Wang (Pacific Northwest National Laboratory) .....	143

<i>Free Radical Reactions of Hydrocarbons at Aqueous Interfaces</i> Kevin R. Wilson (Lawrence Berkeley National Laboratory) .....	147
<i>Ionic Liquids: Radiation Chemistry, Solvation Dynamics and Reactivity Patterns</i> James F. Wishart (Brookhaven National Laboratory) .....	151
<i>Molecular Level Understanding of Hydrogen Bonded Environments</i> Sotiris S. Xantheas (Pacific Northwest National Laboratory) .....	155
<i>Room temperature Single-Molecule Detection and Imaging by Stimulated Raman Scattering Microscopy</i> X. Sunney Xie (Harvard University) .....	159
<b>LIST OF PARTICIPANTS</b> .....	161

An aerial photograph of a green field, possibly a golf course or sports field, with a grid of red and black markers. The word "Abstracts" is written in yellow, italicized font in the center of the image.

*Abstracts*

# Probing Ion Solvation and Charge Transfer at Electrochemical Interfaces Using Nonlinear Soft X Ray Spectroscopy

L. Robert Baker

Department of Chemistry and Biochemistry, The Ohio State University, Columbus, OH 43210

[baker.2364@osu.edu](mailto:baker.2364@osu.edu)

## 1. Program Scope

Understanding electrochemical charge transfer and ion solvation at interfaces is an important challenge with both scientific and technological relevance because these interfacial processes largely determine the performance of batteries, fuel cells, acid–base catalysts, and other electro and photochemical systems. To significantly improve the efficiency of these energy conversion technologies will require a fundamental understanding of the molecular-level processes occurring at the solid–liquid interface that drive electrochemical energy conversion. Interfacial charge transfer in electrochemical systems can proceed by multiple mechanisms: First, charge transfer may occur as the bias-driven motion of electrons or holes from a solid electrode to a liquid phase reactant. In this process electrochemical efficiency is largely determined by the surface electronic structure of the catalyst and the state-dependent charge transfer kinetics that control carrier separation, injection, and trapping at the solid–liquid interface. Second, charge transfer can also occur during an electrochemical reaction via the de-solvation, injection, and intercalation of ions across the interface between a liquid electrolyte and a solid electrode. In this case removing an ion from its solvation shell represents a kinetic barrier to interfacial charge transfer that can strongly influence the rate and efficiency of energy storage and release. Both of these charge transfer mechanisms, which occur at the electrode–electrolyte interface, are critical for understanding and controlling energy flow and conversion efficiency in working electrochemical systems.

To address these important questions, this project aims to directly measure state-dependent charge transfer kinetics and ion solvation and de-solvation dynamics at biased electrochemical interfaces using soft x-ray spectroscopy. Direct observation of these processes will provide important new understanding of the physical processes that determine the efficiency of electrochemical energy conversion. Toward this objective, we are developing a soft x-ray light source for nonlinear spectroscopy. The goal of these experiments is to perform 2-wave mixing of soft x-ray pulse created by high harmonic generation (HHG) with an optical laser pulse and to use this process as a probe of ion coordination geometry and surface electronic structure at working electrode interfaces. This work will extend traditional sum frequency generation (SFG) spectroscopy from the infrared region to the XUV and soft x-ray spectral regions in order to probe core electron resonances with interface specificity. Soft x-ray SFG will provide surface-sensitive visualization of buried interfaces with unprecedented chemical and electronic state specificity. As detailed below, this technique will be applied to the study of ion coordination at biased electrode surfaces as well as metal oxide electrodes used as catalysts for water oxidation.

## 2. Recent Progress

In metal oxide semiconductors, two parameters give rise to two different types of band gaps. First, the charge transfer parameter,  $\Delta$ , can be thought of as the energy splitting between the metal  $3d$  and the O  $2p$  orbitals such that an excitation across this bandgap corresponds to a charge transfer between an O anion and an adjacent metal cation. This bandgap exists in metal oxides regardless of the Hubbard parameter,  $U$ , that governs splitting of the metal  $3d$  orbitals. However, when the effect of  $U$  is also considered, the metal  $3d$  orbitals split into two distinct bands that often straddle the Fermi level energy. Accordingly, in transition metal oxide semiconductors, the conduction band is made up primarily of unoccupied metal  $3d$  states while the valence band is a mixture of occupied O  $2p$  and metal  $3d$  orbitals. In this model the size of the bandgap as well as the exact orbital character of the valence band edge depends on the relative strengths of  $\Delta$  and  $U$ . For example, for  $U > \Delta$  the minimum bandgap is

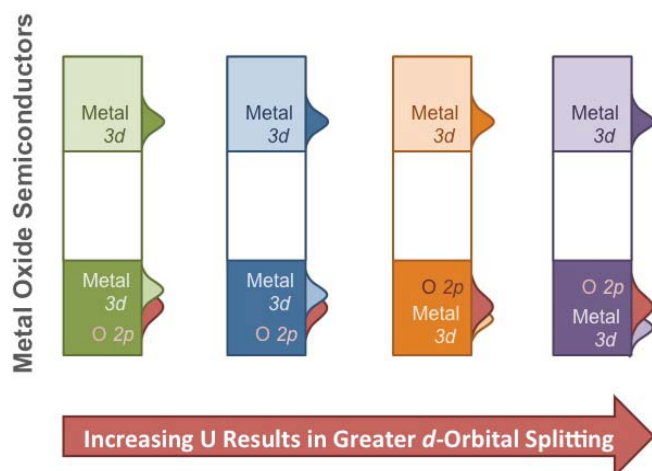


**Fig. 1** Schematic depicting the effect of increasing  $d$ -orbital splitting on the valence band electronic structure of metal oxide semiconductors. As the occupied metal  $d$  states shift to lower energy, the valence band edge becomes increasingly O  $2p$  in character. This has important effects on the bias-dependent charge donor states during electrochemical catalysis.

Cu, it is possible to observe the effect of increasing  $U$  and the accompanying shift of valence band character from metal  $3d$  to O  $2p$  on the overpotential of transition metal oxide electrocatalysts for water oxidation.

To test this hypothesis, we have prepared thin film catalysts of FeOOH,  $\text{Cu}_2\text{O}$ , and mixed  $\text{CuFeO}_2$  and begun to study the activities of these materials for electrochemical water oxidation. In each of these cases, Fe is the  $3+$  oxidation state and Cu is in the  $1+$  oxidation state. The absorption spectra of these catalysts (see Fig. 2A) shows that the mixed-metal  $\text{CuFeO}_2$  has a significantly reduced bandgap compared to either pure FeOOH or  $\text{Cu}_2\text{O}$ . It is currently thought that the reason for this decreased bandgap is the presence of a new metal-metal charge transfer excited state between the valence band maximum (i.e.  $\text{Fe}^{3+}$  states) and the conduction band minimum (i.e.  $\text{Cu}^{1+}$  states). Cyclic voltammetry data shows that of these three materials, only Cu oxide displays activity for water oxidation at low overpotential (see Fig. 2B). This is consistent with our working hypothesis that metal  $d$  states at the valence band edge prevent efficient hole injection. Correlating these electrochemical measurements with linear and nonlinear x-ray spectroscopy will enable us to study the role that the charge donor state plays in determining the efficiency of charge transfer and the overpotential required for electrochemical energy conversion.

We have also made significant progress toward the design and construction of the HHG light source. This includes complete 3D design and fabrication of custom vacuum chambers, design of vacuum compatible motion manipulation for alignment of soft x-ray optics inside the vacuum chambers, ray tracing of the soft x-ray beam to model spot size and

determined by  $\Delta$ , and occupied metal  $3d$  orbitals will be located deep in the valence band while the valence band edge will be composed primarily of O  $2p$  states. Alternatively, for  $U < \Delta$  the minimum bandgap is defined by  $U$ , and the upper edge of the valence band is composed primarily of metal  $3d$  states. In this material a thermalized bandgap excitation does not involve charge transfer between two atoms; rather, it involves only a change in electron configuration and spin state of the  $3d$  metal cation. It is theoretically predicted as well as experimentally observed that  $U$  increases from left to right across a row of transition metals in the periodic table. This effect is schematically depicted in Fig. 1, which shows that as  $U$  increases, the valence band edge of a metal oxide becomes increasingly O  $2p$  in character while the metal  $d$  states shift to lower energy. Consequently, by systematically investigating the series of  $3d$  transition metals from Mn to

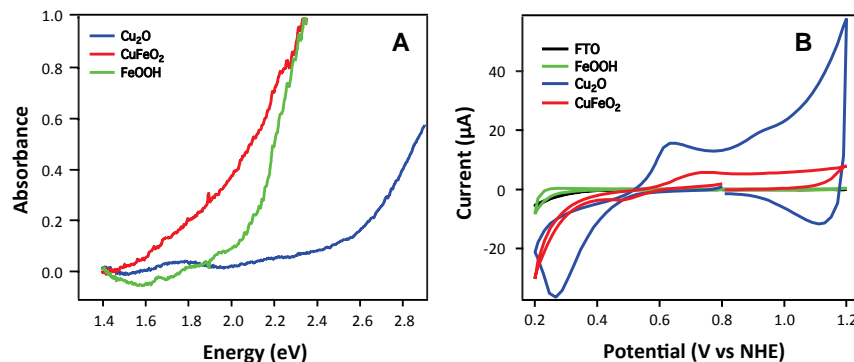


**Fig. 2** Absorption spectra (A) and cyclic voltammetry curves (B) of  $\text{Cu}_2\text{O}$ , FeOOH, and  $\text{CuFeO}_2$ . Cyclic voltammetry curves were obtained in 1M NaOH Ar-purged solution.

aberrations, and creating a design that will enable transient absorption, transient reflectivity, and sum frequency generation experiments simultaneously. Renovation of our laser lab was completed this summer, and this instrument is currently under construction.

### 3. Future Plans

#### 3.1. State Dependent Charge Transfer Efficiency During Electrochemical Water Oxidation

The electronic structure at working solid–liquid interfaces is largely unexplored, even though this interface is responsible for energy conversion in widely used electrochemical catalysts. It is expected that the surface of an electro-catalyst will have a very different electronic structure than the bulk as a result of undercoordination, interface bonding, and chemical and structural defects. Because charge injection occurs directly between surface states and the solvent phase, these states largely determine the rate and efficiency of electrochemical reactions.

Accordingly, soft x-ray spectroscopy will be used to investigate the mechanism of oxidative overpotential during electrochemical water splitting on metal oxide electrodes. It is well known that overpotential limits the efficiency of water oxidation, especially in neutral and acidic solutions. Recent discoveries have shown that this overpotential is greatly reduced if certain metal oxide catalysts are used for O<sub>2</sub> evolution in place of Pt or other noble metal catalysts. Further, a trend has been shown between the measured overpotential and the calculated strength of the metal–oxygen bond for a series of transition metal oxide catalysts. Because metal–oxygen bond strength also scales with other electronic properties of metal oxide semiconductors, such as the relative position of the metal *d* and O 2*p* orbitals in the valence band, it is likely that this correlation points to a more fundamental connection between oxidative efficiency and catalyst electronic structure. Specifically, we plan to use soft x-ray SFG to directly monitor the surface donor and acceptor states during electrochemical O<sub>2</sub> evolution as a function of applied bias on a series of metal oxide anodes. We expect to show that electrochemical efficiency is directly related to the overpotential required to switch the hole donor level between the metal 3*d* and O 2*p* orbitals of the catalyst.

This study will focus on Mn, Fe, Co, Ni and Cu oxide catalysts. In the x-ray SFG experiment, two spectral ranges will be investigated for each catalyst: 1) the metal M<sub>2,3</sub>-edge that varies from 47 eV for Mn to 72 eV for Cu and 2) the O L<sub>1</sub>-edge located at 42 eV (see Fig. 3). Spectra of these two absorption edges at zero bias will show the ground state spectrum of each catalyst surface. Repeating these measurements as the potential is increased up to the voltage necessary for O<sub>2</sub> evolution will show the incremental change in charge state of the catalyst surface with element specificity. From these measurements we will show the relationship between oxidative overpotential and the bias-dependent charge donor level of the metal oxide catalyst with orbital-specific resolution.

#### 3.1. Ion Solvation at Biased Electrode Surfaces

In addition to probing state-specific charge transfer kinetics during electrochemical water oxidation, soft x-ray spectroscopy will also be used to study ion solvation and de-solvation dynamics at biased electrode–electrolyte interfaces. During the charging/discharging cycles of a battery, metal cations are transported between a metal oxide cathode and a carbon anode through a liquid electrolyte. In the charged state of the battery, the cations intercalate into a carbon anode and in the discharged state, the cations intercalate into a metal oxide cathode. While it is possible to spectroscopically probe the coordination geometry of ions in the bulk electrolyte solution as well as the charge state and structure of ions intercalated into an electrode material, to study the

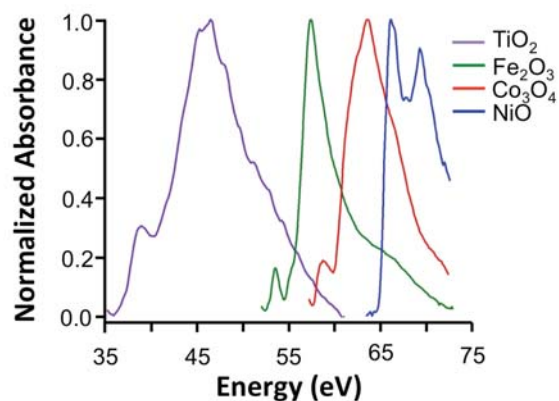


**Fig. 3** Experimental M<sub>2,3</sub> absorption edges of several transition metal oxides measured using a high harmonic source.

solvation structure of ions at the electrode–electrolyte interface is a difficult experimental challenge. The process of ion solvation and de-solvation that occurs as ions transfer between a solid electrode and the liquid electrolyte plays a significant role in determining the rate of energy storage and release. Development of molecular-level models for understanding the process of ion adsorption at interfaces and how solvation and de-solvation dynamics mediate this process will require direct observation of bias-induced ion absorption with the ability to resolve ion solvation geometry with interface specificity.

Soft x-ray spectroscopy is extremely sensitive to the coordination symmetry of ligands around a metal ion because the ligand-induced  $d$  orbital splitting determines the fine structure in spectrum. This is demonstrated in Fig. 4 that shows very different simulated absorption spectra for  $\text{Fe}^{3+}$  ions in octahedral and tetrahedral ligand fields. Similar spectra can be simulated for many other transition metal ions chelated by a variety of ligands using CTM4XAS ligand field multiplet software. This type of spectral simulation has previously enabled accurate interpretation of both ground and excited soft x-ray absorption spectra for metal oxide thin films and can be readily extended to interpret the x-ray spectra of metal ions in solution. Because second order wave mixing of an x-ray beam with an optical beam in an x-ray SFG experiment will probe the same core-hole resonances as an x-ray absorption experiment, but with interface specificity, soft x-ray SFG will enable direct observation of metal ion solvation geometry at solid–liquid interfaces.

Because transition metals display well defined resonances within the soft x-ray spectral range produced by HHG (see Fig. 3) and  $d$  orbital splitting is especially sensitive to changes in ligand coordination symmetry (see Fig. 4), the proposed experiments will focus on transition metal ions in polar solvents. Spectra of metal ions adsorbed to the electrode surface will be measured as a function of applied bias. We anticipate that at increasingly negative bias, the measured spectra will show that the solvation shell around the metal cations becomes asymmetrically distorted until at sufficiently high bias the metal cation is pulled out of the solvation shell and adsorbs directly to the electrode surface. Reversing the bias will result in desorption and re-solvation of the ion from the electrode surface. The fine structure of the x-ray spectrum will show the ligand field coordination symmetry as a function of bias. Phase changes in the surface layer corresponding to decreasing coordination number by exclusion of solvent molecules between the metal ion and the electrode surface will be resolved. Observing the reversibility of these spectral changes in a cyclic voltammetry experiment will reveal the dynamics of ion de-solvation and re-solvation that mediate the kinetics of ion adsorption and desorption, respectively.

#### 4. Publications

N/A

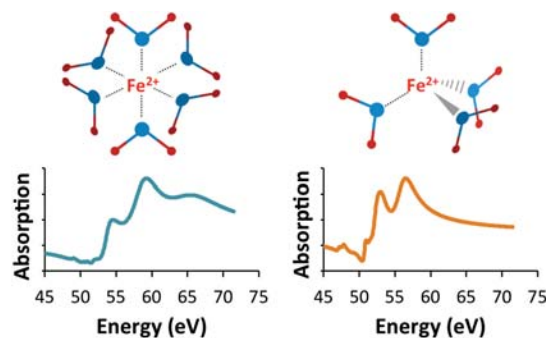


**Fig. 4** Simulated soft x-ray absorption spectrum of  $\text{Fe}^{2+}$  in  $\text{O}_h$  (left) and  $\text{T}_d$  (right) coordination shells.

## FUNDAMENTAL ADVANCES IN RADIATION CHEMISTRY

Principal Investigators:

DM Bartels ([bartels.5@nd.edu](mailto:bartels.5@nd.edu)), I Carmichael, I Janik, JA LaVerne, S Ptasińska  
 Notre Dame Radiation Laboratory, University of Notre Dame, Notre Dame, IN 46556

### SCOPE

*Research in fundamental advances in radiation chemistry is organized around two themes. First, energy deposition and transport seeks to describe how energetic charged particles and photons interact with matter to produce tracks of highly reactive transients, whose recombination and escape ultimately determine the chemical effect of the impinging radiation. The work described in this part is focused on fundamental problems specific to the action of ionizing radiation. Particular projects include investigation of neutron radiolysis in high temperature water, experimental and theoretical investigation of the VUV spectra of liquids up to supercritical conditions, chemistry of highly excited states in spur and track recombination in aromatic hydrocarbon liquids, and investigation of a novel radiation source, the atmospheric pressure plasma jet. The second thrust deals with structure, properties and reactions of free radicals in condensed phases. Challenges being addressed include the experimental and theoretical investigation of solvated electron reaction rates, measurement of radical reaction rates in high temperature water, determination of the redox potentials of hyper-reduced transition metal ions, and investigation of the structure and reactivity of OH radical adducts.*

### PROGRESS AND PLANS

The solvation structure of the hydrated electron has been the subject of debate since its discovery in 1962. For many years a "cavity model" produced by a one-electron pseudopotential in SPC water MD simulations has been broadly accepted as a correct representation, but recently it has been shown that basic properties such as the temperature dependence of the optical spectrum are not reproduced by such models. In response to the controversy, Jungwirth and coworkers performed large scale *ab initio* molecular dynamics simulations with a DFT water cluster embedded in a large classical MD water bath. They find that the local structure has a smaller void surrounded by four waters, each with one OH bond oriented toward the center. In collaboration with workers at Oakland University, we have explored the properties of a minimal model based on the Jungwirth results, consisting of a small water anion cluster embedded in dielectric continuum. We find that just four water molecules are sufficient to provide a robust minimum model at any post-Hartree-Fock level of theory with double-zeta basis set or larger. Additional layers of water molecules do not substantially change the result. In contrast to the assumptions of previous pseudopotential models, the electron has substantial spin density "on" the water molecules. The rms "size" or radius of gyration of the electron in this calculation is in reasonable agreement with the number derived from the experimental optical spectrum. The vertical detachment energy for ejection of the electron is well predicted and the frequency red-shift of the water OH stretch is in excellent agreement with resonance Raman experiments. Using this model with the G4 thermochemistry method reproduces experimental solvation free energy with surprising accuracy. The EPR g-factor shift is in reasonable agreement with experiment. Hyperfine couplings for electrons trapped in low temperature aqueous glasses are correctly calculated. On the basis of all this success, we consider the tetrahedral water cluster with four inward directed OH bonds to be the dominant structural motif of the hydrated electron. The half-century-old controversy is convincingly resolved. Present efforts are exploring the same methodology for electrons in methanol.

Hydroxymethyl radicals  $\bullet\text{CH}_2\text{OH}$  are encountered in many situations in nature, and are often used to study redox processes in solution. A high-temperature radiolysis study of  $\text{N}_2\text{O}$ -saturated aqueous methanol (up to  $300\text{ }^\circ\text{C}$ ) has provided new insight into the self-recombination of  $\bullet\text{CH}_2\text{OH}$  radicals. The self-recombination has been found to follow Arrhenius behavior up to  $300\text{ }^\circ\text{C}$ , with  $12.7 \pm 0.9\text{ kJ mole}^{-1}$  activation energy. The overall recombination is not quite diffusion controlled even at room temperature, implying that both dimerization and disproportionation channels have a significant thermal reaction barrier. Extensive *ab initio* calculations demonstrate with high accuracy that there is no electronic barrier to the dimerization in either gas or aqueous phase. Instead, the barrier is purely entropic (a steric effect) with a very loose transition state which we can model very well by Monte Carlo sampling at Hartree-Fock level. The disproportionation channel in the aqueous phase apparently involves specific water molecules to lower the transition state barrier relative to the gas phase.

Oxidation by the hydroxyl (OH) radical is one of the most widely studied reactions because of its central role in many chemical processes in both nature and industry. Although the redox potential of OH is very positive, direct electron transfer (ET) is rarely observed. If it happens, it mostly proceeds through the formation of an elusive OH adduct intermediate which facilitates ET and subsequent formation of hydroxide anion. Thus the nature of the intermediate bond as well as the type of the solute should determine whether inner sphere or outer sphere ET oxidation will proceed. Using time-resolved resonance Raman spectroscopy we have structurally characterized a variety of OH adducts to neutral sulfur-containing organic compounds, as well as halide/pseudohalide anions. The bond between the OH radical and the oxidized molecule differs depending on the nature of the molecule. In neutral organic sulfides, formation of an OH intermediate dominates the outcome of the oxidation process. The bond of the OH adduct has two-center, three-electron character ( $2c-3e$ , conveniently denoted  $\cdot\cdot$ ) with the frequency of symmetric  $\text{S}:\cdot\text{O}$  stretch centering around  $346\text{ cm}^{-1}$ . From the progression of the stretch overtones we could readily estimate bond dissociation energies in the order of  $\sim 0.4 - 0.6\text{ eV}$ . Oxidation of halide and pseudo-halide anions was also expected to proceed through the formation of OH adducts. Yet from extensive studies of OH-induced oxidation of  $\text{Cl}^-$ ,  $\text{Br}^-$ ,  $\text{I}^-$ ,  $\text{SCN}^-$  we were only able to detect OH adducts to bromide and thiocyanate anions. Although quite elusive and short-lived, these intermediates can be clearly recognized by their characteristic  $2c-3e\text{ X}:\cdot\text{O}$  stretching vibrational frequencies at  $294\text{ cm}^{-1}$  and  $298\text{ cm}^{-1}$  detected in resonance with their transient absorptions at  $360\text{ nm}$  and  $390\text{ nm}$  for  $\text{X} = \text{Br}$  and  $\text{SCN}$ , respectively. From the lack of intermediates detected in the chloride and iodide systems, we conclude that their oxidations by OH radical do not follow the same mechanism. Based on our preliminary studies, we propose that the oxidation mechanism varies in the series from chloride to iodide anion due to substantial differences between their respective redox potentials and solvation energies. This contradicts the widely accepted general oxidation mechanism of halides via an OH adduct intermediate, and makes the OH adduct formation only a special case.

Our recent characterization of an atmospheric pressure plasma jet (APPJ), a low-dose radiation source, indicated a distinctive ring-shape spatial distribution of plasma species. We used optical spectroscopy to study the relative emission intensities of various plasma species ignited in helium flows with and without oxygen addition. The emission spectra of our plasma system were obtained from two regions: one from between the high voltage electrode and the ground electrode (core region) and the other at various radial and axial distances from the jet launched into the air (jet region). The spectrum obtained in the core region of the APPJ in pure helium was

composed of metastable He, He<sub>2</sub>\* dimer, molecular nitrogen N<sub>2</sub> second positive system, N<sub>2</sub><sup>+</sup> first negative system, an atomic hydrogen line H $\alpha$ , hydroxyl radical OH, and atomic oxygen O. Interestingly, with the addition of oxygen (0.5%), the intensities from almost all emission lines except O were diminished. The spectra in the jet region of the APPJ were significantly different from those measured in the core region. In the jet region with pure helium the spectrum was dominated by metastable He, N<sub>2</sub>, N<sub>2</sub><sup>+</sup>, OH, and O. Compared to the core region, the intensity of OH radicals was low in the jet region in pure helium. We observed the effect of air diffusion on the spatial distribution of OH radicals and O atoms along a radial distance from the APPJ, indicating that air diffusion is instrumental in the recombination loss mechanism of both OH radicals and atomic O, especially away from the jet region. Similar to the core region, the intensity of all emission lines except those from O in the jet region decreased with oxygen addition. A ring-shaped profile of reactive plasma species was observed in our study because of high density of helium near the jet axis. In the case of the plasma with oxygen addition, the ring shape was deformed and showed more uniform distribution of reactive plasma species. This experimental work will be complemented by a numerical model, which will provide a qualitative description of certain phenomena observed in the experiment. The model will consist of two parts; background gas dynamics describing the gas flow, and mixing of the helium and oxygen inside and outside the quartz tube. The numerical model will be implemented in a COMSOL Multiphysics simulation package with the help of the Computational Fluid Dynamics and Chemistry modules. The simulation will provide a more accurate description of the spatial distribution of reactive species formed, and presumably explain the ring-shaped profiles of the plasma species.

Polymethyldisiloxanes have a wide variety of applications in the nuclear industry ranging from sealants to long-term containment media, but most of the radiation chemistry studies on these compounds have focused on their polymerization and not overall decomposition and gas production. Gamma radiolysis was performed on polymethyldisiloxanes of different molecular weights from 237 to 14000 Da along with hexamethyldisiloxane in order to determine the effects due to viscosity and end groups. Methane was the major gaseous product with a yield of about 2.5 molecules/100 eV that slightly decreased with increasing molecular weight. Molecular hydrogen has a yield of about half that and it also decreases with increasing molecular weight. Substitution of a phenyl group for the methyl groups in polyphenyldisiloxane resulted in a dramatic decrease in all gaseous yields showing the relative stability that occurs with aromatic compounds under certain radiation types. Infrared spectroscopy was inconclusive, but thermal gravimetric analysis definitely demonstrated an increase in crosslinking with increasing molecular weight. These data can now be used to clarify radiolysis mechanisms for this industrially important class of compounds.

Room temperature EPR spectra of reactive radical anions from octafluorotoluene, decafluoro-*p*-xylene and their partially fluorinated analogues have been obtained with a new, improved version of an Optically Detected Electron Paramagnetic Resonance (ODEPR) spectrometer constructed at the NDRL. The ODEPR signal-to-noise ratio has been greatly enhanced, allowing us to obtain liquid-phase EPR spectra of these previously unavailable radical ions. Octafluorotoluene and decafluoro-*p*-xylene are the simplest representatives of substituted aromatic perfluorocarbons whose radical anions are important reaction intermediates with unusual electronic and spatial structures that have largely eluded characterization. The isotropic spectra we obtained are characterized by the following parameters:  $aF(\textit{ortho}) = 58 \text{ G}$ ,  $aF(\textit{meta}) = 98 \text{ G}$ ,  $aF(\textit{para}) = 182 \text{ G}$ ,  $aF(\text{CF}_3) = 15 \text{ G}$ ,  $g = 2.0050$  for the

octafluorotoluene radical anion;  $a_{\text{F}(\text{ring})} = 31.5 \text{ G}$ ,  $a_{\text{F}(\text{CF}_3)} = 24.4 \text{ G}$ ,  $g = 2.0032$  for the decafluoro-*p*-xylene radical anion. Extensive quantum chemical calculations have been performed in order to support our interpretation of the experimental spectra in these and other partially-fluorinated analogs. While the computed hyperfine splittings, averaged over vibrational motion, are well matched to observation, calculated *g*-factors proved to be in less satisfactory accord. The accompanying energetics suggest that reductive defluorination pathways are strongly influenced by the electron affinities of neutral radical intermediates.

### PUBLICATIONS WITH BES SUPPORT SINCE 2013

- Chipman D.M. *J. Phys. Chem. B* **2013**, **117**, 5148-55 Water from ambient to supercritical conditions with the AMOEBA model.
- El Omar A.K.; Schmidhammer U.; Balcerzyk A.; LaVerne J.; Mostafavi M. *J. Phys Chem. A* **2013**, **117**, 2287-93 Spur reactions observed by picosecond pulse radiolysis in highly concentrated bromide aqueous solutions.
- Janik I.; Marin T.W. *Nucl. Instr. Meth. Phys. Res. A* **2013**, **698**, 44-8 A vacuum ultraviolet filtering monochromator for synchrotron-based spectroscopy.
- Janik I.; Tripathi G.N.R. *J. Chem. Phys* **2013**, **139**, 014302 The nature of the superoxide radical anion in water.
- Janik I.; Tripathi G.N.R. *J. Chem. Phys* **2013**, **138**, 44506. The early events in the OH radical oxidation of dimethyl sulfide in water.
- Jheeta S.; Domaracka A.; Ptasińska S.; Sivaraman B.; Mason N.J. *Chem. Phys. Lett.* **2013**, **556**, 359-64 The irradiation of pure CH<sub>3</sub>OH and 1:1 mixture of NH<sub>3</sub>:CH<sub>3</sub>OH ices at 30 K using low energy electrons.
- Klas M.; Ptasińska S. *Plasma Sources Sci. Technol.* **2013**, **22**, 025013 Characteristics of N<sub>2</sub> and N<sub>2</sub>/O<sub>2</sub> atmospheric pressure glow discharges.
- Mozumder A.; Wojcik M. *Radiat. Phys. Chem.* **2013**, **85**, 167-72 Initial electron-ion distance distribution in irradiated high-mobility liquids: Application of the metropolis method.
- Nuzhdin K.; Bartels D.M. *J. Chem. Phys* **2013**, **138**, 124503-1-8 Hyperfine coupling of the hydrogen atom in high temperature water.
- Kosno K.; Janik I.; Celuch M.; Mirkowski J.; Kisała, J.; Pogocki, D. *Isr. J. Chem.* **2014**, **54**, 302-315 The role of pH in the mechanism of •OH radical induced oxidation of nicotine.
- Han X., Cantrell W.A., Escobar E.E., Ptasińska S. *Eur. Phys. J* **2014**, **D68**, 46. Plasmid DNA Damage Induced by Helium Atmospheric Pressure Plasma Jet.
- Zhang X., Ptasińska S. *J. Phys. D.* **2014**, **47**, 145202. Growth of Silicon Oxynitride Films by Atmospheric Pressure Plasma Jet.
- Bahnev B., Bowden M.D., Styczynska A., Ptasińska S., Mason N.J.; Braithwaite N.St.J. *Eur. Phys. J D* **2014**, **68**, 140-1-5 A novel method for the detection of plasma jet boundaries by exploring DNA damage.
- Han X., Liu Y, Stack M.S., Ptasińska S. *J. Phys.: Conf. Ser.* **2014**, **565**, 012011-1-6 3D Mapping of plasma effective areas via detection of cancer cell damage induced by atmospheric pressure plasma jets.
- Kanjana K.; Walker J.A.; Bartels D.M. *J. Phys. Chem. A* **2015**, **119**, 1830-7 Hydroxymethyl Radical Self-Recombination in High-Temperature Water.
- Rumbach P.; Bartels D.M.; Sankaran R.M.; Go D.B. *Nat Commun* **2015**, **6** The solvation of electrons by an atmospheric-pressure plasma.
- Kumar A., Walker J.A., Bartels D.M., Sevilla M.D. *J. Phys. Chem. A* **2015**, **119** A Simple ab initio Model for the Hydrated Electron that Matches Experiment
- Janik I., Marin T.W. *Rev Sci Inst.*, **2015**, **86**, 015102. Design of an ultrashort optical transmission cell for vacuum ultraviolet spectroscopy of supercritical fluids.
- Arjunan K.P., Sharma V.K., Ptasińska S. *Int. J. Mol. Sci.* **2015**, **16**, 2971-3016 Effects of atmospheric pressure plasmas on isolated and cellular DNA – a review.

## Soft X-ray Spectroscopy and Microscopy of Interfaces Under *in situ* Conditions

Hendrik Bluhm, Mary K. Gilles, David K. Shuh, Musahid Ahmed

MS 6R-2100, 1 Cyclotron Rd, Berkeley, CA-94720

[HBluhm@lbl.gov](mailto:HBluhm@lbl.gov), [MKGilles@lbl.gov](mailto:MKGilles@lbl.gov), [DKShuh@lbl.gov](mailto:DKShuh@lbl.gov), [MAhmed@lbl.gov](mailto:MAhmed@lbl.gov)

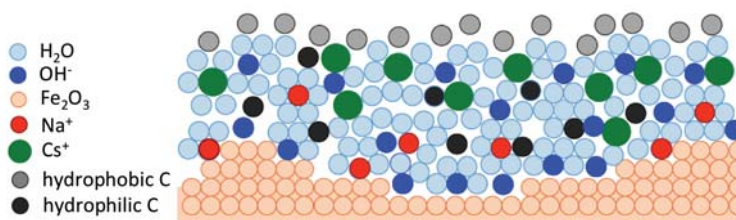
### Program Scope

This scientific program focuses on the molecular-level investigations of interfaces under operating conditions. This is essential for developing fundamental understanding of heterogeneous reactions at solid/vapor, solid/liquid, and liquid vapor interfaces. The high surface sensitivity of ambient pressure X-ray photoelectron spectroscopy (APXPS) (Hendrik Bluhm) combined with tailored *in situ* cells, allows the correlation of the surface chemistry of a solid or liquid with other reaction parameters (e.g., yield, conversion) for a wide variety of pressing problems, such as ion segregation at liquid surfaces, the heterogeneous chemistry of fuel cell electrodes, and ultrafast charge transfer across interfaces. The scanning transmission X-ray microscope (STXM) (Mary Gilles) provides spatially-resolved molecular information on materials important for energy sciences and complements the APXPS investigations by expanding the probe depth and pressure range. The unique capabilities at beamline 11.0.2 enable cutting-edge research on *in operando* interfacial chemistry across a wide range of areas of research, from alternative energy devices to aerosol chemistry. The PI's collaborate with scientists from Sandia National Laboratory (X-ray absorption flame measurements), Pacific Northwest National Laboratory (fundamental atmospheric chemistry) and Berkeley Laboratory (chemical catalysis, X-ray spectroscopy of liquids and electrolytes, photosynthetic systems, and time-resolved X-ray spectroscopy).

### Progress Report

#### *Development of SWAPPS. Hendrik Bluhm.*

Over the past year we have made important progress in the development of standing wave ambient pressure photoelectron spectroscopy (SWAPPS). SWAPPS is a new technique for investigating heterogeneous interfacial processes at liquid/solid interfaces under *in operando* conditions and with chemical and spatial sensitivity on the molecular scale. A complete investigation of heterogeneous processes at liquid/solid interfaces requires measuring the chemical composition of four distinct regions: (1) The bulk liquid, (2) the electrical double layer at the interface, (3) the solid interface in contact with the liquid, and (4) the sub-surface region of the solid. A major obstacle is enhancing the signal from the narrow interfacial region (2, 3) over that originating from the bulk of the liquid layer and solid substrate (1, 4). SWAPPS addresses this challenge and provides detailed chemical information about all four components of the system, as well as the spatial arrangement of chemical species (bulk and interface constituents) along the direction perpendicular to the interface, by tailoring the exciting X-ray wave field into a standing wave that is scanned through the interface of interest and thus provides much increased depth-resolution in XPS experiments. The proof-of-principle experiments focused on mixed NaOH and CsOH thin films on the surface of a thin film of Fe<sub>2</sub>O<sub>3</sub> grown on a Si/Mo multilayer. Rocking curves for all elements in the system (including carbon) showed that Na is preferentially adsorbed at the solution/hematite interface, while Cs is excluded from the interface. Two carbon species were observed as well, one with a binding energy compatible with carboxylic acid or carbonate groups which is distributed throughout the solution, and aliphatic carbon which resides exclusively at the solution/vapor



Schematic representation of the chemical distribution across a thin (Cs,Na)OH/hematite interface, as determined by SWAPPS. (Nemšák et al., Nat. Comm. **2014**, 5, 5441.

interface as expected from its hydrophobic nature. These results indicate that the fully-developed SWAPPS method will be an invaluable tool for the investigation of liquid/vapor interfaces.

***Ambient Pressure Photoemission Spectroscopy of Hybrid Nanoporous Films: Interactions of NH<sub>3</sub> in the Presence of H<sub>2</sub>O. Mary K. Gilles.*** Hybrid materials such as metal organic frameworks (MOFs) are attractive in areas related to gas separation and storage and catalysis. However, exposure to water vapor leads to degradation of some MOFs, limiting their applications. Changes in bonding and competition for binding sites between adsorbate molecules (NH<sub>3</sub>) and water were examined in Cu<sub>3</sub>(btc)<sub>2</sub> (btc=1,3,5-benzenetricarboxylate) thin films using APXPS. Spectra were measured on N 1s, O 1s, and Cu 2p as functions of NH<sub>3</sub> and H<sub>2</sub>O vapor pressures, and on the order in which exposure occurred. Ammonia physisorbs at the Cu<sup>2+</sup> sites and as the loading is increased, the N 1s peak at 400.6 eV shifts by -0.3 eV. This decrease in binding energy indicates a weakening of the ammonia-Cu<sup>2+</sup> interaction that has been attributed to ammonia-ammonia interactions. Upon introduction of H<sub>2</sub>O vapor, ~6% of the NH<sub>3</sub> is displaced by water. The dominant N 1s peak (now shifted to 400.3 eV) develops a shoulder with an increase in binding energy (401.8 eV) due to hydrogen bonding between the adsorbed ammonia and the added water. Instead, if the film is first exposed to water, subsequent addition of ammonia about 80% of the water is displaced (NH<sub>3</sub> binding energy to Cu<sup>2+</sup> is ~2x higher than that of H<sub>2</sub>O). As evidenced by the O 1s spectra, due to hydrogen bonding with the NH<sub>3</sub> connected to Cu<sup>2+</sup>, the remaining water is shifted to a higher binding energy.

Whether water is absorbed first and then mostly replaced by ammonia, or ammonia is absorbed first and a fraction is replaced by water, the spectra indicate that hydrogen bonding between the H<sub>2</sub>O and the NH<sub>3</sub> (now bound to the Cu) further polarizes the ammonia, and enhances electron donation from nitrogen to Cu<sup>2+</sup>. Hence, the increase in the Cu<sup>1+</sup> peak observed in APXPS (reduction of Cu<sup>2+</sup>) results from the presence of both H<sub>2</sub>O and NH<sub>3</sub>.

***Proxies for Sea Salt Aerosol Aging. Mary Gilles.*** Sea salt aerosols (primarily NaCl), produced by wave action, react with strong atmospheric acids (HA), such as nitric and sulfuric acids that condense onto particles during transport. The reaction: NaCl (aq) + HA (aq, g) ↔ NaA (aq) + HCl (aq, g), releases HCl (g) into the atmosphere and the remaining particles are depleted in Cl. STXM/NEXAFS was used to probe the chemistry of NaCl cores coated with weak organic acids (i.e., tartaric, maleic, acetic acids) as a function of hydration/dehydration cycling. These weak organic acids serve as surrogates for complex organic mixtures (secondary organic aerosols) that condense during transport. Because the acid dissociation constants for these acids are 5-10 orders of magnitude smaller than nitric or sulfuric acid it was anticipated they would not undergo similar chemistry. Hydration/dehydration cycles simulated the variable atmospheric conditions aerosols would experience during transport. Under these cycles, the relative solubility of each component in the gas versus aqueous phase becomes more important than the relative acid strength. Ultimately, the loss of the highly volatile HCl product during dehydration drives the acid displacement of weak acids and the reactions of weak acids are greatly enhanced by hydration/dehydration cycles.

### **Proposed Work**

***In operando Spectroscopy of the Heterogeneous Chemistry at Liquid/Solid Interfaces. Hendrik Bluhm.*** We will continue the investigations of liquid/solid interfaces, focusing on the interface of aqueous solutions with iron oxides, which are important both for photo-catalysis and geochemistry. We will investigate the interface of hematite (Fe<sub>2</sub>O<sub>3</sub>) with KOH solutions in photo-catalytic reactions as a function of applied potential and solar illumination. The correlation between the chemical composition of the interface and changes in band bending as a function of electrochemical conditions is of specific interest.

***Chemical Reactions at Aqueous Solution/Vapor Interfaces. Hendrik Bluhm.*** The properties of liquid/vapor interfaces strongly influence the abundance and reactivity of trace gas molecules that are important for many heterogeneous processes in atmospheric and environmental chemistry. To date, little is known about the concentration of solution phase species at the liquid/vapor interface, which can

significantly differ from the bulk solution concentration and is an important quantity in the modeling of heterogeneous reactions at liquid/vapor interfaces.

These open questions will be addressed by developing new methods to study the surface and subsurface chemistry of liquid/vapor interfaces with the same level of detail and control as in the case for solid/vapor interfaces. At the heart of the experiments is the correlation between bulk chemical composition, surface chemical composition, and gas phase composition under reaction conditions, where some of the reaction parameters are: time, bulk liquid composition at the beginning of the experiment, gas phase composition, UV irradiation, and liquid temperature. The basic concept is to use APXPS and partial electron yield (PEY) NEXAFS for surface measurements, and X-ray emission spectroscopy (XES) as well as fluorescence yield (FY) NEXAFS to investigate the bulk composition. Using droplet trains reactions can be studied on the microsecond time scale, while for slower reactions static droplets will be investigated, either deposited on an unreactive substrate or suspended in an optical or acoustic trap. One of the first experiments will address the uptake of SO<sub>2</sub> by water as a function of pH, an important problem in environmental science.

***Water Vapor Uptake Effects on Bonding, Viscosity and Phase. Mary K. Gilles.*** The proposed work focuses on understanding how bonding and viscosity change as water is absorbed onto an interface (APXPS in collaboration with H. Bluhm), the permeation of water through the interface (APXPS), and the transport into the bulk (APXPS, STXM, and Quartz Crystal Microbalance with Dissipation monitoring-QCM-D). Tautomers are isomers formed by the transfer of a  $\alpha$ -hydrogen and movement of a double bond. For aldehydes and ketones, the keto form typically dominates. Hydrogen bonding can lower the tautomerization barrier and influence reactivity and water vapor uptake; enhanced enol formation has been observed with increasing relative humidity. Experiments can provide fundamental insight into the role of hydrogen bonding in tautomeric systems and the energetics of water bonding with each tautomer and subsequent addition of water are ideal for theoretical studies. In amorphous systems, after monolayer absorption, multilayers add and water molecules embed between molecules (plasticization) increasing the distance between molecules and decreasing the viscosity and glass transition temperature. Changes in bonding, viscosity and subsequent water uptake will be examined in chemical systems where a shift in equilibrium bonding configuration occurs where plasticization can affect viscosity. Changes in viscosity will be probed by examining dissipation in a QCM that will be incorporated into the APXPS.

***Metal Ion Coordination Complexes and Clusters: Developing and Exploring the Continuum from Gas-Phase to Bulk Solution Chemistry. David K. Shuh.*** The fundamental chemistry of metal ions in solution is central to technological, environmental, and biological processes. Efforts to understand solution properties of metal ions suffer from complexities introduced by inner-sphere solvation and coordination, and interactions with outer-sphere molecules and ions. An effective approach for probing interactions in metal ion complexes is soft X-ray absorption spectroscopy (XAS) at core levels of light atoms (C, N, O) in coordinating ligands and metal ions. The objective is to explore metal ion coordination chemistry from solution and gas-phase perspectives, using solution XAS and gas-phase VUV/soft X-ray spectroscopies to understand metal ion chemistry in solutions. This will be accomplished by studying bonding in systems that span a range of complexity from gas-phase systems that can be modeled, to bulk solutions where a multitude of interactions with solvent molecules, coordinating ligands, and counter-ions need to be considered. Bridging dimensionality from gas-phase to bulk solution, the research will provide new insights into solution chemistry of metal ions based on a bottom-up approach that incrementally introduces complexity, ultimately describing metal ions in realistic solutions. This research will incorporate an essential collaborative theoretical component with D. Prendergast (LBNL). Experimental efforts will be coordinated with those of Saykally.

**Publications (2014 to date)**

1. Arion, T., et al.: *Appl. Phys. Lett.* **2015**, 106. Artn 121602, Doi 10.1063/1.4916278
2. Carencio, S., et al.: *Small* **2015**, 11, 3045. Doi 10.1002/sml.201402795
3. Dong, A. Y., et al.: *Surface Science* **2015**, 634, 37. Doi 10.1016/j.susc.2014.10.008
4. Eren, B., et al.: *J. Am. Chem. Soc.* **2015**, 137, 11186. Doi 10.1021/jacs.5b07451
5. Eren, B., et al.: *J. Phys. Chem. C* **2015**, 119, 14669. Doi 10.1021/jp512831f
6. Hiltunen, T., et al.: *Phys. Rev. B* **2015**, 91. Artn 075301, Doi 10.1103/Physrevb.91.075301
7. Karslioglu, O., et al.: *Faraday Discuss.* **2015**, 180, 35. Doi 10.1039/c5fd00003c
8. Lampimaki, M., et al.: *J. Phys. Chem. C* **2015**, 119, 7076. Doi 10.1021/jp511340n
9. Mehl, S., et al.: *Phys. Rev. B* **2015**, 91. Artn 085419, Doi 10.1103/Physrevb.91.085419
10. Mueller, D. N., et al.: *Nat. Comm.* **2015**, 6. Artn 6097, Doi 10.1038/Ncomms7097
11. Ng, M. L., et al.: *ChemPhysChem.* **2015**, 16, 923. Doi 10.1002/cphc.201500031
12. Nijem, N., et al.: *Cryst. Growth Des.* **2015**, 15, 2948. Doi 10.1021/acs.cgd.5b00384
13. O'Brien, R. E., et al.: *Environ. Sci. Technol.* **2015**, 49, 4995. Doi 10.1021/acs.est.5b00062
14. Rameshan, C., et al.: *Surface Science* **2015**, 641, 141. Doi 10.1016/j.susc.2015.06.004
15. Stoerzinger, K. A., et al.: *J. Phys. Chem. C* **2015**, 119, 18504. Doi 10.1021/acs.jpcc.5b06621
16. Wang, B. B., et al.: *J. Phys. Chem. A* **2015**, 119, 4498. Doi 10.1021/jp510336q
17. Wei, M. M., et al.: *J. Phys. Chem. C* **2015**, 119, 13590. Doi 10.1021/acs.jpcc.5b01395
18. Yang, Y., et al.: *Nano Res.* **2015**, 8, 227. Doi 10.1007/s12274-014-0639-0
19. Baker, L. R., et al.: *Nano Lett.* **2014**, 14, 5883. Doi 10.1021/Nl502817a
20. Bartels-Rausch, T., et al.: *Atmos. Chem. Phys.* **2014**, 14, 1587. Doi 10.5194/acp-14-1587-2014
21. Du, X. S., et al.: *ECS J. Solid State Sc.* **2014**, 3, Q3045. Doi 10.1149/2.010409jss
22. Frank, J. H., et al.: *App. Phys. B-Lasers O* **2014**, 117, 493. Doi 10.1007/S00340-014-5860-8
23. Jin, L., et al.: *J. Phys. Chem. C* **2014**, 118, 12391. Doi 10.1021/Jp5034855
24. Laskin, J., et al.: *Environ. Sci. & Technol.* **2014**, 48, 12047. Doi 10.1021/Es503432r
25. McCarty, K. F., et al.: *J. Phys. Chem. C* **2014**, 118, 19768. Doi 10.1021/Jp5037603
26. Meihaus, K. R., et al.: *J. Am. Chem. Soc.* **2014**, 136, 6056. Doi 10.1021/ja501569t
27. Miller, D., et al.: *J. Am. Chem. Soc.* **2014**, 136, 6340. Doi 10.1021/ja413125q
28. Minasian, S. G., et al.: *Chem. Sci.* **2014**, 5, 351. Doi 10.1039/C3sc52030g
29. Nemšák, S., et al.: *Nat. Comm.* **2014**, 5. Artn 5441, Doi 10.1038/Ncomms6441
30. Nepl, S., et al.: *Faraday Discuss.* **2014**, 171, 219. Doi 10.1039/C4FD00036F
31. Nijem, N., et al.: *Chem. Comm.* **2014**, 50, 10144. Doi 10.1039/C4cc02327g
32. O'Brien, R. E., et al.: *Geophys. Res. Lett.* **2014**, 41, 4347. Doi 10.1002/2014gl060219
33. Perrine, K. A., et al.: *J. Phys. Chem. C* **2014**, 118, 29378. Doi 10.1021/jp505947h
34. Shavorskiy, A., et al.: *J. Phys. Chem. C* **2014**, 118, 29340. Doi 10.1021/jp505587t
35. Shavorskiy, A., et al.: *Rev. Sci. Instrum.* **2014**, 85. Artn 093102, Doi 10.1063/1.4894208
36. Siefertmann, K. R., et al.: *J. Phys. Chem. Lett.* **2014**, 5, 2753. Doi 10.1021/Jz501264x
37. Starr, D. E., Bluhm, H.: *J. Phys. Chem. C* **2014**, 118, 29209. Doi 10.1021/jp505349f
38. Stoerzinger, K. A., et al.: *J. Phys. Chem. C* **2014**, 118, 19733. Doi 10.1021/Jp502970r
39. Tenney, S. A., et al.: *J. Phys. Chem. C* **2014**, 118, 19252. Doi 10.1021/jp507205t
40. Ward, M. D., et al.: *Inorg. Chem.* **2014**, 53, 6920. Doi 10.1021/Ic500721d
41. Yao, Y. X., et al.: *P. Natl. Acad. Sci. USA* **2014**, 111, 17023. Doi 10.1073/pnas.1416368111

## Surface Chemical Dynamics

N. Camillone III and M. G. White

*Brookhaven National Laboratory, Chemistry Department, Building 555, Upton, NY 11973*

([nicholas@bnl.gov](mailto:nicholas@bnl.gov), [mgwhite@bnl.gov](mailto:mgwhite@bnl.gov))

### 1. Program Scope

This program focuses on fundamental investigations of the dynamics, energetics and morphology-dependence of thermal and photoinduced reactions on planar and nanostructured surfaces that play key roles in energy-related catalysis and photocatalysis. Laser pump-probe methods are used to investigate the dynamics of interfacial charge and energy transfer that lead to adsorbate reaction on metal and metal oxide surfaces. State- and energy-resolved measurements of the gas-phase products are used to infer the dynamics of product formation and desorption. Time-resolved correlation techniques follow surface reactions in real time and are used to infer the dynamics of adsorbate–substrate energy transfer. Measurement of the interfacial electronic structure is used to investigate the impact of adsorbate-surface and cluster-support interactions on the activity of thermal and photoinduced reactions. Capabilities to synthesize and investigate the surface chemical dynamics of arrays of supported metal nanoparticles (NPs) on oxide surfaces include the deposition of size-selected gas-phase clusters as well as solution-phase synthesis and deposition of narrow-size-distribution nanometer-scale particles.

### 2. Recent Progress

***Ultrafast Surface Chemical Dynamics.*** Our ultimate goal is to follow surface chemical processes in real time. Toward this end we investigate the dynamics of substrate–adsorbate energy transfer by injecting energy with  $\sim 100$ -fs near-IR laser pulses to initiate surface reactions by substrate-mediated processes such as desorption induced by multiple electronic transitions and electronic friction. Time-resolved monitoring is achieved by a two-pulse correlation (2PC) method wherein the surface is excited by a “pump” pulse and a time-delayed “probe,” and the delay-dependence of the product yield reports on the energy transfer rate.

One of our primary interests is to understand how the molecule–surface energy transfer that drives surface chemistry depends on the geometry of the surface adsorption site and the nature of the coadsorbed species. Whereas it has been long appreciated that adsorption-site geometry and energetics govern surface chemical processes such as diffusion, desorption and reaction, very little is known about the adsorption-site dependence of the efficiency of molecule–surface energy transfer.

To probe the site-dependence of energy transfer, we have recently investigated in detail the coverage dependence of the desorption dynamics of CO from Pd(111). This system is well-suited to such studies because with increasing coverage the CO site occupancy switches from three-fold-hollow only to bridge-site only, to top-site plus three-fold-hollow site. Thus, we can effectively dial in an adsorption site by controlling the surface coverage, and conduct time-resolved experiments to probe the energy transfer.

In laying the groundwork for these experiments, we reexamined the coverage-dependent evolution of the structure of CO/Pd(111), making careful correlations between features in thermal desorption and electron diffraction measurements. This led us to develop a new but simple recipe for growing adlayers of all coverages, including the  $(2\times 2)$  saturated phase. Along the way we discovered a new  $c(16\times 2)$  structure which we propose is comprised of stripes of the saturated  $(2\times 2)$  structure separated by light domain boundaries. The data also allowed us to estimate the coverage-dependent desorption activation energy, which spans a broad range from  $\sim 0.5$  eV at saturation to  $\sim 1.5$  eV in the zero-coverage limit.

We find a remarkable increase in the photodesorption probability with increasing coverage (Fig. 1), indicating a  $\sim 60$ -fold enhancement for molecules adsorbed at top sites compared to those at three-fold hollow sites. Simulations of the coverage-dependent photoyields using a two-temperature model suggest that the energy transfer rate varies with binding site as follows: three-fold hollow > bridge > atop. This

trend manifests itself as an attenuation of the desorption probability of the more loosely-bound atop molecules compared to what would be expected based on the coverage-dependent activation energies alone. The 2PC measurements (Fig. 2) remain to be fully interpreted, but suggest a more complicated story: the measured decay times for the top site do not appear to follow the expected monotonic trend of weaker coupling with weaker binding. We are currently pursuing possible explanations including an adsorption-site dependence of the preexponential factor.

We have also found that substituting one CO per (2×2) unit cell with an oxygen atom enhances the CO desorption probability by ~3-fold. Our 2PC measurements indicate that the coupling to top-site CO with O-atom neighbors is ~2 times faster than to top-site CO with only CO neighbors. We are working to simulate this behavior within the two-temperature model framework, and performing density functional theory (DFT) cluster calculations of ground and excited electronic states of this system (in collaboration with A. Bhattacharya at the Indian Institute of Science in Bangalore) to understand the coupling.

In parallel we are investigating the ultrafast dynamics of desorption ( $O$ ,  $O_2$ ,  $CO$ ) and reaction ( $O + CO \rightarrow CO_2$ ) on  $TiO_2(110)$ -supported Pd nanoparticles (NPs). These systems provide both the opportunity to explore the size-dependence of the dynamics and serve as more realistic model catalysts for our time-resolved studies. Our initial work has revealed some distinguishing behaviors in the NP thermal and photoinduced chemistry. Most notably, we find that edge/defect sites and limited terrace sizes play important roles in the thermal reaction kinetics, that the cross sections for photoinduced desorption are orders of magnitude larger on the NPs than on the single crystal surfaces, and that the timescales for energy flow are generally longer on the NPs compared to the single crystal, suggesting that the excitation is confined to the NP, as compared to the single crystal. We are currently installing a new oxygen plasma source and XPS system on our UHV system so that we can prepare and characterize clean  $Pd_N/TiO_2(110)$  systems and investigate their thermal and photoinduced chemistry in situ.

**Pump-Probe Studies of Photodesorption and Photooxidation on  $TiO_2(110)$  Surfaces.** Recent work has focused on understanding the underlying electronic properties that control the UV photooxidation efficiency of organic molecules on  $TiO_2(110)$  surfaces. Specifically, work by Henderson and coworkers at PNNL has shown that the co-adsorption of oxygen with simple ketones on a reduced  $TiO_2(110)$  surface greatly enhances the photoyield of radical photoproducts relative to that of the ketone alone. Co-adsorption of oxygen and the ketone also leads to formation of a thermally activated oxygen-ketone complex (e.g., ketone diolate) which is apparently responsible for the observed increase in photoactivity. The reason for this enhanced activity, however, is not clearly understood. To address this issue, we have performed methyl photoyield measurements for a number of ketone molecules (acetaldehyde, acetone, 2-butanone, 2-propanone, acetophenone and trifluoroacetone) with and without co-adsorbed oxygen, to

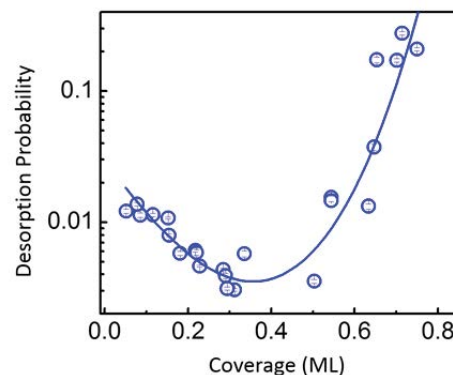


**FIG. 1.** Photoinduced desorption probabilities for CO from Pd(111) as a function of coverage show a dramatic increase as the top site is populated.

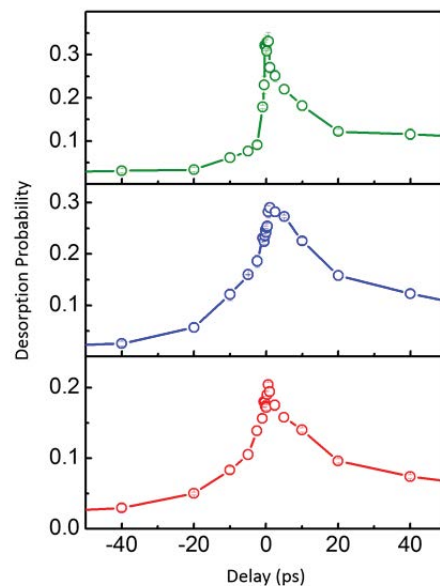


**FIG. 2.** Two-pulse correlation measurements of CO desorption from Pd(111) with adsorption at three-fold hollow sites only, bridge sites only, and top + three-fold-hollow sites (top to bottom).

obtain photoactivity enhancements ratios. We relate the latter to changes in the partial density-of-states (PDOS) at the valence band maximum (VBM) of  $\text{TiO}_2(110)$  for the  $\eta_1$ -bonded ketone and the  $\eta_2$ -bonded ketone-diolate assuming that the photoreaction is induced by resonant electron transfer with thermalized holes at the VBM. The PDOS were obtained from electronic structure calculations using a titania cluster model which correctly describes the band edge positions of bulk titania. The calculations show that the overlap of the molecule-derived  $2p_0$  PDOS with the VBM

generally increases significantly for the  $\eta_2$ -ketone-diolate compared to the  $\eta_1$ -ketone (see Fig. 3). Moreover, the change in PDOS is correlated with the experimental enhancement factors, with trifluoroacetone having the highest, and butanone and pentanone exhibiting the smallest. The results show that for electronically similar systems, the overlap of the PDOS at the VBM is an important factor for controlling the relative efficiency of hole-mediated photoreactions on  $\text{TiO}_2$ .

**Interfacial Electronic Structure of Supported Clusters.** Metal-support interactions can strongly influence catalytic activity through electronic interactions which induce structural changes or the creation of new active sites at the particle-support interface. For example, the catalytic activity of noble metals on reducible oxides for (e.g.,  $\text{TiO}_2$ ,  $\text{CeO}_2$ ) has been attributed to charge transfer interactions that modify the charge state of the metal and stabilize oxygen vacancies on the oxide. In this work, we have explored the role of the metal oxide structure and state of reduction on interfacial charge transfer for a number of small metal oxide nanoclusters ( $\text{MO}_x$ ;  $M = \text{Mo}, \text{W}, \text{Ti}, \text{Nb}$ ) on  $\text{Cu}(111)$  and  $\text{Cu}_2\text{O}/\text{Cu}(111)$  surfaces using mass-selected cluster deposition and DFT calculations. A major advantage of mass-selected deposition is the ability to control the stoichiometry of the clusters, i.e., metal-to-oxygen ratio, thereby allowing studies of “reduced” clusters without post annealing treatment of the surface. Two-photon photoemission (2PPE) measurements of coverage-dependent work function shifts are used to derive surface dipole moments which are sensitive to cluster size, structure and stoichiometry (see Fig. 4). For deposition on  $\text{Cu}(111)$ , the surface dipoles and charge transfer were found to be largest for stoichiometric Mo and W oxide clusters, e.g.,  $\text{Mo}_3\text{O}_9$  and  $\text{W}_3\text{O}_9$ , and smallest for sub-stoichiometric (reduced) clusters of Ti and Nb, e.g.,  $\text{Ti}_3\text{O}_5$  and  $\text{Nb}_4\text{O}_7$ . The surface dipoles generally correlate with DFT-calculated Bader charge transfer, except in cases where the adsorbed cluster structure has a large intrinsic dipole moment. The measured surface dipoles for clusters deposited on the  $\text{Cu}_2\text{O}/\text{Cu}(111)$  thin film are generally much larger than on  $\text{Cu}(111)$  which is attributed to surface polarization associated with deformation of the oxide film resulting from cluster binding. Overall, these experiments demonstrate that coverage dependent work function shifts can be successfully employed to probe charge transfer at

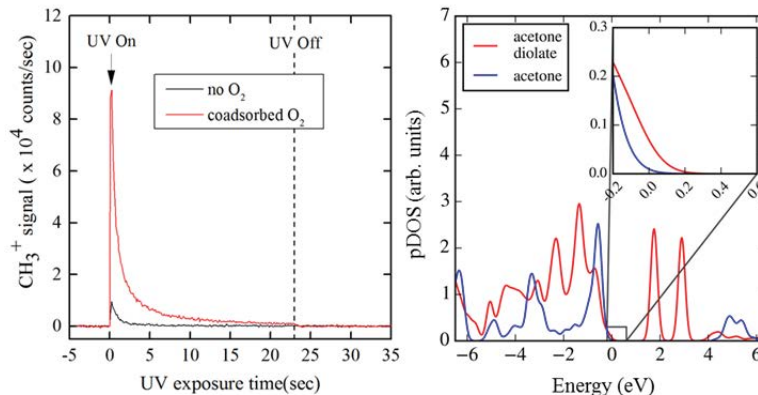


**FIG. 3.** Left: Methyl fragment photoyield versus UV exposure for acetone on  $\text{TiO}_2(110)$  with and without co-adsorbed oxygen. Right: Calculated partial density-of-states for acetone and acetone-diolate on  $\text{TiO}_2(110)$ . Zero energy corresponds to VBM of  $\text{TiO}_2(110)$ .

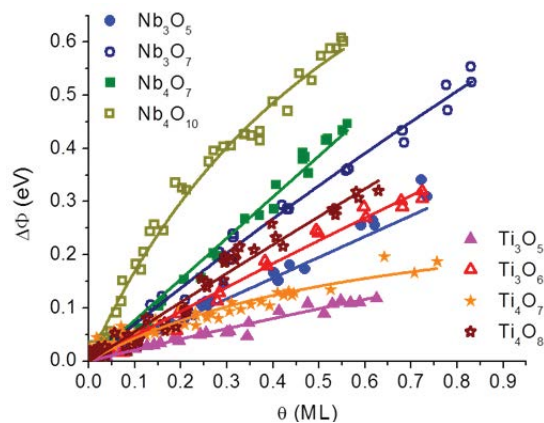


**FIG. 4.** Measured work function shifts for Nb and Ti oxide clusters deposited on a  $\text{Cu}(111)$  surface as measured by 2PPE. The shifts are positive indicating a surface dipole pointing away from the surface and consistent with  $\text{Cu} \rightarrow \text{cluster}$  charge transfer.

cluster-support interfaces which can be combined with other techniques, such as XPS core level shifts, and theoretical calculations to better understand electronic contributions to catalytic activity.

### 3. Future Plans

Our planned work develops three interlinked themes: (i) the chemistry of supported NPs and nanoclusters (NCs), (ii) the exploration of chemical dynamics on ultrafast timescales, and (iii) the photoinduced chemistry of molecular adsorbates. The investigations are motivated by the fundamental need to connect chemical reactivity to chemical dynamics in systems of relevance to catalytic processes—in particular metal and metal-compound NPs and NCs supported on oxide substrates. They are also motivated by fundamental questions of physical changes in the electronic and phonon structure of NPs and their coupling to adsorbates and to the nonmetallic support that may alter dynamics associated with energy flow and reactive processes.

Future work on ultrafast photoinduced reactions will involve modeling of the energy transfer rates to elucidate the adsorption-site- and NP-size-dependent dynamics we have observed. In addition, further experiments on progressively smaller nanoparticles (towards sub-nm) will be pursued to further explore fundamental changes in surface reaction kinetics and dynamics as the size of the metal substrate material is reduced from macroscopic (planar bulk surfaces) to the nanoscale. Future work in surface photochemistry using pump-probe techniques will continue to explore mechanistic aspects of semiconductor photoreactions, including time-resolved studies using a new tunable, ultrafast laser system. New studies in size-selected clusters will focus on mixed metal oxides for which oxide nanoclusters are deposited onto single crystal (e.g., TiO<sub>2</sub>(110)) and thin film metal oxide (e.g., Cu<sub>2</sub>O, MgO) supports to explore cluster-support electronic interactions that can provide a basis for understanding and “tuning” their reactivity.

#### DOE-Sponsored Research Publications (2013–2015)

Influence of Cluster-Support Interactions on Reactivity of Size-Selected Nb<sub>x</sub>O<sub>y</sub> Clusters, M. Nakayama, M. Xue, W. An, P. Liu, and M. G. White, *J. Phys. Chem. C* **119**, 14756-14768 (2015).

Characterization of One-Dimensional Molecular Chains of 4,4'-Biphenyl Diisocyanide on Au(111) by Scanning Tunneling Microscopy, J. Zhou, Y. Li, P. Zahl, P. Sutter, D. J. Stacchiola and M. G. White, *J. Chem. Phys.* **142**, 101901 (2015).

Surface Dipoles and Electron Transfer at the Metal Oxide-Metal Interface: A 2PPE Study of Size-Selected Metal Oxide Clusters Supported on Cu(111), Y. Yang, J. Zhou, M. Nakayama, L. Nie, P. Liu and M. G. White, *J. Phys. Chem. C*, **118**, 13697–13706 (2014).

Photooxidation of Ethanol and 2-Propanol on TiO<sub>2</sub>(110): Evidence for Methyl Radical Ejection, M. D. Kershis and M. G. White, *Phys. Chem. Chem. Phys.* **15**, 17976-17982 (2013).

Exploring Gas-Surface Photoreaction Dynamics using Pixel Imaging Mass Spectrometry (PI<sub>m</sub>MS), M. D. Kershis, D. P. Wilson, M. G. White, J.J. John, A. Nomerotski, M. Brouard, J. Lee, C. Vallance and R. Turchetta, *J. Chem. Phys.* **139**, 084202 (2013).

Dynamics of Acetone Photooxidation on TiO<sub>2</sub>(110): State-resolved Measurements of Methyl Photoproducts, M. D. Kershis, D. P. Wilson and M. G. White, *J. Chem. Phys.*, **138**, 204703 (2013).

Final State Distributions of the Radical Photoproducts from the UV Photooxidation of 2-Butanone on TiO<sub>2</sub>(110), D. P. Wilson, D. P. Sporleder and M. G. White, *J. Phys. Chem. C*, **117**, 9290–9300 (2013).

Photocatalytic Activity of Hydrogen Evolution Over Rh doped SrTiO<sub>3</sub> Prepared by Polymerized Complex Method, P. Shen, J. C. Lofaro, Jr., W. Worner, M. G. White and A. Orlov, *Chem. Eng. J.*, **223**, 200–208 (2013).

## Exceptionally rapid solute radical cation formation following pulse radiolysis

Principal Investigators: Andrew R. Cook and John R. Miller  
 Department of Chemistry, Brookhaven National Laboratory, Upton, NY, 11973 USA  
 acook@bnl.gov, jrmiller@bnl.gov

### Program Scope:

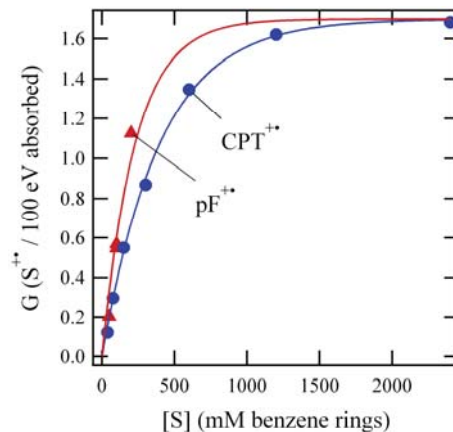
This program applies both photoexcitation and ionization by short pulses of fast electrons to investigate fundamental chemical problems relevant to the production and efficient use of energy and thus obtain unique insights not attainable with other techniques. These studies may play an important role in the development of safer, more effective, and environmentally beneficial processes for the chemical conversion of solar energy. Picosecond pulse radiolysis at the Laser Electron Accelerator Facility (LEAF) is employed to generate and study reactive chemical intermediates or other non-equilibrium states of matter in ways that are complementary to photolysis and electrochemistry and often uniquely accessible by radiolysis. This program also develops new tools for such investigations, applies them to chemical questions, and makes them available to the research community. Advanced experimental capabilities, such as Optical Fiber Single-Shot detection system (OFSS), allow us to work on fascinating systems with 5-10 ps time-resolution that were previously prohibitive for technical reasons.

### Recent Progress:

The radiation chemistry of non-aqueous media is much less understood than that of water, but is an enabling science that makes important contributions to many areas of research in our group. Non-aqueous solvents are often better solvents for dissolving molecules. Low polarity organic solvents allow minimization of energy losses due to electrostatic environment relaxation, which is particularly important for our investigations of charge transport in molecules relevant to OPV, such as conjugated polymers. An emphasis in this poster is placed on solvents where solute radical cations can be made following radiolysis. Important questions include which species can be oxidized in different solvents, and what are the rates and yields?

### “Step” hole capture in chloroform

Contrary to the expectation that solutes are oxidized following pulse radiolysis at normal diffusion controlled rates ( $\sim 10^{10} \text{ M}^{-1}\text{s}^{-1}$ ), in previous work we found unknown and unexpectedly rapid capture of holes in chloroform, observed in OFSS experiments as “Step” increases in absorption within the experimental time resolution of 10~15 ps.<sup>1</sup> While electrons in some molecular liquids have mobilities as large as 100 cm<sup>2</sup>/Vs, this is not true for holes, so it is natural to assume that very fast “step” capture might be exclusive to electrons, which are initially mobile and delocalized after production by ionization and prior to solvation. In contrast, a commonly held expectation is that capture of holes is slow, determined by diffusion of solvent molecular cations. In a solvent like chloroform, with a short-lived radical cation (most live only 1-2 ns), one might expect little oxidation by this initial species, limiting our ability to examine fast chemistry of solute radical cations. Experiments found instead very large yields at 15 ps of holes

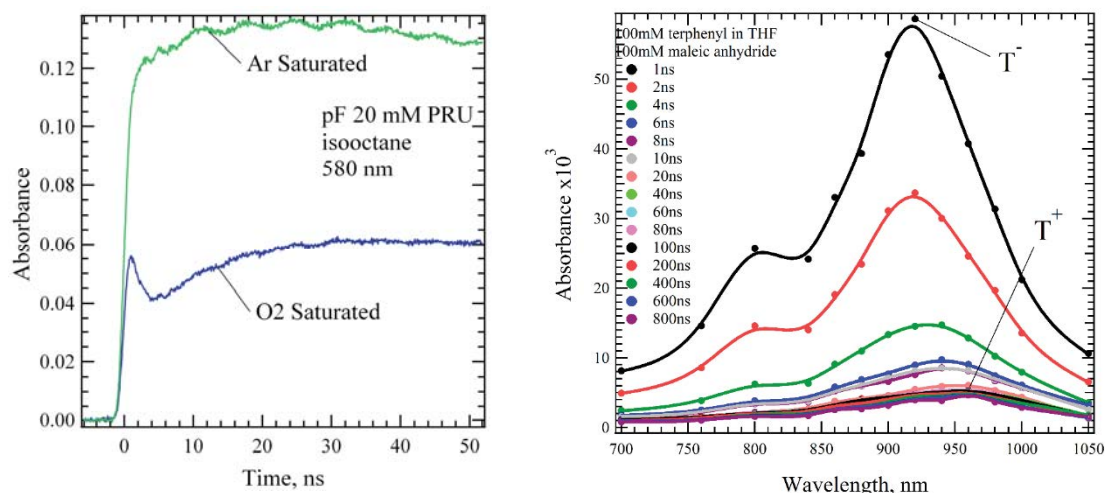


on both polyfluorene (pF) and 4-cyano-4'-n-pentyl-p-terphenyl (CPT), shown in the figure below as a function of the concentration of solute benzene rings. While pF might be oxidized by other radicals formed from fragmentation of the initial solvent radical cation, CPT has a high enough ionization potential to only be oxidized by the initial solvent radical cation. At > 400 mM CPT, the G of  $\sim 1.7/100$  eV absorbed represents capture of nearly all solvent radical cations, a yield that furthermore rivals “Step” capture of electrons in THF we reported in 2011.

This novel fast hole capture may have a large impact on the radiation chemistry of solutes, and provides a new method for studies of solute cations with excellent time resolution. It furthermore is important to understand as it can lead to unexpected chemistry on very fast timescales. The mechanism of capture is not known; it is tempting to draw parallels to that for pre-solvated electrons. Pre-solvated hole capture thus may involve extended hole wavefunctions and possibly coherent hole wavefunction propagation. The fits in the figure use an exponential model analogous to that for pre-solvated electrons:  $f = \exp(-q*[S])$ , where  $f$  is the fraction of holes that survive capture and  $q$  is a quenching coefficient. Values of  $q$  are  $2.5 \text{ M}^{-1}/\text{ring}$  for CPT and  $4.4 \text{ M}^{-1}/\text{ring}$  for pF; these compare favorably to  $q=3.3 \text{ M}^{-1}/\text{ring}$  found for capture of pre-solvated electrons by the pF. The exponential model considers the capture volume in solution, giving a very large distance for 15ps hole capture of 1.5 and 2.3 nm for CPT and pF. These are much larger than typically found for contact distances of reaction, 0.3-0.6 nm. Note that at the highest concentrations of CPT,  $\sim 30\%$  of the radical cations are formed by direct ionization of the solute; this mechanism is linear in solute concentration, and is most important at the highest solute concentrations.

### How general is “Step hole capture ?

An important question is whether this phenomena is unique to chloroform, and if not, to what extent does it occur in other media? Current efforts are aimed at answering these questions, and determining if it can shed light on the mechanism of “Step” hole capture. Initial measures on nanosecond timescales are finding significant amounts of rapidly produced solute radical cations. Two examples are shown below.



The figure on the left shows production of anions and cations of a 20 unit long polyfluorene (pF) in argon saturated isooctane. Addition of oxygen removes pF anions to reveal production of cations by diffusion; extrapolation back to time = 0 shows that at least  $\sim 1/4$  of the ions present at  $< 1$  ns are cations. Due to the high mobility of electrons in isooctane, geminate recombination is far faster than the time resolution of the experiment, so this represents a lower limit for “Step” cation production; OFSS experiments will later make direct measures at 5-10 ps. The figure above

on the right shows radical ion production in THF, with a large concentration of an electron and anion scavenger to reveal Terphenyl radical cations. While the fraction of cations is small, 9.3% of the number of anions, it is actually an astonishing result. THF was shown by Martini, et. al to have a very short radical cation lifetime., 0.5 ps, due to fragmentation to produce a neutral radical and a solvated proton. Because of this, oxidation by solvent radical cations was not previously known or expected in THF. Solute cation production by diffusion is too slow to effectively compete with the 0.5 ps fragmentation. It is likely that “Step” capture is the source of many of the cations above; at this concentration of solute, direct ionization can account for ~1/3 of those observed. Note that like isoctane, the actual number of solute cations produced may be larger due to recombination. A comparison of yields (per 100eV absorbed) of solute cations produced at 0.1-0.4 M solute is given below; the hole lifetime and yield for water were taken from

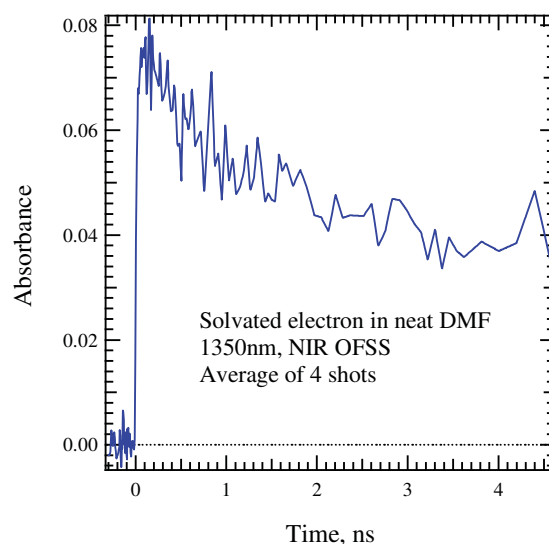
Solvent	Hole lifetime	G(Step)
H <sub>2</sub> O	< 0.04 ps	0
THF	0.5 ps	~0.2
CDCl <sub>3</sub>	1000-2000 ps	1.7

reports from Bradforth’s and Mostafavi’s groups. These data suggest a surprising conclusion: “Step” hole capture is not an exceedingly rapid process, but rather may occur on a few picosecond timescale.

### NIR OFSS experiment development

As noted earlier, the Optical Fiber Single-Shot (OFSS) detection system is a unique tool we developed at BNL for making fast kinetics measurements following pulse radiolysis. This powerful technique provides complete kinetic traces with a time window of ~5ns in a single electron shot, with time resolution of 5-10ps, limited only by the electron pulse width at LEAF. Because it acquires kinetics data in single shots, it is critical to many projects in our group that use samples available in only very small quantities, such as conjugated polymers, as well as those difficult to flow, such as ionic liquids, and solids. The classical delay-line based electron pulse – laser probe technique in such cases is impractical due to accumulated sample degradation. OFSS uses a bundle of optical fibers all cut at different lengths acting as independent and fixed delay lines, the output of which is imaged in the sample and subsequently on signal and reference CCD cameras to read the intensity at each time. CCD cameras limit the useful wavelength range to ~450-950nm.

To enable new work in charge and exciton transport in molecular wires, excess electron solvation in ionic liquids, and other projects, it is necessary to extend the available wavelength range of the experiment. This is currently being developed using InGaAs cameras and custom made NIR achromats, providing the ability to probe kinetics from 950-1650 nm. While implementation is not yet complete, proof of concept experiments have been accomplished. The figure to the right shows data collected at 1350 nm in neat DMF, showing rapid geminate recombination of solvated electrons, using an average of only 4 electron shots, rather than the many thousands that would have been required using the classic delay-line pulse-probe experiment.



**Future Plans:**

**“Step” Cations** Experiments using OFSS will determine yields of solute radical cations produced in 5-10 ps in many media, spanning alkanes, ethers, nitriles, and possibly alcohols. Work will utilize small molecules and conjugated polymers in such media and mixtures, seeking trends to shed light on the mechanism. Measurements in fragmenting solvents will seek correlation between “Step” cation production and initial solvent hole lifetime, a proxy for which will be the computed free energy of fragmentation. A consequence of “Step” capture of holes in certain cases appears to be large amounts of solute excited states produced by rapid recombination. This will be further explored.

A related question is solute cation production in alkanes, where fragmentation has been reported to be as fast as 5-10 ns in solvents such as hexane and isooctane, but our measures show solute radical cation production on longer timescales. Work will explore both “Step” capture of cations in alkanes at 5-10 ps, and seek to determine IP range of solutes that can be oxidized and determine if oxidation is due to the parent radical cation or to a fragment. This approach will be utilized in other solvents as well.

Efforts will be made to observe electrons and holes attached to conjugated polymers in solids – first in dilute matrices and also in neat films. “Step” capture may provide a unique opportunity to make rapid measures of kinetics in these cases.

**NIR OFSS** Implementation of this new technique will be completed, requiring methods to rapidly switch optics between visible and NIR optics. Signal/noise is expected to be increased significantly. This system will then be applied to studies “Step” cations, of charge and exciton transport in conjugated polymers, and excess charge dynamics in ionic liquids (with J. Wishart).

**Publications of DOE sponsored research that have appeared in the last 2 years:**

1. Cook, A. R.; Bird, M. J.; Asaoka, S.; Miller, J. R. "Rapid "Step Capture" of Holes in Chloroform During Pulse Radiolysis" *J. Phys. Chem. A* **2013**, *117*, 7712-7720. doi:10.1021/jp405349u
2. Shkrob, I. A.; Marin, T. W.; Hatcher, J. L.; Cook, A. R.; Szreder, T.; Wishart, J. F. "Radiation Stability of Cations in Ionic Liquids. 2. Improved Radiation Resistance through Charge De localization in 1-Benzylpyridinium" *J. Phys. Chem. B* **2013**, *117*, 14385-14399. doi:10.1021/jp408242b.
3. Zamadar, M.; Cook, A. R.; Lewandowska-Andralojc, A.; Holroyd, R.; Jiang, Y.; Bikalis, J.; Miller, J. R. "Electron Transfer by Excited Benzoquinone Anions: Slow Rates for Two-Electron Transitions" *J. Phys. Chem. A* **2013**, *117*, 8360-8367. doi:10.1021/jp403113u
4. Holroyd, R.; Miller, J. R.; Cook, A. R.; Nishikawa, M. "Pressure Tuning of Electron Attachment to Benzoquinones in Nonpolar Fluids: Continuous Adjustment of Free Energy Changes" *J. Phys. Chem. B* **2014**, *118*, 2164-2171. doi:10.1021/jp412090k
5. Miller, J. R. "Electron Transfer Lower Tunnel Barriers" *Nature Chemistry* **2014**, *6*, 854-855. doi:10.1038/nchem.2059
6. Mani, T.; Grills, D. C.; Miller, J. R. "Vibrational Stark Effects to Identify Ion Pairing and Determine Reduction Potentials in Electrolyte-Free Environments" *J. Am. Chem. Soc.* **2015**, *137*, 1136-1140. doi:10.1021/ja512302c
7. C. A. Zarzana, G.S. Groenewold, B. J. Mincher, S.P. Mezyk, A. Wilden, H. Schmidt, G. Modolo, J.F. Wishart, A.R. Cook "A Comparison of the  $\gamma$ -Radiolysis of TODGA and T(EH)DGA Using UHPLC-ESI-MS Analysis", *Solvent Extraction and Ion Exchange* **2015**, *33*: 431-447.

## Charge and Molecular Dynamics at Heterogeneous Interfaces

Tanja Cuk ([TCuk@lbl.gov](mailto:TCuk@lbl.gov)), Charles Harris ([CBHarris@lbl.gov](mailto:CBHarris@lbl.gov)), and  
David Chandler ([chandler@berkeley.edu](mailto:chandler@berkeley.edu))

Lawrence Berkeley National Laboratory, Chemical Sciences Division, 1 Cyclotron Road,  
Berkeley CA 94720

**I. Program Scope.** One of the greatest challenges in the design of heterogeneous chemical technologies is the limited fundamental understanding of how interfacial properties at solid-liquid and solid-adsorbate interfaces guide the transfer and reorganization of charge. The central research question is to determine how molecules influence charge dynamics at interfaces, and conversely, how these charge dynamics induce molecular changes. Research often targets separately the delocalized charge in the solid and the localized charge in adsorbates or solvated ions. Experimental and theoretical methodologies that target both actors on the same footing are needed to causally link the two sides of the interface. In this program, a range of transient spectroscopic techniques dynamically follow charge transfer from the perspective of charges leaving the solid side, the rise and decay of intermediate molecular species bound from the liquid/adsorbate side, and the purely interfacial electronic states that cannot be thought of distinctly as one or the other. From the theoretical side, molecular dynamics simulations follow the charge reorganizations that accompany this charge transfer and lead to time scales ranging from picoseconds to microseconds.

The *Cuk lab* follows charge transfer and the formation of catalytic intermediates at solid-liquid interfaces through time-resolved spectroscopy coupled to photoactive solid-state devices that control the flow of charge to the interface. An interfacial electric field at the solid-liquid interface separates photo-generated charges that initiate a highly selective and efficient catalytic reaction (here, O<sub>2</sub> evolution or water oxidation). The on-going catalysis allows for the study of sequential reaction steps by surface sensitive transient optical [1], infrared [2], and x-ray spectroscopies that target the dynamics from both sides of the interface. The aim is to deconstruct the steady state product flow into the activation barriers of the different steps of a catalytic reaction.

The *Harris lab* investigates interfacial electronic states between a metal and an adsorbate using two-photon photoemission spectroscopy. Interfacial electrons are measured with time, energy, and momentum resolution to probe charge relaxation, localization, transport, and electronic coupling across the metal adsorbate interface. The systems under study include the NaCl/metal interface to quantify the timescales and energetics of electron trapping at ionic insulator/metal interfaces [3], organic photovoltaic interfaces, and the ionic liquid/metal interface to develop an understanding of ultrafast solvation response relevant to energy applications of ionic liquids [4] and overlap with theoretical studies by David Chandler.

The *Chandler lab* elucidates the dynamics of water and other liquids at solid-liquid interfaces. They use coarse grained models to treat universal features and molecular dynamics simulations with force fields developed by electronic structure calculations to treat atomistic details. Broad ranges of scales in space and time present the principal challenges to this work, challenges that are met with the development of new theoretical perspectives and numerical algorithms. Illustrations include water structure and dynamics at Pt surfaces [5] which exhibit a high degree of dynamic heterogeneity, and ionic melts at electrode surfaces [6] which exhibit order-disorder transitions and super-capacitance.

## **II. Recent Progress and Future Work.**

### A. Catalytic Dynamics by Transient Spectroscopy

While the water oxidation cycle involves the critical step of O–O bond formation, the transition metal oxide radical thought to be the catalytic intermediate required for O–O bond formation has eluded direct observation. We have recently shown [2] that utilizing *in-situ* infrared spectroscopy of an n-SrTiO<sub>3</sub>/aqueous interface and theory (in collaboration with David Prendergast at the Molecular Foundry), a new motion of the oxygen right below the oxyl radical (Ti–O<sup>•</sup>) that reports on it. As shown previously [1], we operate in a range of high photon-to-O<sub>2</sub> quantum efficiency while exciting the photo-catalysis with 266 nm, 500 Hz, 150 fs laser pulses (90% for the 0.1% Nb doped samples, Extended Data Fig. 1), such that almost all the photo-generated holes are expected to evolve into O<sub>2</sub>.

The experiments and associated theory are the first to detect molecularly a catalytic intermediate at its formation at the solid-liquid interface. In doing so, they not only uncover the oxyl radical, but reveal a new way to track a catalytic cycle in this setting. A localized sub-surface vibration of the oxygen directly beneath the oxyl radical uniquely reports on the catalytic intermediate. The integrity of the motion and its appearance with catalytic intermediates at the interface identify sub-surface vibrations to be a molecular probe of catalytic dynamics. Furthermore, the interfacial nature of the vibration couples the catalytic intermediate to the local environment of the solid-liquid interface. Both the electron plasma density in the solid and the librational motion in the electrolyte couple to the sub-surface vibration. Three handles, then, for tracking the catalytic cycle at a solid-liquid interface are demonstrated for the first time: the sub-surface vibration itself, its coupling to electron dynamics, and its coupling to solvation dynamics. Most importantly, by revealing a vibrational motion unique to the intermediate and how that motion couples to solvation dynamics—both thought to determine how catalytic intermediates evolve from one to the next intermediate (here, expected to be O–O by either nucleophilic attack of H<sub>2</sub>O or two neighboring oxyls combining)—the work opens the door to understanding and manipulating a catalytic cycle dynamically.

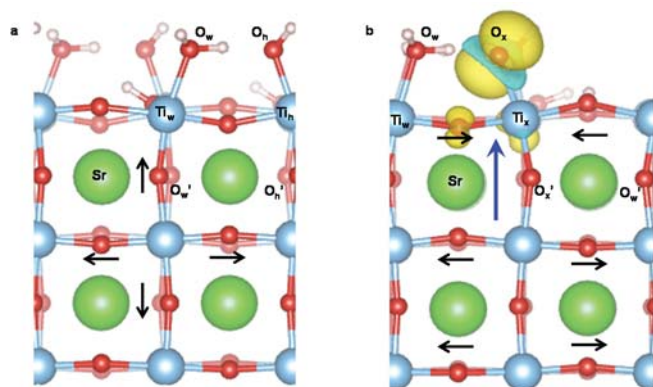


**Figure 1: n-SrTiO<sub>3</sub> before (a) and after excitation (b)**

A cartoon of the sub-surface vibration observed is shown in Fig. 1 by comparing before (Fig. 1a) to after photo-excitation (Fig. 1b). Producing the radical causes a bulk breathing mode to combine with other dark and infrared active modes of the initial configuration to create a new surface mode at roughly the same energy as the bulk breathing mode. The new mode is infrared active due to a large amplitude, Ti–O stretch motion of the O in the SrO layer right below the Ti–O<sup>•</sup> site. Fano lineshapes modified by n-doping and electrolyte conditions show

how the mode weakly couple to the predominant motions within the bulk solid (plasmonic, electronic) and electrolyte (librational) in the same spectral region. The bright mode occurs in a wide range of surface conditions (air vs. electrolyte, pH 2 – 14, % methanol, deuterated electrolyte, and varying holes/cm<sup>2</sup>), which means that while it couples to its environment, the essential motion is robust to surface protonation, solvation environments, number of photo-excited sites, and detailed surface re-structuring.

Future work will involve probing in the infrared at longer time scales, to track the catalytic cycle through O-O bond formation. Ideally, a tunable repetition rate laser will initiate multiple pulses of oxyl radicals to prime the system for O-O bond formation, and to track how the activation barrier for O-O bond formation changes as a function of the number of oxyl radicals at a given time. In a further collaboration with David Prendergast, we are investigating the x-ray signatures of the oxyl radical that we would like to probe in transient x-ray experiments, in collaboration with Musa Ahmed and Hendrik Bluhm.

**B. Ultrafast Excited State Electron Dynamics at Interfaces** One common class of materials our group studies is the organic semiconductor / metal interface whose interfacial electronic structure and electron transport is important to many molecular devices such as organic light emitting diodes. Combining TPPE with a simple Kronig Penney model, we measured the corrugation in the surface potential and resulting band gap opening arising from a periodic phthalocyanine organic lattice on Ag(111) [7]. In a similar system, results from TPPE and DFT calculations identified the hybridization between a metallic state of Ag(111) with the unoccupied molecular orbitals of phthalocyanine [8].

The Harris group has also recently studied ultrathin layers of insulating material, such as alkali halides, on a metal substrates. These systems are important to the emerging fields of micro and nanoelectronic devices that employ the thin insulating material to decouple the molecular properties from the metal electrode. TPPE was used to study the excited state dynamics of ultrathin layers of NaCl on Ag(100), where we observed the first image potential state series for a highly ionic material. These initially delocalized electrons were subsequently found to localize due to trapping at low coordinated defect sites on the NaCl [9]. A recent follow up study on the same system identified an additional deep trap state that emerges at low sample temperatures. This is the first identification of electron localization through multiple metastable trap states at interfaces, and is proposed to correspond to the formation of a small polaron assisted by defect intermediates. These results are currently in preparation for submission. Future studies will seek to identify small polaron formation in a class of alkali halides, and observe the impact of cation identity to the magnitude of self-trapping energy and lifetime stabilization associated with small polaron formation. Additionally, the group will seek to take advantage of NaCl decoupling ability widely exploited in STM experiments to study the decoupled molecular excited states of molecules adsorbed onto the NaCl thin film. These studies will have an impact on the understanding of the fundamental photophysics of nanoelectronic devices.

### **C. Molecular dynamics at solid interfaces**

Chemistry in heterogeneous environments can be dominated by molecular dynamics at the interfaces between liquid and solid matter. Characteristic time scales for this dynamics extend from sub picoseconds to microseconds and beyond. This wide range of scales, the result of complex dynamics of many correlated degrees of freedom, presents challenges to theory. The Chandler group's research overcomes these challenges with novel modeling and sampling techniques.

The Chandler Group's recent work elucidated dynamics of water at metal surfaces, specifically surfaces of Pt [12, 5]. The metal atoms strongly bind oxygen atoms of water molecules, forcing water to adopt geometrical patterns dictated by the geometry of the metal surface. This geometry differs from favorable hydrogen bonding geometries. The intermolecular structure of water molecules attached to the surface is therefore frustrated, resulting in significant dynamic heterogeneity.

In related work, the Chandler Group has also detailed fluctuations of a model of a room-temperature ionic liquid that exhibits super-capacitance due to order-disorder transitions at the electrode-liquid interface [13, 6]. These transitions are surprising in that they manifest large-length scale structure and correlations in the plane parallel to the electrode. Traditional electrochemical modeling neglects such heterogeneity. Future work aims to understand water at other metal surfaces employing improved force fields.

### Recent Publications

1. Waegele, M.M., Chen, X, Herlihy, D.M., and Cuk, T., "How Surface Potential Determines the Kinetics of the First Hole Transfer of Photocatalytic Water Oxidation". *J. Am. Chem. Soc.*, **2014**, 136, 10632-10639.
2. Herlihy, D. M., Waegele, M.M., Chen, X., Permmaju, S., Prengergast, D., and Cuk, T. "Uncovering the Oxyl Radical of Photocatalytic Water Oxidation by its Sub-Surface Vibration", *Science*, Submitted, **2015**.
3. Suich, D. E., Caplins, B. W., Shearer, A. J., Harris, C. B., "Femtosecond Trapping of Free Electrons in Ultrathin Films of NaCl on Ag(100)" *J. Phys. Chem. Lett.*, **2014**, 5, 3073–3077.
4. Muller, E. A., Strader, M. L., Johns, J. E., Yang, A., Caplins, B. W., Shearer, A. J., Suich, D. E., Harris, C. B., "Femtosecond Electron Solvation at the Ionic Liquid/Metal Electrode Interface" *J. Am. Chem. Soc.*, **2013**, 135, 10646-10653.
5. Limmer, D. T., A. P. Willard, P. A. Madden and D. Chandler, "Hydration of metal surfaces can be dynamically heterogeneous and hydrophobic," *Proc. Natl. Acad. Sci. USA* **2013**, 110, 4200-4205.
6. Merlet, C., D. T. Limmer, M. Salanne, R. Van Roij, P. A. Madden, D. Chandler and B. Rotenberg, "The electric double layer has a life of its own," *J. Phys. Chem. C* **2014**, 118, 18291-18298. [Issue cover and commentary by Kornyshev and Qiao devoted to this work.]
7. Caplins, B. W., Shearer, A. J., Suich, D. E., Muller, E. A., Harris, C. B., "Measuring the Electronic Corrugation at the Metal/Organic Interface" *Phys. Rev. B.*, **2014**, 89, 155422.
8. Caplins, B. W., Suich, D. E., Shearer, A. J., Muller, E. A., Harris, C. B., "Metal/Phthalocyanine Hybrid Interface States on Ag(111)" *J. Phys. Chem. Lett.*, **2014**, 5, 1679-1684.
9. Shearer, A. J., Johns, J. E., Caplins, B. W., Suich, D. E., Harris, C. B., "Electron Dynamics of the Buffer Layer and Bilayer Graphene on SiC" *Appl. Phys. Lett.*, **2014**, 104, 231604.
10. Caplins, B.W., Suich, D.E., Shearer, A.J., Harris, C.B., "Quantum Beats at the Metal/Organic Interface" *J. Electron Spectrosc. Relat. Phenom.*, **2015**, 198, 20-25.
11. Caplins, B. W., "Electronic Structure of the Metal/Phthalocyanine Interface Probed by Two-Photon Photoemission" LBNL Thesis, **2014**.
12. Willard, A. P., D. T. Limmer, P. A. Madden and D. Chandler, "Characterizing heterogeneous dynamics at hydrated electrode surfaces," *J. Chem. Phys.* **2013**, 138, 184702.
13. Limmer, D.T., C. Merlet, M. Salanne, D. Chandler, P.A. Madden, R. van Roij, B. Rotenberg, "Charge fluctuations in nano-scale capacitors," *Phys. Rev. Lett.* **2013**, 111, 106102.1-5.
14. Waegele, M.M., Doan, H., and Cuk, T., "Long-lived photoexcited carrier dynamics of d-d excitations in spinel ordered Co<sub>3</sub>O<sub>4</sub>," *J. Phys. Chem. C*, **2014**, 118, 3426.

## Stability of Nano Fluids, Solvent-Exchange Mechanism and Nuclear Quantum Effects. Recent Progress and Future Plans

Liem X. Dang  
Physical Sciences Division  
Pacific Northwest National Laboratory  
Richland, WA 93352  
[liem.dang@pnl.gov](mailto:liem.dang@pnl.gov)

### Background and Significance

Nanofluids are gaining considerable attention because of their potential application in power generation from renewable energy sources such as geothermal, solar, industrial waste heat, and biomass combustion. Nanofluids are liquids that contain a low concentration of nanometer-sized particles. Conventional fluids have poor thermal conductivity compared to solids; the thermal conductivity can be enhanced by dispersing the solid particles in fluids. This fundamental concept has been a topic of interest for a long time. Early studies were confined to only millimeter or micrometer-sized particles. The stability of the suspension is the major challenge of this approach, as large particles tend to settle rapidly. The use of nanoparticles shows promise as a solution to this problem.

The study of thermodynamic and kinetic properties of ions in aqueous and non aqueous solution using statistical mechanics or computer simulation techniques has provided molecular-level details that have advanced our understanding of the chemistry and physics of solvation. Minor differences in ion properties could cause major changes in their role in biological processes. So far, many of the related ion-solvation research studies have focused on the thermodynamics of ion solvation and the hydration structure. The reactivity of ions in solutions requires rearrangement of the hydration shell, which involves the replacement of the solvent molecule from first hydration shell. This process, also known as a solvent-exchange reaction, is believed to be associated with activation volume ( $\Delta V^\ddagger$ ), which is the key indicator of the solvent-exchange mechanism. For example, the exchange process is an associative mechanism when the activation volume is negative and a dissociative mechanism when the activation volume is positive.

Nuclear quantum effects, such as zero-point energy and tunneling, have been shown to affect the structural and dynamical properties of aqueous systems, and a natural question is to what extent this is also true for rate theory results such as the exchange rate between water and an aqueous ion. We performed ring-polymer molecular dynamics (RPMD) simulations to systematically study nuclear quantum effects on the water-exchange rates around water and aqueous chloride, bromide, and iodide ions. These effects were quantified by using the transition state theory (TST), Grote-Hynes (GH) theory, and the reactive flux (RF) method. Our results reveal that tunneling and zero-point energy effects lead to sensible increments in giving rise to larger transmission coefficients in quantum simulations. For the cases of aqueous chloride and bromide, because of their strong interaction with water, the computed quantum transmission coefficients and the residence times are nearly 20% larger than the corresponding classical results, whereas anions such as iodide, exhibit a quantum effect of around 10%. These results are consistent with experimental investigations of anion-bound water vibrational and reorientational motion.

### 1. Nanofluid Stability in Water and Hydrofluorocarbon

Our current research efforts focus on chemical functionalization of the nanoparticle surface to attain stable nanofluid suspensions. A molecular-level understanding of the nanoparticle solvation process and factors influencing dispersion stability is necessary to develop stable and better-performing nanofluids. Computational techniques such as MD simulations can provide more molecular-level insight in to the interfacial behavior of a base fluid with a metal-organic framework (MOF) surface. We studied dispersion stabilities in water and in 1,1,1,3,3-pentafluoropropane (R-245fa), which is a hydrofluorocarbon with a broad range of applications as a blowing agent, solvent, aerosol, and working fluid. First, we focused on the solvent structure around the MOF fragments. We show the radial distribution function RDF plots between chromium atoms of MOF fragment and the carbon atoms on the R-245fa in Figure 1a. We observe that the Cr-C2 RDF has a high intense in the first peak because the fluorine atoms on

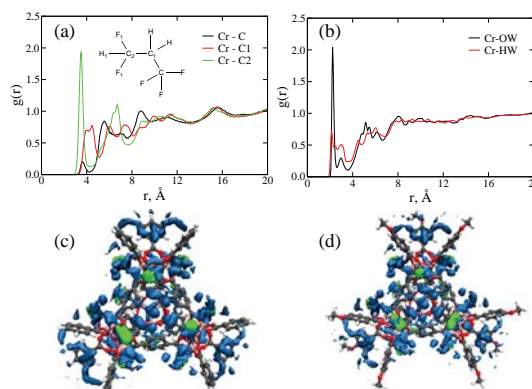


Figure 1. RDFs between chromium atoms of the MOF fragment and the carbon atoms on the R-245fa.

the C2 carbon atom are more partially negative. In Figure 1b, we show the RDF plots between the chromium atoms and water. The first peak of the Cr-OW RDF occurs at 2.24 Å, and is more intense compared to the Cr-HW RDF because of the strong electrostatic interactions between the Cr atoms of MOF and the oxygen in water. Also in Figures 1c and 1d, we show the spatial distribution plots for water and R-245fa around the two types of MOF fragments. These plots clearly show a high water density around the MOF fragment, which clearly indicates that water has a stronger interaction with the MOF fragment than R-245fa. Also, the higher water density in the tetrahedral cavities can be clearly seen; this is because the smaller water molecule can easily penetrate in to the tetrahedral cavity. The significant distribution of R-245fa is found only near the chromium sites of the MOF. R-245fa is mostly composed of fluorine atoms, which are partially negative, and hence has favorable interactions only with the positive Cr sites.

In Figure 2a, we show the computed potential of mean force (PMF) between two MOF fragments with benzoate as modulator in water and R-245fa. Both the PMFs have multiple minima, which indicates that the MOF fragments have solvent-mediated interactions. This behavior is analogous to contact pairs and solvent-separated pairs observed in aqueous salt solutions. The first minimum is at ~22 Å for R-245fa and at ~21.5 Å for water. The first peak in the PMF plot, also called the barrier, is at ~24.5 Å for R-245fa and ~23.5 Å for water. This peak is considered as a transition state for the separation of the two MOF fragments; therefore, the higher the barrier height, the greater the amount of energy needed to separate the MOF fragments. The barrier height is 4.8 kcal/mol for R-245fa and 0.9 kcal/mol for water. These values clearly indicate that MOF fragments have strong attractive interactions in R-245fa compared to water. In other words, these MOF fragments are more dispersible in water compared to R-245fa. The degree to which MOF particles disperse depends on MOF-MOF, MOF-solvent, and solvent-solvent interactions. As evident from Figure 1, the strong interaction between water and MOF particles leads to effective screening of the attractive forces between the MOF fragments. This could be the reason for the better dispersibility of MOF fragments in water.

Figure 2b contains the PMF plots for MOF fragments with 4-methoxybenzoate as the modulator. The first minimum in water is at ~21 Å and in R-245fa at 22 Å. Both the PMFs in this case have fewer wiggles compared to the previous case for benzoate-containing fragments. The barrier is at 26 Å for R-245fa and at 25 Å for water. Similar to the previous case, the barrier for R-245fa is slightly right shifted. The barrier heights are 2.6 kcal/mol for R-245fa and 1.3 kcal/mol for water. Also similar to the previous case, the barrier height for the separation for MOF fragments in R-245fa is greater than that in water. Therefore, even with the methoxy-substituted modulator, the MOF particles tend to disperse better in water than in R-245fa. These results compare well with results obtained from ongoing experiments in our laboratory as illustrated in Figure 2c and 2d. It can be seen in Figure 2c that the nano-MOF particles disperse in water and form a stable suspension, whereas in Figure 2d; the nano-MOF particles precipitate in R-245fa.

## 2. Water-exchange dynamics around $\text{H}_3\text{O}^+$ and $\text{OH}^-$ ions

In this report, we summarize our recent studies of the dynamics of the ion-solvation process. We used the rate theory approach to determine the solvent-exchange rates. Mechanistic properties associated with the water-exchange process, such as PMF, time-dependent transmission coefficients, and the corresponding rate constants, were examined using TST, the RF method, GH theory, and the Impey-Madden-McDonald method. We performed a systematic study using four systems: 1) hydronium ( $\text{H}_3\text{O}^+$ ) and 2) hydroxide ( $\text{OH}^-$ ). In future research, we will focus on understanding the influence of nuclear quantum mechanical effects on the kinetics properties of ions in aqueous solution. Also, because of their ability to respond to the local, nonhomogeneous environment, we are interested in expanding our current methodology to studies of ion-solvation processes at interfaces; we expect a different behavior for these processes.

In Figure 3a, we present PMFs for an  $\text{H}_3\text{O}^+$ - $\text{H}_2\text{O}$  ( $\text{OH}^-$ - $\text{H}_2\text{O}$ ) pair in aqueous solution. The computed PMFs have three distinct features corresponding to three different states of the systems.

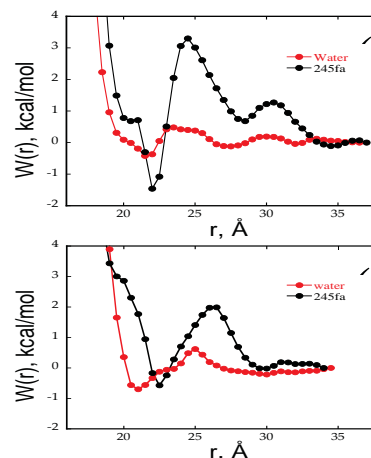


Figure 2. (a) Computed PMF for a pair of MOF fragments in water and R-245fa. (b) Computed PMF for a pair of MOF fragments in water and R-245fa.

The first minimum represents the contact-ion-water-pair (CIWP) state, the barrier top at  $r = r^\ddagger$  represents the transition state, and the third feature is the solvent-separated-ion-water-pair (SSIWP) state. In the CIWP state, the ion and the water are held in close contact by the electrostatic forces; whereas, in the SSIWP state, the solvent screens these forces. Two differences are observed in the PMFs for the  $\text{H}_3\text{O}^+$ -water and  $\text{OH}^-$ -water systems. First, the barrier height is larger for the  $\text{H}_3\text{O}^+$ -water system than for the  $\text{OH}^-$ -water system, and second, the separation corresponding to the transition state for the  $\text{OH}^-$ -water system is larger than that for the  $\text{H}_3\text{O}^+$ -water system. We find these differences quantitatively and conclude that  $\text{H}_3\text{O}^+$ - $\text{H}_2\text{O}$  binding is stronger than  $\text{OH}^-$ - $\text{H}_2\text{O}$  binding. We also find that the coordination number for the  $\text{H}_3\text{O}^+$ -water system (i.e., the number of water molecules that bind to  $\text{H}_3\text{O}^+$  on the average in the CIWP state) is 3, which is consistent with the previously found  $\text{H}_3\text{O}^+(\text{H}_2\text{O})_3$  structure. The Zundel structure<sup>8</sup> ( $\text{H}_2\text{O}\dots\text{H}\dots\text{H}_2\text{O}$ ) is not observed as our model does account for proton transfer. The coordination number for the  $\text{OH}^-$ -water system is 5, which is overestimated in comparison with the previous studies ( $\text{OH}^-(\text{H}_2\text{O})_4$  and  $\text{OH}^-(\text{H}_2\text{O})_3$ ).

The transition rate between the CIWP and SSIWP states (i.e., the water-exchange rate between the first and the second solvation shell around an ion) can be expressed using TST. As expected,  $\tau_{\text{Ist}} = 1/k_{\text{Ist}}$  is smaller for the  $\text{OH}^-$ -water system (i.e., in comparison with  $\text{H}_3\text{O}^+$ , water exchange is faster around  $\text{OH}^-$  because of the smaller barrier height). The shortcoming of TST is that it overestimates the water-exchange rate ( $k_{\text{Ist}}$ ) because of the assumption that, once the ion-water system reaches the barrier top of its PMF from the CIWP state, it goes immediately to the SSIWP state. However, it is likely that barrier recrossing can occur. The probability of actually getting to the SSIWP state is the transmission coefficient  $\kappa$ , and therefore, actual water-exchange rate is  $k = \kappa k_{\text{Ist}}$ .

We use the GH and RF theories to determine the transmission coefficient. In Figure 3b, we show the friction kernel  $\zeta(t)$  calculated for  $\text{H}_3\text{O}^+$  and  $\text{OH}^-$ . The friction  $\zeta(t)$  has two distinguishable components for both the  $\text{H}_3\text{O}^+$ -water and  $\text{OH}^-$ -water systems: 1) a rapid initial drop around 50 to 60 fs and 2) a slow decay on the picosecond time scale. However, it is clear that the  $\text{H}_3\text{O}^+$ -water system experiences larger friction than the  $\text{OH}^-$ -water system. We also found that the barrier frequency for the  $\text{H}_3\text{O}^+$ -water system ( $39 \text{ ps}^{-1}$ ) is larger than that for the  $\text{OH}^-$ -water system ( $21 \text{ ps}^{-1}$ ). The transmission coefficients are  $2.0 \times 10^{-3}$  and  $3.0 \times 10^{-2}$ , respectively, for the  $\text{H}_3\text{O}^+$ -water and  $\text{OH}^-$ -water systems. These values are too low, which means that the CIWP state is extremely stable and transition to the SSIWP state rarely occurs. The term  $\tau_{\text{GH}}$  is water-exchange time scale obtained using GH theory, which is sub-nanosecond for the  $\text{H}_3\text{O}^+$ -water system and an order of magnitude smaller for the  $\text{OH}^-$ -water system. The RF method is very useful for extracting the exact value of transmission coefficient from MD trajectories. From the 10-ns MD trajectory in the NVT ensembles of the  $\text{H}_3\text{O}^+$ -water and  $\text{OH}^-$ -water systems constrained at the transition state, 2500 conformations are collected to perform RF calculations. Using these conformations as the starting ones and releasing the constraint, MD simulations at the NVE ensemble are performed in both backward and forward directions for 2 ps. The value of  $\kappa_{\text{RF}}(t)$  reaches a plateau after a long time as shown in Figure 3c. Averaging over the last 0.5 ps of  $\kappa_{\text{RF}}(t)$  leads to the actual value for the transmission coefficient:  $1.5 \times 10^{-2}$  for the  $\text{H}_3\text{O}^+$ -water system and  $2.4 \times 10^{-2}$  for the  $\text{OH}^-$ -water system. Again, the transmission coefficients are very small, resulting in slow water-exchange time scales. Again, water exchange occurs faster around  $\text{OH}^-$  than around  $\text{H}_3\text{O}^+$ .

For the Impey-Madden-McDonald method, we perform MD simulations of the  $\text{H}_3\text{O}^+$ -water and  $\text{OH}^-$ -water systems for 5 ns in NVT ensemble, saving snapshots every 100 fs. A normalized time correlation function ( $C_p(t;t^*)$ ) for the population of water molecules in the first solvation shell of  $\text{H}_3\text{O}^+$  ( $\text{OH}^-$ ) is calculated from the MD trajectory.  $C_p(t;t^*)$ , as depicted in Figure 3d, clearly distinguishes the  $\text{H}_3\text{O}^+$ -water system from the  $\text{OH}^-$ -water system;  $C_p(t;t^*)$  decays faster for the  $\text{OH}^-$ -water system. It turns out that  $\tau_p$  is one order of magnitude smaller for the  $\text{OH}^-$ -water systems than for the  $\text{H}_3\text{O}^+$ -water system, which similar to the results from using the GH theory.

### 3. Nuclear Quantum Effects in Water Exchange around Lithium and Fluoride Ions

In Figures 4a and 4b, we compare the potentials of mean force for escape of water from the first solvation shell, obtained from classical and quantum simulations of both ions. The barrier heights to exchange of water around  $\text{Li}^+$  in our quantum and classical simulations are 3.8 and 4.0 kcal/mol, respectively, which are within the range of 3.0 to 4.5 given in the literature. For  $\text{F}^-$ , the corresponding barriers are 1.9 and 2.0 kcal/mol. The heights of both barriers are very slightly smaller in the quantum PMFs by 0.2 kcal/mol for  $\text{Li}^+$  and by 0.1 for  $\text{F}^-$ .

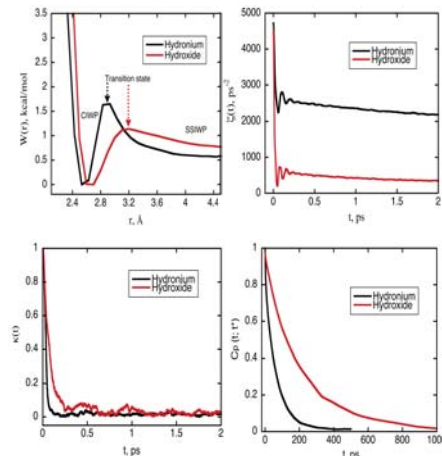


Figure 3. Computed PMFs for the  $\text{H}_3\text{O}^+$ - $\text{H}_2\text{O}$  and  $\text{OH}^-$ - $\text{H}_2\text{O}$  interactions in water as the solvent (3) Same as (3a) for  $\zeta(t)$  (3b) Same as (3a) for  $\kappa(t)$  (3c) Same as (3a) for  $C_p(t;t^*)$  (3d).

This decrease in barrier height for  $F^-$  is less than half the decrease due to nuclear quantum effects than found in the calculations with a rigid-body water model (0.2 kcal/mol), and we shall attribute this below to the absence of competing quantum effects in these rigid-body simulations. The transmission coefficients  $\kappa(t)$  obtained from our classical MD and RPMD simulations are shown in Figure 4c and 4d. In all cases, the plateau value  $\kappa$  is quite small. This implies significant recrossing of the transition state dividing surface, indicating that the ion-water distance  $r$  is not the optimum reaction coordinate for these water-exchange reactions. It is likely that a better coordinate would be a collective function of the positions of all the water molecules involved in hydration, whose rearrangement is necessary for a molecule to leave the first shell. According to our RPMD calculations, the molecular rate transfer of water in the first hydration shell of  $Li^+$  is 136 ps, and in the first shell of  $F^-$ , 20 ps. There are no experimental results with which we can directly compare these values, but neutron scattering experiments suggest that  $\tau \lesssim 100$  ps for both ions. For  $F^-$ , our results are comfortably within this bound, while for  $Li^+$ , the imprecision in the experimental result makes our value reasonable. The molecular rate transfers of  $Li^+$  from earlier computational studies span two orders of magnitude, with values from 25 to 400 ps reported, while those of  $F^-$  are in the 17 to 25 ps range.

#### 4. Conclusions and Outlook

We present a summary of our recent studies of the dynamics of the ion-solvation process. We used the rate theory approach to determine the solvent-exchange rates. Also, analogous to experimental procedures, we computed pressure-dependent rates to determine the activation volume, which is a key indicator for the solvent-exchange mechanism. From our results, we notice that, because of the decrease in barrier heights, TST rate constants increase as pressure increases for all the cases. Therefore, TST results give a negative activation volume, which is indicative of an associative mechanism. We also computed pressure-dependent rate constants using the RF method, which takes in to account recrossing induced by solvent dynamics. We are interested in expanding our current study/method into studies of ion solvation at interfaces. Our future research efforts will focus on understanding the influence of nuclear quantum mechanical effects on the properties of ions in aqueous solution such as the water-exchange rate and the corresponding transmission coefficients using ring-polymer MD techniques.

#### References to publications of DOE sponsored research (2014-Present)

1. Water Exchange Rates and Molecular Mechanism around Aqueous Halide Ions. Annapureddy, H. V. R. and Liem X. Dang. *J. Phys. Chem. B*, 118, 7886 (2014).
2. Understanding the Rates and Molecular Mechanism of Water-Exchange around Aqueous Ions Using Molecular Simulations. Annapureddy, H. V. R. and Liem X. Dang. *J. Phys. Chem. B*, 118, 8917 (2014).
3. Computational Studies of Water-Exchange Rates around Aqueous  $Mg^{2+}$  and  $Be^{2+}$ . Liem X. Dang, *J. Phys. Chem. C*, 118, 29028 (2014).
4. Fluorocarbon Adsorption in Hierarchical Porous Frameworks. Motkuri RK, HVR Annapureddy, M Vijaykumar, HT Schaefer, PF Martin, BP McGrail, Liem X. Dang, R Krishna, and PK Thallapally. *Nature Communications*, 5:4368. DOI: 10.1038/ncomms5368. (2014).
5. Computational Studies of [Bmim][PF<sub>6</sub>]/n-Alcohol Interfaces with Many-Body Potentials. Chang, Tsun-Mei and Liem X. Dang, *J. Phys. Chem. A*, 118, 7186 (2014).
6. Computational Study on the Stability of Nanofluids Containing Metal Organic Frameworks. Harsha V. R. Annapureddy, Satish K. Nune, Radha Kishan Motkuri, Peter B. McGrail and Liem X. Dang. *J. Phys. Chem. B*, 119, 8992 (2015).
7. Nuclear Quantum Effects in Water Exchange around Lithium and Fluoride Ions. David M. Wilkins, David E. Manolopoulos, and Liem X. Dang. *J. Chem. Phys.* 142, 064509 (2015).
8. Water Exchange Dynamics around  $H_3O^+$  and  $OH^-$  Ions. Santanu Roy, Liem X. Dang, *Chemical Physics Letters* 628, 30 (2015).
9. Computer Simulation of Methanol Exchange Dynamics around Cations and Anions. Santanu Roy, Liem X. Dang. *J. Phys. Chem. B*, DOI: 10.1021/acs.jpcc.5b04174. (2015).
10. Computational Study of Molecular Structure and Self-Association of Tri-n-butyl Phosphates in n-Dodecane. Quynh N. Vo, Liem X. Dang, M. Nilsson, Hung D. Nguyen, *J. Phys. Chem. B*, 119, 1588 (2015).

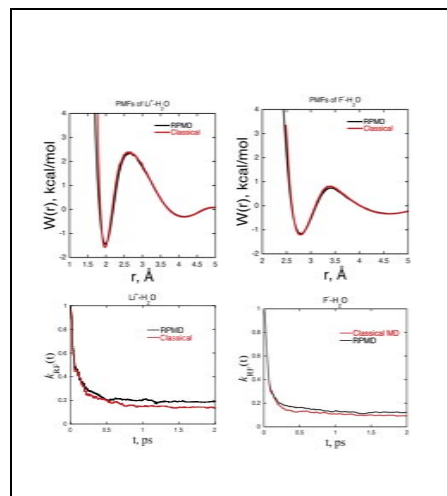


Figure 4. PMFs for escape of water from the first solvation shells of  $Li^+$  (4a) and  $F^-$  (4b) from MD simulations at 298K. Transmission coefficients for the water-exchange reactions around  $Li^+$  (4c) and  $F^-$  (4d).

## Transition Metal-Molecular Interactions Studied with Cluster Ion Infrared Spectroscopy

DE-FG02-96ER14658

Michael A. Duncan

Department of Chemistry, University of Georgia, Athens, GA 30602

maduncan@uga.edu

### **Program Scope**

Our research program investigates gas phase metal clusters and metal cation-molecular complexes as models for heterogeneous catalysis, metal-ligand bonding and metal ion solvation. The clusters studied are molecular sized aggregates of metal or metal oxides. We focus on metal-ligand interactions with species such as benzene or carbon monoxide, and on solvation interactions exemplified by complexes with water, acetonitrile, etc. These studies investigate the nature of the metal-molecular interactions and how they vary with metal composition and cluster size. To obtain size-specific information, we focus on ionized complexes that can be mass selected. Infrared photodissociation spectroscopy is employed to measure the vibrational spectroscopy of these ionized complexes. The vibrational frequencies measured are compared to those for the corresponding free molecular ligands and with the predictions of theory to elucidate the electronic state and geometric structure of the system. Experimental measurements are supplemented with calculations using density functional theory (DFT) with standard functionals such as B3LYP. In new experiments photofragment imaging is employed as a way to probe metal-molecular bond energies.

### **Recent Progress**

The main focus of our recent work has been infrared spectroscopy of transition metal cation-molecular complexes with water, acetylene and benzene. These species are produced by laser vaporization in a pulsed-nozzle cluster source, size-selected with a specially designed reflectron time-of-flight mass spectrometer and studied with infrared photodissociation spectroscopy using an IR optical parametric oscillator laser system (OPO). In studies on complexes of a variety of transition metals, we examine the shift in the frequency for selected vibrational modes in the adsorbate/ligand/solvent molecule that occur upon binding to the metal. The number and frequencies of IR-active modes reveal the structures of these systems, while sudden changes in spectra or dissociation yields reveal the coordination number for the metal ion. In some systems, new bands are found at a certain complex size corresponding to intra-cluster reaction products. In small complexes with strong bonding, we use the method of rare gas "tagging" with argon or neon to enhance dissociation yields. In all of these systems, we employ a close interaction with theory to investigate the details of the metal-molecular interactions that best explain the spectroscopy. We perform density functional theory (DFT) calculations (using Gaussian 09 or GAMESS) and when higher level methods are required, we collaborate with theorists. Our infrared data on these metal ion-molecule complexes provide many examples of unanticipated structural and dynamical information. A crucial aspect of these studies is the infrared laser system, which is an infrared optical parametric oscillator/amplifier system (OPO/OPA; Laser Vision). This system covers the

infrared region of 600–4500  $\text{cm}^{-1}$  with a linewidth of  $\sim 1.0 \text{ cm}^{-1}$ . In new work, we have added a photofragment imaging instrument to our existing molecular beam machine for the study of the dissociation dynamics of mass-selected metal-molecular ions. This new methodology makes it possible to investigate metal-ligand vibrations at lower frequencies and to determine bond energies for hard-to-study cation-molecular complexes.

Transition metal ion-water complexes probe the details of ion solvation. We examine complexes containing a single water molecule, as well as those containing multiple molecules, thus investigating the stepwise solvation process. Recent studies focused on titanium-, and niobium-water systems. Rotationally resolved spectra were obtained for  $\text{Ti}^+(\text{H}_2\text{O})$  and  $\text{Nb}^+(\text{H}_2\text{O})$ , but the spectra obtained did not agree with the predictions of DFT for these complexes. Theory indicates planar  $\text{C}_{2v}$  structures, consistent with expectations for charge-dipole bonding. When a mono-water complex has this structure, its infrared spectrum contains partially resolved rotational structure, as seen previously for the scandium cation-water complex (Figure 1, left). The titanium cation-water complex has a similar spectrum, but the bands are doubled, presumably from spin-orbit interaction (not shown). However, the niobium cation-water complex, which is computed to have the same  $\text{C}_{2v}$  structure, has a very different rotational pattern, seeming to indicate a non-planar structure (Figure 1, right). To improve the computational work on this system, we initiated a collaboration with Sotiris Xantheas and Evangelos Miliordos at Pacific Northwest National Lab. They conducted both multi-reference configuration interaction (MRCI) and single reference coupled cluster [CCSD(T)] calculations combined with basis up to quadruple quality- $\zeta$  on this system. The experiments employ tagging with argon, and so the argon atom position may have a significant influence on these spectra. Therefore, the calculations included this.

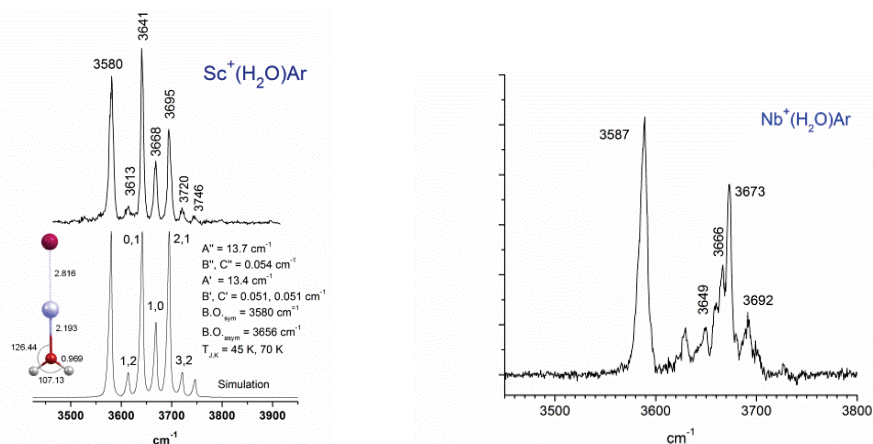


Figure 1. IR spectra in the O–H stretching region for scandium-, titanium- and niobium-water cations. The rotational structure for scandium is consistent with expectations for a  $\text{C}_{2v}$  structure, with a triplet for the asymmetric stretch and a 3:1 intensity alternation from nuclear spin statistics. The niobium spectrum has a very different pattern, with no 3:1 alternation in the line intensities, suggesting a non-planar structure.

Figure 2 (left) shows the minimum energy structure obtained for  $\text{Ar-Nb}^+(\text{H}_2\text{O})$  by Miliordos and Xantheas, which has the argon bent out of the metal-water plane. Initially, we thought this might explain the unusual rotational patterns in the spectrum. However, further investigation of the potential showed that vibrational averaging even in the  $v=0$  level caused the system to have its greatest probability at the planar configuration, thus eliminating this as an explanation for the

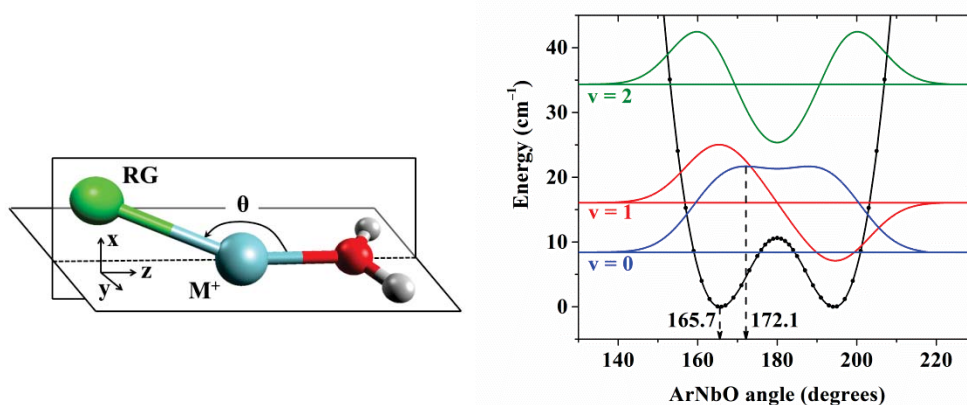


Figure 2. The optimized structure for  $\text{Ar-Nb}^+(\text{H}_2\text{O})$  (left) and the scan of the argon bending potential, with the expectation values of the vibrational wavefunction in this coordinate.

spectrum. We next realized that the 3:1 nuclear spin intensity patterns are only valid for systems in which ortho-para spins states do not equilibrate. Miliordos and Xantheas then calculated the nuclear-electronic spin coupling constants (MHz) of the  $^1\text{H}$  nucleus in the  $\text{M}^+(\text{H}_2\text{O})$  clusters for Sc, V, and Nb. The isotropic Fermi contact terms for niobium and vanadium, which do not exhibit the 3:1 intensity pattern, were much larger (2.17 and 3.6) compared to that for scandium (0.42), which does have the 3:1 pattern. This indicates that vanadium and niobium ions can catalyze the ortho-para nuclear spin interconversion, which then explains the different patterns in the spectra of their complexes.

New experiments have investigated metal ion-acetylene complexes, finding unusual coordination and solvation behavior for the copper system. In the vanadium-acetylene system, intracuster reactions occur forming three-member ( $\text{MC}_2$ ) and five-member ( $\text{MC}_4$ ) metallacycle structures.

Significant progress has been made in the last few months in bringing our new photofragment imaging experiment on-line. The system is now optimized and calibrated and new images have been obtained for the charge-transfer dissociation of  $\text{Ag}^+$ -benzene (Figure 3). The kinetic energy release in this system provides evidence for a bond energy ( $\leq 32.8$  kcal/mol) which is lower than previous estimates.

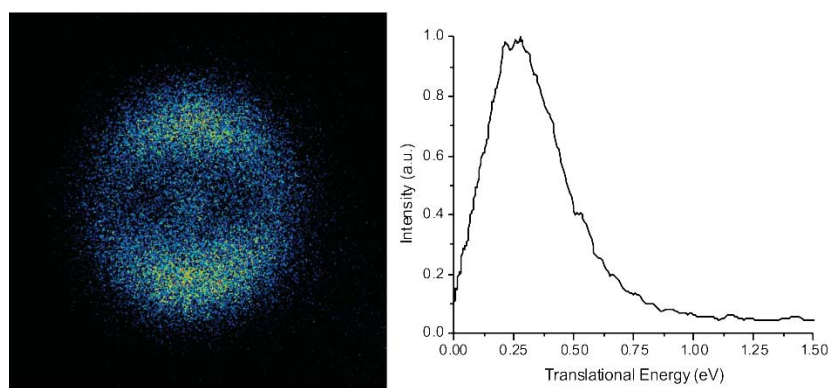


Figure 3. The photofragment image of the benzene cation from the charge-transfer dissociation of  $\text{Ag}^+$ -benzene at 355 nm.

## Future Plans

Our work in the immediate future will continue theory and experiments on metal-water complexes such as those of titanium and niobium, continue the ongoing experiments on vanadium-acetylene complexes, and focus on the continued development of the photofragment imaging experiments. We are particularly interested in applying imaging to the photodissociation of dication-water complexes to obtain improved information about the bond energies in these systems, which are difficult to measure by other methods.

## Publications (1/2013–present) for this Project

1. A. M. Ricks, A. D. Brathwaite, M. A. Duncan, "Coordination and spin states of  $V^+(CO)_n$  clusters revealed by IR spectroscopy," *J. Phys. Chem. A* **117**, 1001–1010 (2013). (Peter Armentrout Festschrift) **DOI:** 10.1021/jp301679m.
2. B. Bandyopadhyay, K. N. Reishus, M. A. Duncan, "Infrared spectroscopy of solvation in small  $Zn^+(H_2O)_n$  Complexes," *J. Phys. Chem. A* **117**, 7794–7803 (2013). **DOI:** 10.1021/jp4046676.
3. A. M. Ricks, A. D. Brathwaite, M. A. Duncan, "IR spectroscopy of  $V^+(CO_2)_n$  clusters: Solvation-induced electron transfer and activation of  $CO_2$ ," *J. Phys. Chem. A* **117**, 11490–11498 (2013). **DOI:** 10.1021/jp4089035.
4. A. D. Brathwaite, M. A. Duncan, "Infrared photodissociation spectroscopy of saturated group IV (Ti, Zr, Hf) metal carbonyl cations," *J. Phys. Chem. A* **117**, 11695–11703 (2013). (Curt Wittig Festschrift). **DOI:** 10.1021/jp400793h.
5. M. Castro, R. Flores, M. A. Duncan, "Theoretical study of nascent solvation in  $Ni^+(\text{benzene})_m$ ,  $m=3$  and 4, clusters," *J. Phys. Chem. A* **117**, 12546–12559 (2013). **DOI:** 10.1021/jp406581m.
6. A. D. Brathwaite, A. M. Ricks, M. A. Duncan, "Infrared spectroscopy of vanadium oxide carbonyl cations," *J. Phys. Chem. A* **117**, 13435–13442 (2013). (Terry Miller festschrift) **DOI:** 10.1021/jp4068697.
7. A. D. Brathwaite, J. A. Maner, M. A. Duncan, "Testing the limits of the 18-electron rule: The gas phase carbonyls of  $Sc^+$  and  $Y^+$ ," *Inorg. Chem.* **53**, 1166–1169 (2014). **DOI:** 10.1021/ic402729g.
8. K. N. Reishus, A. D. Brathwaite, J. D. Mosley, M. A. Duncan, "Infrared Spectroscopy of Coordination versus Solvation in  $Al^+(\text{benzene})_{1-4}$  Complexes," *J. Phys. Chem. A* **118**, 7516–7525 (2014) (Ken Jordan festschrift). **DOI:** 10.1021/jp500778w.
9. A. D. Brathwaite, T. B. Ward, R. S. Walters and M. A. Duncan, "Cation- $\pi$  and CH- $\pi$  Interactions in the Coordination and Solvation of  $Cu^+(\text{acetylene})_n$  Complexes," *J. Phys. Chem. A* **119**, 5658–5667 (2015). **DOI:** 10.1021/acs.jpca.5b03360.

## Confinement, Interfaces, and Ions: Dynamics and Interactions in Water, Proton Transfer, and Room Temperature Ionic Liquid Systems (DE-FG03-84ER13251)

Michael D. Fayer  
Department of Chemistry, Stanford University, Stanford, CA 94305  
fayer@stanford.edu

We examined the dynamics of borohydride ( $\text{BH}_4^-$ ) in water from the perspectives of both the anion and the water using ultrafast two dimensional infrared (2D IR) spectroscopy and IR pump-probe experiments.<sup>7</sup> The dynamics of water molecules interacting with (hydrogen bonded to) anions is a subject that has received a great deal of attention. Borohydride provided the opportunity to examine the anion/water dynamics from the perspective of the anion by studying the B-H stretch using ultrafast IR experiments. It was also possible to look at the dynamics from the water perspective by making measurements on water hydroxyls that are hydrogen bonded to borohydride anions. In addition to the opportunity of measuring the dynamics of an anion hydrogen bonded to water from both sides of the hydrogen bond, the borohydride/water system is interesting because of the special nature of borohydride-water hydrogen bonds, that is, dihydrogen bonds.

Hydrogen bonds occur between a hydrogen bond donor, typically a hydrogen with a partial positive charge that is bonded to a more electronegative element such as oxygen, and a hydrogen bond acceptor which can be a lone pair of an electronegative element, the  $\pi$  electrons of an aromatic ring or multiple bond, or a transition metal center. A special case of hydrogen bonding has also been observed and has been the subject of recent studies, the dihydrogen bond. Because of the relatively low electronegativity of boron, the hydrogens in  $\text{BH}_4^-$  have partial negative charges. This partial negative charge allows the hydrogens to act as hydrogen bond acceptors, in contrast to the usual situation of, e. g, a hydroxyl, which acts as a hydrogen bond donor. Our study focused on the dynamics of borohydride dihydrogen bonds with water. Given the ubiquity of water as a solvent and the widespread use of borohydride as a reducing agent, the borohydride/water system is important in its own right, but it is also useful in understanding dihydrogen bond dynamics.

Borohydride presents the interesting situation in which the H of a water hydroxyl is hydrogen bonded to the H of the borohydride. Thus there is a hydrogen bond between the partially negative H's of the borohydride and the partially positive H's of water. By making IR measurements on the B-H stretch of borohydride and the hydroxyl stretch of water molecules bound to  $\text{BH}_4^-$ , we were able to study the hydrogen bond dynamics from the perspectives of both partners in the dihydrogen bond.

We have examined the dynamics using ultrafast 2D-IR vibrational echo spectroscopy and polarization selective IR pump-probe experiments. Structural evolution of the systems is reflected in spectral diffusion measured with 2D-IR. Measurements of the spectral diffusion of hydroxyls that were bound to borohydride was made possible by a new data analysis procedure that removed the contributions to the data from water hydroxyls bound to other water molecules. The spectral diffusion of the B-H stretch could be measured directly, as the absorption band is well separated from strong water absorptions. In addition, orientational relaxation of water was measured with the pump-probe experiments in the concentrated  $\text{NaBH}_4$  solutions.

The remarkable results are that the B-H stretching mode and the hydroxyls (OD stretch of HOD) bound to the B-Hs show virtually identical spectral diffusion dynamics that are in turn identical to those of the OD stretch of HOD in pure bulk water within relatively small error bars. In bulk water, detailed comparisons of molecular dynamics simulations to 2D-IR data has shown that spectral diffusion, which occurs on two time scales, is associated with hydrogen bond dynamics. Ultrafast dynamics,  $\sim 0.4$  ps, are caused by hydrogen bond length fluctuations, while slower dynamics,  $\sim 1.7$  ps, are caused by randomization of the hydrogen bonding network. Although the hydroxyls and BHs form dihydrogen bonds, the ultrafast fluctuations observed for both the B-H stretch and O-D stretch, which are presumably length fluctuations as in pure water, occur with the same time constants as pure water within error. The slower time scale spectral diffusion (structural dynamics) observed for both the B-H stretch and the O-D stretch for the O-Ds bound to borohydride are also the same as pure bulk water within experimental error. In addition, the orientational relaxation of HOD in the concentrated  $\text{NaBH}_4$  solution (8 water molecules per ion pair) is the same as it is in pure water within a small experimental error. The fact that the dynamics in borohydride solution is the same as in pure water is in contrast to results on other concentrated salt solutions, e.g.,  $\text{KBr}$ , where generally both the spectral diffusion and the orientational relaxation are considerably slower.

The fact that the spectral diffusion of the B-H stretch and the OD stretch bound to borohydride are almost identical to that of the O-D stretch of HOD in bulk water is highly suggestive. The sample used for the measurements was a 1M borohydride solution; so there were no issues of ion pairing or incomplete solvation as the sample is relatively dilute, 55 water molecules per borohydride. The borohydride dynamics are presumably caused by dihydrogen bonded water molecules and the surrounding water. Borohydride is experiencing the same structural fluctuations as its solvating water. Borohydride is tetrahedral. It has a calculated radius for the isolated anion of  $\sim 1.9$  Å compared to water's  $\sim 1.35$  Å. Therefore, borohydride is larger than water. (If a water molecule plus the two H-bonds it accepts from other water molecules, which gives water an effective tetrahedral character are considered, the sizes are more similar.) The tetrahedral arrangement of the B-H bonds may permit water to dihydrogen bond to it without greatly perturbing the nominally tetrahedral hydrogen bonding structure of the surrounding water. The results suggest that the hydrogen bonding does not enforce strained structures on the dihydrogen bound waters but rather can allow the water to coordinate at angles native to the bulk water structure. The net result is that borohydride anion does not greatly change the structure or dynamics of the surrounding water in contrast to simple anions like  $\text{Br}^-$ , which is solvated by six water molecules and destroys the local tetrahedral environment.

Aqueous proton transfer is important in a wide variety of chemical and biological systems, and the effect of confined environments on proton transfer is relevant to many important topics, including fuel cell membranes. Reverse micelles (RMs), consisting of aggregated surfactant molecules encapsulating a core water pool within a hydrophobic organic phase, provide simple and experimentally accessible systems for studying confined aqueous environments.

Proton transfer kinetics in both ionic and neutral reverse micelles were studied by time-correlated single photon counting (TCSPC) investigations of the fluorescent photoacid 8-hydroxypyrene-1,3,6-trisulfonate (HPTS).<sup>9</sup> Orientational dynamics of dissolved probe molecules in the water pools of the reverse micelles were also investigated by time dependent fluorescence anisotropy measurements of MPTS, the methoxy derivative of HPTS. These experiments were compared to the same experiments in bulk water. The studies were conducted on reverse micelles with a wide range of water nanopool sizes. It was found that in ionic reverse micelles (surfactant Aerosol OT, AOT), orientational motion (fluorescence anisotropy decay) of MPTS was relatively unhindered, consistent with MPTS being located in

the water core of the reverse micelle away from the water-surfactant interface for the larger reverse micelles, although for very small RMs interaction with the interface was evident. In non-ionic reverse micelles (surfactant Igepal CO-520, Igepal), however, orientational anisotropy for all RM sizes displayed a slow multiexponential decay consistent with wobbling-in-a-cone behavior, indicating MPTS is located at the water-surfactant interface. HPTS proton transfer in ionic reverse micelles followed kinetics qualitatively like those in bulk water, albeit slower, with the long-time power law time dependence associated with recombination of the proton with the dissociated photoacid suggesting a modified diffusion-controlled process. However, the power law exponents in the ionic reverse micelles are smaller ( $\sim -0.55$ ) than in bulk water ( $-1.1$ ). In neutral reverse micelles, proton transfer kinetics did not show discernible power law behavior, and were best represented by a two component model with one relatively water-exposed population, and a population with a faster fluorescence lifetime and negligible proton transfer. We explained the Igepal results on the basis of close association between the probe and the neutral water-surfactant interface, with the probe experiencing a distribution of more and less water-like environments.

In addition, the observation in bulk water of a power law  $t^{-1.1}$  for diffusion-controlled recombination was in contrast to the theoretical prediction of  $t^{-1.5}$  and previously reported observations. Greatly improved experimental methodology enabled accurate determination of the proton transfer time dependence. The fluorescence spectrum is composed of a peak for the protonated HPTS and a peak for the deprotonated species, which is substantially red shifted but still overlaps with the protonated peak. To obtain accurate proton transfer kinetics, the full time dependent spectra of both peaks were recorded, in contrast to previous studies where a single wavelength of the protonated HPTS fluorescence was measured. By using the full time dependent spectra, the true time dependence of the protonated band was obtained. The same procedures were used for all of the samples.

In addition to the research outlined briefly above, we have conducted detailed studies of the dynamics of solutes in room temperature ionic liquids (RTILs) and discovered and theoretically explicated a new physical phenomenon required to interpret the experimental results.<sup>8,10,11,4</sup> We have performed the first 2D IR experiments on metal organic frameworks (MOFs) to observe framework dynamics and how they are influenced by filling the pores with solvent.<sup>5</sup> We have also performed a variety of studies using ultrafast IR methods of the dynamics of surfactants in planar bilayers and vesicles.<sup>1,2,3,6</sup>

Our future work will expand our investigations of proton transfer in fuel cell membranes using photoacids to directly observe proton transfer in the nanochannels of the membranes and ultrafast IR experiments to study the dynamics of nanoconfined water in the channels. We will investigate four different commercial fuel cell membranes to understand how the chemical and structural differences of the membranes affect proton transport in the membrane channels. We will continue our studies of the dynamics of complex ions in water. Based on the results on the borohydride tetrahedral anion described above, we will use 2D IR and other IR experiments to investigate a tetrahedral cation, ammonium, by studying both the ammonium stretch and the hydroxyl stretch of water bound to ammonium. As with borohydride, these experiments will measure dynamics from both the ion and water perspectives. We will also study the selenocyanate anion in water to understand the influence of hydrogen bonding interactions on the anion. We are expanding our studies of RTILs, particularly to understand dynamics and interactions of CO<sub>2</sub> in RTILs. RTILs are being developed for carbon capture applications. We are also using selenocyanate, because of its long vibrational lifetime, as a dynamical probe of water nanopools in reverse micelles and in RTILs. In RMs, the studies will be performed as a function of the size of the water nanopool, and in RTILs, the studies will be performed as a

function of the alkyl chain length on the alkyl-methyl imidazolium cations. In the studies of RTILs, we are also performing experiments on imidazolium cations that have been synthesized to have a  $-SeCN$  moiety, which provides a probe of the RTILs with a long lifetime. The cations with  $SeCN$  will be dilute, and will yield dynamical information from what is in essence the RTIL cation without an additional vibrational probe molecule. In the RTIL experiments, we will also use optical heterodyne detected optical Kerr effect experiments to provide a dynamical observable that can be measured from  $<100$  fs to microseconds.

### Publications – Last Two Years

1. “Dynamics in the Interior of AOT Lamellae Investigated with 2D IR Spectroscopy,” S. K. Karthick Kumar, A. Tamimi, and Michael D. Fayer *J. Am. Chem. Soc.* **135**, 5118-5126 (2013).
2. “Ultrafast Structural Dynamics Inside Planar Phospholipid Multibilayer Model Cell Membranes Measured with 2D IR Spectroscopy,” Oksana Kel, Amr Tamimi, Megan C. Thielges, and Michael D. Fayer *J. Am. Chem. Soc.* **135**, 11063-11074 (2013).
3. “Size Dependent Ultrafast Structural Dynamics inside Phospholipid Vesicle Bilayers Measured with 2D IR Vibrational Echo Spectroscopy,” Oksana Kel, Amr Tamimi, and Michael D. Fayer *Proc. Nat. Acad. Sci. U.S.A.* **111**, 918-923 (2014).
4. “Dynamics and structure of room temperature ionic liquids,” Michael D. Fayer *Chem. Phys. Lett.* **616-617**, 259-274 (2014).
5. “Structural Dynamics inside a Functionalized Metal-Organic Framework Probed by Ultrafast 2D IR Spectroscopy,” Jun Nishida, Honghan Fei, Amr Tamimi, Sonja Pullen, Sascha Ott, Seth M. Cohen, and Michael D. Fayer *Proc. Nat. Acad. Sci. U.S.A.* **111**, 18442-18447 (2014).
6. “The Influence of Cholesterol on Fast Dynamics Inside of Vesicle and Planar Phospholipid Bilayers Measured with 2D IR Spectroscopy,” Oksana Kel, Amr Tamimi, and Michael D. Fayer *J. Phys. Chem. B* **119**, 8852-8862 (2015).
7. “Dynamics of Dihydrogen Bonding in Aqueous Solutions of Sodium Borohydride,” Chiara H. Giammanco, Patrick L. Kramer, and Michael D. Fayer *J. Phys. Chem. B* **119**, 3546-3559 (2015).
8. “Dynamics of water, methanol, and ethanol in a room temperature ionic liquid,” Patrick L. Kramer, Chiara H. Giammanco, and Michael D. Fayer *J. Chem. Phys.* **142**, 212408 (2015).
9. “Proton Transfer in Ionic and Neutral Reverse Micelles,” Christian Lawler and Michael D. Fayer *J. Phys. Chem. B* ASAP (2015).
10. “Observation and Theory of Reorientation-Induced Spectral Diffusion in Polarization-Selective 2D IR Spectroscopy,” Patrick L. Kramer, Jun Nishida, Chiara H. Giammanco, Amr Tamimi, and Michael D. Fayer *J. Chem. Phys.* **142**, 184505 (2015).
11. “Separation of Experimental 2D IR Frequency-Frequency Correlation Functions into Structural and Reorientation-induced Contributions,” Patrick L. Kramer, Jun Nishida, and Michael D. Fayer *J. Chem. Phys.* submitted (2015).

## Chemical Kinetics and Dynamics at Interfaces

### *Fundamentals of Solvation under Extreme Conditions*

**John L. Fulton**

Physical Sciences Division  
Pacific Northwest National Laboratory  
902 Battelle Blvd., Mail Stop K2-57  
Richland, WA 99354  
[john.fulton@pnl.gov](mailto:john.fulton@pnl.gov)

Collaborators: G. K. Schenter, C. J. Mundy, M. Baer, E. J. Bylaska, N. Govind, M. Galib.

### **Program Scope**

The primary objective of this project is to describe, on a molecular level, the solvent/solute structure and dynamics in fluids such as water under extremely non-ideal conditions. The scope of studies includes solute–solvent interactions, clustering, ion-pair formation, and hydrogen bonding occurring under extremes of temperature, concentration and pH. The effort entails the use of spectroscopic techniques such as x-ray absorption fine structure (XAFS) spectroscopy, high-energy x-ray scattering, coupled with theoretical methods such as molecular dynamics (MD-XAFS), and electronic structure calculations in order to test and refine structural models of these systems. In total, these methods allow for a comprehensive assessment of solvation and the chemical state of an ion or solute under any condition. The research is answering major scientific questions in areas related to geochemistry, biochemistry, and sustainable nuclear energy (aqueous ion chemistry and corrosion). This program provides the structural information that is the scientific basis for the chemical thermodynamic data and models in these systems under non-ideal conditions.

### **Recent Progress**

***Water under pressure.*** The H-bonding structure of water to a large extent governs the local- and long-range hydration structure of cations and anions. This is one of the reasons that enormous effort has been made to accurately measure and predict the structure of pure water. A recent x-ray diffraction (XRD) benchmark study (JCP 138, 074506, 2013) is widely viewed as the most accurate and significantly improved assessment of pure water structure under ambient conditions. While measurements have been made at high pressure, they lack the needed spatial resolution and low noise of this new standard for ambient conditions. A new style of pressure cell (PNNL) was used to obtain high-resolution measurements of water up to 3.6 kbar. The approach involves the use of a specially mounted, thin diamond window (250 $\mu$ m thick x 3 mm diameter) and a high-energy x-ray (115 keV) beamline. This work was a collaborative effort with L. Skinner and C. Benmore at Argonne, who are the developers of refinement methods to quantitatively recover the O-O pair distribution ( $g_{OO}(R)$ ) from x-ray scattering data. As shown by the  $g_{OO}(R)$  data in Figure 1, over this moderate pressure range, there are large structural changes that occur as the pressure is increased up to 3.6 kbar ( $\rho = 1.12$  g/ml). It is interesting that the changes in the measured peak positions and amplitudes in the  $g_{OO}(r)$ , between low and high pressure, mimic the structural changes that are observed between low density amorphous ice (LDA) and high density amorphous (HDA) ice structures.

This new benchmark, high-pressure data provides a second state point (with the ambient data) for a rigorous test of water models. In Figure 1, these measurements are compared to simulated structure from DFT-MD (revPBE-D3) and from an empirically-based water potential (TIP4P/2005). This work is in collaboration with C. Mundy, G. Schenter and M. Galib at PNNL.

It is commonly believed that DFT-based water is over-structured. However through inclusion of longer-range dispersion (D3) and through the judicious choice of specific functionals and basis sets an excellent outcome is achieved. Table 1 reports an error analysis comparing three different simulation protocols to the ambient and high-pressure experimental data. As shown by the simulated structure in Figure 1 and in the error analysis in Table 1, DFT-MD (revPBE-D3) best represents the structure of water under these two conditions. This is a remarkable outcome since the TIP4P/2005 empirical potential is held to be one of the most accurate representations of water structure.

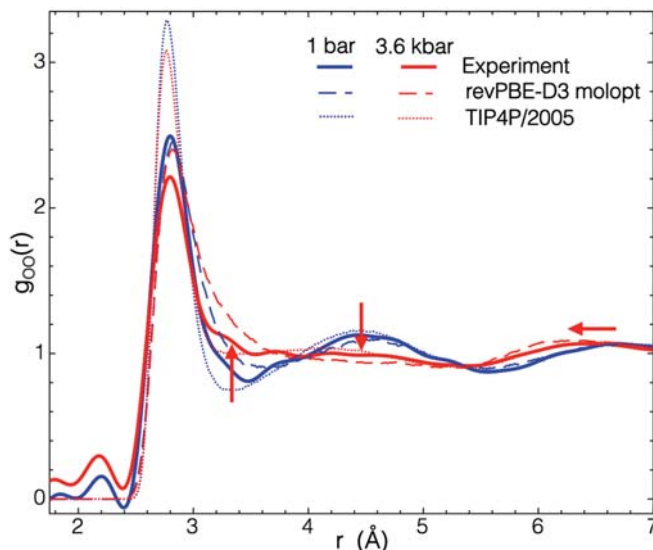


Figure 1. Measured O-O pair distribution functions at 1 bar and 3.6 kbar. Comparisons are made with MD simulations from DFT (revPBE-D3 molopt) and from empirical (TIP4P/2005) interaction potentials.

Table 1.  $\chi_{OO}$  agreement factors (weighted sum of squares) between simulation and experiment for the three MD models studied over the range  $0 < r < 10 \text{ \AA}$  (lower is better agreement). The mW (Moore and Molinero) method is another empirical potential.

Method	1 bar	3.6 kbar
revPBE-D3 MOLOPT	0.033	0.048
TIP4P/2005	0.078	0.072
mW	0.052	0.184
Experimental error	0.014	0.013

The structural changes observed at high pressure (3.6 kbar) are characterized in revPBE-D3 by a) the number of hydrogen bonds in the first shell are nearly unchanged at approximately four, b) under ambient pressure the first-shell H-bonding arrangement is approximately tetrahedral whereas at high pressure this arrangement becomes significantly distorted, c) this symmetry distortion occurs as a fifth water starts to encroach upon the first shell through a non H-bonding interaction.

**A revised picture of  $\text{Na}^+$  hydration.** Continuing improvements in synchrotron-based x-ray optics and detectors offers opportunities to measure aqueous structure with unprecedented detail. The structure of hydrated  $\text{Na}^+$  was measured using both the high-resolution XRD technique described above and with a first-of-its-kind EXAFS study of aqueous  $\text{Na}^+$ . The results alter the established structural values for this system.

The EXAFS spectrum has not previously been evaluated for aqueous  $\text{Na}^+$  because of the many factors limiting the data quality during acquisition of EXAFS spectra at low X-ray energies (1 keV). These include achieving constant high x-ray flux at the sample, stable beam position, harmonic-free beam, stable sample detectors and finally properly accounting for the strong X-ray absorption by the sample. The combination of a very high-flux, low-energy undulator source, an improved X-ray monochromator, as well as an improved detector has allowed the acquisition of high-quality EXAFS spectra sufficient for a quantitative treatment of the higher-order scattering paths that are required to determine the  $\text{Na}^+$  aqueous structure. The method also involves using a low-Z EXAFS cell that incorporates 200 nm thick  $\text{Si}_3\text{N}_4$  x-ray transmission windows to contain the flowing liquid in a high-vacuum chamber.

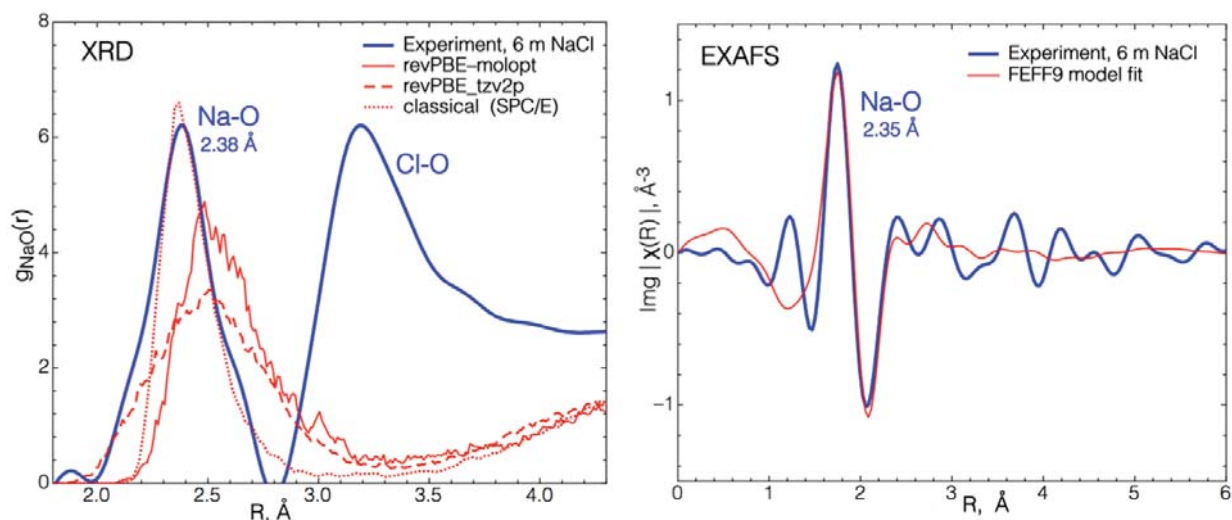


Figure 2. XRD (left) and EXAFS (right) measurement of  $g_{\text{NaO}}(R)$  compared to simulated values from DFT and from SPC/E models. The measured XRD spectrum also contains the structural contribution from Cl-O interaction of water hydrating the first solvent shell about  $\text{Cl}^-$ .

Figure 2 shows the XRD and the EXAFS spectra for 6 m NaCl and reports their measured first-shell Na-O distances of 2.38 and 2.35 Å, respectively. These distances are substantially shorter than the accepted literature value of about 2.44 Å and the measurements show that the first-shell waters are significantly more ordered than expected. These new results are especially important given the huge role of aqueous  $\text{Na}^+$  in biochemical and geochemical systems.

We have previously shown that DFT-based simulations predict ion-water structure with very high fidelity for divalent cations (e.g. transition metals). The DFT-based simulations accurately represent the repulsive part of the pair potential that mostly dominates the structural interaction of water with di- and tri-valent cations. There is however a known difficulty with monovalent cations. Figure 2 also compares the experimental structure with the simulated structure using either DFT (revPBE) or empirical (SPC/E) potential models. The Na-O structure from the DFT simulation is too disordered and at a substantially longer Na-O distance than the experimental value. The classical potential reasonably captures the experimental structure. The current hypothesis is that small DFT errors in describing the shape and depth of the attractive well of the Na/water pair potential become especially important for monovalent ions. The challenges of using DFT-based methods for monovalent cations is currently an area of active study.

## Future Plans

The objective is to gain a fundamental understanding of the molecular structure that provides the basis for understanding ion chemistry and dynamics. We propose exploring ion-water structure for systems in which the local structure has not yet been measured or the structure is not yet fully understood. Our goal is to identify the underlying structural factors that govern the macroscopic properties of ions that have so far eluded a comprehensive theoretical treatment. The proposed work also involves a comprehensive study of ion pairing in concentrated solutions and at high temperatures. The objective is to describe how the ion pair structure is governed by a range of different types of solvent interactions.

## References to publications of DOE sponsored research (2013 - present)

1. V.-T. Pham, J. L. Fulton, "Ion-pairing in aqueous  $\text{CaCl}_2$  and  $\text{RbBr}$  solutions: simultaneous structural refinement of XAFS and XRD data.", **J. Chem. Phys.**, 138, 044201, (2013)
2. S. Bogatko, E. Cauet, E. Bylaska, G. K. Schenter, J. L. Fulton, J. H. Weare, "Hydration Structure and Dynamics of Aqueous  $\text{Ca}^{2+}$  using Ab Initio Molecular Dynamics: Comparison with  $\text{Zn}^{2+}$ ,  $\text{Fe}^{3+}$ , and  $\text{Al}^{3+}$ ." **Chemistry: A European Journal**, 19, 3047, (2013)
3. "The Aerobic Oxidation of Bromide to Dibromine Catalyzed by Homogeneous Oxidation Catalysts and Initiated by Nitrate in Acetic Acid." Partenheimer W, John L. Fulton, Christine M. Sorensen, Van-Thai Pham, and Yongsheng Chen. **Advanced Synthesis & Catalysis** 387, 130-137, (2014).
4. "Persistent ion pairing in aqueous hydrochloric acid" Marcel D. Baer, John L. Fulton, Mahalingam Balasubramanian, Gregory K. Schenter, and Christopher J. Mundy, **J. Phys. Chem. B**, 118, 7211 (2014) (Feature Article)
5. John C. Linehan, Mahalingam Balasubramanian, John L. Fulton, "Homogeneous catalysis: from metal atoms to small clusters", In "XAFS Techniques for Catalysts, Nanomaterials, and Surfaces", Yasuhiro Iwasawa, Kiyotaka Asakura, and Mizuki Tada, editors, Springer, New York, 2015 in press.
6. Gregory K. Schenter, John L. Fulton, "Molecular Dynamics Simulations and XAFS (MD-XAFS)", In "XAFS Techniques for Catalysts, Nanomaterials, and Surfaces", Yasuhiro Iwasawa, Kiyotaka Asakura, and Mizuki Tada, editors, Springer, New York, 2015 in press.
7. John L. Fulton, Niranjan Govind, Thomas Huthwelker, Eric J. Bylaska, Aleksei Vjunov, Sonia Pin, Tricia D. Smurthwaite, "Electronic and Chemical State of Aluminum from the Single- (K) and Double-Electron Excitation ( $\text{KL}_{\text{II\&III}}$ ,  $\text{KL}_1$ ) X-ray Absorption Near-Edge Spectra of alpha-Alumina, Sodium Aluminate, Aqueous  $\text{Al}^{3+} \cdot (\text{H}_2\text{O})_6$ , and Aqueous  $\text{Al}(\text{OH})_4^-$ ", **J. Phys. Chem. B**, 119, 8380-8388, 2015.

## Probing Chromophore Energetics and Couplings for Singlet Fission in Solar Cell Applications

DE-FG02-13ER16393

Etienne Garand

Department of Chemistry, University of Wisconsin-Madison, Madison, WI 53706

[egarand@chem.wisc.edu](mailto:egarand@chem.wisc.edu)

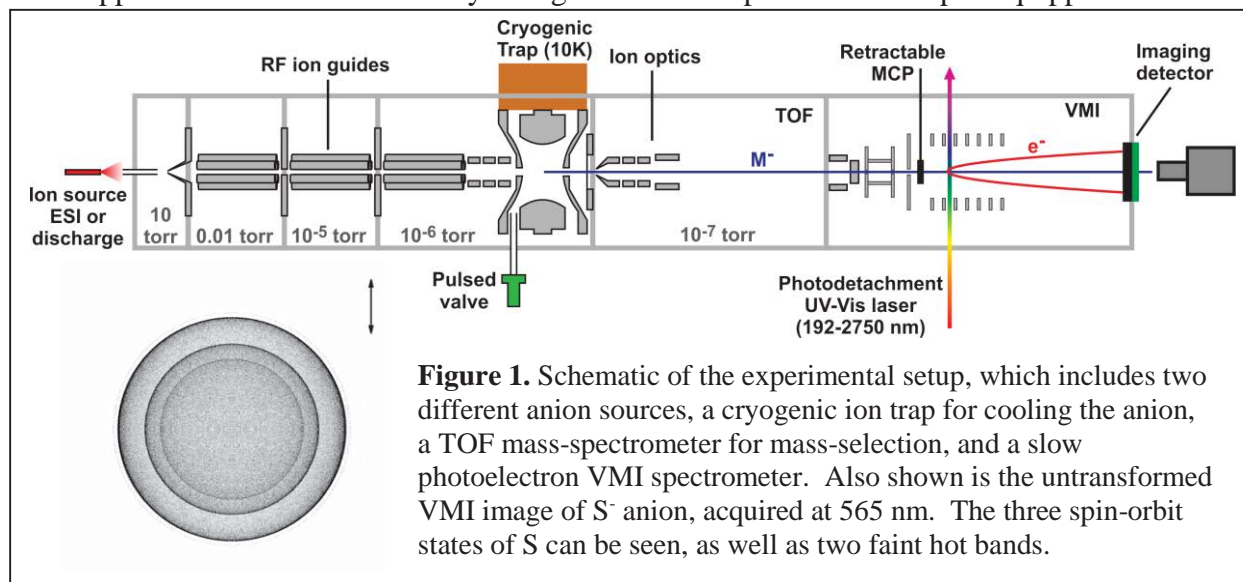
### *Program scope*

Our studies aim to provide a molecular-level understanding of processes that can improve efficiencies of alternative sources of energy, such as those found in dye-sensitized solar cells. In particular, the mechanisms and molecular requirements for efficient exciton multiplication through singlet fission will be explored using high-resolution anion photoelectron (PE) spectroscopy. More specific aims are (1) to probe the evolution of the electronic structure as a function of cluster size to understand singlet fission in crystals, (2) to explore the relationship between the nature of linkers and the electronic structure in covalently-bonded chromophore dimers, and (3) to highlight the differences, including exciton delocalization and the effects of solvent interactions, between the crystalline species and the isolated covalently-bonded dimers.

The electronic states of organic chromophore clusters and covalently-bonded dimers will be probed via PE spectroscopy of mass-selected anion precursors. Starting from the radical anion with a doublet ground state, all the low-lying singlet and triplet states of the neutral molecule that involve removal of a single electron can be accessed via one-photon photodetachment. Therefore, with the exception of the doubly excited state, all the electronic states relevant to singlet fission are accessible on equal footing in our experiments. This makes PE spectroscopy an ideal method for probing the couplings present between these states. Using anions also provide the added advantage of mass selection, which is crucial for studying the behavior of singlet fission as a function of cluster size. To extract precise information about the electronic state energies and couplings, it is important to obtain well-resolved PE spectra. This can be achieved by using the slow electron velocity-map imaging (SEVI) technique which combines velocity-map imaging (VMI) detection with tunable lasers to yield PE spectrum with sub-meV resolution. Additionally, we can reduce temperature related resolution limitations by collisionally cooling the anions to  $\sim 10$  K in a cryogenic radio-frequency ion trap prior to laser photodetachment. Comparisons of the different chromophore systems can reveal the electronic interactions responsible for the observed differences in their singlet fission efficiency. The results can also be used to benchmark theoretical methods.

## Progress

Since the start of this program in July 2013, we have designed and built the cryogenic SEVI apparatus shown schematically in Figure 1. The experimental setup is equipped with both



a heated oven expansion discharge source and an electrospray ionization source. The anions generated by either source are guided through differential pumping regions into a cryogenic ion trap using homebuilt RF ion guides. Inside the quadrupole ion trap, the anions are cooled via collisions with helium buffer gas. Residence time inside the trap is typically 50-90 ms to ensure temperature equilibrium before the anions are gently extracted into a linear time-of-flight mass spectrometer, which has a resolution of  $m/\Delta m \sim 800$ . A pulsed re-referencing scheme allows only the anions with a specific mass into the VMI region where they are intersected with the gently focused output of a tunable pulsed UV-Vis laser. Photoelectrons, velocity focused by the VMI optics, are mapped onto a detector assembly consisting of imaging quality micro-channel plates and a phosphor screen. The resulting image is captured by a 2048x2048 pixel camera triggered by the time-of-flight timing, providing both the conventional PE spectra via angular integration as well as anisotropy information on the individual vibronic transitions. The construction of the instrument was completed in the spring of 2015 and we are currently fine-tuning it, i.e. developing the ion sources for stable production of radical anions and optimizing SEVI imaging resolution. Plans are in place to install a reflectron in the time-of-flight region to incorporate additional capability of acquiring infrared spectra of the anions via cryogenic infrared vibrational predissociation spectroscopy.

To carry out the proposed experiments, we have redesigned the SEVI VMI setup to allow for better focusing and less noise operations. A schematic of the new design is shown in Figure 2. A series of 40 evenly spaced plates extend the entire VMI region, giving us a well-defined electric field environment, while two layers of mu-metal shielding encase the entire electrode stack. The electrodes are resistively coupled (or grounded) with only three adjustable voltage parameters. One of the voltage remains fixed to define the forward kinetic energy of the electrons. VMI focus is determined by adjusting the other two voltages, where one corrects the energy aberration and the other brings the focal plane onto the detector. Therefore, the day-to-day operation of this VMI is not more difficult than the traditional three-plate VMI, while the

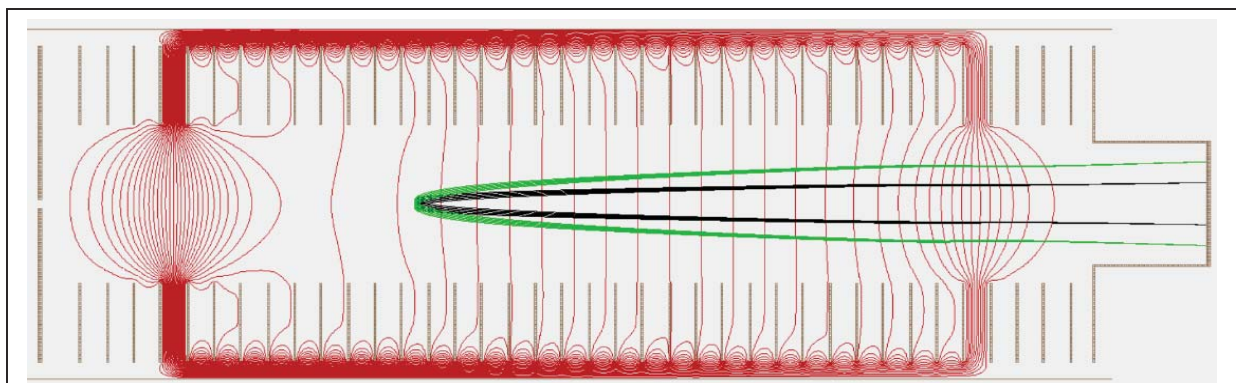


**Figure 2:** Schematic of the aberration corrected SEVI VMI setup. For the simulated electron flight path, 0.1 eV electrons are shown in black, 0.4 eV electrons are shown in green. The electric field lines are shown in red.

conditions of operation should be more forgiving. During the designing process, we found that the best VMI focus across the image is achieved when the photoelectrons are formed on a slightly curved electric field line, which is difficult to obtain against a flat repeller plate. Hence, we replaced the repeller plate with a series of open plates which can provide a smooth gradient to

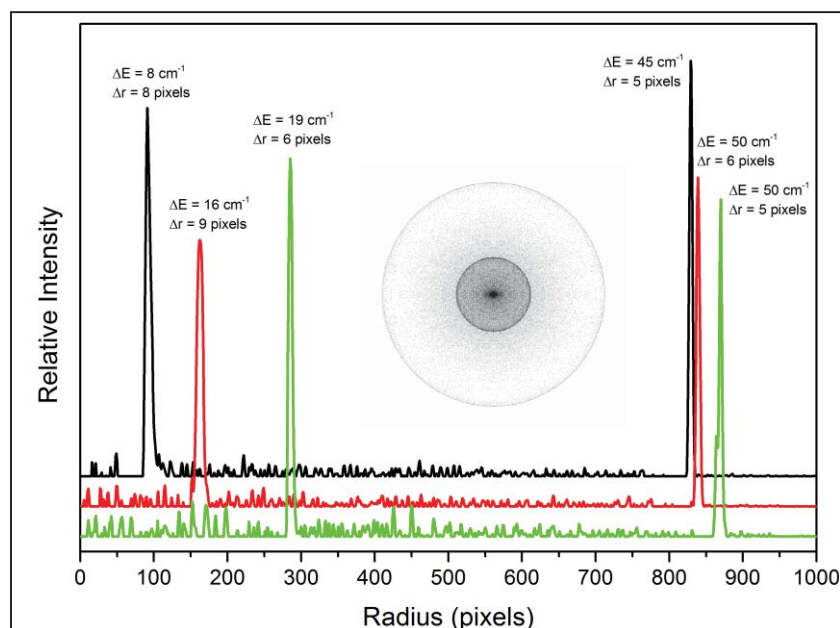


**Figure 3:** SEVI spectra of  $\text{Br}^-$ , demonstrating the consistency of the VMI focus for electrons with various eKE. The highest energy peak here correspond to  $\text{eKE} = 4115 \text{ cm}^{-1}$ . The center image is the inverse Abel transformed image of the green spectrum.

give the right curvature at the interaction region. The VMI focus is also dictated by the physical width of the laser beam because the electrons are formed on a sloping electric field. By stretching out the extraction region, we can provide a gentler sloping field, and therefore minimize the blurring effect from the laser beam width. Figure 3 shows a series of PE spectra of  $\text{Br}^-$  anion, acquired with the same VMI settings at various photon energies. The widths in pixels are consistent for all the peaks despite their  $\sim 0.5 \text{ eV}$  difference in energy. This should give us a wider range

of the image where the focus is optimal. Work is currently underway to further improve the optimal focus of the VMI setup. Finally, our design should also minimize the “noise” electrons formed from the electrodes when the laser energy is higher than the work function of stainless steel. Notably the electrodes near the interaction region are open, minimizing the surface area exposed to stray photons. This aspect is particularly important when studying the excited states of the polyacene molecules, which typically require photons with energies greater than 4 eV.

Concurrent to implementing the new VMI design, we also began investigating the formation of the polyacene radical anions. The difficulty here lies in its unstable nature and its relatively low electron affinity. Three approaches are being tested. First, a strong reducing agent is added to polyacene solution, where a faint color change can be observed indicating the polyacene has been reduced. Electrospray of the reduced solution has yielded radical anion signals, however source conditions need to be optimized for signal stability. The other method utilizes electrochemistry to controllably reduce the polyacene species, many of which has known, albeit high, redox potentials. We have successfully interfaced an electrochemical flow cell to the electrospray source, making it feasible to extend its use to the polyacenes. Finally, we've designed and built an oven discharge source, which has a proven record of producing a variety of radical anions. We are currently working on interfacing such an effusive beam source with the RF ion guides.

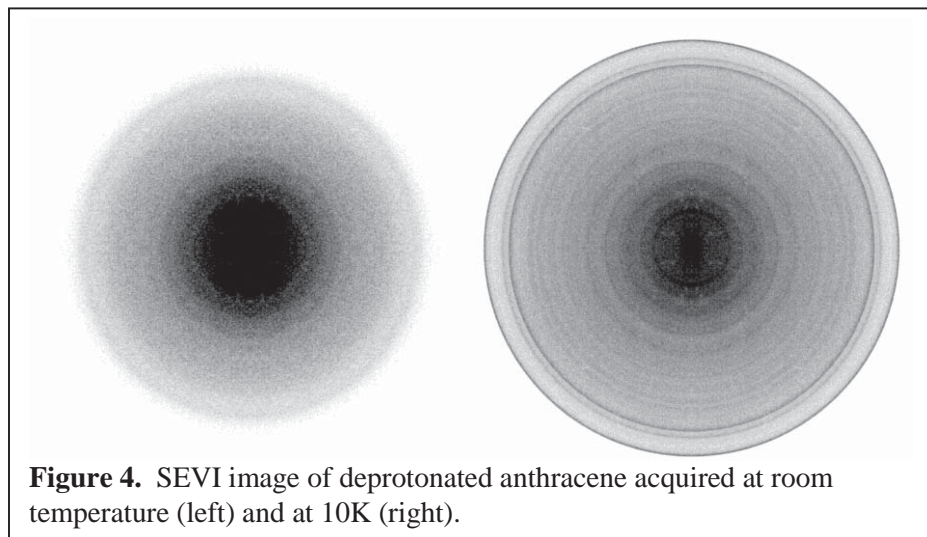


**Figure 4.** SEVI image of deprotonated anthracene acquired at room temperature (left) and at 10K (right).

Lastly, we have successfully tested the cooling capability of our instrument by acquiring the SEVI image of deprotonated anthracene anion at room temperature and at 10K. The results are shown in Figure 4. The advantage of using cooled anions is immediately obvious from the quality of the

images. Notably, the amount of internal energies available in these molecules at room temperature is quite significant, severely degrading the spectral resolution. This would only worsen for the large polyacenes, making cooling absolutely vital for the experiments.

### *Future plans*

Our immediate plan in the next year is to complete the testing of the cryogenic SEVI apparatus. Specifically, improved energy resolution and ease of use will be demonstrated with atomic and simple molecular anions. Additional changes will be made to further minimize “noise” electrons at high photon energies. We will also determine the conditions required for coupling the electrospray source with chemical and electrochemical reduction processes and optimize the oven discharge source. We aim to acquire the well-resolved PE spectra of anthracene and tetracene anions, as well as the dimers of these species in the next year. We will probe the ground states of the neutral species to validate our experimental and theoretical techniques. After which, we will focus our studies on the low-lying excited states that are relevant in the singlet fission process. The analysis of the results will be aided by infrared spectroscopy of the radical anions which can be acquired using our CIVS instrument.

## Reactions and Transformations

Phillip L. Geissler (plgeissler@lbl.gov), Musahid Ahmed (mahmed@lbl.gov),  
David Chandler (saykally@berkeley.edu), Rich Saykally (saykally@berkeley.edu)

Lawrence Berkeley National Laboratory, Chemical Sciences Division, 1 Cyclotron Road,  
Berkeley, CA 94720

### Program Scope

A significant gap exists between basic studies of molecular chemical physics and the operation of real devices and natural systems. This program comprises nascent efforts to establish the chemical methods and insight that will enable understanding of systems that are profoundly complex in composition, heterogeneity, preparation, and organization. The problems are multifaceted, and the case studies span a broad range of materials and behaviors. But a long-term unifying theme runs through these efforts: transitioning from the chemical physics of precisely specified model systems to transformations within the disordered and incompletely controlled environments that feature in energy applications.

Applying novel methods of theory and numerical simulation, Chandler's research group seeks to understand dynamics at soft interfaces, especially those of water, and the emergent phase behavior of water and other materials, sometimes driven to extreme conditions and far from equilibrium. Ahmed probes chemistry of liquids, surfaces and interfaces under various environments, coupling novel reactors to mass spectrometry, lasers and X-ray spectroscopies. Saykally's group uses liquid microjet technology to study the details of water evaporation and CO<sub>2</sub> dissolution without the obfuscating effects of condensation that have plagued previous studies. A new effort by Geissler's and Chandler's groups will focus on the dynamics of self-assembly, clarifying the time-dependent organization of molecular and nanoscale components into spatial patterns that promote new kinds of chemical reactivity.

### Recent Progress

Recent work from Chandler's group illustrating the importance of interfacial fluctuations include a numerical study of water evaporation using the method of transition path sampling, an analysis of hydrophobic effects at the water-oil surfaces and of pre-melting at the water-ice interface. These studies and associated treatments of coarsening and phase behaviors are challenging because relaxation of interfacial fluctuations extend over a broad range of time scales. The slowest processes are associated with vitrification and the formation of various amorphous ice phases.

Saykally's group has quantified the water evaporation coefficient (0.6), which has been highly controversial, and is a critical parameter in models of climate and cloud dynamics. Ammonium sulfate, the most common ionic solute in atmospheric aerosols, was shown to have no statistically significant effect on the rate, whereas sodium perchlorate effected a 25% reduction. The presence of acetic acid-a surface active component of natural aerosols- was likewise shown not to effect significant changes in the evaporation rate. Most recently, we have determined that addition of up to 0.5M concentrations of HCl has similarly negligible effects on the rate(unpublished). Using newly developed liquid microjet mixing technology, the first X-ray absorption spectra of aqueous carbonates, including the short-lived carbonic acid species itself, have been measured as a function

of pH to characterize the evolution of electronic structure and hydration structure of carbonate, bicarbonate, carbonic acid and dissolved CO<sub>2</sub>.

The chemical composition of melanin was elucidated by Ahmed using synchrotron based photoionization mass spectrometry in conjunction with statistical analysis which allowed correlation of color with chemical structures. Secondary Ion Mass Spectrometry (SIMS) in combination with FTIR spectroscopy was employed to study the gas plasma flux on endotoxin lipid A film. This study shows that lipid A film deactivation is sensitive to the magnitude of reactive species flux. The extent of surface modification appears to be significantly different under low and high flux conditions and a chemical model was proposed to explain this effect. The growth mechanisms of Ag nanoparticles controlled by plasmon-induced charge transfer in Ag-TiO<sub>2</sub> films were explored via electron and optical imaging and numerical simulation.

Geissler's group has explored the extension of path sampling techniques to the long and highly chaotic trajectories characteristic of self-assembly. This approach leverages and extends simulation tools developed in the context of barrier-crossing dynamics, e.g., chemical reactions. As a unique goal, we seek capabilities to sample trajectories beyond those representative of average behavior. These rare but important pathways foreshadow dramatic susceptibilities to external fields and also provide practical guidance in searching for combinations of control parameters that foster successful ordering. As a step towards this end, we have identified a class of techniques that hold promise for importance sampling of long assembly trajectories, explaining as well why other approaches suffer from problematically low acceptance probabilities.

### **Future Plans**

A new direction in this program is to perform mass spectrometry under ambient conditions to probe chemistry of surfaces and interfaces under aqueous environments. This is achieved via Drop Desorption Electrospray Ionization (Drop-DESI) where a liquid junction (drop) is scanned across a surface of interest. Very recently, an ion trap mass spectrometer has been procured to enhance capabilities in sensitivity and is able to analyze ions generated from various ion sources. The ability to sample under ambient conditions allows the possibility to probe chemical reactions on surfaces. Here we propose to build microfluidic reactors, where pH, temperature and chemical constituents can be changed, and Drop-DESI by rastering over the surface could probe chemical change.

A second thrust would be to use the liquid junction drop as a reactor itself. Reactants will be introduced into a microdroplet (100-500 μm diameters) at constant linear speeds (i.e. adjustable flow rates in volume/time). Tunable IR lasers and X-ray synchrotron radiation will be focused on the droplet for absorption type measurements. The outgoing capillary will differentially pump the liquid droplet to an electrospray unit and into the mass spectrometer. Product evolution will be monitored via mass spectrometry, while transient intermediates will be captured either by vibrational or electronic spectroscopy. Preliminary experiments of the reaction of 1 nm palladium nanoparticles encapsulated within generation 4 hydroxylated PAMAM dendrimers with a strong oxidizing agent, iodobenzene dichloride has been probed via mass spectrometry and X-ray absorption spectroscopy directly in solution (Figure 1). In collaboration with scientists at PNNL, a System for Analysis at the Liquid Vacuum Interface (SALVI) device is being incorporated for interrogation with mass spectrometry and X-ray spectroscopy to provide a window to probe liquids in a high vacuum environment.

Saykally plans to complete a detailed study of water evaporation rates as a function of pH, comparing solutions of HCl and NaOH, as a means of addressing the controversial interfacial behavior of hydrated protons and hydroxide, respectively. We will further perfect microjet-based mixing system for generating short lived species, e.g. carbonic acid, in liquid microjets for study by X-ray spectroscopy. We will apply this technology to the study of hydration and hydrolysis of carbon dioxide, nitrogen oxides, and sulfur oxides, including temperature dependence. We also plan to construct a new endstation designed to use our liquid microjet mixing technology to address the carbonate system via X-ray photoelectron spectroscopy (XPS), in collaboration with LBL beamline scientists. While XAS probes the *empty* orbitals of a system, XPS probes its filled orbitals, providing complementary details of electronic and geometric structure and hydration. We will study the properties of aqueous carbonic acid, and its interactions with  $\text{Ca}^{2+}$  and  $\text{Mg}^{2+}$  ions, as well as other salts. Fundamental insights gained from these studies are expected to facilitate the development of  $\text{CO}_2$  sequestering schemes based on saline aquifer burial. Similar investigations of nitrogen and sulfur oxides will be explored.

Chandler's and Geissler's groups plan to pursue new fundamental studies of self-assembly. A range of model systems, from the realistic (e.g., the sedimentation of polyhedral nanocrystals in aqueous solution) to the idealized (e.g., the emergence of flower-like patterns from a binary system of disks in two dimensions), may be examined in support of their overarching goal – to develop computational tools, theoretical perspectives, and physical insight for understanding the patterned aggregation of molecularly structured components in strongly fluctuating environments. One strategy is to construct long trajectories in gradual stages from shorter trajectory slices that each connect a small number of metastable intermediates. These partial transition paths can therefore be sampled efficiently with standard path sampling tools. In order to focus attention on productive segments of time evolution, we impose constraints on complete reconstructed pathways, which must connect initial and final states. By exploiting the natural segmentation of slow dynamics in complex systems, we in effect turn the central hurdle of TPS into an asset. Landscapes for self-assembly can be explored more deeply by exerting biases on trajectory sampling other than, or in addition to, the constraint of successful ordering, focusing attention on revealing dynamics whose statistical weight is negligible in the ensemble of typical aggregation pathways.

Chandler also plans coarse-grained modeling of coarsening and grain-boundary structures, and at order-disorder transitions in membranes and the role of those transitions on the forces that organize clustering of trans-membrane particles.

### Recent Publications

T.R. Gingrich and P.L. Geissler, "Preserving correlation between trajectories for efficient path sampling," *J. Chem. Phys.* (2015) **142**, 234104, doi: 10.1063/1.4922343

Z. Liu, N. Destouches, G. Vitrant, Y. Lefkir, T. Epicier, F. Vocanson, S. Bakhti, Y. Fang, B. Bandyopadhyay, and M. Ahmed, "Understanding the Growth Mechanisms of Ag Nanoparticles Controlled by Plasmon-Induced Charge Transfers in Ag-TiO<sub>2</sub> Films," *J. Phys. Chem. C*, (2015) 119, 9496, DOI: 10.1021/acs.jpcc.5b01350

S. Y. Liu, M. Shawkey, D. Parkinson, T. Troy and M. Ahmed, "Elucidation of the chemical composition of avian melanin," *RSC Advances*, (2014), 4, 40396, DOI: 10.1039/C4RA06606E

H-W. Chang, C-C. Hsu, M. Ahmed, S-Y. Liu, Y. Fang, J. Seog, G. S. Oehrlein, and D. B. Graves, "Plasma Flux Dependent Lipid A Deactivation," *J. Phys. D: Appl. Phys.*, (2014) 47 224015

S. Neppl, A. Shavorskiy, I. Zegkinoglou, M. Fraund, D. S. Slaughter, T. Troy, M. P. Ziemkiewicz, M. Ahmed, S. Gul, B. Rude, J. Z. Zhang, A. S. Termsin, P-A. Glans, Y-S. Liu, C. H. Wu, J. Guo, M. Salmeron, H. Bluhm, and Oliver Gessner, "Capturing interfacial photo-electrochemical dynamics with picosecond time-resolved X-ray photoelectron spectroscopy," *Faraday Discuss.*, (2014), 171, 219, DOI: 10.1039/C4FD00036F

Varilly, P., and D. Chandler, "Water evaporation: a transition path sampling study," *J. Phys. Chem. B* 117, 1419-1428 (2013).

Willard, A. P., and D. Chandler, "The molecular structure of the interface between water and a hydrophobic substrate is liquid-vapor like," *J. Chem. Phys.* 141, 18C519 (2014).

Limmer, D. T., and D. Chandler, "Premelting, fluctuations and coarse-graining of water-ice interfaces," *J. Chem. Phys.* 141, 18C505 (2014).

Limmer, D. T., and D. Chandler, "The putative liquid-liquid transition is a liquid-solid transition in atomistic models of water, Part II," *J. Chem. Phys.* 138, 214504.1-15 (2013).

Limmer, D. T., and D. Chandler, "Corresponding states for mesostructure and dynamics of supercooled water," *Faraday Discuss.* 167, 485-498 (2013).

Limmer, D. T., and D. Chandler, "Time scales of supercooled water and implications for reversible polyamorphism," *Mol. Phys.* (2015). DOI:10.1080/00268976.2015.1029552

Limmer, D.T., and D. Chandler, "Comment on 'Spontaneous liquid-liquid phase separation of water'," *Phys. Rev. E* 91, 016301 (2015).

Keys, A. S., J. P. Garrahan, and D. Chandler, "Calorimetric glass transition explained by hierarchical dynamic facilitation," *Proc. Natl. Acad. Sci. USA* 110, 4482-4487 (2013).

Limmer, D.T., and D. Chandler, "Theory of amorphous ices," *Proc. Natl. Acad. Sci. USA*. 111, 9413-9418 (2014).

\*Duffey, K.C., Shih, O., Wong, N.L., Drisdell, W.S., Saykally, R.J., and Cohen, R.C. "Evaporation kinetics of aqueous acetic acid droplets: effects of soluble organic aerosol components on the mechanism of water evaporation" *Phys. Chem. Chem. Phys.* 2013, 15 (28), 11634-11639. \*Cover Article.

Lam, R. K., England, A. H., Smith, J. W., Rizzuto, A. M., Shih, O., Prendergast, D., Saykally, R. J., "The hydration structure of dissolved carbon dioxide from X-ray absorption spectroscopy" *Chem. Phys. Lett.*, 633, 214-217 (2015). \*Editor's Choice

Lam, R. K., England, A. H., Sheardy, A. T., Shih, O., Smith, J. W., Rizzuto, A. M., Prendergast, D., Saykally, R. J., "The hydration structure of aqueous carbonic acid from X-ray absorption spectroscopy" *Chem. Phys. Lett.*, 614, 282-286 (2014) \*Cover Article.

R.J. Saykally, "Air/Water Interface: Two Sides of the Acid Base Story" *Nature Chem.* 5, 82-84 (2013). DOI: 10.1038/nchem.1556

## Chemical Kinetics and Dynamics at Interfaces

*Laser induced reactions in solids and at surfaces*

**Wayne P. Hess (PI) Alan G. Joly and Kenneth Beck**

Physical Sciences Division  
Pacific Northwest National Laboratory  
P.O. Box 999, Mail Stop K8-88,  
Richland, WA 99352, USA  
[wayne.hess@pnnl.gov](mailto:wayne.hess@pnnl.gov)

Additional collaborators include: P.Z. El-Khoury, Y. Gong, S.J. Peppernick, M.T.E. Halliday  
D. Hu, R.F. Haglund Jr., A.L. Shluger, P.V. Sushko, V.A. Apkarian and M. Zamkov

### Program Scope

The chemistry and physics of electronically excited solids and surfaces is relevant to the fields of photocatalysis, radiation chemistry, and solar energy conversion. Irradiation of solid surfaces by UV, or higher energy photons, produces energetic species such as core holes and free electrons, that relax to form electron-hole pairs, excitons, plasmons, and other transient species capable of driving surface and bulk reactions. The interaction between light, metals and insulators is fundamentally important in catalysis, microelectronics, sensor technology, and materials processing. Photostimulated desorption studies, of atoms or molecules, provide a direct window into these important processes and are particularly indicative of electronic excited state dynamics. Greater understanding is gained using a combined experiment/theory approach. We therefore use *ab initio* calculations to model results from our laser desorption and photoemission experiments. The interaction between light and metal nano objects can lead to intense field enhancement and strong optical absorption through excitation of surface plasmon polaritons. Such plasmon excitation can be used for a variety of purposes such as ultrasensitive chemical detection, solar energy generation, or to drive chemical reactions. Large field enhancements can be localized at particular sites by careful design of nanoscale structures. Similar to near field optics, field localization below the diffraction limit can be obtained. The dynamics of plasmonics excitations is complex and we use finite difference time domain calculations to model field enhancements and optical properties of complex structures including substrate couplings or interactions with dielectric materials.

### Approach:

We are developing a combined photoemission electron microscopy (PEEM) and femtosecond laser approach to probe plasmonic nanostructures such as solid metal particles or lithographically produced nanostructures such as gratings, trenches, or nanohole arrays. We then correlate PEEM images with scanning electron microscopy or surface enhanced Raman spectroscopy (or the spatially resolved tip-enhanced implementation). Finite difference time domain (FDTD) calculations are used to interpret field enhancements measured by the electron and optical techniques. The effects of extreme electric field enhancement on Raman spectra is investigated using plasmonic nanostructures constructed from a metal nanoparticles or metal covered atomic force microscopy (AFM) tips on thin film metal/silica substrates. The Raman scattering from molecules positioned between these structures show greatly enhanced scattering and often highly perturbed spectra depending on nanogap dimensions or whether a conductive junction is created between tip and substrate. In photodesorption studies, photon energies are chosen to excite

specific surface structural features that lead to particular desorption reactions. The photon energy selective approach takes advantage of energetic differences between surface and bulk exciton states and probes the surface exciton directly. We measure velocities and state distributions of desorbed atoms or molecules from ionic crystals using resonance enhanced multiphoton ionization and time-of-flight mass spectrometry. Application of this approach to controlling the yield and state distributions of desorbed species requires detailed knowledge of the atomic structure, optical properties, and electronic structure. We have demonstrated surface-selective excitation and reaction on alkali halides and generalized our exciton model to oxide materials and shown that desorbed atom product states can be selected by careful choice of laser wavelength, pulse duration, and delay between laser pulses.

### **Recent Progress**

Nonlinear PEEM of isolated nanoholes in gold thin films map propagating surface plasmons (PSPs) launched from the lithographically patterned plasmonic structures. Individual holes constitute an efficient and fundamental light coupling structure in metal substrates that are easily produced and combined into more complex structures. For hole diameters ranging from 200 nm to several microns, we found that PSPs generated by 780 nm low-angle 15 fs laser pulses exhibit elongated ring-like interference patterns surrounding the hole. A notable agreement between finite difference time domain simulations and experiment corroborates our assignment of the observed photoemission patterns to PSPs launched from isolated nanoholes and probed through nonlinear photoemission. Systematically increasing hole diameter enhanced the efficiency of near field emission, as described by a simple and intuitive geometrical model, which accounts for the observed and simulated diameter dependent plasmonic response. This effort paves the way for designing nanohole assemblies where optical coupling and subsequent plasmon propagation can be rationally controlled.

We extended our above approach to nanohole arrays lithographically patterned in gold thin films. Again, PEEM was used to map PSPs launched from various array structures. Strong near field photoemission patterns are observed in the PEEM images and recorded photoemission patterns are attributed to constructive and destructive interferences between PSPs launched from the individual nanoholes which comprise the array. In examining the nanohole array geometry-dependent photoemission patterns, we find that the launched propagating SPPs can be manipulated and focused by changing the separation between the nanoholes. We then demonstrated how varying the array geometry (hole diameter, pitch, and number of rows/columns) leads to intense localized photoemission and identified optimal array geometries for efficient light coupling and interferometric plasmonic lensing. We concluded that the focal lengths of the array-based interferometric plasmonic lenses can be tuned by varying the incidence angle and wavelength of the driving laser field and that the overall efficiency of the lenses can be controlled by changing the nanohole diameters and by varying the row and column numbers of the nanohole array. With the aid of finite-difference time-domain simulations, optimal interferometric focusing of propagating SPPs can be achieved. We then demonstrated a preliminary application of interferometric plasmonic lensing by enhancing the photoemission from the vertex of a gold triangle using a nanohole array coupling and focusing element.

We recorded time-resolved nonlinear photoemission electron microscopy (tr-PEEM) images of propagating surface plasmons launched from a lithographically patterned rectangular trench on a flat gold surface. Our tr-PEEM scheme involves a pair of identical, spatially separated, and interferometrically-locked femtosecond laser pulses. The use of spatially and temporally offset pump and probe pulse pairs allows the determination of the plasmon group velocity (0.95c). Using a combination of tr-PEEM and FDTD simulations, we determined that the upper limit

for the  $1/e$  decay length of the plasmon field is 88  $\mu\text{m}$ . Power dependent PEEM images provide experimental evidence for a sequential coherent nonlinear photoemission process, in which one laser source launches a PSP through a linear interaction, and the second subsequently probes the PSP *via* two-photon photoemission. The recorded time-resolved movies of a PSP allow us to directly measure various properties of the surface-bound wave packet, including its carrier wavelength (783 nm) and group velocity. In addition, tr-PEEM images reveal that the launched PSP may be detected at least 250 microns away from the coupling trench structure. The experimentally measured PSP properties demonstrate that surface plasmons propagating on nominally flat gold surfaces may potentially be harnessed for use in mesoscale plasmonic devices, chiefly incorporated into plasmonic circuits of a few hundred microns in size.

### Future Plans

Future plans include extending time-resolved non-linear PEEM studies which offers both nanometer spatial and fs time resolution. It should be possible to capture spatially resolved field enhancement, and subsequent decay dynamics, following 800 nm fs laser excitation. Using PEEM we have measured plasmonic enhancement factors, without the presence of a molecular emitter as in surface enhanced Raman scattering (SERS). We now have the tools needed to correlate field enhancement with SERS and the tip enhanced version (TERS) response and by adding time-resolved PEEM (stabilized using a recently constructed Mach-Zhender interferometer) the path opens to an entirely new set of measurements capable of correlating structure and dynamics of a variety of designer plasmonic constructs (e.g. gaps between surface structures drawn by focused ion beam lithography or between AFM tip and surface structure). The inclusion of helium ion lithography into our arsenal, now allows sub 10 nm structures to be fabricated enabling correlated femtosecond PEEM with transmission electron microscopy (TEM) and tip-enhanced Raman spectroscopy to study plasmon resonant photoemission from noble metal nanostructures and time-resolved PEEM to probe dynamics of metal and hybrid (metal:insulator or meta material) nanostructures. We will interrogate such metal-insulator systems using a variety of advanced techniques including: x-ray and ultraviolet photoelectron spectroscopy (XPS, UPS) femtosecond nonlinear photoemission, PEEM, SERS, TERS, TEM (and energy resolved variants) for spatially-resolved Raman and EELS spectroscopy. Femtosecond time-resolved PEEM can reveal spatially resolved ultrafast dynamics and is a powerful tool for studying the near-surface electronic states of nanostructures or plasmonic devices. We have recently developed capabilities to perform energy-resolved two-photon photoemission using a hemispherical analyzer XPS instrument. In combination we expect these two techniques will provide spatially-resolved electronic state dynamics of nanostructured metal-insulator materials.

### References to publications of DOE BES sponsored research (2013 to present)

1. S.J. Peppernick, A.G. Joly, K.M. Beck and W.P. Hess, J. Wang, Y.C. Wang and W.D. Wei, "Two-Photon Photoemission Microscopy of a Plasmonic Silver Nanoparticle Trimer," *Appl. Phys. A* **112**, 35 (2013).
2. A. Polyakov, C. Senft, K.F. Thompson, J. Feng, S. Cabrini, P.J. Schuck, H.A. Padmore, S.J. Peppernick, and W.P. Hess, "Plasmon enhanced photocathode for high brightness and high repetition rate x-ray sources" *Phys. Rev. Lett.* **110**, 076802 (2013).
3. P.Z. El-Khoury, S.J. Peppernick, D. Hu, A.G. Joly, and W.P. Hess "The Origin of Surface-Enhanced Raman Scattering of 4,4'-Biphenyldicarboxylate on Silver Substrates" *J. Phys. Chem. C*, **117**, 7260 (2013).
4. S.J. Peppernick, A.G. Joly, K.M. Beck, and W.P. Hess "Plasmon-Induced Optical Field Enhancement studied by Correlated Scanning and Photoemission Electron Microscopy", *J. Chem.*

- Phys.* **138**, 154701 (2013).
5. P.Z. El-Khoury, D. Hu, V.A. Apkarian and W.P. Hess, "Raman Scattering at Plasmonic Junctions Shorted by Conductive Molecular Bridges" *Nano Lett.* **13**, 1858 (2013).
  6. M.T.E. Halliday, A.G. Joly, W.P. Hess, P.V. Sushko and A.L. Shluger, "Photodesorption of Br-atoms from crystalline CsBr thin films grown on LiF and KBr(100)," *J. Phys. Chem. C*, **117**, 1302 (2013).
  7. P.Z. El-Khoury, W.P. Hess, "A Theoretical Investigation of Raman from a Single 1,3-Propanedithiol Molecule." *Chem. Phys. Lett.* **581**, 57 (2013).
  8. P.Z. El-Khoury, D. Hu, and W.P. Hess, "Junction Plasmon Induced Molecular Reorientation" *J. Phys. Chem. Lett.* **4**, 3435 (2013).
  9. P.Z. El-Khoury, E.J. Bylaska, and W.P. Hess, "Time Domain Simulations of Chemical Bonding Effects in Surface-Enhanced Spectroscopy." *J. Chem. Phys.* **139**, 174303 (2013).
  10. P.Z. El-Khoury, W.P. Hess, "Vibronic Raman Scattering at the Quantum Limit of Plasmons" *Nano Lett.* **14**, 4114 (2014).
  11. P.Z. El-Khoury, K. Honkala, W.P. Hess, "Electronic and Vibrational Properties of Meso-Tetraphenylporphyrin on Silver Substrates." *J. Phys. Chem. A* **118**, 8115 (2014).
  12. Patrick Z. El-Khoury, Wayne Hess, "Vibronic Raman Scattering at the Quantum Limit of Plasmons" *Nano Lett.* **14**, 4114 (2014).
  13. Y. Gong, A.G. Joly, P.Z. El-Khoury, and W.P. Hess, "Nonlinear Photoemission Electron Micrographs of Plasmonic Nanoholes in Gold Thin Films" *J. Phys. Chem. C* **118**, 25671 (2014).
  14. P.Z. El-Khoury, T.W. Ueltschi, A.L. Mifflin, D. Hu, and W.P. Hess, "Frequency Resolved Nano-scale Chemical Imaging of 4,4'-Dimercaptostilbene on Silver" *J. Phys. Chem. C* **118**, 27525 (2014).
  15. Y. Gong, A.G. Joly, P.Z. El-Khoury and W.P. Hess, "Interferometric Plasmonic Lensing with Nanohole Arrays" *J. Phys. Chem. Lett.* **5**, 4243 (2014).
  16. P.Z. El-Khoury, E. Khon, Y. Gong, A.G. Joly, P. Abellan, J.E. Evans, N.D. Browning, D. Hu, M. Zamkov, W.P. Hess, "Electric Field Enhancement in a Self-Assembled 2D Array of Silver Nanospheres", *J. Chem. Phys.* **141**, 214308 (2014).
  17. Y. Gong, A.G. Joly, P.Z. El-Khoury, L.M. Kong and W.P. Hess "High Brightness Plasmon-Enhanced Nanostructured Gold Photoemitter" *Phys. Rev. Appl.* **2**, 064012 (2014).
  18. P.Z. El-Khoury, Y. Gong, P. Abellan, B.W. Arey, A.G. Joly, D. Hu, J.E. Evans, N.D. Browning, W.P. Hess "Tip-Enhanced Raman Nanographs: Mapping Topography and Local Electric Fields" *Nano Lett.* **15**, 2385 (2015).
  19. Y. Gong, Alan G. Joly, Dehong Hu, Patrick Z. El-Khoury and Wayne P. Hess, "Ultrafast Imaging of Surface Plasmons Propagating on a Gold Surface" *Nano Lett.* **15**, 3472 (2015).
  20. R.B. Davidson II, J.I. Ziegler, G. Vargas, S.M. Avanesyan, Y. Gong, W. Hess, R.F. Haglund Jr., "Efficient Forward Second-Harmonic Generation from Planar Archimedean Nanospirals" *Nanophotonics*, **4**, 108 (2015).
  21. M.T.E Halliday, W.P Hess, A L Shluger, "Structure and properties of electronic and hole centers in CsBr from theoretical calculations" *J. Phys. Condens. Matter* **27**, 245501 (2015).
  22. P.Z. El-Khoury, G.E. Johnson, I.V. Novikova, Y. Gong, A.G. Joly, J.E. Evans, M. Zamkov, J. Laskin and W.P. Hess "Enhanced Raman Scattering from Aromatic Dithiols Electrosprayed into Plasmonic Nanojunctions" *Faraday Discuss.* **2015**, DOI: 10.1039/C5FD00036J
  23. S.A. Fischer, T.W. Ueltschi, P.Z. El-Khoury, A.L. Mifflin, W.P. Hess, H.F. Wang, C.J. Cramer, and N. Govind, "Molecular Dynamics and Static Normal Mode Analysis: The C-H Region of DMSO as a Case Study" *J. Phys. Chem. B* (2015) DOI: 10.1021/acs.jpcc.5b03323.

## Spectroscopic Imaging of Molecular Functions at Surfaces

*Wilson Ho*

Department of Physics & Astronomy and of Chemistry  
University of California, Irvine  
Irvine, CA 92697-4575 USA

[wilsonho@uci.edu](mailto:wilsonho@uci.edu)

### **Program Scope:**

This project focuses on the understanding of the nature of the chemical bonds and interactions through single molecule spectromicroscopy using the newly developed inelastic tunneling probe (itProbe) with the scanning tunneling microscope (STM). It can be argued that chemistry is dictated by the outer electron densities of the interacting molecules. The presence of an atom or molecule defines the potential energy surface in space. As two molecules approach each other, or when two atoms form a bond, the overall potential energy surface becomes modified from those of isolated entities. Specifically, itProbe provides an image related to the two-dimensional slice of the potential energy surface at a chosen height above the surface. Comparison of measurements to density functional theory (DFT) calculations gives insights into the origin of the contrast in the itProbe images by relating them to the potential energy surface of the composite CO-tip with the species adsorbed on the surface. Changes in the CO vibrational energy, intensity, and line shape trace back to variations in the electron density on the surface. Contrast in the itProbe image corresponds to contours of constant CO vibrational energy. The itProbe with the STM has the capability to resolve atomic scale variations in the potential energy surface. Changes in the electron density indicate electron rearrangement that can be used to define bonding and molecular interactions. These experiments with the STM would lead to an understanding of the inner machinery of single molecules that are not possible with other approaches, providing information on the electronic, vibrational, and structural properties, as well as the relation of these properties to the reactivity, chemical sensing, self-assembly, and other chemical interactions. Results from these studies yield the molecular basis for understanding properties, processes, and phenomena in chemical and physical systems over different length scales from the atomic to macroscopic ensembles. The experiments rely on the unique properties of the STM operating at 600 mK. Results from this project provide new insights into surface chemistry and catalysis, environmental processes and energy generation, electronic processing and electron transport through molecules as in molecular electronics.

### **Recent Progress:**

The most recent results obtained during the past year are described in this report, highlighting the spectroscopic imaging of the molecular structure and the nature of intermolecular interactions responsible for self-assembly. The arrangement of atoms in a molecule implicates its physical and chemical properties. The STM previously has provided spatially resolved electronic and vibrational signatures of single molecules. However, the spatial distributions of these signatures do not relate directly to the geometric structures of the

molecules. When a CO-terminated tip is scanned over adsorbed species, the energy, intensity, and line shape of the lowest energy vibration, the hindered translational mode of CO, show spatial variations, the origin of contrast seen in the itProbe images. These variations in the CO vibration are detected by inelastic electron tunneling spectroscopy (IETS) with the STM. Spatial imaging at a selected energy within the peak of the hindered translational mode of the CO-tip yields direct visualization of the skeletal structure of the molecule and intermolecular electron density rearrangement. The combined capabilities of the STM suggest the possibility of relating the structure (electronic, vibrational, and geometric) and function in chemistry.

During this grant period, the itProbe was used to image 1,3-difluorobenzene ( $C_6H_4F_2$ ), hexafluorobenzene ( $C_6F_6$ ), and benzene ( $C_6H_6$ ) on Ag(110) surface. These results visualize halogen bonding that leads to intermolecular interactions responsible for self-assembly of ordered two-dimensional islands. The number and location of the fluorine atoms influence the nature of the intermolecular interactions that cause differences in the translational and rotational orders of the molecules within the self-assembly. An example of a self-assembled island of 1,3-difluorobenzene in Fig. 1 shows clearly the locations of the two C-F bonds. The island shows translational order but orientation disorder due to the two C-F bonds. The intermolecular

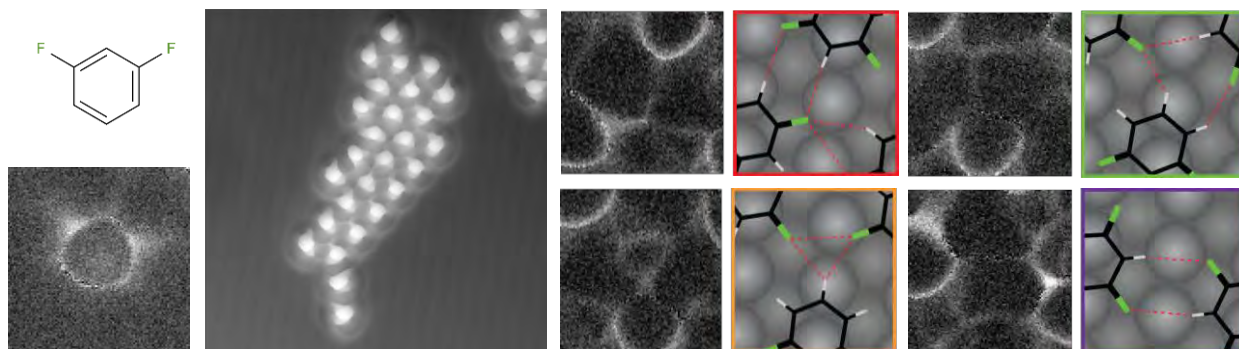


**Fig. 1:** 1,3-difluorobenzene on Ag(110) showing the schematic molecular structure (leftmost top); itProbe image of the skeletal structure of the molecule (the two “ears” are the positions of the two C-F bonds), (leftmost bottom); island of self-assembled molecules revealing the two “ears” in each molecule (second from left); the different types of bonds in the island are imaged by itProbe and are shown in the right half of the figure with schematic diagrams corresponding to the itProbe images.

interactions are mainly hydrogen bonding between the F and the H and the less frequent halogen bonding between two F atoms due to the 1:2 ratio of F:H in each molecule.

When all the H atoms are replaced by F atoms, the self-assembly of  $C_6F_6$  would not be expected because the electronegative F atoms around the molecule would suggest a repulsive interaction between the molecules. However, islands of  $C_6F_6$  are formed with translational and rotational ordering of the molecules in each island. Indeed, a rich network of intermolecular interactions is revealed by the itProbe images. Instead of negative point charge depicting each F atom, the spatial distribution of the charge density in the C-F bond needs to be considered. Bonding of F to the C leads to a decrease of charge at the end of the F (sigma hole) due to charge sharing from F to the C atom and a concomitant charge accumulation around the equator of the F atom. This charge redistribution leads to favorable electrostatic interaction between two F atoms if the end of one F atom points to the side or the equator of the other F atom. Thus the two C-F

bonds should deviate significantly from a linear geometry to optimize electrostatic interaction between the two C-F bonds. The itProbe image of the intermolecular interactions that lead to the self-assembly of  $C_6F_6$  molecules is shown in Fig. 2. In addition, all six C-F bonds in each molecule are clearly revealed in each molecule. Side bonding between two C-F bonds is seen in the itProbe image, creating the rich intermolecular network that leads to translational and rotational order for molecules in the self-assembled islands. The molecules are all tilted at  $11^\circ$  from the vertical in order to optimize bonding and lowering of energy for the assembly.

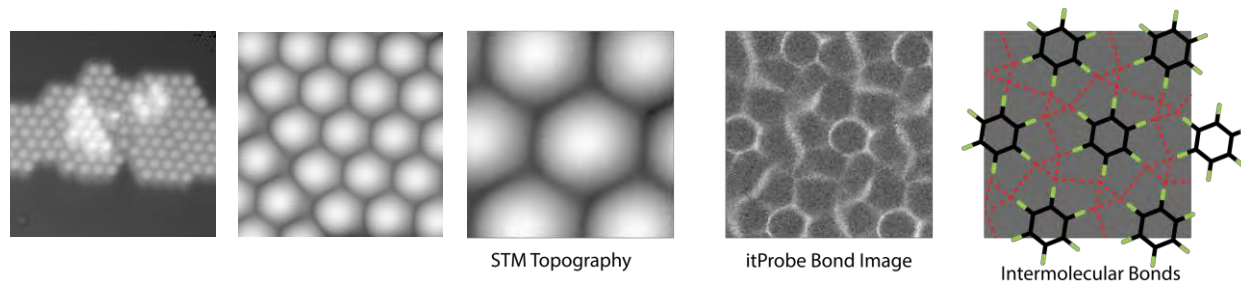


**Fig. 2:** Self-assembly of an island of  $C_6F_6$  with partial second layer formation (leftmost panel); zoom in of the first layer (second from left); zoom in further (STM topography); itProbe image of the bonds for 6  $C_6F_6$  molecules (itProbe Bond Image); schematic diagram showing intermolecular bonds in red dashed lines (Intermolecular Bonds).

Significant differences separate  $C_6H_6$  from  $C_6F_6$  (or  $C_6H_4F_2$ ) for benzene without fluorine. Self-assembly of  $C_6H_6$  does not occur as clearly seen in Fig. 3 where molecules adsorb in isolation for similar coverages as the fluorinated benzene molecules. The lack of island formation suggests that the intermolecular interactions between  $C_6H_6$  molecules are weak, certainly weaker than the interaction of each molecule with the Ag(110) surface. The  $C_6H_6$  molecules preferentially adsorb at step edges because the adsorption energy is higher. Structural images of  $C_6H_6$  molecules obtained by itProbe provide new insights into the concept of the size and shape of molecules. For  $C_6H_6$  adsorbed on the flat terrace of Ag(110) compared to the known molecular geometry, the skeletal structure shows a larger size and has the rectangular symmetry of the substrate surface. In contrast, a molecule at the step edge has a size close to the known structure of  $C_6H_6$  and the expected hexagonal symmetry. The CO-tip maps out the spatial variations in the potential energy surface above the  $C_6H_6$  that affect the vibrational mode of the CO. The potential energy surface is defined primarily by the  $C_6H_6$  electron density and the associated potential energy surface. The itProbe images reveal that a benzene molecule has variable size and shape as seen by a CO molecule at a certain height above it. The itProbe senses changes in the CO hindered translational vibration that depends on the spatial variations in the potential energy surface defined predominantly by the adsorbed  $C_6H_6$ .

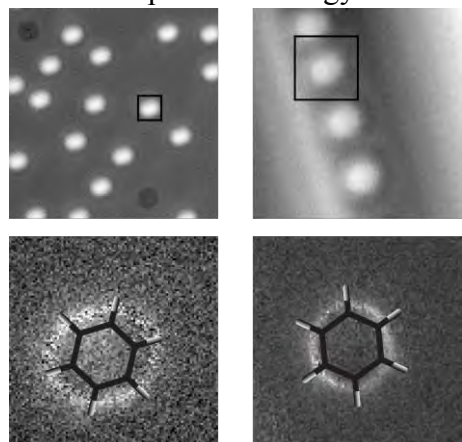


**Fig. 3:** Topographic (z) images of  $C_6H_6$  molecules adsorbed on the terrace (top left panel) and step edge (top right panel), and the corresponding itProbe images (bottom panels) of single  $C_6H_6$  molecules selected by the black squares in the z-images. The known skeletal structure of  $C_6H_6$  is overlapped for comparison of size and shape.

The ability of the STM to image molecular structure is an important addition to its previously shown capabilities for manipulation and the determination of the electronic and vibrational properties. These results suggest opportunities to relate structure and function in chemistry at the single molecule level.

### **Future Plans:**

The relationship among the molecular composition, structure, bonding, and reactivity is one of the central dogmatic principles in chemistry. The itProbe images the structure and bonding in single molecules and interactions between molecules that are responsible for the formation of larger molecular structures. Experiments are in progress to measure by the itProbe the size and shape of C<sub>6</sub>H<sub>6</sub> on a substrate with a different symmetry, specifically Cu(111) to contrast with the Ag(110) substrate. The focus of future plans lies in elucidating the nature of traditionally classified bonds, specifically the ionic, covalent, coordination, hydrogen, and van der Waals bonds. In addition, using the itProbe, it has been possible to reveal unexpected interactions between atoms, particularly when one of the participating partners is a H atom. The lightest element exhibits notoriously quantum mechanical properties and a H atom has been imaged to be shared in multi-centered bonds. Specific systems for investigation in the future plans include azulene, isocyanides (e.g. 1,4-phenylene diisocyanide), and NaCl.

### **References to Publications of DOE Sponsored Research:**

[1] “*Interplay between Electronic Properties and Interatomic Spacing in Artificial Gold Chains on NiAl(110)*”, N. Nilius, T.M. Wallis, M. Persson, and W. Ho, *J. Phys. Chem. C* **118**, 29001-29006 (2014). Additional support is obtained for N.N. from the Deutsche Forschungsgemeinschaft Fellowship, and for M.P. from the Swedish Research Council.

[2] “*Rotational Spectromicroscopy: Imaging the Orbital Interaction between Molecular Hydrogen and an Adsorbed Molecule*”, S. Li, D. Yuan, A. Yu, G. Czap, R. Wu, and W. Ho, *Phys. Rev. Lett.* **114**, 206101 (2015). Additional support is obtained for S.L. A.Y., and D.Y. from the NSF Center for Chemical Innovation: Chemistry at the Space-Time Limit.

[3] “*Single-Molecule Rotational and Vibrational Spectroscopy and Microscopy with the Scanning Tunneling Microscope*”, A. Yu, S. Li, G. Czap, and W. Ho, *J. Phys. Chem. C*, DOI: 10.1021/acs.jpcc.5b00494 (2015). Additional support is obtained for A.Y. and S.L. from the NSF Center for Chemical Innovation: Chemistry at the Space-Time Limit.

## Development of Approaches to Model Excited State Charge and Energy Transfer in Solution

**Lead PI:** Christine Isborn, University of California Merced

**PI:** Aurora Clark, Washington State University

**PI:** Thomas Markland, Stanford University

The aim of this recently funded project (started 9/1/2015) is to develop accurate and efficient theoretical methods to compute ground and excited states, as well as the ability to treat the dynamics of electrons, protons, and excitations in the presence of solvent fluctuations occurring over a range of time-scales. To address such a challenge requires accurate and efficient methods to compute ground and excited states, as well as the ability to treat the dynamics of electrons, protons, and excitations in the presence of solvent. This project aims to provide a unified approach to treat these processes in large chemical systems by creating a highly scalable computational approach that accurately and efficiently computes electronic ground and excited states.

This project will involve the development by Isborn of the GPU accelerated time-dependent density functional theory code within TERACHEM. The speed-up of the computations allows TERACHEM to perform fully quantum mechanical ground and excited state calculation on molecules of unprecedented size (~10,000 electrons). The convergence of excited state properties and how they may differ from those of the ground state will be examined, QM/MM interfaces will be tuned for better agreement with experimental hydration free energies and aqueous absorption spectra, TDDFT functionals that are accurate for large-scale aqueous excited state calculations (including explicit solvent) will be determined, and the real-time TDDFT method will be benchmarked and developed to provide a more accurate and efficient fully ab initio model for electron transfer dynamics.

This will be combined with Markland's work to treat the quantum dynamics of nuclei on single adiabatic surfaces, via the ring polymer molecular dynamics (RPMD) approach, and also for electronically non-adiabatic processes via techniques based on combining semiclassical trajectory-based approaches with those based on direct evolution of the reduced density matrix. This project will further develop Markland's recent method to treat nonadiabatic dynamics in which the reduced density matrix is evolved by using a semiclassical approximation within a generalized quantum master equation (GQME) framework. The major advantage of using semiclassical approaches to directly evolve the reduced density matrix in this way is that the problem of calculating the long time evolution of the quantum system, i.e. the motion of the proton and electron states, is mapped onto a series of short time trajectories. Hence this approach (i.) takes advantage of the short time accuracy of semiclassical trajectories (ii.) reduces the cost of each trajectory and the cost due to failure of any particular trajectory (iii.) allows for mass computational parallelization of the trajectories.

Clark will utilize recently introduced methods that use data analytics techniques to decompose the roles of ultrafast processes from longer scale organizational features, which can be used in conjunction with Markov chain models to elucidate the role of solute-solvent organizational structure in the dynamics. To fully realize the effects of solute-solvent coupling upon reactivity, a detailed understanding of the multiscale dynamics and correlations between solute and solvent motion must be also invoked. Thus, new data analytics techniques of Clark are needed that decouple ultrafast processes from longer scale organizational features, which can be used to understand free energy landscapes that include solute-solvent structure.

By integrating these methods, a hierarchical computational approach for solution phase reactions will be obtained. The research targets improved accuracy for ground and excited states in aqueous solution, with a specific focus on excited state proton transfer, electron transfer (ET) and proton coupled electron transfer (PCET) reactions. Modeling of excited states in solution is necessary for studying photoinitiated PCET and heterogeneous/homogeneous photocatalysis, as well as other energy transfer related processes.

The results will provide more accurate and efficient theoretical models for solution phase reactions that will be used to achieve a deeper understanding of the role of solvent and hydrogen bonding in excited state and electron transfer processes. The development and combination of these computational approaches will enable the broader computational community to access solution phase reactivity at an unprecedented level of chemical complexity, and thus true predictive models will be developed that aid in experimental interpretation and the rational design of solution-mediated processes.

THEORY OF THE REACTION DYNAMICS OF SMALL MOLECULES  
ON METAL SURFACES

Bret E. Jackson

Department of Chemistry  
104 LGRT  
710 North Pleasant Street  
University of Massachusetts  
Amherst, MA 01003  
jackson@chem.umass.eduProgram Scope

Our objective is to develop realistic theoretical models for molecule-metal interactions important in catalysis and other surface processes. The dissociative adsorption of molecules on metals, Eley-Rideal and Langmuir-Hinshelwood reactions, recombinative desorption and sticking are all of interest. To help elucidate the experiments that study these processes, we examine how the reaction dynamics depend upon the nature of the molecule-metal interaction, as well as experimental variables such as substrate temperature, beam energy, angle of impact, and the internal states of the molecules. Electronic structure methods based on Density Functional Theory (DFT) are used to compute each molecule-metal potential energy surface (PES). Both time-dependent quantum scattering techniques and quasi-classical methods are used to examine the reaction dynamics. Effort is directed towards developing improved quantum methods that can accurately describe reactions, as well as include the effects of temperature (lattice vibration) and electronic excitations.

Recent Progress

The dissociative chemisorption of methane on a Ni catalyst is the rate-limiting step in the chief industrial process for H<sub>2</sub> production. This reaction, where a single C-H bond breaks, leaving CH<sub>3</sub> and H fragments bound to the surface, has a high barrier and a correspondingly small dissociative sticking probability that increases exponentially with collision energy below saturation. The reaction has an unusually strong dependence on the temperature of the substrate, and is also enhanced by vibrational excitation of the methane, but in a non-statistical fashion. Much of our recent work has focused on this reaction in an attempt to understand how methane reactivity varies with the temperature of the metal, the translational and vibrational energy in the molecule, and the properties of the metal surface. Using DFT to locate the transition state on several Ni and Pt surfaces, we find that vibrational motion of the metal atom over which the molecule dissociates changes the height of the barrier to dissociation. From this we have developed models that accurately introduce the effects of lattice motion (substrate temperature) into our scattering calculations. We describe the reaction dynamics using a fully quantum approach based on the Reaction Path Hamiltonian (RPH). Our PES is harmonic for small displacements away from the reaction (or minimum energy) path, and if we ignore anharmonic terms for larger displacements, we can use DFT to compute a reasonably accurate PES that includes all 15 molecular degrees of freedom. We expand the total wavefunction in the adiabatic vibrational states of the molecule, and evolve it in time. We have used this approach, based entirely on *ab initio* data, to elucidate experimental studies of methane dissociative adsorption by the Utz (Tufts) and Beck (EPFL) groups on Ni(100), Ni(111), and Pt(110)-(1x2), with much success.

Recent experimental studies of CH<sub>4</sub> dissociation on Pt(111) by the Beck group show that the saturation coverage of CH<sub>3</sub> on the surface increases with both the translational energy and vibrational excitation of the incident molecule. We used DFT to examine how the dissociation barrier is modified by the presence of chemisorbed H and CH<sub>3</sub> fragments, finding that this barrier increases as the surface coverage of reaction products increases [1]. Using these results, we developed kinetic models that were able to reproduce and explain the saturation behavior observed in the experimental uptake curves, publishing a joint paper with the Beck group [1]. In another study, we used a purely classical RPH to examine methane reactions on Ni(100) and Ni(111) [2]. First, we showed that the perturbative assumptions made in our quantum RPH model are valid. Second, we showed that classical trajectory methods overestimated the reaction probability of molecules in the ground vibrational state at lower energies, due to an unphysical flow of zero point energy within the molecule [2].

In collaboration with the Kroes group (Leiden) we have used AIMD, *ab initio* molecular dynamics, to study methane dissociation on moving Pt(111) and Ni(111) surfaces. In AIMD, one computes the instantaneous forces on the particles “on the fly”, using DFT in our case, eliminating the need to construct approximate many-dimensional PESs. This is a collaboration with the Beck and Utz groups, who are performing experiments on these metal surfaces at high energies, where classical methods should be accurate. The first set of studies, on Pt(111), verified that our sudden treatment of molecular motion parallel to the surface was accurate[4]. It also confirmed that reactions at lower energies occurred close to the top sites, where the barriers were lowest. These studies allowed us to benchmark the accuracy of our DFT-based PES, confirming that the barrier was too low, as suspected. Finally, this work suggested that our treatment of molecular rotation could be improved. We explored methods for doing this in a subsequent paper [5]. In particular, we showed that a sudden treatment of molecular rotation was easily implemented, leading to better results. New AIMD results for Ni(111) were shown to be consistent with our earlier work. We also significantly expanded our basis set and coupling order, demonstrating full convergence for our RPH-based approach [5].

Exciting the vibrational modes of methane can significantly enhance reactivity. This increase, relative to that from putting the same amount of energy into translational motion, the so-called efficacy, is different for different vibrational modes, as well as for the same mode on different metal surfaces. We showed that on Ni(100) the symmetric stretch significantly softens at the transition state and is strongly coupled to the reaction coordinate. As a result there is a large vibrational efficacy for this mode, as observed by two experimental groups. We demonstrated how the efficacies for vibrational enhancement are related to transitions from higher to lower energy vibrationally adiabatic states, or to the ground state, with the excess energy going into motion along the reaction path, which corresponds to bond breaking at the transition state. We have been able to elucidate similar behavior on Ni(111) [5]. Overall, agreement with experiment has been good, in terms of both the magnitude of the reactivity over a broad range of incident energies and temperatures, and the efficacies of the different vibrational modes for promoting reaction. More importantly, our approach made it possible to follow the flow of energy within the molecule as it dissociates, providing a detailed understanding of how translational, vibrational and lattice energy contribute to reactivity. Our work on this was summarized in a invited Feature Article in *J. Phys. Chem.* [7].

We computed a new, more accurate, PES for methane dissociation on Ni(111), and have focused on several recent experiments involving the isotopologues of methane, CH<sub>x</sub>D<sub>4-x</sub>. Of particular interest are bond-selective reactions (by vibrational excitation) and the effects of mass, tunneling, and zero point energy on reactivity. In a recent study of the dissociative chemisorption of CHD<sub>3</sub> on Ni(111) we found that the symmetric stretches of the CD<sub>3</sub> group were more

efficacious at promoting C-D bond scission than the antisymmetric  $\text{CD}_3$  stretches [8]. In addition, while we could get 100% bond-selectivity by exciting the C-H stretch, exciting either C-D stretch mode was not as selective. These reactions exhibited an interesting (but explainable) variation with temperature and energy.

We have examined the dissociative chemisorption of  $\text{H}_2\text{O}$ ,  $\text{HOD}$  and  $\text{D}_2\text{O}$  on  $\text{Ni}(111)$  using our RPH approach [9]. This was motivated by recent experimental results from the Beck group, who are the very first to measure dissociative sticking probabilities for water on a metal surface. Mode-selective chemistry is observed, as for methane, with both stretch modes strongly enhancing reactivity. The effects of lattice motion are more complicated than for methane, with several types of motion able to modify the barrier to reaction. Overall, agreement with experiment was good.

In a collaboration with the experimental group of Art Utz, we looked more closely into the variation in reactivity of  $\text{CH}_4$  on  $\text{Ni}(111)$  with temperature [12]. They were able, for the first time, to measure the variation in the dissociative sticking probability over a large temperature range, providing a more rigorous test for our models. Our new PES and RPH-based scattering calculation accurately reproduced this variation. Moreover, we were able to show why the variation was so strong below threshold, and were able to relate this threshold energy to properties of our PES.

In other (minor) work we co-authored a book chapter in a Springer text aimed at a more general audience, focusing on quantum effects in reactions [3]. We also have a brief Comment appearing in *Phys. Rev. Lett.*, regarding an earlier study in that journal that examined H atom trapping and sticking on graphene at very low temperatures [6]. Finally, we contributed to two studies that used statistical models to examine the scattering and sticking of H atoms on graphene surfaces [10,11].

### Future Plans

We have computed a new, more accurate, PES for methane dissociation on  $\text{Ni}(111)$ , and now have our first PES for the reaction on  $\text{Pt}(111)$ . We will continue to use the new  $\text{Ni}(111)$  surface in studies focused on several recent experiments involving the isotopologues of methane,  $\text{CH}_x\text{D}_{4-x}$ . Of particular interest are bond-selective reactions (by vibrational excitation) and the effects of mass, tunneling, and zero point energy on reactivity. We will also explore some improvements to our RPH-based scattering approach, particularly our treatment of molecular rotation. These PESs will also be used in our on-going collaboration with the Beck and Utz groups, who are making new measurements of  $\text{CD}_3\text{H}$  dissociation on  $\text{Pt}(111)$  and  $\text{Ni}(111)$ , respectively. We have not yet applied our RPH-based approach to  $\text{Pt}(111)$ , and it will be interesting to explore the mode-specific chemistry that has been observed on that metal. Also of interest is the relative reactivity of the  $\text{Ni}(111)$  and  $\text{Pt}(111)$  surfaces. Our earlier work found the Pt surface to be more reactive than the Ni, but experiment suggests that the difference is much larger than our study found. The behavior of the methyl group during the dissociation is different on the two metals, and this may play a role. We are also beginning to explore the reactions of other molecules. In addition to water, we are interested in the dissociative chemisorption of  $\text{CO}_2$  and  $\text{NH}_3$ . It will be interesting to see if these other systems exhibit the strong temperature effects, mode-selectivity and bond-specificity of the methane reactions.

We also have an ongoing project examining H-Ag interactions, motivated by experiments in the Wodtke group (MPI, Göttingen). In particular, we are examining scattering, subsurface

penetration and thermal desorption, in collaboration with the Lemoine group in Toulouse, and Sven Nave in Orsay.

DOE-Sponsored Publications (past 2 years)

[1] H. Ueta, L. Chen, R. D. Beck, I. Colón-Díaz and B. Jackson, “Quantum state-resolved CH<sub>4</sub> dissociation on Pt(111): Coverage dependent barrier heights from experiment and density functional theory,” *Phys. Chem. Chem. Phys.* 15, 20526 – 20535 (2013).

[2] M. Mastromatteo and B. Jackson, “The dissociative chemisorption of methane on Ni(100) and Ni(111): Classical and quantum studies based on the Reaction Path Hamiltonian,” *J. Chem. Phys.* 139, 194701-1 – 9 (2013).

[3] C. Díaz, A. Gross, B. Jackson and G.-J. Kroes, “Elementary Molecule-Surface Scattering Processes Relevant to Heterogeneous Catalysis: Insights from Quantum Dynamics Calculations,” in *Molecular Quantum Dynamics*, Springer Series Physical Chemistry in Action, pp. 31 – 58, 2014, ed. F. Gatti.

[4] F. Nattino, H. Ueta, H. Chadwick, M. van Reijzen, R. D. Beck, B. Jackson, M. C. van Hemert, and G.J. Kroes, “Ab Initio Molecular Dynamics Calculations versus Quantum-State Resolved Experiments on CHD<sub>3</sub> + Pt(111): New Insights into a Prototypical Gas-Surface Reaction,” *J. Phys. Chem. Lett.* 5, 1294-1299 (2014).

[5] B. Jackson, F. Nattino, and G.J. Kroes, “Dissociative chemisorption of methane on metal surfaces: Tests of dynamical assumptions using quantum models and ab initio molecular dynamics,” *J. Chem. Phys.* 141, 054102 (2014).

[6] B. Lepetit and B. Jackson, Reply to “Comment, *Phys. Rev. Lett.* 113, LTK1078 (2014),” *Phys. Rev. Lett.* LSK1108 (2014).

[7] S. Nave, A. K. Tiwari and B. Jackson, “The Dissociative Chemisorption of Methane on Ni and Pt Surfaces: Mode-specific Chemistry and the Effects of Lattice Motion,” *J. Phys. Chem. A* 118, 9615-9631 (2014).

[8]. H. Guo and B. Jackson, “Mode- and Bond- Selective Chemistry on Metal Surfaces: The Dissociative Chemisorption of CHD<sub>3</sub> on Ni(111),” *J. Phys. Chem. C* 119, 14769-14779 (2015).

[9]. A. Farjamnia and B. Jackson, “The Dissociative Chemisorption of Water on Ni(111): Mode- and Bond- Selective Chemistry on Metal Surfaces,” *J. Chem. Phys.* 142, 234705 (2015).

[10]. M. Bonfanti, B. Jackson, K. H. Hughes, I. Burghardt and R. Martinazzo, “Quantum Dynamics of Hydrogen Atoms on Graphene: I. System-bath Modeling,” *J. Chem. Phys.* (accepted).

[11]. M. Bonfanti, B. Jackson, K. H. Hughes, I. Burghardt and R. Martinazzo, “Quantum Dynamics of Hydrogen Atoms on Graphene: II. Sticking,” *J. Chem. Phys.* (accepted).

[12]. V. L. Campbell, N. Chen, H. Guo, B. Jackson and A. L. Utz, “Substrate Vibrations as Promoters of Chemical Reactivity on Metal Surfaces,” *J. Phys. Chem. C* (accepted).

## DE-FG02-07ER15889: Probing catalytic activity in defect sites in transition metal oxides and sulfides using cluster models: A combined experimental and theoretical approach

Caroline Chick Jarrold and Krishnan Raghavachari

Indiana University, Department of Chemistry, 800 East Kirkwood Ave.

Bloomington, IN 47405

[cjarrold@indiana.edu](mailto:cjarrold@indiana.edu), [kraghava@indiana.edu](mailto:kraghava@indiana.edu)

### I. Program Scope

Our research program combines experimental and computational methods to study a range of cluster models for heterogeneous catalytic materials. The focus of our studies has been transition metal oxide and sulfide clusters in lower-than-traditional oxidation states, and their chemical and physical interactions with water. More recent efforts have included cluster-alcohol reactivity studies to further investigate the importance of  $-H$  mobility in  $M_xO_y^- + H_2O \rightarrow M_xO_{y+1}^- + H_2$  reaction kinetics, and the introduction of unsaturated hydrocarbons in the cluster water reaction to evaluate their potential role as sacrificial reagents in full-cycle processes. The goal is to model and understand the role of various processes involved in  $H_2$  production from photocatalytic decomposition of water using Group 6 (Mo and W) oxides and sulfides. The experiments and calculations are designed to probe fundamental, cluster-substrate molecular-scale interactions that are governed by charge state, peculiar oxidation states, and unique molecular structures.

The general strategy of our studies continues to be as follows: (1) Determine how the molecular and electronic structures of transition metal suboxide and subsulfide clusters evolve as a function of oxidation state by reconciling anion photoelectron spectra of the bare clusters with high-level DFT calculations. Anions are of particular interest because of the propensity of metal oxide and sulfides to accumulate electrons in applied systems. (2) Measure and analyze the kinetics of cluster reactivity with water, with and without the inclusion of sacrificial reagents. (3) Dissect possible reaction mechanisms computationally, to determine whether catalytically relevant interactions are involved. (4) Verify these challenging computational studies by spectroscopic investigation [typically, anion photoelectron (PE) spectroscopy] of observed reactive intermediates. (5) Probe the effect of local electronic excitation on bare clusters and cluster complexes, to evaluate photocatalytic processes. The overarching goal of this project is to identify particular defect structures that balance structural stability with electronic activity, both of which are necessary for a site to be simultaneously robust and catalytically active, and to find trends and patterns in activity that can lead to improvement of existing applied catalytic systems, or the discovery of new systems.

### II. Recent Progress

A. Non- and Anti-Arrhenius behavior in  $M_xO_y^- + H_2O$  ( $M = Mo, W$ ) reactions. We recently installed a

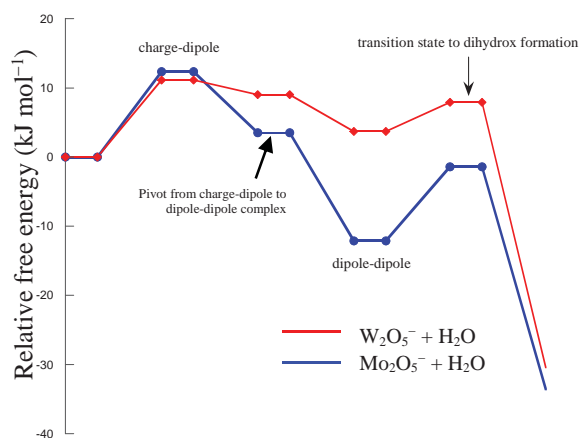


**Figure 1.** Schematic showing calculated free energies along entrance channel for  $M_xO_y^- + H_2O$  reactions

temperature variable high-pressure fast-flow reactor into the apparatus used in all DOE-funded studies of the Group 6 transition metal suboxide reactions with water, which either result in  $H_2$  production [ $M_xO_y^- + H_2O \rightarrow M_xO_{y+1}^- + H_2$  ( $M = Mo, W$ ;  $x = 2 - 4$ ;  $y$  typically  $\leq 2x$ )] or addition products [ $M_xO_y^- + H_2O \rightarrow M_xO_{y+1}H_2^-$ ]. Based on results of systematic experiments on the temperature dependence of  $M_xO_y^- + H_2O$  reaction rates,  $Mo_xO_y^- + H_2O$  reactions exhibit anti-Arrhenius behavior, while  $W_xO_y^- + H_2O$  reaction rates have near-zero temperature dependence or are Arrhenius, with low barrier. Overall,  $Mo_xO_y^- + H_2O$  rate constants are higher than their  $W_xO_y^-$  analogs. However, previous calculations on the  $M_xO_y^- + H_2O$  reaction path energy for  $M = Mo$  and  $W$  have showed

that once water has dissociatively added to the cluster to form a dihydroxide complex, barriers for the structural rearrangements necessary to produce  $H_2$  are *higher* for  $Mo_xO_y^-$  clusters than for  $W_xO_y^-$  clusters. While this result explained the observation of  $Mo_xO_yH_2^-$  trapped intermediates not seen for  $W_xO_y^-$  analogs, it did not elucidate what governs the relative overall  $M_xO_y^- + H_2O$  rate constants.

Additional calculations on initial cluster-water electrostatic interactions have shown that the dipole-dipole complexes that lead to dihydroxide formation are more strongly bound for  $Mo_xO_y^- \cdot H_2O$  complexes compared to  $W_xO_y^- \cdot H_2O$  analogs. The consequence is shown schematically in Figure 1: The overall barrier to forming a covalently bound complex is submerged for  $Mo_2O_5^- + H_2O$ , while the  $W_2O_5^- + H_2O$  reaction has a net positive free energy barrier. The magnitude of the  $M_xO_y^- + H_2O$  rate constants, ca.  $10^{-11}$  to  $10^{-13}$   $cm^3$  molecule $^{-1}s^{-1}$ , are in line with gas-phase radical reactions, and are on the same scale as entropy barrier-limited reaction rates using the Eyring's  $\frac{k_B T}{hp} e^{\Delta S/R}$ . We conclude that calculations of barriers along the full reaction pathway are useful for understanding the reaction product distributions we observe, while the measured rate constants are to a large extent governed by the initial electrostatic interactions between the cluster and reactant.

B. Role of electrostatic interactions versus  $-H$  mobility in  $M_xO_y^- + ROH$  ( $R = H, CH_3, C_2H_5$ ) reactions. To test the computationally-predicted importance of  $-H$  mobility in the  $M_xO_y^- + H_2O \rightarrow M_xO_{y+1}^- + H_2$  reaction mechanism,  $ROH$  ( $R = CH_3, C_2H_5$ ) was substituted for  $H_2O$  with the idea that the alkyl group would be slow relative to  $-H$ , and that verification of the mechanism could be made with the observation of additional trapped intermediates. Based on strong similarities between  $M_xO_y^- + ROH$  and  $M_xO_y^- + H_2O$  product distributions as well as the anion photoelectron spectra of the long-lived intermediates, examples of which are shown in Figure 2, it is evident that water and small alcohols follow completely analogous pathways in reactions with  $M_xO_y^-$  clusters. However,  $M_xO_y^- + ROH$  product distributions include several  $M_xO_{y+2}R_2^-$  products for which there is no analog in reactions with water. This observation supports the mechanism of proton mobility, since it suggests that the evolution of  $RH$  from the  $M_xO_y^- + ROH$  reaction is slowed sufficiently to allow for the addition of a second  $ROH$ , which then leads to fast  $H_2$  production.

The rate constants measured for the  $M_xO_y^- + ROH$  reactions showed interesting variations. While the  $M_xO_y^- + CH_3CH_2OH$  reaction rates were a factor of 3 slower than analogous reactions with water, the  $M_xO_y^- + CH_3OH$  rates were a factor of 20 slower. Given the findings summarized in Sec. II.A., this result again points to the importance of the weakly-bound complexes. The entropy-barrier for complex formation is higher for  $ROH$  than for  $H_2O$ , but the  $CH_3CH_2OH$  complex is more strongly bound than the  $CH_3OH$  complex, and is therefore less likely to dissociate before proceeding to form the hydroxide-alkoxide complex.

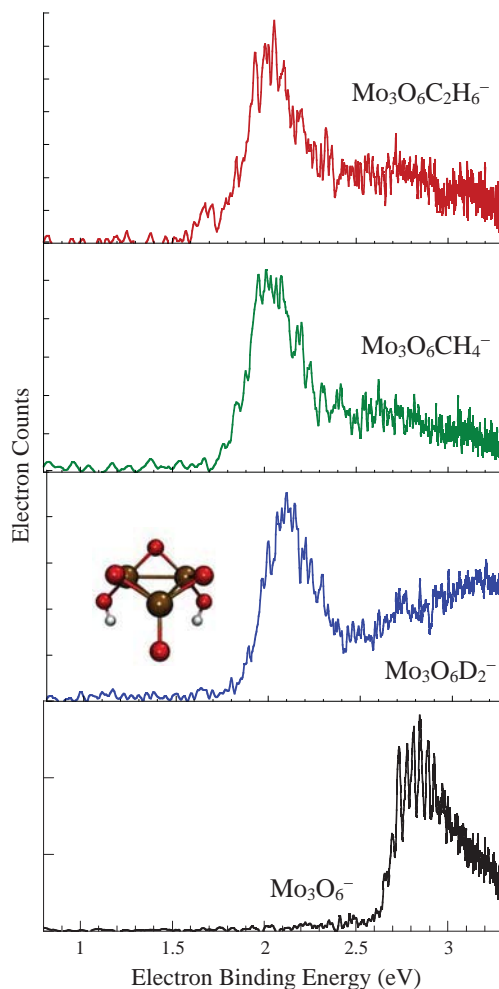


**Figure 2.** Photoelectron spectra (3.49 eV photon energy) of trapped intermediates formed in  $Mo_3O_5^- + EtOH, MeOH$  and  $D_2O$  reactions. The  $Mo_3O_6^-$  spectrum is included to demonstrate the spectral resolution.

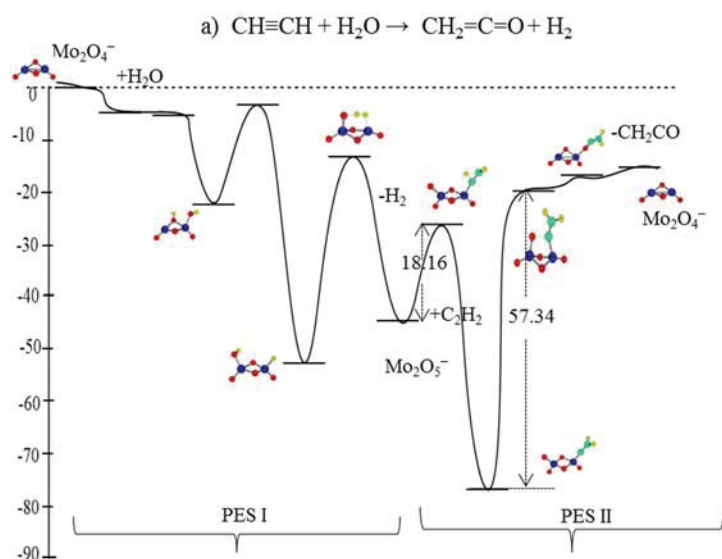
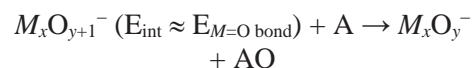
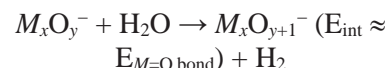


**Figure 3.** Reaction path free energy (kcal mol<sup>-1</sup>, 298K) for the Mo<sub>2</sub>O<sub>4</sub><sup>2-</sup> cluster-mediated C<sub>2</sub>H<sub>2</sub> + H<sub>2</sub>O → H<sub>2</sub> + C<sub>2</sub>H<sub>2</sub>O reaction.

and the use of ethylene in this process is marginally endothermic. On the other hand, calculations predict that strongly-bound complex formation relative to the final products may terminate the process if internal energy dissipates on the timescale of the two reactions. To evaluate the feasibility of this approach, we implemented studies using C<sub>2</sub>H<sub>4</sub> as a sacrificial reagent for W<sub>x</sub>O<sub>y</sub><sup>-</sup> + H<sub>2</sub>O reactions. A snapshot of the results for the *x* = 2 series, shown in Figure 4, demonstrates that (1) sequential oxidation by water appears to be significantly slowed for H<sub>2</sub>O/C<sub>2</sub>H<sub>4</sub> mixes relative to H<sub>2</sub>O/Ne, and (2) the weakly bound W<sub>2</sub>O<sub>5</sub><sup>-</sup>·C<sub>2</sub>H<sub>4</sub> complex that appears when the clusters are exposed to only C<sub>2</sub>H<sub>4</sub> is significantly depleted when H<sub>2</sub>O is present. While neither of these observations directly confirm that C<sub>2</sub>H<sub>4</sub> is acting as a sacrificial reagent, the results are promising.

**D. Reactivity of Metal Sulfides with Water:** We have carried out a density functional investigation of the electronic structures and chemical reactions of trimetallic Mo and W sulfide (M<sub>3</sub>S<sub>x</sub><sup>-</sup>, *x* = 3-4) cluster anions with water. In particular, the M<sub>3</sub>S<sub>4</sub><sup>-</sup> cluster has a structural motif containing a threefold coordinated S seen in molybdenum sulfide clusters in solution chemistry that show catalytic activity for hydrogen generation from water. In all cases, the reaction proceeds via three distinct steps: 1) Initial dissociation of water to form a thiol and metal-hydroxide bond 2) Subsequent hydrogen migration resulting in the formation of a metal hydride and 3) Evolution of molecular hydrogen which leaves behind an oxidized form of the original metal sulfide cluster. While both metals (Mo and W) follow the same trend of reaction energy profiles, W is found to bear the lower energy barriers and larger exothermicities. Moreover, our study reveals that the energetic barriers for these trimetallic clusters for reaction with water are significantly lower

C. Use of sacrificial reagents to regenerate suboxide states in M<sub>x</sub>O<sub>y</sub><sup>-</sup> + H<sub>2</sub>O reactions. Much of the work to date has involved transition metal suboxide reactions with water that generate H<sub>2</sub>, but then leave the metal oxide cluster in higher and unreactive oxidation states. An ideal full-cycle process includes a sacrificial reagent that reduces the transition metal oxide cluster before it dissipates the internal energy gained from the new M=O bond formation:



Computationally, we have determined that both CO and C<sub>2</sub>H<sub>2</sub> as sacrificial reagents provide an exothermic path,

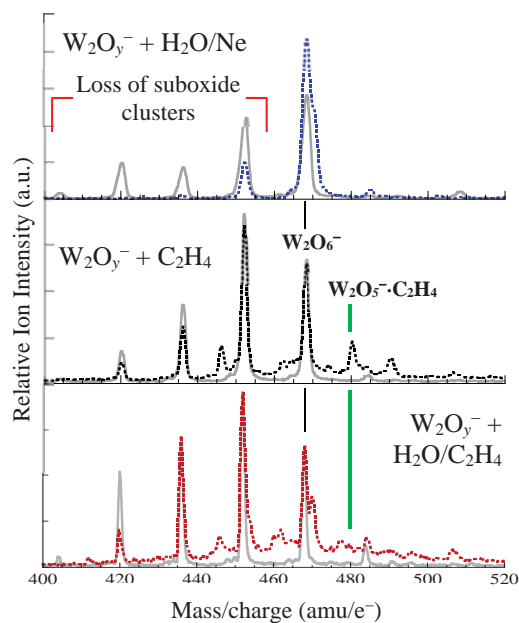


**Figure 4.** Initial W<sub>2</sub>O<sub>y</sub><sup>-</sup> cluster distributions (gray traces) and final distributions after reacting with H<sub>2</sub>O/Ne, C<sub>2</sub>H<sub>4</sub>, and H<sub>2</sub>O/C<sub>2</sub>H<sub>4</sub>. path

than the previously studied bimetallic clusters ( $M_2S_x^-$ ) throughout the course of the reaction. We conclude that these metal sulfide clusters show promise of catalytic activity for hydrogen evolution from water.

### III. Future Plans

The enduring strength of the research program is the synergistic interplay between theory and experiment. The primary goal is to complete the catalytic cycle using sacrificial reagents as outlines above. Several strategies such as the use of flashlamps and/or collision-induced dissociation to overcome the deep wells in sacrificial reagent processes, and using  $H_2^{18}O$  to help determine whether sacrificial reagents are working as conceived will follow. The other goals are the use of metal sulfides in the catalytic role, and the use of theory to establish the connection between the reactivity of clusters and that on surfaces and in the solution phase.

### IV. References to publications of DOE sponsored research that have appeared in 2013–present or that have been accepted for publication

1. “Direct Reduction of Alkyl Halides at Silver in Dimethylformamide: Effects of Position and Identity of the Halogen”, Lauren M. Strawsine, Arkajyoti Sengupta, Krishnan Raghavachari, and Dennis G. Peters, *ChemElectroChem.* **2**, 726–736 (2015). <http://dx.doi.org/10.1002/celec.201402410>
2. “Hydroxyl Migration in Heterotrimetallic Clusters: An Assessment of Fluxionality Pathways”, Debashis Adhikari and Krishnan Raghavachari, *J. Phys. Chem. A* **118**, 11047-11055 (2014). <http://dx.doi.org/10.1021/jp5080835>
3. “Comparative study of water reactions with  $Mo_2O_y^-$  and  $W_2O_y^-$  clusters: A combined experimental and theoretical investigation,” Manisha Ray, Sarah E. Waller, Arjun Saha, Krishnan Raghavachari, and Caroline Chick Jarrold, *J. Chem. Phys.* **141**, 104310(1-9) (2014) <http://dx.doi.org/10.1063/1.4894760>.
4. “Electronic Structures and Water Reactivity of Mixed Metal Sulfide Cluster Anions,” Arjun Saha and Krishnan Raghavachari, *J. Chem. Phys.* **141**, 074305(1-9) (2014); <http://dx.doi.org/10.1063/1.4892671>.
5. “RH and  $H_2$  production in reactions between ROH and small molybdenum oxide cluster anions,” Sarah E. Waller and Caroline Chick Jarrold, *J. Phys. Chem. A* **118**, 8493-8504 (2014); <http://dx.doi.org/10.1021/jp502021k>.
6. “Electrochemical Reduction of 2-chloro-N-phenylacetamides at Carbon and Silver Cathodes in Dimethylformamide”, Erick M. Pasciak, Arkajyoti Sengupta, Mohammad S. Mubarak, Krishnan Raghavachari and Dennis G. Peters, *Electrochim. Acta* **127**, 159-166 (2014). <http://dx.doi.org/10.1016/j.electacta.2014.01.133>.
7. “A Simple Relationship Between Oxidation State and Electron Affinity in Gas-Phase Metal-oxo Complexes,” Sarah E. Waller, Manisha Ray, Bruce L. Yoder, and Caroline Chick Jarrold, *J. Phys. Chem. A* **117**, 13919-13925 (2013). <http://pubs.acs.org/doi/abs/10.1021/jp4097666#>.
8. “Hydrogen Evolution from Water through Metal Sulfide Reactions”, Arjun Saha and Krishnan Raghavachari, *J. Chem. Phys.* **139**, 204301(1-12) (2013). <http://dx.doi.org/10.1063/1.4830096>.
9. "New Insights on Photocatalytic  $H_2$  Liberation from Water using Transition Metal Oxides: Lessons from Cluster Models of Molybdenum and Tungsten Oxides," Raghunath O. Ramabhadran, Jennifer E. Mann, Sarah E. Waller, David W. Rothgeb, Caroline Chick Jarrold and Krishnan Raghavachari, *J. Amer. Chem. Soc.*, **135**, 17039-17051 (2013). <http://dx.doi.org/10.1021/ja4076309>.

## Critical evaluation of theoretical models for aqueous chemistry and CO<sub>2</sub> activation in the temperature-controlled cluster regime

RE: DE-FG02-00ER15066 and DE-FG02-06ER15800

Program Managers: Dr. Mark Pederson and Dr. Gregory Fiechtner

K. D. Jordan (jordan@pitt.edu), Dept. of Chemistry, University of Pittsburgh, Pittsburgh, PA 15260

M. A. Johnson (mark.johnson@yale.edu), Dept. of Chemistry, Yale University, New Haven, CT 06520

### Program Scope:

Our joint program exploits size-selected clusters as a medium with which to unravel molecular level pictures of key transient species in condensed phase and interfacial chemistry that are relevant to the mediation of radiation damaged systems and the catalytic activation of small molecules (CO<sub>2</sub>, H<sub>2</sub>O). In the past year, we have made dramatic advances in understanding the nature of the hydrated proton at the surface of water as well as the intramolecular distortions at play in the assembly of the building blocks that form room temperature ionic liquids (IL).

### I. Unraveling the spectral character of the proton defect in water clusters

One of the most important species in aqueous chemistry is the hydrated proton. In our 2014 CPIMS abstract, we reported a significant advance in the observation of the bands associated with the proton defect in the three-dimensional, cage-like H<sup>+</sup>(H<sub>2</sub>O)<sub>*n*=21</sub> cluster.[1] We then extended this experimental observation (see Fig. 1) to include the cluster size-dependence of the transitions[2] as well as initiated an extensive theoretical effort to understand the locations and breadths of these bands.[3] The latter work was carried out jointly with Sotiris Xantheas and Shawn Kathmann at PNNL, who are also CPIMS PIs. The key theoretical results are summarized in Table 1, which reports the hydronium OH stretch shifts obtained from harmonic and anharmonic (VPT2) calculations on the H<sub>3</sub>O<sup>+</sup>, H<sub>9</sub>O<sub>4</sub><sup>+</sup>, and H<sub>21</sub>O<sub>10</sub><sup>+</sup> motifs cut out of the *n* = 21 cluster. One set of VPT2 calculations were carried out

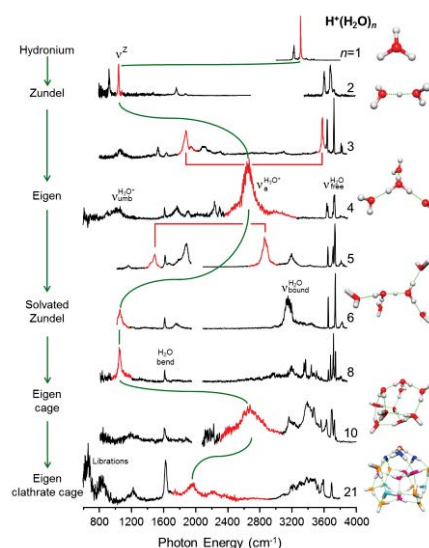


**Fig. 1.** Survey of the cluster size-dependence of the spectral signatures of the excess proton in selected H<sup>+</sup>(H<sub>2</sub>O)<sub>*n*</sub> clusters.

using the standard approach and included all vibrational modes. The other is a three-mode model including only the three hydronium OH stretch vibrations. In both cases the cubic and quartic couplings required for the VPT analysis were obtained from B3LYP calculations. As seen from the table, the simple 3-mode model semi-quantitatively reproduces the trends of the full VPT calculations, which, in turn, are in good overall agreement with experiment. In an important conceptual advance, we demonstrated that *much of the increase in the red shift of the  $H_3O^+$  OH stretch vibration with growing hydration of the ion is due to electric field effects rather than delocalization of the charge onto the hydration shells.*

Interestingly, the spectrum of the  $n = 21$  cluster is quite similar to that of bulk dilute acid where the broad continuum absorption from 1000-3000  $cm^{-1}$  has been attributed to the excess proton. This strongly suggests that water clusters in the size range around  $n = 20$  are, in fact, useful models for the condensed phase behavior and, as such, warrant further investigation.

## II. Excess electron-induced, water-network mediated intracuster proton transfer

In this joint experimental/theoretical study, we characterized the way that water clusters mediate electron capture by pyridine. This paper reporting the experimental results and theoretical analysis has been accepted for publication in *J. Chem. Phys.*[6] The key issue here is that in isolation, the  $Py^-$  radical anion is a transient negative ion (i.e., scattering resonance) while in solution, Py is known to undergo rapid proton transfer to form the neutral pyridinium radical ( $PyH^{(0)}$ ) upon scavenging an excess electron. As such, this system presents an excellent platform in which to follow the competition between stabilization of the radical anion resonance and intracuster proton transfer as water molecules are sequentially added to the  $[Py \cdot (H_2O)_n]^-$ . Understanding the diffuse spectra displayed by this system has taken several years to disentangle, and by integrating negative ion photoelectron spectroscopy, Ar-tagged and electron autodetachment vibrational spectroscopies with theoretical predictions, we identify the “tipping point” for intra-cluster proton transfer to be at the tri-hydrate. That system is particularly interesting because three types of structures are all present in the cold clusters prepared in the laboratory: (1) proton-transferred structures  $PyH^{(0)} \cdot (OH^-) \cdot (H_2O)_n$ , (2) hydrated  $Py^-$  ions, and (3) dipole-bound anions in which the excess electron is bound in the net dipole field of the pyridine

Table 1. Calculated vibrational frequencies of  $H_3O^+$ ,  $H_9O_4^+$ , and a  $H_{21}O_{10}^+$  cluster extracted from the  $n = 21$  cluster.

Species	Frequency ( $cm^{-1}$ ) <sup>a</sup>		
	Harmonic	Anharmonic VPT2	
		Model <sup>b</sup>	Full
$H_3O^+$	3510 (s)	3344	3348
	3606 (a)	3430	3417
$H_9O_4^+$	2990 (s)	2718	2664
	2869 (a)	2547	2599
$H_{21}O_{10}^+$	2822 (s)	2516	2617
	2604 (a)	2242	2100

<sup>a</sup>In the calculations the energies of the two asymmetric vibrations are slightly split, and only the average is reported in the Table.

<sup>b</sup>The model includes only the three hydronium OH stretch vibrations.

and water molecules. The formation of hydroxide ions is found to be complete by  $n = 5$ , at which point the  $\text{PyH}^{(0)}$  radical is retained in the primary solvation shell of the anion.

### III. Intramolecular distortions and fundamental interactions in ionic liquids (IL)

Clusters provide a unique medium in which to clarify the structural implications of spectral features displayed by the bulk liquids, which are becoming increasingly important as media for catalytic activation of  $\text{CO}_2$ . Our first efforts in this area were to first establish the spectra of the isolated ionic components of commonly used ILs [e.g.,  $\text{EMIM}^+$ , butyltrimethylammonium $^+$ ,  $\text{BF}_4^-$ , bis(trifluoromethylsulfonyl)imide, ( $\text{Tf}_2\text{N}^-$ )] so that the intramolecular signatures could be used to follow structural changes that occur upon assembly of the ions.[4,5] This initial survey led to a more extensive theoretical analysis of the molecular physics underlying the bands displayed by the isolated EMIM cation and several analogues with representative spectra displayed in Fig. 2. These were chosen to disentangle the origin of key features commonly used to indicate formation of directional H-bonds in the liquid. An important conclusion of this effort was reported in [4], where we quantified the appearance of “extra bands” arising from intramolecular Fermi resonance interactions in the isolated ions. We then followed how the signatures of the isolated ions evolved as the ions are assembled, both in neutral ion pairs and in odd-numbered combinations where the growing cluster is charged.[5]

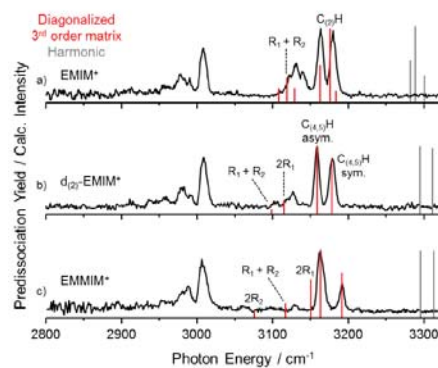


**Fig. 2.** Anharmonic analysis of the ethylmethylimidazolium cation (EMIM) upon substitution at the  $\text{C}_{(2)}$ -H position by (b) D and (c)  $\text{CH}_3$ . The extra bands near  $3125\text{ cm}^{-1}$ , originally assigned as red-shifted features due to H-bonding in the liquid ILs (e.g.,  $\text{EMIM}/\text{BF}_4$ ), are found to be present in the isolated cations and are traced to intramolecular Fermi resonance interactions.

### IV. Plans for the next year

#### *Origin of the band broadening in protonated water clusters*

The identification of the band locations and structures at play in the protonated water clusters carried out in the past two years provides an excellent foundation upon which to address the next important question regarding the spectra of dilute acids: The origin of the dramatic spectral broadening in the OH stretching manifold associated with the proton defect. On the experimental side, we have already obtained isotopomer-selective spectra of trace isotopically labeled clusters (e.g.,  $\text{H}^+(\text{D}_2\text{O})_4$ ), and thus can directly challenge the nature of the anharmonic couplings due to mixing between identical OH oscillators. In another approach, we have also obtained spectra of the isotopologues of the hydronium ion bound to a rigid H-bond acceptor manifold in the 18-crown-6/ $\text{H}_3\text{O}^+$  complexes. The next step will involve identifying the theoretical origin of these shapes, with particular attention to the role of heavy particle excursions at the vibrational zero-point level, thus generating breadth not from thermally induced fluctuations, but rather from the intrinsic spectrum of the OK systems. We have also obtained

spectra of the hydrated hydroxide ion over the region  $600 - 4000 \text{ cm}^{-1}$ , and demonstrated that the bands originally assigned to the OH stretches bound to the hydroxide ion in the first hydration shell actually lie much lower in energy than indicated in our initial report on this system in 2003, which only covered the range above  $2200 \text{ cm}^{-1}$ . The H-bonded bands are quite complex, and the anharmonic analysis of the patterns will be a prominent aspect of our work in the next year.

#### *Decomposition of the intermolecular interactions at play in small clusters of ionic liquids*

The results of these first studies indicate that electrostatic interactions dominate the structural motifs, thus raising the question of whether H-bonding is present under any circumstances. We have therefore initiated a study to follow the evolution of the EMIM complexed with a variety of anions with increasing proton affinities (halides, acetate) to identify the onset of strong red-shifts and intensity enhancements qualitatively in line with classical H-bonding. This effort will likely involve the use of symmetry-adapted perturbation theory (SAPT) to dissect the dispersion. The calculations show that the interactions are highly non-additive, and that polarization effects are significantly larger in magnitude than charge-transfer contributions.

#### *Papers in the past two years under this grant*

1. "Spectral signature of the proton defect in a three-dimensional water network through cryogenic vibrational spectroscopy of the "magic"  $\text{H}^+(\text{H}_2\text{O})_{21}$  cluster", J. A. Fournier, C. J. Johnson, C. T. Wolke, G. H. Weddle, A. B. Wolk, and M. A. Johnson, *Science*, 344, 1009 (2014).
2. "Site-specific vibrational spectral signatures of water molecules in the "magic"  $\text{H}_3\text{O}^+(\text{H}_2\text{O})_{20}$  and  $\text{Cs}^+(\text{H}_2\text{O})_{20}$  clusters", Joseph A. Fournier, Conrad T. Wolke, Christopher J. Johnson, Mark A. Johnson, Nadja Heine, Sandy Gewinner, Wieland Schöllkopf, Tim K. Esser, Matias R. Fagiani, Harald Knorke, Knut R. Asmis, *Proc. Natl. Acad. Sci. USA*, **111**, 18132-18137 (2014).
3. "Snapshots of proton accommodation at a microscopic water surface: understanding the vibrational spectral signatures of the charge defect in cryogenically cooled  $\text{H}^+(\text{H}_2\text{O})_{n=2-28}$  clusters", J. A. Fournier, C. T. Wolke, M. A. Johnson, T. T. Odbadrakh, K. D. Jordan, S. M. Kathmann, and S. S. Xantheas, *J. Phys. Chem. A*, in press (Feature Article) (2015).
4. "Comparison of the local binding motifs in the imidazolium-based ionic liquids [EMIM][BF<sub>4</sub>] and [EMMIM][BF<sub>4</sub>] through cryogenic ion vibrational predissociation spectroscopy: Unraveling the roles of anharmonicity and intermolecular interactions," Joseph A. Fournier, Conrad T. Wolke, Christopher J. Johnson, Anne B. McCoy, and Mark A. Johnson, *J. Chem. Phys.*, **17**, 8518-8529 (2015).
5. "Understanding the ionic liquid [NC4111][Tf<sub>2</sub>N] from individual building blocks: An IR-spectroscopic study," Kenny Hanke, Martin Kaufmann, Gerhard Schwaab, Martina Havenith, Conrad T. Wolke, Olga Gorlova, Mark A. Johnson, Bishnu Kar, Wolfram Sander, Elsa Sanchez-Garcia, *Phys. Chem. Chem. Phys.*, **17**, 8518 (2015).
6. 3. "Water Network-Mediated Electron-Induced Proton Transfer in Anionic  $[\text{C}_5\text{H}_5\text{N}^-(\text{H}_2\text{O})_n]$  Clusters: Size-Dependent Formation of the Pyridinium Radical for  $n > 3$ ", A. F. DeBlase, C. T. Wolke, G. H. Weddle, K. A. Archer, K. D. Jordan, J. T. Kelly, G. S. Tschumper, N. I. Hammer, and M. A. Johnson, *Accepted, J. Chem. Phys.*

## *Nucleation Chemical Physics*

Shawn M. Kathmann  
Physical Sciences Division  
Pacific Northwest National Laboratory  
902 Battelle Blvd.  
Mail Stop K1-83  
Richland, WA 99352  
[shawn.kathmann@pnl.gov](mailto:shawn.kathmann@pnl.gov)

### **Program Scope**

The objective of this work is to develop an understanding of the chemical physics governing nucleation. The thermodynamics and kinetics of the embryos of the nucleating phase are important because they have a strong dependence on size, shape and composition and differ significantly from bulk or isolated molecules. The technological need in these areas is to control chemical transformations to produce specific atomic or molecular products without generating undesired byproducts, or nanoparticles with specific properties. Computing reaction barriers and understanding condensed phase mechanisms is much more complicated than those in the gas phase because the reactants are surrounded by solvent molecules and the configurations, energy flow, quantum and classical electric fields and potentials, and ground and excited state electronic structure of the entire statistical assembly must be considered.

### **Recent Progress and Future Directions**

#### *Charge and Field Fluctuations in Aqueous NaCl*

The observations of luminescence during crystallization as well as electric field induced crystallization suggest that the process of crystallization may not be purely classical but also involves an essential electronic structure component. Strong electric field fluctuations may play an important role in this process by providing the necessary driving force for the observed electronic structure changes.

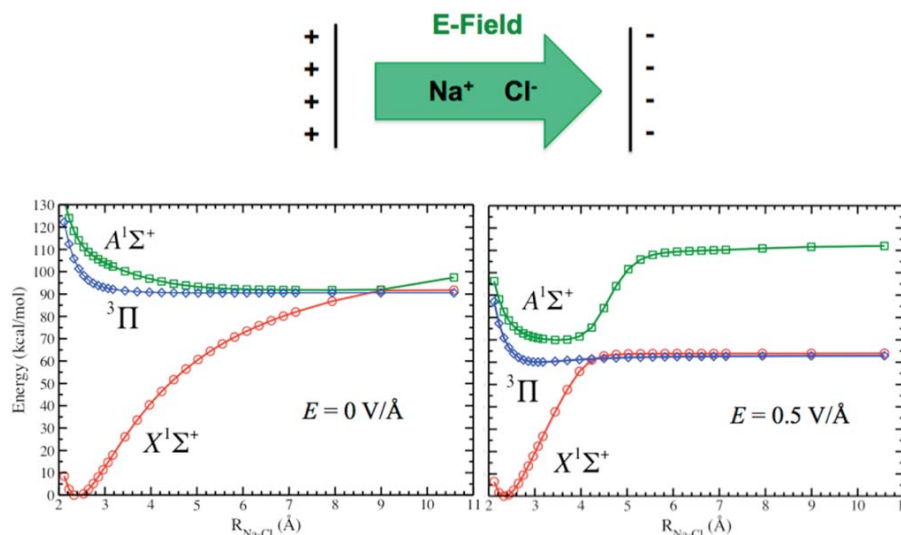


**Figure 1.** Adiabatic potential energy curves for the NaCl dimer in vacuum without (left) and with (right) an external electric field of 0.5 V/Å pointing from Na<sup>+</sup> toward Cl<sup>-</sup> (top). The influence of the electric field moves the zero field avoided crossing from 9 to 4 Å, and the first excited singlet and triplet states become stabilized by about 30 kcal/mol relative to the ground singlet state minimum.

Here we provide an initial benchmark analysis to understand the influence of electric fields on ground and excited electronic states of the NaCl dimer (see Figure 1). Our high-level electronic structure calculations

using MOLPRO (MRCI/aug-cc-pvtz) on the NaCl dimer show that an electric field of  $0.5 \text{ V/\AA}$  can dramatically alter the electronic states available to the system. As a consistency check we computed the ensemble averaged electric field distributions inside aqueous electrolytes and discovered that they are extremely large and thus may alter the ground and excited electronic states in the condensed phase. The importance of electric field fluctuations driving electron transfer has been a topic of intense research since the seminal work of Marcus. The main objective of this work is to provide basic understanding of the fluctuations in charge, electric potentials, and electric fields, both classically and quantum mechanically, for concentrated aqueous NaCl electrolytes. For example, using various isomers of  $(\text{H}_2\text{O})_6$  as a prototypical system, one can readily

see the differences between quantum and classical voltage distributions shown in Figure 2. Our published calculations and analyses provide the first steps toward understanding the magnitude and fluctuations of charge, classical point charge sources of electric potentials and fields in aqueous electrolytes and what role these fields may play in driving charge redistribution/transfer during crystallization as well as inducing crystal formation itself.

#### *Quantum Voltages and Valence Electrons*

Voltages and fields inside matter are relevant to crystallization, materials science, biology, catalysis, and aqueous chemistry. The variation of voltages in matter can be measured by electron holography. Complimentary, using modern supercomputers and a sufficiently accurate level of theory allow the prediction of quantum voltages with spatial resolutions of bulk systems well beyond what can be currently measured. Of particular interest is Bethe's Mean Inner Potential ( $V_o$ ) – the spatial average of these quantum voltages referenced to the vacuum. We have established a protocol to reliably evaluate  $V_o$  from quantum calculations. Voltages are very sensitive to the distribution of electrons and provide metrics to understand interactions in condensed phases (see Fig. 3). We find excellent agreement with measurements of  $V_o$  for vitrified water and salt crystals. The changes in  $V_o$  upon bond formation in a  $\text{H}_2\text{O}$  molecule reveal a far-field picture where an increase in electron density results in a decrease in voltage due to better screening of the nuclear cores. We found that, in contrast to the positive definite voltages of isolated atoms, once the electrons are allowed to transfer and redistribute to

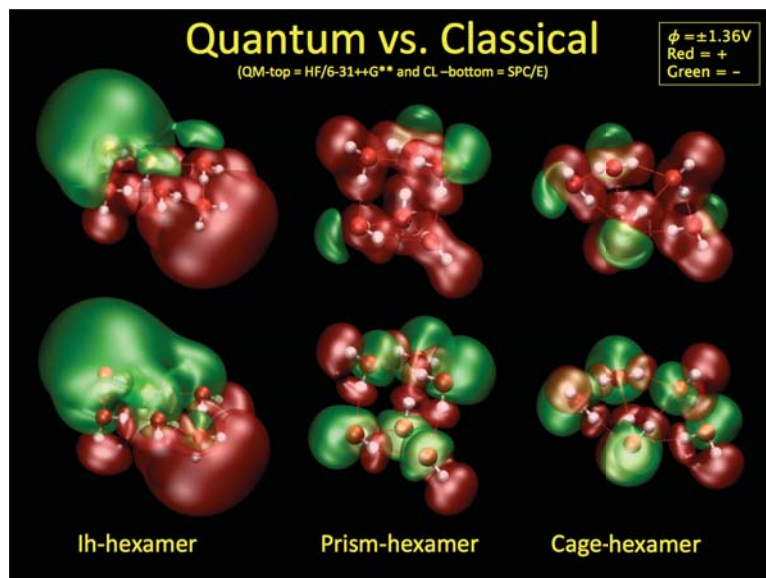


**Figure 2.** Quantum (top) versus classical (bottom) voltage isosurfaces ( $\phi$ ) for the Ih, prism, and cage isomers of the water hexamer, where the red and green isosurfaces are at  $+1.36\text{V}$  and  $-1.36\text{V}$ , respectively. The nuclear configurations are exactly the same for consistency. The quantum voltages are from HF/6-31++G\*\* level of theory and basis set and the classical voltages are due to the SPC/E point charges.

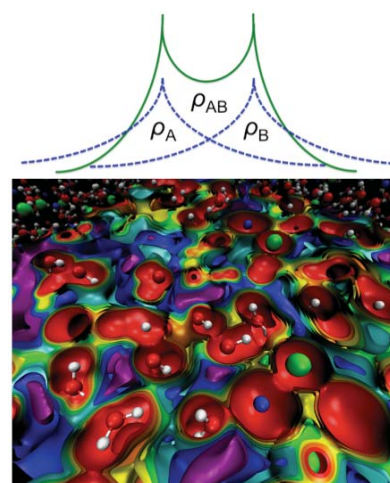


**Figure 3.** As atoms and molecules come together to form liquids and solids their electrons redistribute and this is reflected in the voltage distributions.

form bonds, lone pairs of electrons, and ions such that about 40% of the total volume of the bulk electrolyte contains negative voltages.

#### *Vibrational Spectroscopy and Electric Fields*

The influence of electric fields on the vibrational response of molecules has a long history and is relevant to many chemical processes in condensed phases and their interfaces. The central concept is the use of a particular vibrational mode as a kind of antenna or probe capable of sensing the *effective* electric field fluctuations due to its surrounding environment. Early work in this area employed continuum descriptions of electrostatics while more recent work utilized electric fields arising from classical point charges. Here we will explore the electric fields arising from quantum mechanical charge distributions for  $\text{H}_3\text{O}^+$  in small water clusters. Thus, this work stands as distinct from previous studies in that we are approaching the electric field coupling to vibrational shifts from an *ab initio* perspective yielding more “exact” electric field strengths in the absolute sense as there is much uncertainty in these fields from continuum, point charges, or polarizable sources. Specifically, the electric fields on the Hydrogen atom sites are calculated as those arising from the quantum mechanical charge densities of all the other atoms in the system excluding only those atoms with the water molecule for which the field is being evaluated. It is in this sense that these fields must be considered as *effective* electric fields arising from the surrounding atoms as this construction formally neglects the electric fields arising from the atoms within the molecule for which the field is being probed as well as the response of the surrounding environment to this probe’s charge distribution. These internal electric fields are found to be (left) 0.8, (center) 1.1, and (right) 1.1  $\text{V}/\text{\AA}$  for the structures shown in Figure 4. We find that once the 2<sup>nd</sup> solvation layer of water molecules is present, the electric fields on the H sites within  $\text{H}_3\text{O}^+$  stop increasing as more water molecules are added. We have discovered several interesting aspects within this work and must continue working to delve deeper into the connections between vibrational spectroscopy and internal and externally applied fields.

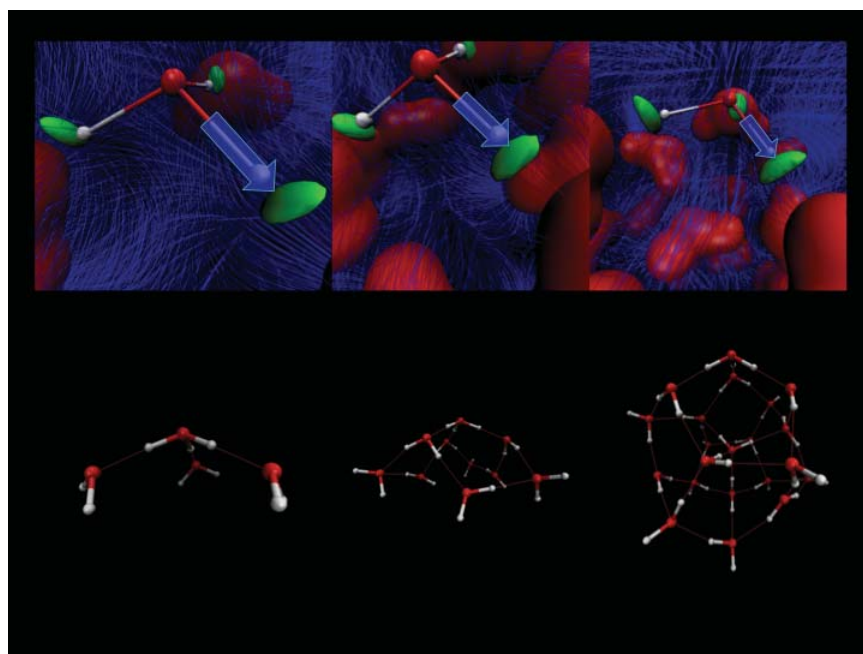


**Figure 4.** (upper panel) Quantum negative voltage isosurfaces (green) represent lone pairs of the adjacent  $\text{H}_2\text{O}$  molecules to the H atoms of  $\text{H}_3\text{O}^+$ . As a result, the quantum electric field lines (blue) at the H atom sites, generated by the  $\text{H}_2\text{O}$  molecules, are directed toward the lone pairs along the OH bonds (shown as blue arrows). The  $\text{H}_2\text{O}$  molecules are enclosed by positive voltage isosurfaces (red). (lower panel) Molecular structures left, center, and right for the images in the upper panel. The O and H atoms are shown as red and white spheres, respectively.

Direct PNNL collaborators on this project include M. Valiev, G.K. Schenter, C.J. Mundy, X. Wang, J. Fulton, L. Dang, and M. Baer and Postdoctoral Fellow Bernhard Sellner. Outside collaborations with the University College London include Stephen Cox and Angelos Michaelides on ice nucleation (Chemistry), Jake Stinson and Ian Ford on sulfuric acid-water nucleation as well as Mark Johnson at Yale on connections between electric fields and vibrational spectroscopy have been mutually beneficial.

*Acknowledgement:* This research was performed in part using the DOE NERSC facility. Battelle operates PNNL for DOE.

### **Publications of DOE Sponsored Research (2013-present)**

- Communication** – H. Wen, G.L. Hou, S.M. Kathmann, M. Valiev, and X.B. Wang, “Solute anisotropy effects in hydrated anion and neutral clusters”, *Journal of Chemical Physics*, **138**, 031101 (2013).
- S.J. Cox, Z. Raza, S.M. Kathmann, B. Slater, and A. Michaelides, “The Microscopic Features of Heterogeneous Ice Nucleation May Affect the Macroscopic Morphology of Atmospheric Ice Crystals”, *Faraday Discussions*, in press (2013).
- S.M. Kathmann, B. Sellner, A.J. Alexander, and M. Valiev, “Beyond Classical Theories”, *Proceedings of the 19<sup>th</sup> International Conference on Nucleation and Atmospheric Aerosols - AIP Conference Proceedings*, **1527**, 109, doi:10.1063/1.4803215 (2013).
- J.L. Stinson, S.M. Kathmann, and I.J. Ford, “Empirical Valence bonds: A reactive classical potential for sulphuric acid and water”, *Proceedings of the 19<sup>th</sup> International Conference on Nucleation and Atmospheric Aerosols - AIP Conference Proceedings*, **1527**, 266, doi:10.1063/1.4803255 (2013).
- Cover Article** – B. Sellner, M. Valiev, and S.M. Kathmann, “Charge and Electric Field Fluctuations in Aqueous NaCl Electrolytes”, *Journal of Physical Chemistry B*, **117**, 10869 (2013). This work was highlighted in DOE’s Pulse (Science and Technology Highlights from the DOE National Laboratories), “*Strong forces at work in simple table salt*”, #397, Sept. 16, (2013) <http://web.ornl.gov/info/news/pulse/no397/story3.shtml>
- J.L. Stinson, S.M. Kathmann, and I.J. Ford, “Dynamical consequences of a constraint on the Langevin thermostat in molecular cluster simulation”, *Molecular Physics*, DOI:10.1080/00268976.2014.917732 (2014).
- J.L. Stinson, S.M. Kathmann, and I.J. Ford, “Investigating the significance of zero-point motion in small molecular clusters of sulphuric acid and water”, *Journal of Chemical Physics*, **140**, 024306 (2014).
- B. Sellner and S.M. Kathmann, “A Matter of Quantum Voltages”, **Invited - Special Issue** of *Journal of Chemical Physics*, **141**, 18C534 (2014).
- S.J. Cox, S.M. Kathmann, B. Slater, and A. Michaelides, "Molecular simulations of heterogeneous ice nucleation. I. Controlling ice nucleation through surface hydrophilicity", *Journal of Chemical Physics*, **142**, 184704 (2015).
- S.J. Cox, S.M. Kathmann, B. Slater, and A. Michaelides, "Molecular Simulations of Heterogeneous Ice Nucleation. II. Peeling back the Layers", *Journal of Chemical Physics*, **142**, 184705 (2015).
- Feature Cover Article** - J.A. Fournier, C.T. Wolke, M.A. Johnson, T.T. Odbadrakh, K.D. Jordan, S.M. Kathmann and S.S. Xantheas, “Snapshots of Proton Accommodation at a Microscopic Water Surface: Understanding the Vibrational Spectral Signatures of the Charge Defect in Cryogenically Cooled  $H^+(H_2O)_{n=2-28}$  Clusters”, *Journal of Physical Chemistry A*, **119**, 9425 (2015).
- J.L. Stinson, S.M. Kathmann, and I.J. Ford, “A classical reactive potential for molecular clusters of sulphuric acid and water”, *Molecular Physics*, **in press** (2015).

## Chemical Kinetics and Dynamics at Interfaces

*Structure and Reactivity of Ices, Oxides, and Amorphous Materials*

**Bruce D. Kay (PI), R. Scott Smith, and Zdenek Dohnálek**

Chemical and Materials Sciences Division

Pacific Northwest National Laboratory

P.O. Box 999, Mail Stop K8-88

Richland, Washington 99352

bruce.kay@pnl.gov

Collaborators include: GA Kimmel, RA May, and NG Petrik

### Program Scope

The objective of this program is to examine physiochemical phenomena occurring at the surface and within the bulk of ices, oxides, and amorphous materials. The microscopic details of physisorption, chemisorption, and reactivity of these materials are important to unravel the kinetics and dynamic mechanisms involved in heterogeneous (i.e., gas/liquid) processes. This fundamental research is relevant to solvation and liquid solutions, glasses and deeply supercooled liquids, heterogeneous catalysis, environmental chemistry, and astrochemistry. Our research provides a quantitative understanding of elementary kinetic processes in these complex systems. For example, the reactivity and solvation of polar molecules on ice surfaces play an important role in complicated reaction processes that occur in the environment. These same molecular processes are germane to understanding dissolution, precipitation, and crystallization kinetics in multiphase, multicomponent, complex systems. Amorphous solid water (ASW) is of special importance for many reasons, including the open question over its applicability as a model for liquid water, and fundamental interest in the properties of glassy materials. In addition to the properties of ASW itself, understanding the intermolecular interactions between ASW and an adsorbate is important in such diverse areas as solvation in aqueous solutions, cryobiology, and desorption phenomena in cometary and interstellar ices. Metal oxides are often used as catalysts or as supports for catalysts, making the interaction of adsorbates with their surfaces of much interest. Additionally, oxide interfaces are important in the subsurface environment; specifically, molecular-level interactions at mineral surfaces are responsible for the transport and reactivity of subsurface contaminants. Thus, detailed molecular-level studies are germane to DOE programs in environmental restoration, waste processing, and contaminant fate and transport.

Our approach is to use molecular beams to synthesize “chemically tailored” nanoscale films as model systems to study ices, amorphous materials, supercooled liquids, and metal oxides. In addition to their utility as a synthetic tool, molecular beams are ideally suited for investigating the heterogeneous chemical properties of these novel films. Modulated molecular beam techniques enable us to determine the adsorption, diffusion, sequestration, reaction, and desorption kinetics in real-time. In support of the experimental studies, kinetic modeling and simulation techniques are used to analyze and interpret the experimental data.

### Recent Progress and Future Directions

***Adsorption, Desorption, and Displacement Kinetics of H<sub>2</sub>O and CO<sub>2</sub> on TiO<sub>2</sub>(110) and Forsterite, Mg<sub>2</sub>SiO<sub>4</sub>(011) Surfaces*** Understanding the interaction dynamics of water and carbon dioxide with mineral surfaces is requisite for determining the feasibility of carbon capture and sequestration strategies whose goal is the formation of carbonates. Unfortunately mineral surfaces are complicated, making experimental determination of these interactions difficult. For

example olivines, which are orthosilicates and comprise a large fraction of the earth's upper mantle, can have silicon, oxygen, and cation (Mg, Fe, Ca, etc.) surface adsorption sites. Impurities, such as cation substitutions that occur in "real-world" minerals, add a further level of complexity. In order to be able to interpret the results from a more complex system, a well-characterized  $\text{TiO}_2(110)$  crystal was used as a model oxide surface. While clearly not as complex as a true mineral surface, it has the advantage of having both metal and oxygen surface sites and as such should be a good reference point for interpreting results from more complicated substrates. In a recent study we examined in detail the adsorbate-substrate interaction kinetics of  $\text{CO}_2$  and  $\text{H}_2\text{O}$  on a well-characterized  $\text{TiO}_2(110)$  substrate (Reference #6). Following that work, we explored the interactions of  $\text{CO}_2$  and  $\text{H}_2\text{O}$  on the more complicated natural mineral crystal, forsterite,  $\text{Mg}_2\text{SiO}_4(011)$  (Reference #7). Below we summarize the results for  $\text{H}_2\text{O}$  and  $\text{CO}_2$  adsorption on both  $\text{TiO}_2$  and Forsterite ( $\text{Mg}_2\text{SiO}_4$ ).

Temperature programmed desorption (TPD) and molecular beam techniques were used to determine the adsorption, desorption, and displacement kinetics of  $\text{H}_2\text{O}$  and  $\text{CO}_2$  on a  $\text{TiO}_2(110)$  surface. The TPD for  $\text{H}_2\text{O}$  and  $\text{CO}_2$  have well-resolved peaks corresponding to desorption from bridge-bonded oxygen ( $\text{O}_b$ ), five-fold coordinated Ti ( $\text{Ti}_{5c}$ ), and oxygen vacancies ( $\text{V}_o$ ) sites in order of increasing peak temperature. The results show that both species preferentially bind to the highest binding energy available, first occupying defects, followed by  $\text{Ti}_{5c}$  sites, and then  $\text{O}_b$  sites. Analysis of the saturated monolayer peak for both molecules reveals that the corresponding adsorption energies on all sites are greater for  $\text{H}_2\text{O}$  than for  $\text{CO}_2$ . Using sequential adsorption, we showed that, independent of the dose order ( $\text{H}_2\text{O}$  first then  $\text{CO}_2$  and vice versa),  $\text{H}_2\text{O}$  displaces  $\text{CO}_2$  from any occupied site before reaching the desorption temperature. Isothermal experiments reveal that the onset of  $\text{H}_2\text{O}$  displacement of  $\text{CO}_2$  occurs between 75 and 80 K. These results indicate that  $\text{H}_2\text{O}$  preferentially binds to the highest energy binding sites available and displaces  $\text{CO}_2$  if necessary. These results show that the relative strength of the adsorbate-substrate interactions is the dominant factor in the competitive adsorption/displacement kinetics.

The same experimental molecular beam techniques described above were applied to study the interactions of  $\text{CO}_2$  and  $\text{H}_2\text{O}$  with a natural mineral crystal, forsterite,  $\text{Mg}_2\text{SiO}_4(011)$ . An X-ray photoelectron spectroscopy (XPS) analysis of our sample revealed that ~10–15% of the cation content was iron, i.e., the molecular formula was approximately  $\text{Mg}_{1.8}\text{Fe}_{0.2}\text{SiO}_4$ . The XPS data showed the existence of O, Mg, Si, and Fe on the surface, and because of the presence of all four atomic species, the surface was expected to give rise to a broad distribution of adsorbate binding energies. In fact, contrary to the results on  $\text{TiO}_2(110)$ , the TPD results on forsterite showed that neither  $\text{CO}_2$  nor  $\text{H}_2\text{O}$  has distinct sub-monolayer desorption peaks but instead both have a broad continuous desorption feature that evolves smoothly to multilayer desorption. Inversion analysis of the monolayer coverage desorption spectra for both molecules reveals that the corresponding binding energies for  $\text{H}_2\text{O}$  are greater than that for  $\text{CO}_2$  on all sites. The relative strength of the  $\text{H}_2\text{O}$  and  $\text{CO}_2$  substrate interaction energy appears to be the dominant factor in the competitive adsorption and displacement kinetics. In experiments in which the two adsorbates are co-dosed,  $\text{H}_2\text{O}$  preferentially binds to the highest-energy binding sites available and displaces  $\text{CO}_2$ . The onset of significant  $\text{CO}_2$  displacement by  $\text{H}_2\text{O}$  occurs between 65 and 75 K.

We find no experimental evidence for the dissociation or reaction of either  $\text{CO}_2$  or  $\text{H}_2\text{O}$  on forsterite. Of course, current experiments in which forsterite is used as a model substrate for carbonation to form  $\text{MgCO}_3$  are at elevated pressures (>100 atm) and temperatures (>300 K) that

cannot be replicated in our ultrahigh vacuum based experiments. However, theoretical studies that are trying to determine the fundamental energetics should be able to use our data as a benchmark for the accuracy of their calculations and adsorption models.

***The release of trapped gases from amorphous solid water films. “Top-down” crystallization-induced crack propagation probed using the molecular volcano*** Amorphous solid water (ASW) is a kinetically metastable form of water which is created when water vapor impinges on a substrate below 130 K. When heated, or allowed to sit for a fantastically long time, ASW converts to thermodynamically stable crystalline ice. Crystallization of ASW can result in structural changes in the film. For example, when an inert gas ( $\text{CCl}_4$ , Ar,  $\text{CO}_2$ , Kr, Xe, CO,  $\text{N}_2$ ,  $\text{O}_2$ , and others) is deposited underneath an ASW overlayer, the inert gas desorption is delayed until crystallization of the ASW overlayer. We have previously termed the episodic release of trapped gases from ASW the “molecular volcano”. The observed abrupt desorption is likely due to the formation of cracks that accompany the crystallization kinetics and form a connected release pathway.

The volcano peak was used to determine the crystallization induced crack propagation mechanism. In these experiments an inert gas layer was deposited at various positions in the ASW film. The results showed that the closer to the top of the film the layer was deposited, the earlier in temperature (time) the volcano desorption peak occurred. Through a series of experiments we were able to show conclusively that the direction of crack formation begins at the ASW/vacuum interface and moves downward into the film. Isothermal desorption experiments where the overlayer thickness was varied were used to measure the crack propagation rate. The results revealed that after an induction period, cracks propagate linearly in time with an Arrhenius temperature dependent velocity and activation energy of 54 kJ/mol. A two-step kinetic model in which nucleation and crystallization occurs in an induction zone near the top of the film followed by the propagation of a crystallization/crack front into the film is in good agreement with the temperature programmed desorption results. (This work is described in publications #1 and #2 below).

Based on these results we have begun to explore methods to directly determine the crystallization mechanism of ASW films. In this work, simultaneous TPD and reflection absorption infrared (RAIRS) spectra are obtained. The TPD experiments reveal information about surface crystallization whereas the FTIR experiments reveal information about bulk crystallization. Preliminary results show that the isothermal TPD spectra are independent of thickness and the FTIR results show that the crystallization time increases with thickness. These results support the “top-down” crystallization mechanism suggested by the “volcano” papers. Future work will focus on quantifying the crystallization kinetics and parsing out the nucleation and growth rates.

***Probing Toluene and Ethylbenzene Stable Glass Formation using Inert Gas Permeation*** Amorphous materials, also known as glasses, have technological applications in numerous fields including optical and material science, bioscience, polymer chemistry, pharmaceuticals, and food science, to name just a few. Vapor deposition of a substance onto a low temperature substrate (below its  $T_g$ ) is one method capable of achieving the rapid cooling needed to create amorphous materials. Ediger et al. have recently shown that the thermodynamic and kinetic stability of organic glasses (e.g. o-terphenyl, indomethacin, and others) grown using vapor deposition is dependent on the substrate growth temperature. Glasses with relatively low heat capacity, low enthalpy, high density, and increased kinetic stability are called “stable glasses”. We have previously developed a method to measure the translational diffusivity of supercooled liquids at

temperatures near their  $T_g$ . In this technique, an amorphous film is vapor deposited on top of an inert gas layer. The composite film is heated and, at the temperature the amorphous film transforms into a supercooled liquid, the inert gas can diffuse through the overlayer. The main idea is that the inert gas remains trapped under the overlayer until the amorphous solid transforms into a supercooled liquid.

In a recent paper (#9) we use inert gas permeation to investigate the formation of stable glasses of toluene and ethylbenzene. The effect of deposition temperature ( $T_{dep}$ ) on the kinetic stability of the vapor deposited glasses is determined using Kr desorption spectra from within sandwich layers of either toluene or ethylbenzene. The results for toluene show that the most stable glass is formed at  $T_{dep} = 0.92 T_g$ , although stable glass formation was observed for deposition temperatures from 0.85 to 0.95  $T_g$ . Similar results were found for ethylbenzene. These results are consistent with recent calorimetric studies and demonstrate that the inert gas permeation technique provides a direct method to observe the onset of molecular translation motion that accompanies the glass to supercooled liquid transition. The permeation technique has the potential for use in studying mixed/complicated composite films that would be difficult to study using calorimetry alone. This technique will be used in the future to explore stable glass formation in other vapor deposited systems and in more complicated composite films.

#### References to Publications of DOE sponsored Research (2013 - present)

1. R. A. May, R. S. Smith and B. D. Kay, "The release of trapped gases from amorphous solid water films. I. "Top-down" crystallization-induced crack propagation probed using the molecular volcano", J. Chem. Phys. **138**, 104501 (2013).
2. R. A. May, R. S. Smith and B. D. Kay, "The release of trapped gases from amorphous solid water films. II. "Bottom-up" induced desorption pathways", J. Chem. Phys. **138**, 104502 (2013).
3. R. A. May, R. S. Smith and B. D. Kay, "Mobility of supercooled liquid toluene, ethylbenzene, and benzene near their glass transition temperatures investigated using inert gas permeation", J. Phys. Chem. A **117**, 11881-11889 (2013).
4. G. A. Kimmel, T. Zubkov, R. S. Smith, N. G. Petrik and B. D. Kay, "Turning things downside up: Adsorbate induced water flipping on  $pt(111)$ ", J. Chem. Phys. **141**, 18C515 (2014).
5. V. Molinero and B. D. Kay, "Preface: Special topic on interfacial and confined water", J. Chem. Phys. **141**, 18C101 (2014).
6. R. S. Smith, Z. J. Li, L. Chen, Z. Dohnalek and B. D. Kay, "Adsorption, desorption, and displacement kinetics of  $H_2O$  and  $CO_2$  on  $TiO_2(110)$ ", J. Phys. Chem. B **118**, 8054-8061 (2014).
7. R. S. Smith, Z. J. Li, Z. Dohnalek and B. D. Kay, "Adsorption, desorption, and displacement kinetics of  $H_2O$  and  $CO_2$  on forsterite,  $Mg_2SiO_4(011)$ ", J. Phys. Chem. C **118**, 29091-29100 (2014).
8. R. S. Smith, J. Matthiesen and B. D. Kay, "Desorption kinetics of methanol, ethanol, and water from graphene", J. Phys. Chem. A **118**, 8242-8250 (2014).
9. R. S. Smith, R. A. May and B. D. Kay, "Probing toluene and ethylbenzene stable glass formation using inert gas permeation", Journal of Physical Chemistry Letters (2015), DOI: 10.1021/acs.jpcclett.5b01611.
10. K. Thürmer, C. Yuan, G. A. Kimmel, B. D. Kay and R. S. Smith, "Weak interactions between water and clathrate-forming gases at low pressures", Surface Science **641**, 216-223 (2015).

## Probing Ultrafast Electron (De)localization Dynamics in Mixed Valence Complexes Using Femtosecond X-ray Spectroscopy

**Lead PI:** Prof. Munira Khalil, University of Washington, Seattle, [mkhalil@uw.edu](mailto:mkhalil@uw.edu)

**Co-PI:** Dr. Niranjan Govind, EMSL, Pacific Northwest National Laboratory

**Co-PI:** Prof. Shaul Mukamel, University of California, Irvine

**Co-PI:** Dr. Robert Schoenlein, Lawrence Berkeley National Laboratory

### PROGRAM SCOPE:

The overall goal of this research program is to understand valence electron and vibrational motion following metal-to-metal charge transfer (MMCT) excitation in the following mixed valence complexes dissolved in aqueous solution:  $[(\text{NH}_3)_5\text{Ru}^{\text{III}}\text{NCFe}^{\text{II}}(\text{CN})_5]^-$  (**1**, FeRu), *trans*- $[(\text{NC})_5\text{Fe}^{\text{II}}\text{CNPt}^{\text{IV}}(\text{NH}_3)_4\text{NCFe}^{\text{II}}(\text{CN})_5]^{4-}$  (**2**, FePtFe) and *trans*- $[(\text{NC})_5\text{Fe}^{\text{III}}\text{CNRu}^{\text{II}}(\text{L})_4\text{NCFe}^{\text{III}}(\text{CN})_5]^{4-}$  (**3**, FeRuFe, L=pyridine). The project objectives are (i) to observe the time-dependent re-arrangement of *d* electrons across two transition metal sites and the bridging ligand following photoinduced MMCT excitation on a sub-50 fs timescale using femtosecond X-ray pulses generated at LCLS (ii) to simulate femtosecond X-ray absorption and emission spectra of solvated, photo-excited, transition metal mixed valence complexes using a realistic treatment of multi-electron correlations/transitions, spin-orbit coupling and final state lifetime effects and to propose and study the feasibility of nonlinear X-ray experiments on solvated transition metal mixed valence systems using future X-FEL light sources and (iii) to determine the role of coupled electronic and vibrational motions during ultrafast photoinduced charge transfer.

### RESEARCH PROGRESS AND FUTURE PLANS:

**Development of Two-Dimensional Vibrational-Electronic (2D VE) Spectroscopy to Measure Coherently Coupled Vibrational and Electronic Motions (Khalil)** We have developed a Fourier transform (FT) 2D vibrational-electronic (2D VE) spectroscopy employing a novel mid-IR and optical pulse sequence. This new femtosecond third-order nonlinear spectroscopy provides the high time and frequency resolutions of existing 2D FT techniques, but is sensitive to cross-peaks containing IR and electronic dipole moment cross terms. We use 2D VE spectroscopy to help understand the vibrational-electronic couplings in the cyanide-bridged transition metal mixed valence complex FeRu (Complex **1**) dissolved in formamide. The amplitude of the cross-peaks in the 2D VE spectra reveal that three of the four intramolecular cyanide stretching vibrations are coherently coupled to the MMCT electronic transition. Analysis of the 2D VE lineshapes reveals positive and negative frequency correlations of the cyanide stretching modes with the charge transfer transition. We will use this spectroscopy to measure the vibrational-electronic couplings in other mixed valence complexes over the next two years. In the next years, we will also develop the complementary 2D EV spectroscopy where the fate of coherent vibrational motion will be explored on various electronic surfaces following charge transfer with a sequence of optical pulses. We believe that the 2D VE and 2D EV techniques will find wide applicability in fields of chemistry, biology, and material science, specifically in mode-selective chemistry, coupled vibrational and electron transfer, proton and electron transfer processes, and the study of materials with strong electronic correlations where vibrations have been shown to coherently drive electronic phase transitions. We are also working to detail the selection rules for these new spectroscopies and show how the spectroscopic observables measure parameters from commonly used vibronic Hamiltonians.

### Equilibrium X-ray Absorption (XA) and Resonant Inelastic X-ray Scattering (RIXS) Spectra of Transition Metal Mixed Valence Complexes at the Fe K-edge and Fe L-edges in Solution. (Khalil, Schoenlein)

In order to understand the electronic configuration in the ground state of the transition metal complexes, we have obtained equilibrium XA, X-ray emission (XE) and RIXS spectra in water for Complexes **1** and **2** and model complexes  $\text{Fe}(\text{II})\text{CN}_6$  and  $\text{Fe}(\text{III})\text{CN}_6$  at the Fe L-edge and the Fe K-edge. A subset of the data is shown in Figure 1. The spectra reveal that the oxidation state of the iron atom in

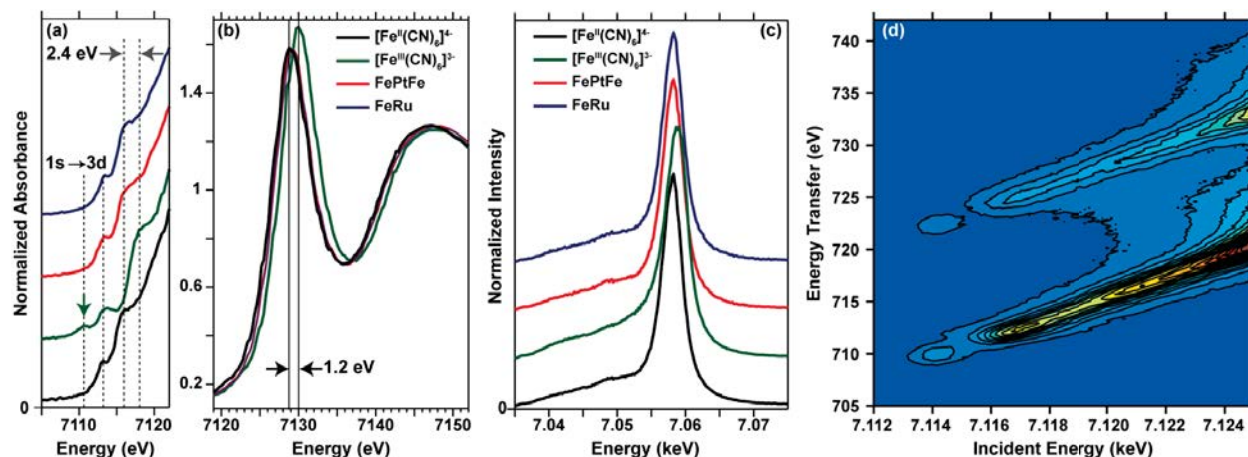


**Figure 1** (a-b) Static XANES spectra of reference complexes ( $[\text{Fe}^{\text{II}}(\text{CN})_6]^{4-}$ ,  $[\text{Fe}^{\text{III}}(\text{CN})_6]^{3-}$ ) and mixed valence compounds FeRu and FePtFe taken at ALS BL 10.3.2 where (a) shows multiple pre-edge features shifting from Fe(II) to Fe(III) and (b) shows a clear increase in energy and slight increase in relative intensity for the edge energy in Fe(III) vs Fe(II). (c) Equilibrium Fe K $\beta$  XE spectra of reference complexes ( $[\text{Fe}^{\text{II}}(\text{CN})_6]^{4-}$ ,  $[\text{Fe}^{\text{III}}(\text{CN})_6]^{3-}$ ) and mixed valence compounds FeRu and FePtFe taken at BL 7-ID at APS. (d) Fe K $\alpha$  RIXS spectra of the FeRu taken at BL 7-ID at APS. The spectra show a clear distinction between the Fe(II) complexes, which include the ground state mixed valence compounds, and the Fe(III) complex, which replicates the Fe state after MMCT photoexcitation. All complexes were dissolved in water to an iron concentration of at least 30 mM and flowed through a jet or capillary set-up.

FePtFe complex is Fe(II) and that of FeRu is also Fe(II) in the ground electronic state. The XANES and EXAFS spectra are currently being analyzed to obtain information about electronic configuration and bonding geometry around the Fe atoms. The EXAFS spectra will provide us with detailed information about the bond lengths between the Fe-C and Fe-N atoms. We will compare the experimental spectra with the simulated XANES spectra (as described below). The successful collection of equilibrium spectra will allow us to validate parameters in the simulation/computational codes for correctly modelling the electronic structure of the solvated mixed valence complexes. Additionally, the static spectra serve as necessary preliminary data for ultrafast XA/XE experiments that are planned for Oct. 2015 at the XPP instrument at LCLS.

In a related effort, the Schoenlein group has focused on the CN- bridged mixed valence transition-metal complex  $\text{Ru}^{\text{II}}\text{-CN-Cr}^{\text{III}}\text{-CN-Ru}^{\text{II}}$  complex as a prototypical model system. The strong electronic coupling between electron transfer donors (D) and acceptors (A) gives rise to very intense MMCT absorption bands at 500 nm in aqueous solution. Compared to the typical CN-bridged model complex ( $\text{Ru}^{\text{II}}\text{-CN-Ru}^{\text{III}}$ ), the use of the covalently linked  $\text{Cr}^{\text{III}}$  electron acceptor leads to remarkably long-lived charge-separated intermediates, attributed to the existence of electronic states of different spin multiplicity that effectively inhibit back electron transfer (BET). The first time-resolved X-ray spectroscopy (XANES) and equilibrium RIXS studies of this complex have recently been conducted at APS beamline 7-ID. Transient XANES at the Cr K-edge monitors changes in the local coordination geometry, changes in the spin multiplicity and electronic structure, and indicate BET on the time scale of  $\sim 35$  nsec. Detailed analysis of changes in pre-edge features in the XANES energy region is presently underway, and will be coupled with high-level ab initio calculations will provide an unprecedented view of electron delocalization dynamics in transition metal mixed valence systems. For these experiments, we have successfully synthesized the Ru-Cr-Ru compound (in collaboration with Prof. T.-K. Kim, U. Pusan), and have characterized the local structure (ground state) in the vicinity of the Cr atom via EXAFS measurements at the Advanced Light Source BL6.

**Ab Initio Molecular Dynamics/Molecular Mechanics (AIMD/MM), XA spectroscopy, UV/Vis and IR Spectroscopy of Model Complexes [Fe(CN)<sub>6</sub><sup>4-</sup> & Fe(CN)<sub>6</sub><sup>3-</sup>] in Water (Govind)** In order to study solvated model Fe(CN)<sub>6</sub><sup>4-</sup> and Fe(CN)<sub>6</sub><sup>3-</sup> complexes in water, we have performed extensive AIMD/MM dynamics simulations. The model complex was placed in a 40 Å cubic box and solvated with 2116 randomly placed water molecules to give a density close to 1 g/cm<sup>3</sup> (water density at standard temperature-pressure). The complex was treated quantum mechanically (QM), while the rest of the system (the water bath) was treated at the molecular mechanics (MM) level. Three K<sup>+</sup> cations and four K<sup>+</sup> cations were randomly placed in the solvation environment for the Fe(CN)<sub>6</sub><sup>3-</sup> and Fe(CN)<sub>6</sub><sup>4-</sup> complexes, respectively, to neutralize the charge of the solvation box. The water molecules, which comprise the MM region, were treated with the SPC/E water model. AIMD/MM molecular dynamics simulations were performed at 298.15 K (NVT) for 10 ps after equilibration. For the SPC/E water model, the SHAKE algorithm was used to keep the water molecules rigid (constraining the bond lengths and bond angle). The QM region (i.e., complexes) were described at the density functional theory (DFT) level of theory with the generalized-gradient approximation (GGA) functional of Perdew, Burke, and Enzerhof (PBE). The complexes, which comprise the QM region in the models, were allowed to move freely (i.e., SHAKE was not applied). Following the AIMD/MM runs, we extracted approximately 150 frames of the complex with a shell of water molecules from the trajectory to perform the XANES and UV/Vis spectra calculations. In addition to the shell of waters, the COSMO implicit solvent model was also included in all the frames to treat the far field. IR spectra were calculated directly from the AIMD/MM trajectory via the autocorrelation of the velocities. The Fe K-edge XANES and UV/Vis spectra were calculated with TDDFT. We have extended our TDDFT code to capture the quadrupole transitions in the Fe K-edge XANES. Our calculations are in excellent agreement with the experiments of Khalil and co-workers. We are in the process of preparing a joint manuscript covering this work.

**AIMD/MM, XA, UV/Vis and IR Spectroscopy of Dimer Complex [Fe(CN)<sub>5</sub>-CN-Ru(NH<sub>3</sub>)<sub>5</sub>] in Water and Formamide (Govind)** A similar protocol, as described above, was also applied to the solvated dimer complex FeRu in water and formamide. The dimer complex model involved the solvation in a simulation box containing the dimer complex with 2109 water molecules to give a density close to 1 g/cm<sup>3</sup>. The second model involved the solvation of the box with 953 formamide molecules to give a density close to the formamide density of 1.13 g/cm<sup>3</sup> at STP. For the MM water molecule region, the SPC/E force-field was applied as with the previous model complex cases. For the MM formamide region in the second model, the GAFF force-field parameters were applied along with the Columbic charges derived by Andersson et al. via ab initio calculations. The SHAKE algorithm was used to fix hydrogen bearing bonds in formamide. As with the model complexes, the QM complex region was unconstrained. The details of the AIMD/MM simulations are the same as that for the model complexes. We have completed our AIMD/MM calculations of the dimer complex in water and are in the process of completing the calculations in formamide. The XANES, UV/Vis and IR spectra, as in the model complexes, will be calculated here. The goal of this study is to elucidate the structural and spectroscopic differences of the dimer complex in water and formamide as has been discussed by Khalil and co-workers. These results will be summarized in a joint paper focusing on the dimer complexes in water and formamide.

**Simulating Valence-to-Core X-ray Emission Spectroscopy (Govind, Mukamel)** Valence to core X-ray emission spectroscopy (VtC-XES) is a sensitive tool to identify ligands and characterize ligand valence orbitals in transition metal complexes. The VtC-XES features arise on the high energy tail of the much stronger Kβ<sub>1,3</sub> lines (Kβ main line). They represent transitions from the occupied valence orbitals with ligand s- or p- character and metal p-character to the (metal) core 1s orbital. Usually a VtC-XES spectrum can be divided into two regions called Kβ'' and Kβ<sub>2,5</sub>. Kβ'' features are related to transitions involving valence orbitals with mainly ligand s-character, which can be used to identify the chelating atoms. Kβ<sub>2,5</sub> peaks are determined by valence orbitals with heavy ligand p-character and some metal p-character, which contain the information of chemical bonds between the metal center and ligands. Compared with X-ray absorption techniques like XANES and EXAFS, an advantage of XES is that it does not require

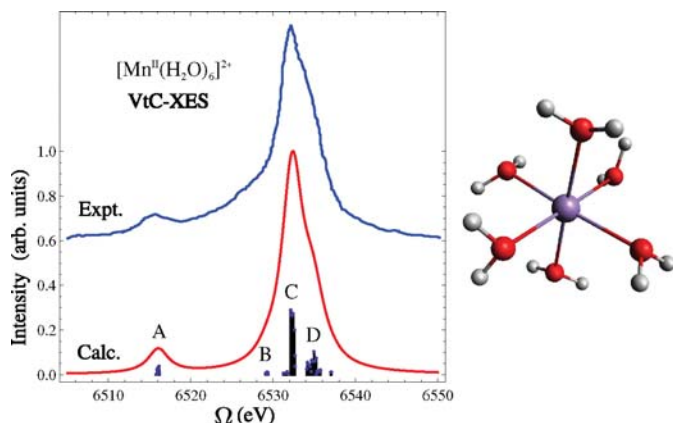


**Figure 2.** VtC emission spectrum of  $\text{Mn}^{\text{II}}(\text{H}_2\text{O})_6]^{2+}$

as reference to simulate VtC-XES spectra. In contrast with the single-particle DFT approach, which provides a reliable description of single configuration dominant VtC X-ray emission processes our approach is well-suited to describe emission processes with multiconfigurational character. We have applied our approach to calculate the K-edge VtC-XES spectra of seven low- and high-spin model complexes involving Cr, Mn and Fe transition metal (TM) centers with different oxidation states. Specifically, we have chosen the following TM complexes:  $[\text{Cr}^{\text{III}}(\text{NH}_3)_6]^{3+}$ ,  $[\text{Cr}^0(\text{CO})_6]$ ;  $\text{Mn}^{\text{II}}(\text{H}_2\text{O})_6]^{2+}$ ,  $[\text{Mn}^{\text{II}}(\text{CN})_5\text{N}]^{3-}$ ;  $[\text{Fe}^{\text{II}}(\text{CN})_6]^{4-}$ ;  $[\text{Fe}^{\text{III}}(\text{CN})_6]^{3-}$  and  $[\text{Fe}^{\text{II}}(\text{CN})_5(\text{NO})]^{2-}$ . We have studied the dominant spin states of these complexes, that is, the high-spin quartet for  $[\text{Cr}^{\text{III}}(\text{NH}_3)_6]^{3+}$ , the low-spin singlet for  $[\text{Cr}^0(\text{CO})_6]$ , the high-spin sextet for  $\text{Mn}^{\text{II}}(\text{H}_2\text{O})_6]^{2+}$ , the low-spin doublet for  $[\text{Mn}^{\text{II}}(\text{CN})_5\text{N}]^{3-}$ , the low-spin singlet for  $[\text{Fe}^{\text{II}}(\text{CN})_6]^{4-}$ , the low-spin doublet for  $[\text{Fe}^{\text{III}}(\text{CN})_6]^{3-}$ , and the low-spin singlet for  $[\text{Fe}^{\text{II}}(\text{CN})_5(\text{NO})]^{2-}$ . Our calculated results are in excellent agreement with experiment. An example is provided in Figure 2. Our paper, where we detail our approach and findings, is currently under review in JCTC. We are extending the above benchmark study to calculate the VtC-XES of the model complexes  $[\text{Fe}(\text{CN})_6]^{4-}$  &  $[\text{Fe}(\text{CN})_6]^{3-}$  in water. In addition, this analysis will also be performed for the mixed valence FeRu dimer, FePtFe and RuCrRu complexes in water. This data has just been acquired by the Khalil and Schoenlein groups at the APS beamline (described earlier).

**Calculating Electron Transfer Rates (Mukamel)** Khalil and coworkers have carried out a series of nonlinear IR and vibrational-electronic spectroscopy studies to investigate the charge transfer and vibrational energy relaxation dynamics of several typical vibrational modes in the Fe-Pt-Fe trimer and Fe-Ru dimer complexes. These systems are important models to understand photoinduced charge transfer and chemical reactions in transition metal complexes. With the kinetic and vibrational-electronic coupling parameters obtained from these experiments, we plan to construct simple model Hamiltonians to describe the dimer and trimer systems, with which one can recover the experimental charge transfer and vibrational relaxation dynamics. Using a Green's function approach, electron transfer rate expressions with vibrational effect will be derived and how each specific vibrational mode affects the ultrafast electron transfer in the studied system will be analyzed. With the knowledge, we can further study how to control electron transfer in these systems with differently shaped IR pulses.

#### **DOE SUPPORTED PUBLICATIONS (09/01/14 - present)**

1. Courtney, Trevor L.; Fox, Zachary W.; Estergreen, Laura; Khalil, Munira. Measuring Coherently Coupled Intramolecular Vibrational and Charge-Transfer Dynamics with Two-Dimensional Vibrational-Electronic Spectroscopy. *The Journal of Physical Chemistry Letters* **2015**, *6*, 1286-1292.
2. Zhang, Yu; Mukamel, Shaul; Khalil, Munira; Govind, Niranjan. Simulating Valence-to-Core X-ray Emission Spectroscopy of Transition Metal Complexes with Time-Dependent Density Functional Theory. *Journal of Chemical Theory and Computation* **2015**, (in review)

## Chemical Kinetics and Dynamics at Interfaces

### *Non-Thermal Reactions at Surfaces and Interfaces*

**Greg A. Kimmel (PI) and Nikolay G. Petrik**

Chemical and Materials Sciences Division  
 Pacific Northwest National Laboratory  
 P.O. Box 999, Mail Stop K8-88  
 Richland, WA 99352  
[gregory.kimmel@pnnl.gov](mailto:gregory.kimmel@pnnl.gov)

Collaborators include: BD Kay and RS Smith

### Program Scope

The objectives of this program are to investigate 1) thermal and non-thermal reactions at surfaces and interfaces, and 2) the structure of thin adsorbate films and how this influences the thermal and non-thermal chemistry. Energetic processes at surfaces and interfaces are important in fields such as photocatalysis, radiation chemistry, radiation biology, waste processing, and advanced materials synthesis. Low-energy excitations (e.g. excitons, electrons, and holes) frequently play a dominant role in these energetic processes. For example, in radiation-induced processes, the high energy primary particles produce numerous, chemically active, secondary electrons with energies that are typically less than ~100 eV. In photocatalysis, non-thermal reactions are often initiated by holes or (conduction band) electrons produced by the absorption of visible and/or UV photons in the substrate. In addition, the presence of surfaces or interfaces modifies the physics and chemistry compared to what occurs in the bulk.

We use quadrupole mass spectroscopy, infrared reflection-absorption spectroscopy (IRAS), and other ultra-high vacuum (UHV) surface science techniques to investigate thermal, electron-stimulated, and photon-stimulated reactions at surfaces and interfaces, in nanoscale materials, and in thin molecular solids. Since the structure of water near interface plays a crucial role in the thermal and non-thermal chemistry occurring there, a significant component of our work involves investigating the structure of aqueous interfaces. A key element of our approach is the use of well-characterized model systems to unravel the complex non-thermal chemistry occurring at surfaces and interfaces. This work addresses several important issues, including understanding how the various types of low-energy excitations initiate reactions at interfaces, the relationship between the water structure near an interface and the non-thermal reactions, energy transfer at surfaces and interfaces, and new reaction pathways at surfaces.

### Recent Progress

#### *Turning things downside up: Adsorbate induced water flipping on Pt(111)*

Water-metal interfaces are important for many areas of science and technology including corrosion, electrochemistry, and electrolysis. These interfaces are interesting in part due to the complex ways in which the hydrogen bonding arrangement within the water network adapts to the presence of a symmetry-breaking 2-dimensional interface. The changes in the hydrogen bonding network at metal interfaces are also related to how water adapts to hydrophilic and hydrophobic solutes.

We have examined the adsorption of the weakly bound species N<sub>2</sub>, O<sub>2</sub>, CO and Kr on the ( $\sqrt{37} \times \sqrt{37}$ )R25.3° water monolayer on Pt(111) using a combination of molecular beam dosing, infrared reflection absorption spectroscopy (IRAS), and temperature programmed desorption (TPD). In contrast to multilayer crystalline ice, the adsorbate-free water monolayer is characterized by a lack of dangling OH bonds protruding into the vacuum (H-up). Instead, the non-hydrogen-bonded OH groups are oriented downward (H-down) to maximize their interaction with the underlying Pt(111) substrate. Adsorption of Kr and O<sub>2</sub> have little effect on the structure and vibrational spectrum of the “ $\sqrt{37}$ ” water monolayer

while adsorption of both  $N_2$ , and  $CO$  are effective in “flipping” H-down water molecules into an H-up configuration (see Figure 1). This “flipping” occurs readily upon adsorption at temperatures as low as 20 K and the water monolayer transforms back to the H-down, “ $\sqrt{37}$ ” structure upon adsorbate desorption above 35 K, indicating small energy differences and barriers between the H-down and H-up configurations. The results suggest that converting water in the first layer from H-down to H-up is mediated by the electrostatic interactions between the water and the adsorbates.

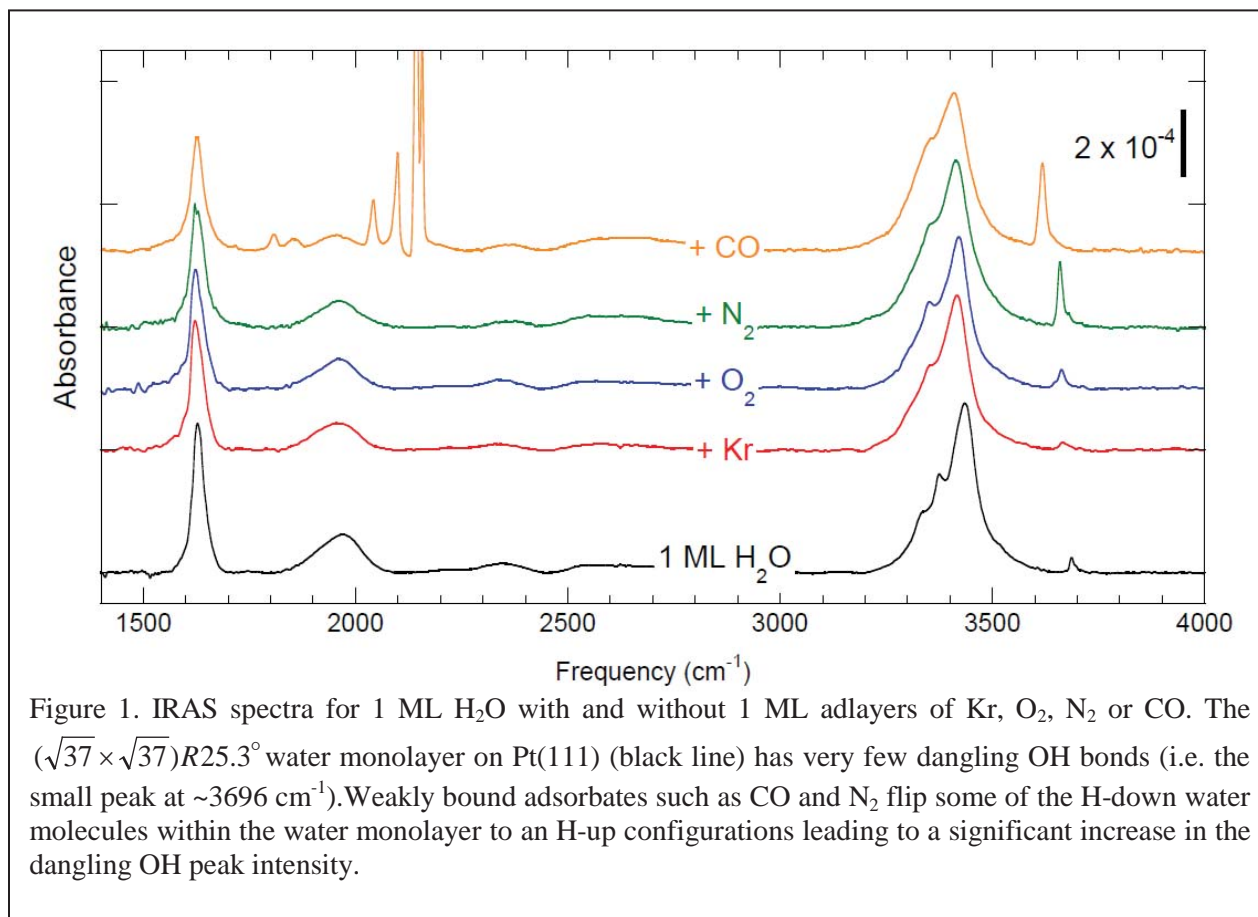


Figure 1. IRAS spectra for 1 ML  $H_2O$  with and without 1 ML adlayers of Kr,  $O_2$ ,  $N_2$  or  $CO$ . The  $(\sqrt{37} \times \sqrt{37})R25.3^\circ$  water monolayer on Pt(111) (black line) has very few dangling OH bonds (i.e. the small peak at  $\sim 3696 \text{ cm}^{-1}$ ). Weakly bound adsorbates such as  $CO$  and  $N_2$  flip some of the H-down water molecules within the water monolayer to an H-up configurations leading to a significant increase in the dangling OH peak intensity.

This work was done in collaboration with B. D. Kay and R. S. Smith and is published in reference 4.

### ***Insights into Acetone Photochemistry on Rutile $TiO_2(110)$ .***

$TiO_2$  is a widely used photocatalyst. Its ability to oxidize organic contaminants makes it useful, for example, in air and water purification systems and as a thin-film coating for self-cleaning surfaces. As a result of titanium oxide’s practical applications and its potential use in photocatalytic water spitting, it has been the subject of a tremendous amount of research. We have previously investigated in detail the photooxidation of  $CO$  to  $CO_2$  on  $TiO_2(110)$ . Those experiments showed that the  $CO_2$  is ejected from the surface with a non-cosine angular distribution that provided valuable information about the reaction pathway. Recently, we have extended our investigation of photooxidation reactions on  $TiO_2(110)$  to more complex molecules, this time focusing on acetone.

We have used IRAS, angle-resolved PSD and other methods to investigate the thermal- and photon-stimulated reactions of the acetone co-adsorbed with oxygen on rutile  $TiO_2(110)$  and irradiated with UV photons with energy above the bandgap. Our results show that the acetone photochemistry on  $TiO_2(110)$  involves two distinct photochemical reaction pathways. One reaction pathway proceeds via a

previously-proposed acetone diolate intermediate (see Figure 2). This reaction pathway is most evident for initial coverages of acetone that are less than or approximately equal to the coverage of oxygen adatoms on an oxidized  $\text{TiO}_2(110)$  surface, but it occurs for all acetone coverages studied (i.e. 0 – 0.6 monolayers). IRAS spectra show  $\eta^2$ -acetone diolate forms via thermally-activated reactions between chemisorbed oxygen and acetone. Angle-resolved measurements of the  $\text{CH}_3$  radicals that are ejected from the acetone diolate during UV irradiation show that they have a distribution that is peaked at  $\sim \pm 66^\circ$  from the normal  $[110]$  vector in the  $[\bar{1}10]$  azimuth (i.e. perpendicular to the rows of bridging oxygen ( $\text{O}_b$ ) and  $\text{Ti}_{5c}$  ions), consistent with the expected orientation of the  $\text{C}-\text{CH}_3$  bonds in  $\eta^2$ -acetone diolate on  $\text{TiO}_2(110)$ . After UV irradiation, the acetone diolate peaks disappear from the IRAS spectra and new peaks that are associated with the  $\eta^2$ -acetate are observed. The results provide direct signatures of the previously-proposed 2-step mechanism of the acetone photooxidation on  $\text{TiO}_2(110)$ .

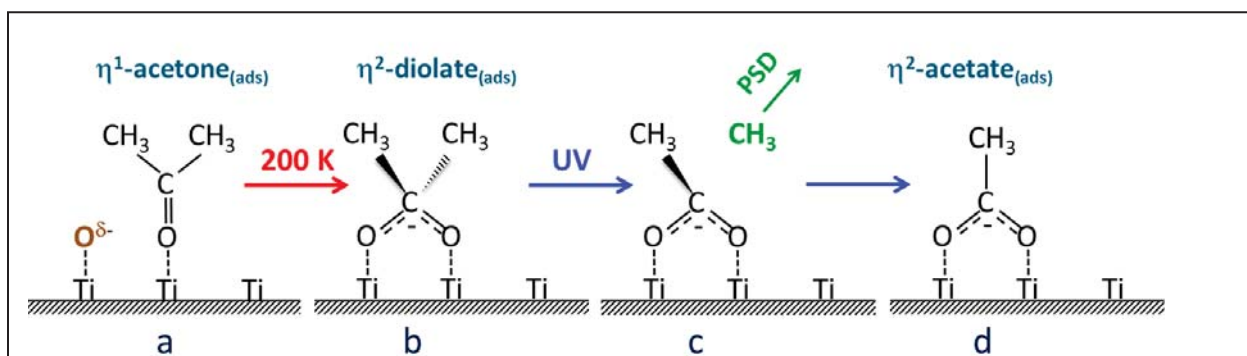


Figure 2. Schematic of the reaction channel for acetone adsorbed on oxidized  $\text{TiO}_2(110)$  that leads to  $\text{CH}_3$  emission off-normal to the surface via the acetone diolate intermediate.

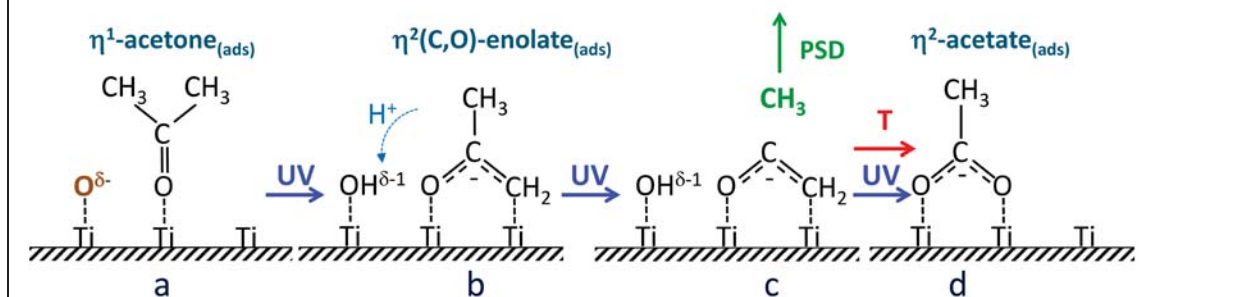


Figure 3. Schematic of the reaction channel for acetone adsorbed on oxidized  $\text{TiO}_2(110)$  that leads to  $\text{CH}_3$  emission normal to the surface via the acetone enolate intermediate.

We also find a second reaction channel in which the methyl fragments are ejected along the surface normal (see Figure 3). This normal component of the PSD distribution is associated with a different precursor molecule and indicates that a second, previously unknown, photochemical reaction channel exists for acetone on this surface. The “normal” component grows with acetone coverage in the 0–0.6 ML range, and it becomes a significant reaction channel for acetone coverages at the upper end of this range. Both reaction channels lead to the ejection of  $\text{CH}_3$  during UV irradiation and to the eventual desorption of ketene at the same temperature during post-irradiation TPD (corresponding to thermal decomposition of surface acetate). Both components of the  $\text{CH}_3$  PSD angular distribution are relatively narrow as compared to the cosine distribution characteristic for desorption of thermally-equilibrated

molecules, indicating both channels are the result of non-thermal bond-breaking events. Although we cannot make a definitive assignment of the second reaction channel, the results suggest that acetone-enolate, produced by non-thermal reactions in the acetone adsorbed on oxidized TiO<sub>2</sub>(110), is the photo-active species responsible for the normal component observed in the CH<sub>3</sub> AR-PSD measurements.

This work is published in references 5 and 6.

### Future Directions:

Important questions remain concerning the factors that determine the structure of thin water films on various substrates. We plan to continue investigating the structure of thin water films on non-metal surfaces, such as oxides, and on metals where the first layer of water does not wet the substrate. For the non-thermal reactions in water films, we will use IRAS to characterize the electron-stimulated reaction products and precursors. We will also continue our investigations into the photochemistry of small molecules on TiO<sub>2</sub>(110).

### References to publications of DOE-sponsored research (FY 2013 – present)

- [1] Nikolay G. Petrik and Greg A. Kimmel, “Probing the photochemistry of chemisorbed oxygen on TiO<sub>2</sub>(110) with Kr and other co-adsorbates,” *Phys. Chem. Chem. Phys.* **16**, 2338 – 2346 (2014) (DOI: 10.1039/c3cp54195a).
- [2] Nikolay G. Petrik, Rhiannon J. Monckton, Sven P. K. Koehler and Greg A. Kimmel, “Electron-stimulated reactions in layered CO/H<sub>2</sub>O films: Hydrogen atom diffusion and the sequential hydrogenation of CO to methanol,” *J. Chem. Phys.* **140**, 204710 (2014) (DOI: 10.1063/1.4878658).
- [3] Nikolay G. Petrik, Rhiannon J. Monckton, Sven P. K. Koehler and Greg A. Kimmel, “Distance-dependent radiation chemistry: Oxidation versus hydrogenation of CO in electron-irradiated H<sub>2</sub>O/CO/H<sub>2</sub>O ices,” *J. Phys. Chem.*, **118**, 27483 (2014). (DOI: 10.1021/jp509785d).
- [4] Greg A. Kimmel, Tykhon Zubkov, R. Scott Smith, Nikolay G. Petrik and Bruce D. Kay, “Turning things downside up: Adsorbate induced water flipping on Pt(111),” *J. Chem. Phys.*, **141**, 18C515 (2014) (DOI: 10.1063.4896226).
- [5] Nikolay G. Petrik, Michael A. Henderson, and Greg A. Kimmel, “Insights into Acetone Photochemistry on Rutile TiO<sub>2</sub>(110). 1. Off-Normal CH<sub>3</sub> Ejection from Acetone Diolate,” *J. Phys. Chem. C.*, **119**, 12262 (2015). (DOI: 10.1021/acs.jpcc.5b02477).
- [6] Nikolay G. Petrik, Michael A. Henderson, and Greg A. Kimmel, “Insights into Acetone Photochemistry on Rutile TiO<sub>2</sub>(110). 2. New Photodesorption Channel with CH<sub>3</sub> Ejection along the Surface Normal,” *J. Phys. Chem. C.*, **119**, 12273 (2015). (DOI: 10.1021/acs.jpcc.5b02478).
- [7] Konrad Thürmer, Chunqing Yuan, Greg A. Kimmel, Bruce D. Kay, R. Scott Smith, “Weak interactions between water and clathrate-forming gases at low pressures,” *Surf. Sci.* **641**, 216-223 (2015). (DOI: 10.1016/j.susc.2015.07.013).
- [8] Nikolay G. Petrik and Greg A. Kimmel, “Reaction Kinetics of Water Molecules with Oxygen Vacancies on Rutile TiO<sub>2</sub>(110),” *J. Phys. Chem.* **accepted**.

## Interfacial Radiation Sciences

Jay A. LaVerne, David M. Bartels, Ian Carmichael, Sylwia Ptasinska  
Notre Dame Radiation Laboratory, University of Notre Dame, Notre Dame, IN 46556  
[laverne.1@nd.edu](mailto:laverne.1@nd.edu), [bartels.5@nd.edu](mailto:bartels.5@nd.edu), [carmichael.1@nd.edu](mailto:carmichael.1@nd.edu), [sylwia.ptasinska.1@nd.edu](mailto:sylwia.ptasinska.1@nd.edu)

### Program Scope

A wide range of disciplines and techniques are used to probe chemical effects induced at interfaces by radiation. Fundamental radiation chemical effects in homogeneous media continue to be a major effort at the NDRL and this program utilizes that expertise to examine much more complicated heterogeneous systems with their wide variety of challenges. Areas being addressed relevant to the nuclear power industry include construction materials commonly found in reactors or in the storage of waste fuel and proposed newer cladding materials. This work extends our extensive knowledge on the radiolysis of water and aqueous solutions to include the effects due to an added interface. Another active area of research involves probing the precise interactions occurring at gas – solid interfaces using advanced X-ray photoelectron spectroscopy techniques. In particular, emphasis has been given to gases at GaP and GaAs surfaces because of their use in photoelectrochemical devices.

### Recent Progress and Future Plans

The radiolysis of a variety of iron oxide powders with different amounts of associated water has been performed using gamma rays and 5 MeV  $^4\text{He}$  ions <sup>1</sup>. Adsorbed water was characterized by both temperature programmed desorption and diffuse reflection infrared Fourier transform spectroscopy to reveal a variety of active sites on the surface. Molecular hydrogen production was found only from water adsorbed on  $\text{Fe}_2\text{O}_3$ , and the yield was several orders of magnitude greater than that from bulk water. Aqueous slurries of  $\text{FeO}$ ,  $\text{Fe}_3\text{O}_4$  and  $\text{Fe}_2\text{O}_3$ , examined as a function of water fraction, gave different yields of  $\text{H}_2$  depending on the oxide type and the amount of water. Examination of the iron oxide powders following irradiation during X-ray diffraction showed no change in crystal structure. Raman spectroscopy of the oxides revealed the formation of islands of  $\text{Fe}_2\text{O}_3$  on the surfaces of  $\text{FeO}$  and  $\text{Fe}_3\text{O}_4$ . X-ray photoelectron spectroscopy of the oxides revealed the general formation of new oxygen species following radiolysis.

Two copper oxides, cuprous and cupric oxide, were characterized using a variety of surface techniques including scanning electron microscopy, temperature programmed desorption, diffuse reflectance infrared Fourier transform spectroscopy, Raman spectroscopy, X-ray photoelectron spectroscopy and X-ray diffraction to analyze changes in the oxide surface following irradiation with gamma rays and 5 MeV  $^4\text{He}$  ions <sup>2</sup>. The radiation chemical yield for  $\text{H}_2$  was also measured for copper oxide powders with adsorbed water as well as with slurries containing various amounts of water. The yield of  $\text{H}_2$  was found to be slightly greater than the yield expected for bulk water radiolysis indicating some small radiation chemical effect of the oxide surface on water. X-ray photoelectron spectroscopy indicated that the amount of OH groups present on the cuprous oxide surface decreased as a result of the irradiation while the cupric oxide surface had an apparent increase in OH groups on the surface. This result suggests that the mechanism for the formation of  $\text{H}_2$  differs based on the surface composition and structure of the oxide.

Other popular construction materials used in the nuclear power industry such as  $\text{Al}_2\text{O}_3$  will be examined at the molecular level following radiolysis by gamma rays and  $^4\text{He}$  ions. Zircaloy is

a common cladding material, but it is known to spontaneously reduce water at high temperatures leading to potentially disastrous results as witnessed at Fukushima. One of the more promoted alloys for use as cladding in the future generation of nuclear reactors is SiC, which has undergone considerable material science studies and proven to be very stable under a variety of thermal conditions. However, little is known about the radiation chemistry of SiC and systematic studies will be undertaken to understand the effects of radiation on the chemistry of water in association with SiC and surface oxidation of the material.

A detailed molecular-level understanding of gas-solid interfacial interactions, especially under operational conditions, is important, both from the applied and fundamental points of view. Recently, fundamental investigations probing water adsorption and dissociation onto surfaces of GaP- and GaAs-based photoelectrodes, which can be incorporated into photoelectrochemical (PEC) solar cells, were conducted in order to elucidate the water effects on surfaces upon CO<sub>2</sub> reduction<sup>3-5</sup> and water splitting<sup>6-8</sup>. However, due to our limited knowledge of the material and electronic structures of such semiconductor surfaces, especially under realistic conditions, there is no comprehensive understanding of molecular chemistry at the water/electrode interface<sup>9-11</sup>. Photoelectrodes, especially under operational conditions, usually suffer from a variety of issues, including a short lifetime due to photocorrosion and decreased electron extraction efficiency due to the formation of oxides on the electrodes' surface<sup>8-11</sup>. Because PEC processes occur in an aqueous environment, it is essential to understand the nature of H<sub>2</sub>O interactions with semiconductors and the possible oxidation and reduction mechanisms at the H<sub>2</sub>O/semiconductor interface<sup>4,7</sup>. Characterization of interfacial interactions between several molecular gases and GaAs(100) or GaP(111) surfaces were carried out by X-ray photoelectron spectroscopy (XPS), which is one of the surface sensitive techniques used most widely<sup>12</sup>. Moreover, our advanced *in situ* instrumentation, *i.e.*, near-ambient pressure XPS (NAP XPS), enabled us to explore the gas/solid interfacial chemistry at elevated pressures (up to the mbar range) and temperatures (up to 773 K).

We have reported the evolution of photoemission spectra from GaAs(100) over wide ranges of pressures and temperatures for the three oxidants, N<sub>2</sub>O, NO, and O<sub>2</sub><sup>13</sup>. Our results indicated that, for these three gases, the oxidation processes at the gas/semiconductor interface are distinctly different. The extent of surface oxidation was determined primarily by the following factors related to the oxidants: chemical bond dissociation energies, the presence of unpaired electrons, electron affinities, and dipole moments, all of which affect the kinetics and energetics of adsorption and oxidation. NO has the greatest ability to oxidize the surface at temperatures below 473 K, while O<sub>2</sub> is the more efficient oxidant at higher temperatures. N<sub>2</sub>O oxidizes GaAs gradually with increases in pressure and temperature, but it does not produce oxidation to any great degree. The open-shell structure of NO enables it to be adsorbed and to dissociate, even at room temperature, which results in surface oxidation. At higher temperatures, the extent of oxidation due to NO interactions depends on gas pressure, *i.e.*, the number of NO molecules that are adsorbed onto the surface. In the case of O<sub>2</sub>, surface oxidation is determined by the dissociation of O-O bonds, which can be facilitated at higher temperatures. In the case of N<sub>2</sub>O, despite the fact that it has the lowest bond dissociation energy, interactions between this molecule and GaAs are weaker. Our study on the reactivity of GaAs surfaces with various oxidants can be used to model processes in which charge carriers that are photogenerated in the bulk of a semiconductor migrate to the surface and interact with the adsorbant<sup>10</sup>.

In addition to detecting the final products of gas dissociation onto surfaces, we were able to detect intermediate species through *in situ* tracking of physicochemical processes on the surface. Knowing the intermediate species allows us to deduce the reaction pathways and to obtain a comprehensive picture of surface oxidation at close to ambient conditions, which cannot be achieved with the standard XPS technique. For example, in the case of the H<sub>2</sub>O/GaP(111) interface, we observed the formation of final products with a different degree of oxidation and hydroxylation, O<sub>n</sub>•Ga•(OH)<sub>3-n</sub> where 0 ≤ n ≤ 1, via a Ga<sub>2</sub>O-like intermediate species<sup>14</sup>.

Although we have proposed mechanisms that may explain the nature of the oxidant interactions with the GaAs and GaP surfaces, they should be confirmed with results from computational modeling, which we plan to perform with the LLNL group. Moving forward, we will extend this study to other III-V semiconductor materials such as GaSb and GaN, in order to understand the effects of the counter ion on surface oxidation in Ga-based materials. We also plan to study an entire PEC device in which GaP acts as a photoelectrode for water splitting. In such a case the surface chemistry of this PEC solar cell will be also monitored under *operando* conditions using the NAP XPS system.

## References

- (1) Reiff, S. C.; La Verne, J. A. Radiation-Induced Chemical Changes to Iron Oxides. *J. Phys. Chem. B* **2015**, *119*, 7358-7365.
- (2) Reiff, S. C.; La Verne, J. A. Gamma and He Ion Radiolysis of Copper Oxides. *J. Phys. Chem. C* **2015**, *119*, 8821-8828.
- (3) Barton, E. E.; Rampulla, D. M.; Bocarsly, A. B. Selective solar-driven reduction of CO<sub>2</sub> to methanol using a catalyzed p-GaP based photoelectrochemical cell. *J. Am. Chem. Soc.* **2008**, *130*, 6342-+.
- (4) Jeon, S.; Kim, H.; Goddard, W. A., III; Atwater, H. A. DFT Study of Water Adsorption and Decomposition on a Ga-Rich GaP(001)(2x4) Surface. *J. Phys. Chem. C* **2012**, *116*, 17604-17612.
- (5) Munoz-Garcia, A. B.; Carter, E. A. Non-innocent Dissociation of H<sub>2</sub>O on GaP(110): Implications for Electrochemical Reduction of CO<sub>2</sub>. *J. Am. Chem. Soc.* **2012**, *134*, 13600-13603.
- (6) Lewerenz, H.-J.; Peter, L. *Photoelectrochemical Water Splitting: Materials, Processes and Architectures*; Royal Society of Chemistry: Cambridge, GBR, 2013.
- (7) Wood, B. C.; Schwegler, E.; Choi, W. I.; Ogitsu, T. Hydrogen-Bond Dynamics of Water at the Interface with InP/GaP(001) and the Implications for Photoelectrochemistry. *J. Am. Chem. Soc.* **2013**, *135*, 15774-15783.
- (8) Wood, B. C.; Schwegler, E.; Choi, W. I.; Ogitsu, T. Surface Chemistry of GaP(001) and InP(001) in Contact with Water. *J. Phys. Chem. C* **2014**, *118*, 1062-1070.
- (9) May, M. M.; Supplie, O.; Hoehn, C.; van de Krol, R.; Lewerenz, H.-J.; Hannappel, T. The interface of GaP(100) and H<sub>2</sub>O studied by photoemission and reflection anisotropy spectroscopy. *New J. Phys.* **2013**, *15*.
- (10) Wood, B. C.; Ogitsu, T.; Schwegler, E. Ab initio modeling of water-semiconductor interfaces for photocatalytic water splitting: role of surface oxygen and hydroxyl. *J. Photon. Energy.* **2011**, *1*.
- (11) Wood, B. C.; Ogitsu, T.; Schwegler, E. Local structural models of complex oxygen-and hydroxyl-rich GaP/InP(001) surfaces. *J. Chem. Phys.* **2012**, *136*.
- (12) Bagus, P. S.; Ilton, E. S.; Nelin, C. J. The interpretation of XPS spectra: Insights into materials properties. *Sur. Sci. Rep.* **2013**, *68*, 273-304.
- (13) Zhang, X.; Ptasinska, S. Evolution of Surface-Assisted Oxidation of GaAs (100) by Gas-Phase N<sub>2</sub>O, NO, and O<sub>2</sub><sup>-</sup> under Near-Ambient Pressure Conditions. *J. Phys. Chem. C* **2015**, *119*, 262-270.
- (14) Zhang, X.; Ptasinska, S. Distinct and dramatic water dissociation on GaP(111) tracked by near-ambient pressure X-ray photoelectron spectroscopy. *Phys. Chem. Chem. Phys.* **2015**, *17*, 3909-3918.

**Publications with BES support (2013-2015)**

- Jheeta, S.; Domaracka, A.; Ptasinska, S.; Sivaraman, B.; Mason, N. J. The Irradiation of Pure CH<sub>3</sub>OH and 1:1 NH<sub>3</sub>:CH<sub>3</sub>OH Ices at 30K Using Low Energy Electrons. *Chem. Phys. Lett.* **2013** 556 359-64.
- Dhiman, S.; LaVerne, J. A. Radiolysis of Simple Quaternary Ammonium Salt Components of Amberlite Resin. *J. Nucl. Mater.* **2013**, 436, 8-13.
- Lousada, C. M.; LaVerne, J. A.; Jonsson, M. Enhanced Hydrogen Formation During the Catalytic Decomposition of H<sub>2</sub>O<sub>2</sub> on Metal Oxide Surfaces in the Presence of HO Radical Scavengers *Phys. Chem. Chem. Phys.* **2013**, 15, 12674-19.
- Mincher, B. J.; Mezyk, S. P.; Elias, G.; Groenewold, G. S.; LaVerne, J. A.; Nilsson, A. R.; Pearson, J.; Schmitt, N. C.; Tillotson, R. D. and Olsen, L. G. The Radiation Chemistry of CMPO: Part 2. Alpha Radiolysis. *Solv. Extr. Ion Exch.* **2014** 32, 167-78.
- Zhang, X. Q.; Lamere, E.; Liu, X. Y.; Furdyna, J. K. and Ptasinska, S. Morphology Dependence of Interfacial Oxidation States of Gallium Arsenide Under Near Ambient Conditions. *Appl. Phys. Lett.* **2014** 104, 181602.
- Zhang, X. Q.; Lamere, E.; Liu, X.; Furdyna, J. K. and Ptasinska, S. Interface Chemistry of H<sub>2</sub>O on GaAs Nanowires Probed by Near Ambient Pressure X-ray Photoelectron Spectroscopy. *Chem. Phys. Lett.* **2014** 605, 51-5.
- Zhang, X. Q. and Ptasinska, S. Dissociative Adsorption of Water on an H<sub>2</sub>O/GaAs(100) Interface: *In Situ* Near-Ambient Pressure XPS Studies. *J. Phys. Chem. C* **2014** 118, 4259-66.
- Zhang, X.; Ptasinska S. Growth of Silicon Oxynitride Films by Atmospheric Pressure Plasma Jet. *J. Phys. D.* **2014** 47, 145202.
- Plekan, O.; Feyer, V.; Ptasinska, S.; Tsud, N.; Prince, K. C. Cyclic Dipeptide Immobilization on Au(111) and Cu(110) Surfaces. *Phys. Chem. Chem. Phys.* **2014** 16, 6657-65.
- Sun, F.; Zhang, T.; Jobbins, M. M.; Guo, Z.; Zhang, X.; Zheng, Z.; Tang, D.; Ptasinska, S.; Luo, T. Molecular Bridge Enables Anomalous Enhancement in Thermal Transport across Hard-Soft Material Interfaces. *Adv. Mat.* **2014** 26, 6093-9.
- Zhang, X.; Ptasinska S. Evolution of Surface-assisted Oxidation of GaAs (100) by Gas-phase N<sub>2</sub>O, NO, and O<sub>2</sub> Under Near-ambient Pressure Conditions. *J. Phys. Chem. C* **2015** 119, 262-70.
- Zhang, X.; Ptasinska, S. Distinct and Dramatic Water Dissociation on GaP (111) Tracked by Near Ambient Pressure XPS. *Phys. Chem. Chem. Phys.* **2015** 17, 3909-18.
- Plekan, O.; Feyer, V.; Cassidy, A.; Lyamayev, V.; Tsud, N.; Ptasinska, S.; Reiff, S.; Acres, R. G.; Prince, K. C. Functionalisation and Immobilisation of an Au(110) Surface Via Uracil and 2-Thiouracil Anchored Layer. *Phys. Chem. Chem. Phys.* **2015** 17, 15181-92
- Reiff, S. C.; La Verne, J. A. Radiation-Induced Chemical Changes to Iron Oxides. *J. Phys. Chem. B* **2015** 119, 7358-65.
- Reiff, S. C.; La Verne, J. A. Gamma and He Ion Radiolysis of Copper Oxides. *J. Phys. Chem. C* **2015** 119, 8821-8.
- Leay, L.; Bower, W.; Horne, G.; Wady, P.; Baidak, A.; Pottinger, M.; Nancekievill, M.; Smith, A. D.; Watson, S.; Green, P. R.; Lennox, B.; LaVerne, J.A.; Pimblott, S.M. I. Development of Irradiation Capabilities to Address the Challenges of the Nuclear Industry. *Nucl. Meth. Phys. Res. B* **2015** 343, 62-9.

## *Single-Molecule Interfacial Electron Transfer*

**H. Peter Lu**

Bowling Green State University  
Department of Chemistry and Center for Photochemical Sciences  
Bowling Green, OH 43403  
[hplu@bgsu.edu](mailto:hplu@bgsu.edu)

### **Program Scope**

We develop and apply single-molecule high spatial and temporal resolved techniques to study molecular dynamics in condensed phase and at interfaces, especially, the complex reaction dynamics associated with electron and energy transfer rate processes. The complexity and inhomogeneity of the interfacial ET dynamics often present a major challenge for a molecular level comprehension of the intrinsically complex systems, which calls for both higher spatial and temporal resolutions at ultimate single-molecule and single-particle sensitivities. Combined single-molecule spectroscopy and electrochemical atomic force microscopy (E-Chem AFM) approaches are unique for heterogeneous and complex interfacial electron transfer systems because the static and dynamic inhomogeneities can be identified and characterized by studying one molecule at a specific nanoscale surface site at a time. Single-molecule spectroscopy reveals statistical distributions correlated with microscopic parameters and their fluctuations, which are often hidden in ensemble-averaged measurements. The goal of our project is to integrate and apply these spectroscopic imaging and topographic scanning techniques to measure the energy flow and electron flow between molecules and substrate surfaces as a function of surface site geometry and molecular structure. We have been primarily focusing on studying interfacial electron transfer under ambient condition and electrolyte solution involving both single crystal and colloidal TiO<sub>2</sub> and related substrates. The resulting molecular level understanding of the fundamental interfacial electron transfer processes will be important for developing efficient light harvesting systems and broadly applicable to problems in fundamental chemistry and physics.

### **Recent Progress**

**Single-Molecule Interfacial Electron Transfer Dynamics of Porphyrin on TiO<sub>2</sub> Nanoparticles: Dissecting the Complex Electronic Coupling Dependent Dynamics.** The photosensitized interfacial electron transfer (ET) dynamics of the Zn(II)-5,10,15,20-tetra (3-carboxyphenyl) porphyrin (*m*-ZnTCPP)-TiO<sub>2</sub> nanoparticle (NP) system has been studied using single-molecule photon-stamping spectroscopy. The single-molecule fluorescence intensity trajectories of *m*-ZnTCPP on TiO<sub>2</sub> NP surface show fluctuations and blinking between bright and dark states, which are attributed to the variations in the reactivity of interfacial ET, i.e., intermittent interfacial electron transfer dynamics, a typical dynamically disordered chemical dynamics (Figure 1). We show the effect of anchoring group binding geometry (*meta* or *para*), hence electronic coupling of sensitizer (*m/p*-ZnTCPP) and TiO<sub>2</sub> substrate, on interfacial ET dynamics. The nonexponential autocorrelation function decay and the power-law distribution of the dark-time probability density provide a detailed characterization of the inhomogeneous interfacial ET dynamics sensitive to the molecular structure, molecular environment, and molecule-substrate electronic coupling (Figure 2). Overall, our results strongly suggest that the fluctuation and even intermittency of excited-state chemical reactivity are intrinsic and general properties of molecular systems that involve strong molecule-substrate interactions.

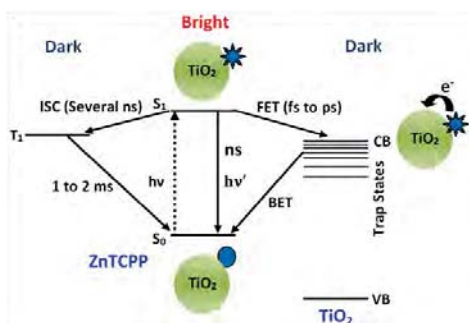


**Figure 1.** Schematic diagram showing energy levels and photoinduced processes involved in ZnTCPP/TiO<sub>2</sub> system. CB: conduction band; VB: Valence band; ISC: intersystem crossing. In ZnTCPP/TiO<sub>2</sub> system the photoexcited single-molecule involves either radiative emission to yield a photon that contributes to a bright state or involves non-radiative electron transfer process that contributes to the dark state.

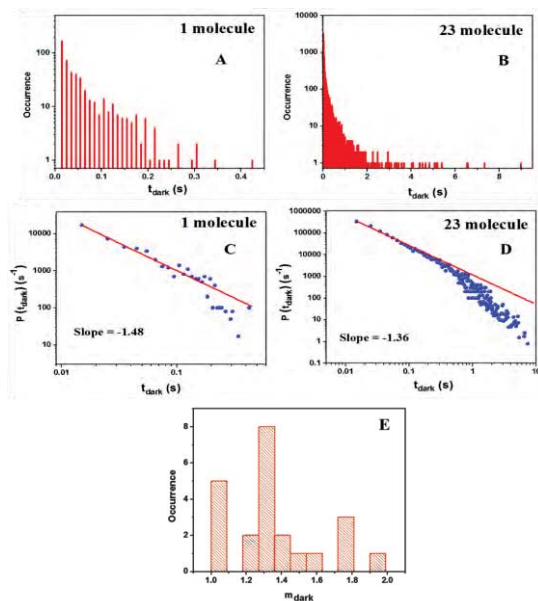


**Figure 2.** Distributions of dark-time durations of *m*-ZnTCPP on TiO<sub>2</sub> NP surface for (A) 1 molecule and (B) 23 molecules. Probability densities of the dark-time durations of *m*-ZnTCPP on TiO<sub>2</sub> NP surface for (C) 1 molecule and (D) 23 molecules. In log-log scale plots (C, D) the solid lines are linear fits indicating power-law behavior. The power-law exponent, which is the slope of the linear fits, is also indicated in the figures. (E) The Histogram of power-law exponents ( $m_{\text{dark}}$ ), for 23 different molecules of *m*-ZnTCPP on TiO<sub>2</sub> NP surface.

### Single-Molecule Interfacial Electron Transfer Dynamics of Porphyrin on TiO<sub>2</sub> Nanoparticles: Dissecting Driving Force and Electron Accepting State Density Dependent Dynamics.

Single-molecule photonstamping spectroscopy correlated with electrochemistry was used to analyzing complex interfacial electron transfer (ET) dynamics by probing *m*-ZnTCPP molecule anchored to TiO<sub>2</sub> NP surface while electrochemically controlling the energetically-accessible surface states of TiO<sub>2</sub> NPs (Figure 3). Application of negative potential raises the electron density in TiO<sub>2</sub> NPs, resulting in hindered forward ET and enhanced backward ET due to the changes of the driving force and the occupancy of acceptor states. However, density of states plays a dominant role in dictating the interfacial ET dynamics (Figure 4).

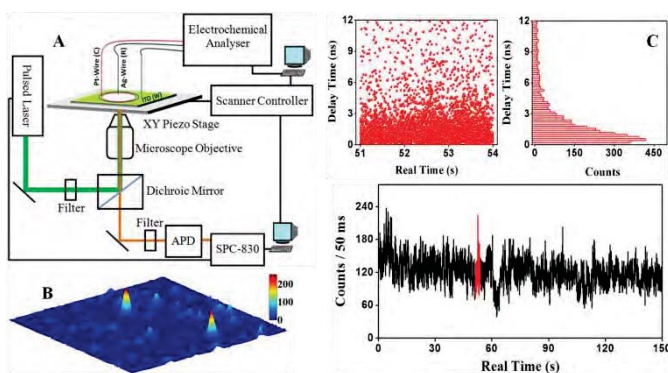


**Figure 3.** (A) Schematic representation of experimental setup for spectroelectrochemistry correlated with photon-stamping spectroscopy. (B) Single-molecule confocal fluorescence images of *m*-ZnTCPP on TiO<sub>2</sub> NPs-coated ITO surface with -0.60 V applied potential (10  $\mu\text{m}$  x 10  $\mu\text{m}$ ). (C) Typical experimental photon-stamping trajectories for a particular time window (in red) of single-molecule fluorescence trajectory.

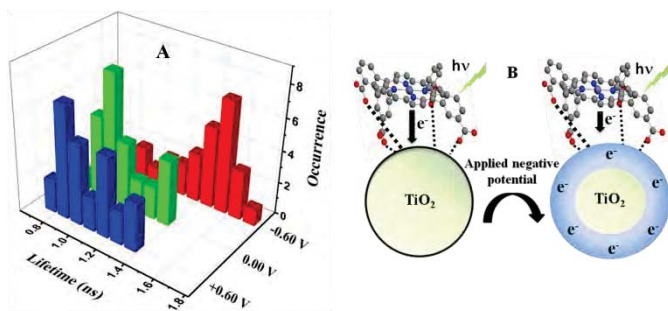


**Figure 4.** Fluorescence lifetime distributions of *m*-ZnTCPP on TiO<sub>2</sub> NPs-coated ITO surface in presence of 0.1 M NaCl aqueous electrolyte with +0.60 V, 0.00 V and -0.60 V applied potential. (B) Schematic depiction of interfacial ET in absence and presence of applied electric bias. In absence of electric bias the efficiency of photoinduced ET is high (indicated by

large arrow), whereas the application of negative potential raises the electron density in TiO<sub>2</sub> NPs, leading to decrease in the efficiency of ET (indicated by small arrow).

**Comparative Studies of Interfacial Electron Transfer Dynamics at Different Energy Substrates: Suppressed Fluorescence Blinking of Single-Molecules on Doped Semiconductors.** Photo-induced, interfacial electron transfer (ET) dynamics between *m*-ZnTCPP and Sn-doped In<sub>2</sub>O<sub>3</sub> (ITO) film has been studied using single-molecule photon-stamping spectroscopy. The observed ET dynamics of single *m*-ZnTCPP adsorbed on ITO was compared with that of *m*-ZnTCPP adsorbed on TiO<sub>2</sub> NPs with and without applied electric potential. Compared to *m*-ZnTCPP on TiO<sub>2</sub> NP surface, *m*-ZnTCPP on ITO surface shows reduced lifetime as well as suppressed blinking and quasi-continuous distribution of fluorescence intensities, presumably due to higher electron density in ITO (Figure 5). The higher electron density leads to the occupancy of CB acceptor states/trap states, which supports a higher backward electron transfer (BET) rate that results in quasi-continuous distribution of fluorescence intensities. The dependence of BET rate on electron density and charge trapping is consistent with our previous observations of quasi-continuous distribution of fluorescence intensities of *m*-ZnTCPP on TiO<sub>2</sub> NPs with applied negative potential across the dye-TiO<sub>2</sub> interface. The quasi-continuous distribution of fluorescence intensities in both case of *m*-ZnTCPP on ITO surface and *m*-ZnTCPP on TiO<sub>2</sub> NPs with applied negative potential indicates that the electron density/occupancy in the semiconductor plays a dominant role in dictating the changes in rates of charge transfer in our system, rather than the relative energetics between electron in semiconductor and the oxidized sensitizer.

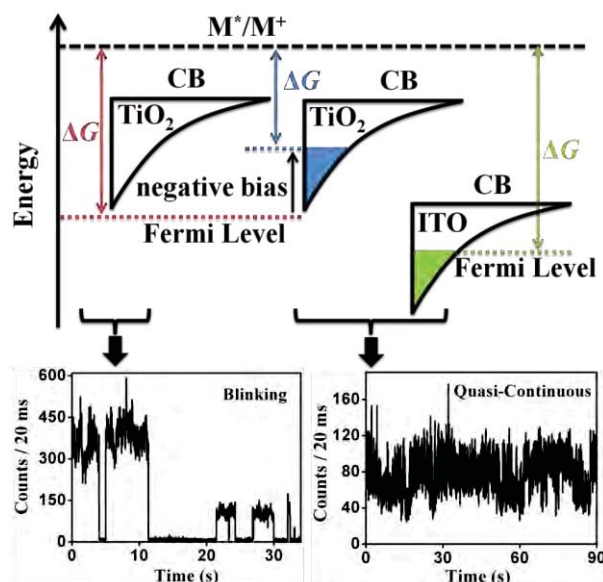


**Figure 5:** Schematic illustration of the sub-bandgap or trap states, Fermi level, and forward ET free energy driving force ( $\Delta G$ ) for ITO, TiO<sub>2</sub> NPs, and TiO<sub>2</sub> NPs with applied negative bias:  $M^*/M^+$  indicate excited state energy of *m*-ZnTCPP. In TiO<sub>2</sub> the Fermi level lies below the trap states, application of negative potential raises the TiO<sub>2</sub> Fermi level, which leads to occupancy of CB electron acceptor states as well as decrease in  $\Delta G$  value. Blue area denotes electron acceptor states unavailable for electron injection from *m*-ZnTCPP excited state. In case of ITO the Fermi level lies above the conduction band edge and the forward ET free energy driving force ( $\Delta G$ )

is also large compared to that of TiO<sub>2</sub>. (**Lower Panel**) Typical Single-molecule fluorescence emission trajectories of *m*-ZnTCPP on ITO surface. Unlike *m*-ZnTCPP on ITO surface (**Lower right**), *m*-ZnTCPP adsorbed on TiO<sub>2</sub> NPs show fluorescence intensity trajectories with distinct bright and dark states (**Lower left**).

### Future Research Plans

In interfacial ET systems, a BET process is possible by thermal de-trapping of the electrons from the total electron density of the reduced semiconductor and recombining the electrons with the oxidized dye molecules. Compared to ultrafast FET processes, BET processes take place at a longer time-scale, ranging from sub-nanoseconds to several milliseconds, probably due to the existence of trap states and non-Brownian diffusion motions of the electrons in semiconductors. Furthermore, the dynamics of the BET processes are often non-exponential or dispersive. Ensemble averaged approaches, while valuable, cannot resolve important nanoscale aspects of interfacial ET. In particular, the geometry of the adsorption site, the orientation and motion of the adsorbed molecule, and their relationship to the excited state dynamics, are often averaged out as the ensemble-averaged measurements cannot dissect complex interfacial ET processes at a site specific level. The difficulty comes from both intrinsic spatial and temporal inhomogeneities of the interfacial electron transfer dynamics, which can be identified, measured, and analyzed by studying specific one molecule at a time and a location at an interface. One of the most significant characteristics of our approach is that we will interrogate the complex interfacial electron transfer dynamics by actively pin-point energetic manipulation of the surface interaction and electronic couplings, beyond the conventional excitation and observation. We plan to study the FET and BET dynamics by manipulating the electric field distribution at the interface and the energetic trapping state distributions in the TiO<sub>2</sub> materials. Furthermore, We will continue our systematic studies of the electronic coupling strength between excited states of dye molecule and the semiconductors as well as metal catalysis surfaces, including (i) the use of externally controlled local electric field to manipulate the surface energetic state density and chemical activities; (ii) the use of different anchoring groups presenting different electronic coupling of the molecules and substrate surfaces; and by (iii) the use of different semiconductor nanoscale systems and catalytically active metal surfaces for systematic analysis of the surface state energetics and electron transfer accepting site density on the ET dynamics. We will use AFM tip enhanced single-molecule spectroscopic imaging to analyse the detailed spatial and temporal distributions and dynamics in the complex interfacial electron transfer systems.

### Publications of DOE sponsored research (FY2013-2015)

1. Yufan He, Jin Cao, Vishal Govind Rao, Bharat Dhital, and H. Peter Lu, "High-spatial resolved interfacial electron transfer imaging analysis by simultaneous lifetime imaging and AFM topographic imaging," Submitted (2015).
2. Vishal Govind Rao, Bharat Dhital, and H. Peter Lu, "Driving Force and Electron Accepting State Density Dependent Interfacial Electron Transfer Dynamics: Suppressed Fluorescence Blinking of Single-Molecules on Doped Semiconductors," Submitted (2015).
3. Vishal Govind Rao, Bharat Dhital, and H. Peter Lu, "Single-Molecule Interfacial Electron Transfer Dynamics of Porphyrin on TiO<sub>2</sub> Nanoparticles: Dissecting Driving Force and Electron Accepting State Density Dependent Dynamics," *Chemical Communication*, in press (2015).
4. Vishal Govind Rao, Bharat Dhital, Yufan He, H. Peter Lu, "Single-Molecule Interfacial Electron Transfer Dynamics of Porphyrin on TiO<sub>2</sub> Nanoparticles: Dissecting the Complex Electronic Coupling Dependent Dynamics," *J. Phys. Chem. C.*, **118**, 20209-20221 (2014).
5. H. Peter Lu, "Single-Molecule Interfacial Electron Transfer Dynamics," an invited book chapter in *Handbook of Spectroscopy*, Second Edition (G. Gauglitz and D. S. Moore. Eds), p. 877-910, Wiley-VCH Verlag GmbH & Co. (2014).

## Solution Reactivity and Mechanisms through Pulse Radiolysis

Sergei V. Lymar

Chemistry Department, Brookhaven National Laboratory, Upton, NY 11973-5000

e-mail: lymar@bnl.gov

### Scope

This program applies pulse radiolysis for investigating reactive intermediates and inorganic reaction mechanisms. The specific systems are selected based on their fundamental significance or importance in energy and environmental problems.

The first project investigates physical chemistry of nitrogen oxides and their congeneric oxoacids and oxoanions. These species play an essential role in environmental chemistry, particularly in the terrestrial nitrogen cycle, pollution, bioremediation, and ozone depletion. Nitrogen-oxygen intermediates are also central to the radiation-induced reactions that occur in nuclear fuel processing and within attendant nuclear waste. Equally important are the biochemical roles of nitrogen oxides. We apply time-resolved techniques for elucidation of the prospective reactions in terms of their thermodynamics, rates and mechanisms, focusing on the positive nitrogen oxidation states, whose chemistry is of the greatest current interest.

The second project deals with radiation chemistry in polar aprotic solvents. Due to their solubilizing properties, low nucleophilicity, and large electrochemical window, these solvents are widely used in mechanistic studies of transition metal complexes including those relevant to redox catalysis. Our recent studies have shown that pulse radiolysis, particularly combined with time-resolved infrared detection (TRIR), is a powerful technique for gaining mechanistic insights into the dynamics of redox catalysis in polar aprotic solvents through probing normally inaccessible catalysts' oxidation states. However, this research is hampered by insufficient understanding of primary radiolysis species in these solvents and by the deficiency of methods for directing their reactivity toward generating strong reductants or oxidants that can be used for initiating useful redox chemistry. Our recent work has been focused on acetonitrile, which is our solvent of choice for a number of planned TRIR mechanistic studies.

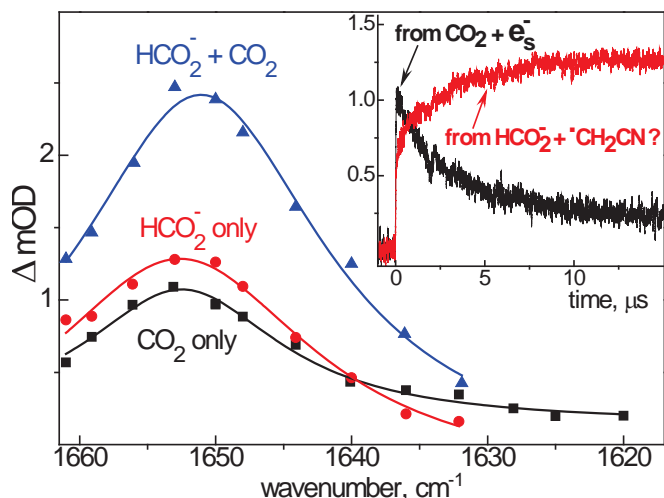
The goal of the third project has been to gain mechanistic insight into redox catalysis through characterization of the catalyst transients involved in the catalytic cycle, with the focus on water oxidation catalysis, which remains the greatest challenge in the photochemical water splitting. The major difficulty here has been in detection and characterization of the reaction intermediates. In this project, we apply time-resolved techniques to clarify the nature of the catalyst transients formed during water oxidation, thereby providing information that is critical to performing accurate mechanistic analyses.

This abstract summarizes recent results from the last two projects; the first project was presented in detail at the previous meeting.

Collaborators on these projects include M. Valiev (PNNL),<sup>1</sup> J. Hurst (WSU, emeritus),<sup>2-5</sup> D. Polyansky (BNL),<sup>4</sup> and D. Grills (BNL).<sup>6</sup>

### Recent progress

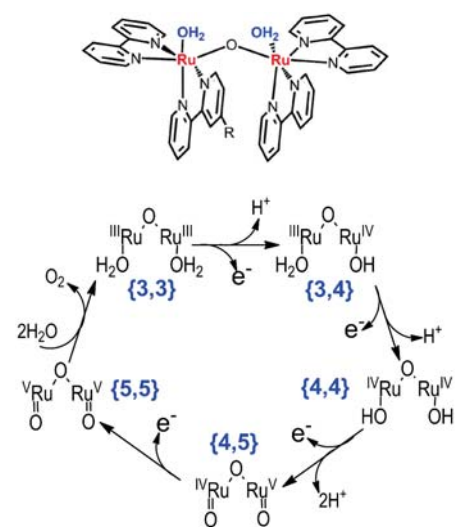
*CO<sub>2</sub><sup>•-</sup> radical in acetonitrile.* (with David C. Grills) The only reducing species generated by pulse radiolysis in MeCN is the solvated electron (e<sub>s</sub><sup>-</sup>), which we used for initiating the reductive chemistry of a Mn complex: Mn(HCO<sub>2</sub>)(<sup>t</sup>Bu<sub>2</sub>-bpy)(CO)<sub>3</sub> + e<sub>s</sub><sup>-</sup> → Mn<sup>•</sup>(<sup>t</sup>Bu<sub>2</sub>-bpy)(CO)<sub>3</sub> + HCO<sub>2</sub><sup>-</sup>.<sup>6</sup>



We also observed that addition of formate ( $\text{HCO}_2^-$ ) nearly doubles the radiation yield of the  $\text{Mn}(\text{HCO}_2)(^t\text{Bu}_2\text{-bpy})(\text{CO})_3$  reduction. A similar effect of formate was detected in the reduction of nitrobenzyl compounds and attributed to the reducing action of the  $\text{CO}_2^{\bullet-}$  radical ( $E^0(\text{CO}_2/\text{CO}_2^-)_{\text{aq}} = -1.9 \text{ V NHE}^{7-8}$ ) produced via H-atom abstraction from  $\text{HCO}_2^-$  by the radiolytically-generated  $^{\bullet}\text{CH}_2\text{CN}$  radical.<sup>9</sup> From literature,<sup>7-8,10</sup> we estimate  $BDE(\text{H}-\text{CO}_2^-) \approx 92 \text{ kcal/mol}$ . Because  $BDE(\text{H}-\text{CH}_2\text{CN})$  is  $\sim 97 \text{ kcal/mol}$ , such a reaction is feasible, but both the previous and our attempts to detect the

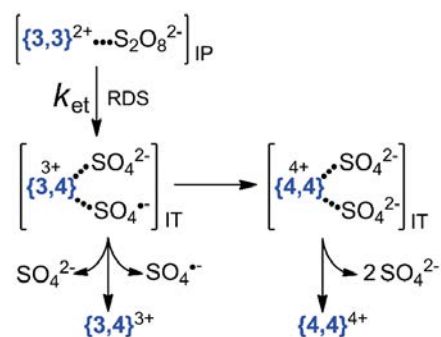
characteristic UV absorption of  $\text{CO}_2^{\bullet-}$  were unsuccessful, raising doubts about the intermediacy of formate-derived  $\text{CO}_2^{\bullet-}$ . However, using TRIR we did observe this radical as shown in Figure above. To our knowledge, this is the first direct IR detection of  $\text{CO}_2^{\bullet-}$  in solution. The results clearly indicate that comparable  $\text{CO}_2^{\bullet-}$  amounts are produced by  $\text{CO}_2$  electron capture and through oxidation of  $\text{HCO}_2^-$  by solvent radicals. However, the nature of the latter process, particularly the origin of the fast initial  $\text{CO}_2^{\bullet-}$  rise, and the  $\text{CO}_2^{\bullet-}$  decay pattern are not as yet understood. We will further explore these features and also broaden the approach to include secondary alcohols and alkoxides, whose  $\alpha\text{-C-H}$   $BDE$ s are even lower than that in  $\text{HCO}_2^-$  (e.g., we estimate  $BDE$  of  $\sim 85 \text{ kcal/mol}$  for  $\alpha\text{-C-H}$  in  $\text{Me}_2\text{C}(\text{H})\text{O}^-$ ). We thus anticipate that alkoxides will be more efficient than formate in intercepting the C-centered solvent radicals and generating very strong reductants (e.g.,  $E^0(\text{Me}_2\text{CO}/\text{Me}_2^{\bullet}\text{CO}^-)_{\text{aq}} = -2.1 \text{ V NHE}$ ).

*Intermediates in Water Oxidation Catalysis.*<sup>2-5</sup> (with James K. Hurst) Of all structurally defined, homogeneous catalysts that have been examined, the dimeric  $\mu$ -oxo-bridged ruthenium ion *cis,cis*-



$[(\text{bpy})_2(\text{H}_2\text{O})\text{Ru}^{\text{III}}-\text{O}-\text{Ru}^{\text{III}}(\text{OH}_2)(\text{bpy})_2]^{4+}$  (known as the “blue dimer”), where  $\text{bpy} = 2,2'$ -bipyridine (denoted  $\{3,3\}$  and shown to the left), has been the most extensively studied. Water oxidation by the “blue dimer” involves its progressive oxidation with the attendant loss of protons to the ruthenyl  $\{5,5\}$  state. However, the properties of the catalyst’s unstable oxidation states above  $\{3,4\}$  and the catalysis mechanism remain in dispute.

We determined that one-electron oxidation of  $\{3,3\}$  to  $\{3,4\}$  by  $\text{S}_2\text{O}_8^{2-}$  occurs through concurrent reaction pathways corresponding to the three protic forms of  $\{3,3\}$ . Free energy correlations of the rate constants, transient species dynamics determined by pulse radiolysis, and medium and temperature dependencies all suggest that the rate determining step in these reactions is a strongly non-adiabatic dissociative electron transfer within a precursor ion pair leading to the  $\{3,4\}|\text{SO}_4^{2-}|\text{SO}_4^{\bullet-}$  ion triple (IT in Scheme below). As deduced from  $\text{SO}_4^{\bullet-}$  scavenging experiments, this radical then either oxidizes  $\{3,4\}$  to  $\{4,4\}$  within the ion triple, effecting a net two-electron oxidation of  $\{3,3\}$ , or escapes in solution with  $\sim 25 \%$  probability to react with additional  $\{3,3\}$ , that is, effecting sequential one-



electron oxidations. These unusual reactions provide a clean way to generate  $\{3,4\}$ , which has made possible pulse radiolysis application for assessment of the  $\{3,4\}$  reactivity toward oxidizing radicals and obtaining and characterization of the  $\{4,4\}$  state, including its electronic spectrum and direct measurement of its comproportionation ( $\{3,3\} + \{4,4\} \rightarrow 2\{3,4\}$ ) and disproportionation ( $2\{4,4\} \rightarrow \{3,4\} + \{4,5\}$ ). These are the two most important spontaneous processes that control the catalyst's energy efficiency.

For the reaction of  $\{3,4\}$  with  $\text{OH}^\bullet$ , the transient spectrum indicates stoichiometric *reduction* of  $\{3,4\}$  to  $\{3,3\}$ . This reaction constitutes a clear example of a rare type of reaction known as “oxidant-induced reduction” and requires that the bipyridine ligand undergoes oxidation leading to net hydroxylation of the ring (Scheme below). This reaction is interesting within the context of water oxidation because a mechanism for catalysis involves water attack on  $\{5,5\}$  that may result in addition of the nascent OH-fragment to the ligand, which could



be the initial step in oxidative degradation of the “blue dimer” and/or  $\text{O}_2$ -forming pathways involving non-innocent participation of the ligand.

*Planned work will investigate:*

- Nature and radiation yields of primary acetonitrile radiolysis products.
- Techniques for directing primary radiolysis species toward generating strong reductants or oxidants in acetonitrile.
- Novel pathways for generating nitroxyl species ( $^1\text{HNO}$  and  $^3\text{NO}^-$ ) and their reactivity, including their self-decay and spin-forbidden ground state bond breaking/making reactions.
- Energetics and redox reactivity of trioxodinitrate ( $\text{HN}_2\text{O}_3^-/\text{N}_2\text{O}_3^{2-}$ ) species, and their nitroxyl release mechanism.
- Redox and radical chemistry in the nitrite/nitrate system, including: formation pathways and thermodynamics of nitrate radical anion,  $\text{NO}_3^{2-}$ ; rates and mechanisms of its acid-catalyzed and redox reactions.

**References** (DOE sponsored publications in 2014-present are marked with asterisk)

- (1\*)Shaikh, N.; Valiev, M.; Lyman, S. V. "Decomposition of Amino Diazeniumdiolates (NONOates): Molecular Mechanisms" *J. Inorg. Biochem.* **2014**, *141*, 28-35.
- (2)Cape, J. L.; Lyman, S. V.; Lightbody, T.; Hurst, J. K. *Inorg. Chem.* **2009**, *48*, 4400-4410.
- (3)Stull, J. A.; Britt, R. D.; McHale, J. L.; Knorr, F. J.; Lyman, S. V.; Hurst, J. K. *J. Am. Chem. Soc.* **2012**, *134*, 19973-19976.
- (4\*)Polyanskiy, D. E.; Hurst, J. K.; Lyman, S. V. "Application of Pulse Radiolysis to Mechanistic Investigations of Water Oxidation Catalysis" *Eur. J. Inorg. Chem.* **2014**, 619-634.
- (5\*)Hurst, J. K.; Roemeling, M. D.; Lyman, S. V. "Mechanistic Insight into Peroxydisulfate Reactivity: Oxidation of the *cis,cis*- $[\text{Ru}(\text{bpy})_2(\text{OH})_2]_2\text{O}^{4+}$  “Blue Dimer”" *J. Phys. Chem. B* **2015**, *119*, 7749-7760.

- (6\*)Grills, D. C.; Farrington, J. A.; Layne, B. H.; Lymar, S. V.; Mello, B. A.; Preses, J. M.; Wishart, J. F. "Mechanism of the Formation of a Mn-Based CO<sub>2</sub> Reduction Catalyst Revealed by Pulse Radiolysis with Time-Resolved Infrared Detection" *J. Am. Chem. Soc.* **2014**, *136*, 5563-5566.
- (7)Armstrong, D. A.; Huie, R. E.; Lymar, S.; Koppenol, W. H.; Merényi, G.; Neta, P.; Stanbury, D. M.; Steenken, S.; Wardman, P. *Bioinorg. React. Mech.* **2013**, *9*, 59-61.
- (8\*)Armstrong, D. A.; Huie, R. E.; Lymar, S.; Koppenol, W. H.; Merényi, G.; Neta, P.; Ruscic, B.; Stanbury, D. M.; Steenken, S.; Wardman, P. "Standard Electrode Potentials Involving Radicals in Aqueous Solution: Inorganic Radicals" *Pure Appl. Chem.*, *accepted*.
- (9)Burrows, H. D.; Kosower, E. M. *J. Phys. Chem.* **1974**, *78*, 112-117.
- (10)Wagman, D. D.; Evans, W. H.; Parker, V. B.; Schumm, R. H.; Halow, I.; Bailey, S. M.; Churney, K. L.; Nuttall, R. L. *J. Phys. Chem. Ref. Data* **1982**, *11*, Suppl. 2.

## ***Ab initio* approach to interfacial processes in hydrogen bonded fluids**

Christopher J. Mundy  
 Physical Sciences Division  
 Pacific Northwest National Laboratory  
 902 Battelle Blvd, Mail Stop K1-83  
 Richland, WA 99352  
[chris.mundy@pnnl.gov](mailto:chris.mundy@pnnl.gov)

### **Program Scope**

The long-term objective of this research is to develop a fundamental understanding of processes, such as transport mechanisms and chemical transformations, at interfaces of hydrogen-bonded liquids. Liquid surfaces and interfaces play a central role in many chemical, physical, and biological processes. Many important processes occur at the interface between water and a hydrophobic liquid. Separation techniques are possible because of the hydrophobic/hydrophilic properties of liquid/liquid interfaces. Reactions that proceed at interfaces are also highly dependent on the interactions between the interfacial solvent and solute molecules. The interfacial structure and properties of molecules at interfaces are generally very different from those in the bulk liquid. Therefore, an understanding of the chemical and physical properties of these systems is dependent on an understanding of the interfacial molecular structure. The adsorption and distribution of ions at aqueous liquid interfaces are fundamental processes encountered in a wide range of physical systems. In particular, the manner in which solvent molecules solvate ions at the interface is relevant to problems in a variety of areas. Another major focus lies in the development of models of molecular interaction of water and ions that can be parameterized from high-level first principles electronic structure calculations and benchmarked by experimental measurements. These models will be used with appropriate simulation techniques for sampling statistical mechanical ensembles to obtain the desired properties.

### **Progress Report**

#### A molecular model of nanoscale hydrodynamics [1]

In this work, we construct a particle-based model to capture the nanoscale fluctuation hydrodynamics and the hydrophobicity effect.

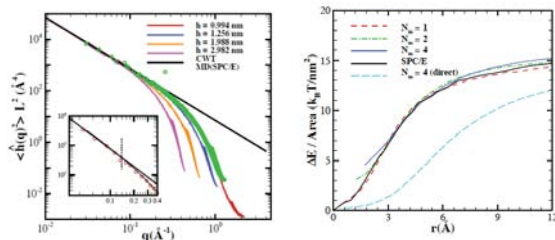


**Figure 1:** (Left) Capillary wave spectrum as a function of resolution of our model as compared to MD (green) and theory (black). (Right) The free energy of solvation for cavities of different radius at different resolutions of the model. Cyan is the free energy of solvation of a coarse representation in the absence of compressibility and capillarity.

Following the pioneering work of Lum-Chandler-Weeks we seek to add the microscopic concepts of compressibility and surface tension to a well smoothed dissipative particle dynamics model that correctly captures macroscopic flow as described by Navier-Stokes. The advantage to our formulation is that we are using a Lagrangian based method and can easily perform the molecular dynamics of a reduced model (Navier-Stokes) with the microscopic concepts of compressibility and

capillarity. To this end, our model can reproduce surface tensions and solvation free energies of small spheres as directly compared to molecular simulation (see **Figure 1**).

### The role of short-range structure in hydrophobic solvation [4]

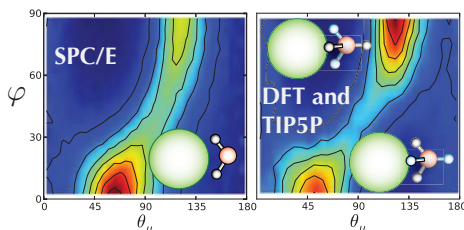


**Figure 2:** Schematic of the solvation patterns of different water models around a hard sphere [4]. The left panel is SPC/E water and shows only one distinct population for the orientation of water around the hard sphere favoring the configurations consistent with donation of hydrogen bonds. The right panel shows the results of TIP5P and DFT water models where there is clear population in both donating and accepting configurations.

Here we study the structural and electrostatic consequences of the various broken symmetries that arise from inserting the simplest model of an uncharged ion core, a hard sphere solute of varying radius into water as described by two classical water models, SPC/E and TIP5P, and by state-of-the-art quantum density functional calculations. We show, the solvent response to a hard sphere (HS) solvation generate special configurations that are particularly sensitive to small differences between donor and acceptor hydrogen bonds and to local variations in the induced charge density as shown in **Figure 2** [4]. This system provides a stringent test of classical water models in a

physically important application where accurate quantum calculations can be carried out to assess their predictions. These results have implications for nonzero ionic charge and needed improvements to the Born model. In our study we derive explicit expressions for the calculation of the potential at the center of the HS cavity due to the structure of water. Thus, the relationship between local hydration structure and the cavity potential provides an important insight into the sensitivity of hydration free energies to forms of molecular interaction (*e.g.* quantum versus classical). These results in conjunction with our previous studies provide further evidence that the differences in the solvent response to broken symmetries have measurable consequences that can influence the underlying thermodynamics of ions in solution.

### Acids in the vicinity of the air-water interface [3,5]

The role of the first solvation shell as an important ingredient for ion adsorption has led to a unique program at PNNL to determine the accurate local hydration structure of ions using X-ray adsorption fine structure (EXAFS) in conjunction with molecular dynamics (MD) using *ab initio* based interaction potentials. Although there is a theoretical and experimental consensus that ions can be present at the air-water interface, there is no such consensus regarding the self-ions of water ( $\text{H}_3\text{O}^+$  and  $\text{OH}^-$ ) that comprise acids and bases. Recently we have established the use of *ab initio* based interaction potentials to study hydrochloric acid (HCl) over a variety of concentrations [5]. Our recent joint simulation/experimental study has verified the emergence and experimental assignment of a contracted contact ion pair between chlorine and  $\text{H}_3\text{O}^+$  moiety. This observation and prediction suggests a picture of acids where the chloride anion is not a mere spectator but an active participant in the determination of the activity of the excess proton. In our previous study it was found that the solvation structure of  $\text{HNO}_3$  in bulk at high concentrations resembled the interfacial solvation of  $\text{HNO}_3$  at low concentrations (*e.g.* isolated

molecule). The differences in the local solvation structure between  $\text{HNO}_3$  under interfacial and bulk solvation was correlated to the measured degree of dissociation in both environments.

Extensions of the aforementioned work on nitric acid were initiated to explain the observed proton exchange from HCl to DCl in molecular beam experiments on the liquid-air interface of salty glycerol solutions [3]. To this end we performed *ab initio* MD simulations and computed the potentials of mean force (PMF) for acid dissociation of HCl in bulk and in the vicinity of the air-water interface.

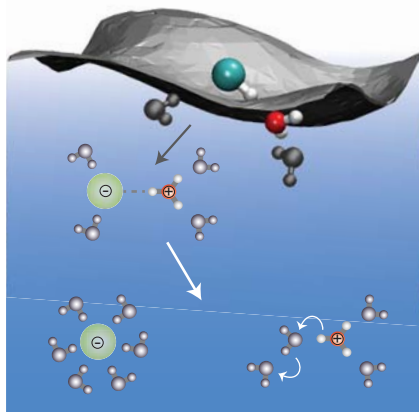


**Figure 3:** A schematic depicting the possible channels for acid dissociation in the vicinity of the air-water interface [3]

Our finding, consistent with our previous studies on nitric acid, is that the preponderance of the contracted contact ion-pair between chlorine and  $\text{H}_3\text{O}^+$  in high concentration HCl is observed at low concentrations of HCl in the vicinity of the air-water interface. The abundance of this contracted ion pair at the air-water interface preconditions the likelihood for fast proton exchange as shown schematically in **Figure 3**. Moreover, when the acid is changed to HBr no fast proton exchange is observed. This was also corroborated in our simulations where we found that HBr has little to no propensity to form contact ion pairs and favors reactive channels to complete

dissociation.

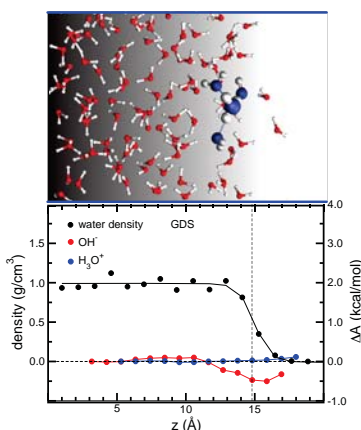


**Figure 4:** Intrinsic free energies of adsorption for  $\text{H}_3\text{O}^+$  (blue) and  $\text{OH}^-$  (red) at the air water interface (black) [5].

Connections of the aforementioned work to our recent study of the intrinsic PMFs of  $\text{H}_3\text{O}^+$  to the air-water interface[5] can provide clues to understanding the controversial topic of the surface propensity of protons to the air-water interface. Indeed, our intrinsic PMFs indicate that there is no strong driving or repelling force for the isolated  $\text{H}_3\text{O}^+$  to air-water interface as shown in **Figure 4**. Rather our research suggests a picture where the correlated interactions of the proton and the counter ion must be considered to form a complete picture of acids in the vicinity of the air-water interface. This is distinct from our understanding of the inorganic electrolytes where the independent ion picture seems to hold for concentrations below 1 M.

### Future directions

We are currently extending this work to investigate the solvent response of charged hard spheres using multiple representations of the molecular interaction for water (*e.g.* TIP5P, SPC/E, flavors of DFT). Our preliminary results are shown in and suggest that is not possible with a single parameterization of a water model to reproduce the solvent response of a quantum based interaction to neutral, positive, or negative charged hard spheres.

**Acknowledgements.** This work was performed with Yan Levin (Brazil) John D. Weeks (U. Maryland), D.J. Tobias (UC-I), Ilja Siepmann (U. Minn.), and I.-F.W. Kuo (LLNL), Greg

Schenter (PNNL), Marcel D. Baer (PNNL), Shawn M. Kathmann, Abe Stern (UC-I), Joost VandeVondele (U. Zurich), Greg Kimmel (PNNL), John Fulton (PNNL), and Roger Rousseau (PNNL). We also acknowledge computer resources from NERSC and a 2008-2012 INCITE award. Battelle operates Pacific Northwest National Laboratory for the US Department of Energy.

**Publications with BES support (2014-present):**

1. Lei, H.; **Mundy, CJ**; Schenter, GK; Voulgarakis NK, "Modeling nanoscale hydrodynamics by smoothed dissipative particle dynamics," *Journal of Chemical Physics* **142**, 194504 (2015)
2. Chun, J; Schenter, GK; **Mundy, CJ**, "The role of solvent heterogeneity in determining the dispersion interaction between nanoassemblies," *Journal of Physical Chemistry B* **119**, 5873 (2015)
3. Baer, MD; Tobias, DJ; **Mundy, CJ**, "Investigation of Interfacial and Bulk Dissociation of HBr, HCl, and HNO<sub>3</sub> Using Density Functional Theory-Based Molecular Dynamics Simulations," *Journal of Physical Chemistry B*, DOI: 10.1021/jp5062896
4. Remsing, RC; Baer, MD; Schenter, GK; **Mundy, CJ**; Weeks, JD, "The Role of Broken Symmetry in Solvation of a Spherical Cavity in Classical and Quantum Water Models," *Journal of Physical Chemistry Letters* **5**, 2767 (2014)
5. Baer, MD; Kuo, I-FW; Tobias, DJ; **Mundy, CJ**, "Toward a unified picture of the water self-ions at the air-water interface," *Journal of Physical Chemistry B* **118**, 8364 (2014)
6. Pluharova, E; Baer, MD; **Mundy, CJ**; Schmidt, B; Jungwirth, P, "Aqueous Cation-Amide Binding: Free Energies and IR Spectral Signatures by Ab Initio Molecular Dynamics," *Journal of Physical Chemistry Letters* **5**, 2235 (2014)
7. Baer, MD; Fulton, JL; Balasubramanian, M; Schenter, GK; **Mundy, CJ**, "Persistent ion-pairing in aqueous hydrochloric acid," (Frontiers Article) *Journal of Physical Chemistry B* **118**, 7211 (2014).

## DYNAMIC STUDIES OF PHOTO- AND ELECTRON-INDUCED REACTIONS ON NANOSTRUCTURED SURFACES - DE-FG02-90ER14104

**Richard Osgood,**

Center for Integrated Science and Engineering, Columbia University, New York, NY 10027, [Osgood@columbia.edu](mailto:Osgood@columbia.edu)

### Program Scope or Definition:

Our current research program seeks to examine the photon- and electron-initiated reaction mechanisms, and nonequilibrium-excited dynamics effects, occurring with excitation of adsorbates on well-characterized metal-oxide surfaces, comparing both in single-crystal and in nanocrystalline forms. Our program has developed and improved a new synthesis method for uncapped nanocrystals with specific orientation and atomic structure *in situ* in UHV. STM-based nanocrystallography is used to identify the atomic structure and orientation of these nanocrystals and their adsorbates, including subtle effects such as moiré patterns. In order to explore the dynamics of surface reactions, 3 types of excitation are applied to adsorbate-covered surfaces: (a) thermal excitation in temperature programmed desorption (TPD) experiments, (b) irradiation with monochromated light from a UV lamp, and (c) excitation with the electric charge, injected from an STM tip. The last method allows single-molecule resolved studies. The resulting chemistry and surface dynamics are investigated via imaging of the reaction fragments in the vicinity of the reaction sites.

Our initial studies included an ordered series of alkanes, while our most recent experiments have been directed toward charge-induced reactions of trimethylacetic acid (TMAA) adsorbed on single-crystal TiO<sub>2</sub>(110) surfaces and TiO<sub>2</sub> nanocrystals prepared on a Au(111) substrate. TMAA was chosen since it is known to exhibit light-induced chemistry on TiO<sub>2</sub>, this photo-chemistry has been examined extensively in experiments by our DOE PNNL colleagues. Our current research has shown that metal-supported TiO<sub>2</sub> nanocrystals are active for UV light-induced desorption of TMAA with efficiencies comparable to those of single-crystal surfaces. Also STM tip-induced desorption of TMAA has been demonstrated on the TiO<sub>2</sub>(110) surface by application of negative sample biases that inject electronic holes into the substrate. Mechanical strain-induced modulation of adsorbate surface dynamics on TiO<sub>2</sub>(110) has been observed. Finally, in collaborative project, the surface chemistry of deuterated CH<sub>3</sub>OH on a set of iron oxide reconstructions of Fe<sub>3</sub>O<sub>4</sub> has been initiated.

### Recent Progress:

#### *STM studies of photoreactions on supported single-crystal & single-nanocrystal TiO<sub>2</sub>.*

In order to establish the dynamics of light-induced reactions on TiO<sub>2</sub> surfaces that could serve as a platform for more complex studies of single-molecule charge-induced reactions, a series of experiments has been carried out, in which surfaces with adsorbed target molecules were controllably exposed to photon-energy-tuned UV light. Trimethyl acetic acid (TMAA) was chosen as a model photoreaction active molecule due to its ease of handling and the existence of numerous prior studies of its photoreactivity, including DOE Labs (e.g. PNNL). UV doses were administered using a Xe-Hg arc lamp, which was spectrally narrowed with a monochromator to a 15 nm bandwidth. Using this apparatus, the photoreactivity of TMAA on the surfaces of both a single-crystal rutile(110) bulk crystal or a TiO<sub>2</sub> nanocrystal sample, grown on a Au(111) substrate, was explored. In the case of single-crystal rutile(110) surface individual TMAA molecules were clearly visible in the STM images, thus allowing measurement of their areal density simply via direct “counting” of the molecules in a known area. Thus the molecular desorption rates could be measured from the images of TMAA-rutile(110) surface before and after UV doses. Typical data from a TMAA photo-depletion experiment is shown in **Fig. 1** (blue data). Using this approach, a  $5 \times 10^{-5}$  quantum efficiency of this light-induced process was measured for  $\lambda = 305$ .

However, the identical experiment with 360 nm UV light did not show noticeable desorption even after a 4.5-hour dose. While photolysis of TMAA on single-crystal TiO<sub>2</sub> surface is a well-studied reaction, our experiments are the *first spectrally resolved measurements*. Our results also directly demonstrate hole-mediated dynamics of this photoreaction. Indeed, the energy of  $\lambda = 360$  nm photons is well above the TiO<sub>2</sub> bandgap and such light is readily adsorbed in TiO<sub>2</sub> bulk. However, the adsorption depth for 360 nm light is 250 nm, which is much greater than diffusion range of holes in TiO<sub>2</sub> (10 nm) thus explaining negligible reaction rates. In comparison, the adsorption depth for the 305 nm light is 13 nm, thus allowing the photoreaction rate to be determined.

In addition, single-site resolved TMAA photolysis experiments have been performed with our TiO<sub>2</sub> nanocrystals prepared on the Au(111).[2] This procedure leads to the formation of 10–30 nm wide and 1–3 nm tall crystallites with predominantly a rutile (100) orientation of their top face. Since this was the first study of TMAA interaction on TiO<sub>2</sub> nanocrystals, our initial experiments explored the adsorption state of TMAA on these nanocrystals. Using both STM imaging and temperature programmed desorption (TPD) spectroscopy, our experiments established that TMAA readily adsorbs on the TiO<sub>2</sub> nanocrystal surfaces at 300K with the local surface density of the adsorbed molecules being comparable to that on the single-crystal rutile(110) surface. The adsorbed molecules follow a nearly identical thermal decomposition pattern for nano-TiO<sub>2</sub> and rutile(110) with the important exception being that nanocrystals of TiO<sub>2</sub> generate more dehydrogenated products compared to bulk single-crystal (110).

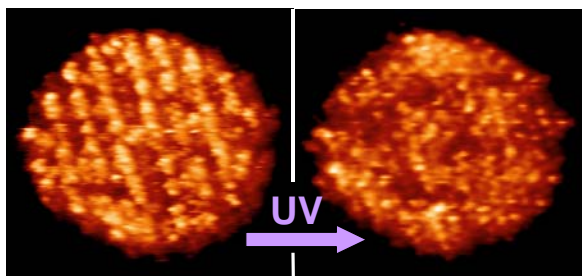


**Fig. 2:** 25 × 25 nm STM images on TMAA-covered TiO<sub>2</sub> nanocrystal on Au(111) substrate before (left) and after (right) a dose of 300nm UV light.

ments, which compared TPD spectra from as-prepared with spectra from UV-irradiated TMAA/nano-TiO<sub>2</sub>/Au(111) surfaces, as shown in the insert in **Fig. 1**. Using these TPD-based measurements, the UV irradiation time dependence of TMAA photodesorption from nano-TiO<sub>2</sub>/Au(111) surface was determined for  $\lambda = 305$ nm. These data are shown in **Fig. 1** together with the photodesorption data from a (110) surface. The comparison of the time constants of the

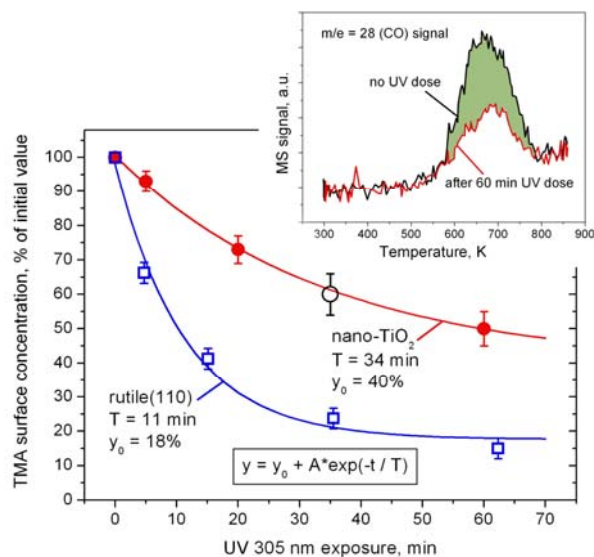


**Fig 1:** Cumulative plot showing the dynamics of TMAA desorption from nano-TiO<sub>2</sub>/Au(111) (red symbols) and rutile(110) (the blue symbols) surfaces induced by 305 nm UV light. The rutile(110) data was based on STM images and the nano-TiO<sub>2</sub> data was derived from pre- and post-irradiation TPD data, as shown in insert.

One example from a photo-reaction experiment is shown in **Fig. 2**. The left STM image shows a TMAA-saturated 20nm-wide TiO<sub>2</sub> nanocrystal and the left image shows the same nanocrystal after a 15min exposure to 305nm UV light. Light-induced desorption from the crystal is evident from the surface molecular density; counting of individual molecules suggests that ~50% of the initially adsorbed TMAA molecules have been removed by irradiation. This result was further supported by independent TPD experi-

two curves indicates that the efficiency of TMAA photodesorption on nano-TiO<sub>2</sub>/Au(111) is ~ 4 times lower than that on rutile(110). This ratio of efficiencies can be explained through the difference in optical paths of UV light in the samples. *To the best of our knowledge, this is the first atomically-resolved study of any photo-induced reaction on the surfaces of TiO<sub>2</sub> nanocrystals.*[6]

### ***Studies of STM tip-induced surface reactions***

As a next step towards understanding dynamics on a single-molecule scale, a number of experiments have been performed, in which surface reactions were triggered by charges, injected from an STM tip. Earlier, we have demonstrated electron-induced chemistry of halo-hydrocarbons on TiO<sub>2</sub> surface.[1] Recently, we have explored the possibility of initiation of the

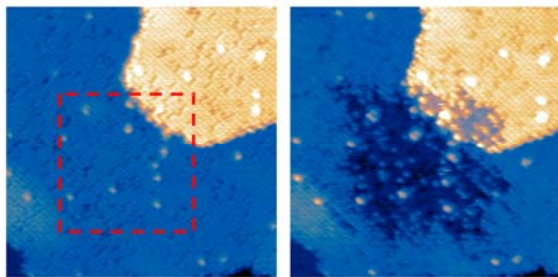


**Fig. 3:** Two STM images showing the same 40 × 40nm area of TMAA-saturated (110) surface before (left) and after (right) the smaller area, marked with the red square, had been scanned with -3.5 V sample bias.

TMAA photodesorption reaction on rutile(110) surface by controlled variations of the sample bias voltage. TMAA photodesorption is known to be activated by the electronic holes, generated in the TiO<sub>2</sub> bulk by UV light. Thus in the case of STM tip-induced experiments, the holes were created by application of negative sample biases. Several experimental protocols have been tested and the results of one such experiment is shown in **Fig. 3**. In this figure the left STM image shows TMAA-saturated rutile(110) surface. After taking the image a smaller 20 × 20 nm area of the surface was scanned with  $V = - 3.5V$  bias for 400sec in

total. Then the original 40 × 40nm area was imaged again at the normal +1.5V bias. It can be seen from the left image in **Fig. 3** that the virtually all TMA surface species have desorbed as a result of the negative bias application. This tip-induced reaction exhibits a clear energy threshold; thus in our experiments it was shown that  $V = - 3.0V$  bias causes no detectable TMAA desorption at identical conditions to the experiments shown in **Fig. 3**.

### ***Catalytic studies on iron-oxide surfaces.***

In order to expand our oxide-substrate capability to other materials of interest, our group, has begun to examine processes on Fe<sub>3</sub>O<sub>4</sub>(111) surfaces.[4] In particular, we chose to study the surface reactivity of deuterated methanol, which is of interest for fuel-cell applications. The unique combination of STM and TPD capabilities of our experimental chamber allowed us to relate specific reactivity patterns to different surface phases of Fe<sub>3</sub>O<sub>4</sub>(111) that included Fe<sub>2</sub>O<sub>3</sub>(0001) and FeO(111). These surface phases were formed by varying the sample preparation conditions; the phases could be easily distinguished in STM images. Methanol species were observed to be dissociatively adsorbed only on the Fe-terminated Fe<sub>3</sub>O<sub>4</sub>(111) surface and physisorbed on the O-terminated FeO(111) surfaces. On Fe sites, methanol is first dissociated into methoxy (CD<sub>3</sub>O) attached to surface-terminating Fe ions and D-atom atop the under-coordinated oxygen sites of Fe<sub>3</sub>O<sub>4</sub>(111). A fraction of these surface species then recombined to desorb as molecular methanol (CD<sub>3</sub>OD) from the surface at 365 K. Methoxy (CD<sub>3</sub>O) is further dissociated into formaldehyde (CD<sub>2</sub>O) and D-atoms at higher temperatures. The gas-phase formaldehyde (CD<sub>2</sub>O) and methanol molecules recombinatively desorb from the surface at 635 K. From a more general point of view, our work has shown that reaction of methanol on the iron-oxide surface is shown to have high sensitivity to atomic-level surface reconstruction.

### ***Stress-Induced Reactivity on Oxide Surfaces.***

Our Group has recently demonstrated the use of nanoscale local strain to control surface reactions on oxide surfaces [3,5]. Thus we have used STM imaging in an UHV environment to show that this strain locally alters reactivity of the surface. This change may be used in conjunction understand the role of strain in controlling reaction dynamics on a strained surface. Our experiments used a nanoscale template of extremely small, buried-atom Ar clusters to provide nm-scale strain in near-surface layers of metal oxides, as shown in **Fig. 4**. These buried Ar clusters were prepared by a low-energy (i.e. 1-2 kV) ion beam in combination with high-temperature annealing. In the vicinity of the buried Ar blister, the atomic layers are deformed upward and a local strain field is established.

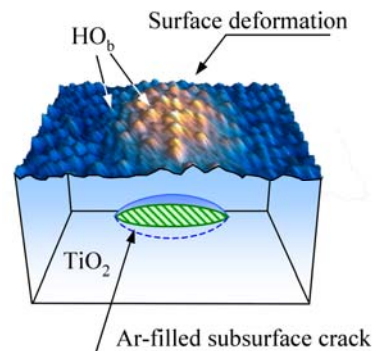


**Fig. 4:** 3D cross-sectional figure combining STM image of rutile(110) with OH groups, distributed on the surface, and schematic sketch of a buried Ar cluster.

### **Future Plans**

Our most recent experiments have showed that local (i.e. atomic scale) strain in  $\text{TiO}_2$  layers results in a change in the reactivity of that surface and, in particular, in change of the binding energy of hydrogen atoms, which are the simplest adsorbates on the rutile(110) surface.[5] *Our goal is now to understand the relationship between photo- and tip-reaction dynamics and surface strain.* The O-H bond energy deviations due to surface strain have been deduced by collecting local OH concentration data on the surface protrusions of different dimensions and using the statistical physics to process this data. Our plans for the coming year are to examine tip-induced surface fragment dynamics on  $\text{TiO}_2$  and to begin examination of reactions on other oxide surfaces

### **Recent Grant-Sponsored Publications**

1. D. V. Potapenko, Z. Li, R. Osgood, "Dissociation of single 2-chloroanthracene molecules by STM-tip electron injection." *J. Chem. Phys.* **116**, 4679 (2012)
2. D.V. Potapenko, Z. Li, Y. Lou, R. M. Osgood Jr., "2-Propanol reactivity on *in situ* prepared Au(111)-supported  $\text{TiO}_2$  nanocrystals." *J. Catal.* **297**, 281-288 (2012)
3. D.V. Potapenko, Z. Li, J.W. Kysar, R.M. Osgood, "Nanoscale strain engineering on the surface of a bulk  $\text{TiO}_2$  crystal" *Nano Lett.* **14**, 6185 (2014)
4. Z. Li, D.V. Potapenko, K.T. Rim, M. Flytzani-Stephanopoulos, G.W. Flynn, R.M. Osgood, X.-D. Wen, and E.R. Batista, "Reactions of Deuterated Methanol ( $\text{CD}_3\text{OD}$ ) on  $\text{Fe}_3\text{O}_4(111)$ " *J. Phys. Chem. C* **119**, 1113 (2015)
5. Z. Li, D.V. Potapenko, R.M. Osgood, "Controlling surface reactions with nanopatterned surface elastic strain" *ASC Nano* **9**, 82 (2015)
6. D.V. Potapenko, Z. Li, R.M. Osgood, "Photocatalysis on nano- $\text{TiO}_2/\text{Au}(111)$ : adsorption and photodecomposition of TMAA" Submitted (July 2015)
7. D.V. Potapenko, R.M. Osgood, "Exploration of diffusion in solids with Temperature Programmed Out-diffusion method: Ar in  $\text{TiO}_2$ ", in preparation.
8. D.V. Potapenko, G.T. Gomes, and R.M. Osgood, "Modification of O-H bond energy with surface strain on rutile  $\text{TiO}_2(110)$  surface.", in preparation.

## Studies of surface adsorbate electronic structure and femtochemistry at the fundamental length and time scales

*Hrvoje Petek*

*Department of Physics and Astronomy and Chemistry  
University of Pittsburgh*

We study the dynamical properties of solid surfaces on the femtosecond temporal and nanometer spatial scales by time-resolved photoemission and scanning tunneling microscopy methods. The chemical and physical properties at molecule-solid interfaces are fundamentally important to solar energy conversion processes. Here we report on the recent results on the first experimental detection of excitons in metals and CO<sub>2</sub> Capture by metal-organic chains on Au surfaces.

**Transient excitons at Ag(111) surface.** In the field-theoretic description of light-matter interaction, the absorption of a photon creating an electron-hole pair is an instantaneous process. At the instant of interaction, a photon induces a nonadiabatic transition in a metal to create an electron-hole pair interacting via the bare Coulomb interaction. This primary transition causes fast deviations from the initial charge density equilibrium of the system, which in turn couples to the dynamical polarization or screening response of the surrounding electronic density within a few lattice sites from the disturbance. The excitation evolves from this *transient excitonic* state, where a bound state of the electron-hole pair exists, to the fully screened state of the system, where a metal does not support a locally bound state of the Coulomb potential, on the time scale of formation of the screening charge density through the virtual single-particle and collective plasma excitations. In the case of a metal surface, the self-consistent linear response to creation of an external charge has the classical analog of perfect screening in the image charge. The image charge through the associated image potential supports a Rydberg series of image potential states. The transient exciton created by the interaction of a surface state electron with a photon can recombine to regenerate the coherent field (reflection), undergo a second-order scattering process with overall energy and momentum conservation (Drude absorption), or evolve into energy conserving asymptotic states such as the image potential states. In a nonlinear multiphoton photoemission experiment, additional absorption of photon can excite the electron above the vacuum level, with the resulting photoemission spectrum capturing the dynamics of the transient exciton evolving into the fully screened image potential state.

In order to study the coherent interaction of light with metals, we developed a coherent three-dimensional multi-photon photoemission (3D-*mPP*) spectroscopy technique. In the case of Ag(111), we employ 3D-*mPP* to resolve for the first time the transient excitonic response of a metal. With single color, broadly tunable <15 fs pulse excitation in the visible spectrum, we excite *mPP* from Ag(111) surfaces, and image the resulting energy vs. parallel momentum distributions. The *mPP* spectra exhibit features, which cannot be attributed to single particle excitations among the well-known surface and bulk bands of Ag. In the case of 3PP from Ag(111) surface, a nondispersive feature, which dominates the spectra, appears when the laser is tuned near the two-photon resonant excitation from the Shockley surface state (SS) to the image potential state. The nondispersive character of the spectrum and the momentum range corresponding to the

SS attribute this feature to a localized state that is created by exciting an electron from the SS, namely the transient exciton.

In order to obtain further information on this newly discovered transient exciton, we perform time-resolved *m*PP measurements with interferometric scanning of identical pump-probe pulses. Interferometric time-resolved photoemission movies with different excitation wavelengths identify the coherent pathways and timescales for 3PP via the transient exciton resonance of Ag(111) surface. Interferograms, such as in Fig. 1 for the normal emission from Ag(111) surface, contain information on the coherent interactions leading to the 3PP process. Fourier transforming the interferograms obtains 2D photoelectron spectra, which correlate the components of the coherent polarization excited in the sample with the final state energies in the 3PP spectra. The 2D spectra manifest the evolution of the transient exciton into the fully screened image potential state on the time scale of dephasing of the surface plasmon of Ag. Remarkably, at higher excitation fluences it is possible to drive high-order processes up to 9PP via the excitation of the transient exciton in Ag. In parallel with these experimental studies, we are developing the many-body theory of the ultrafast excitonic response of metals.

The transient exciton at Ag(111) surface can be observed with 15 fs laser pulses due to the unusual screening properties at Ag surfaces. We plan to explore the transient exciton response on adsorbate modified Ag surfaces and on thin metal films on semiconductor surfaces. The transient excitons and polaritonic responses of Ag and Cu surfaces are representative of the ultrafast optical responses of solid-state materials. Thus, similar coherent responses are likely to have a role in the conversion of solar to electrical and chemical energy in organic and inorganic semiconducting materials.

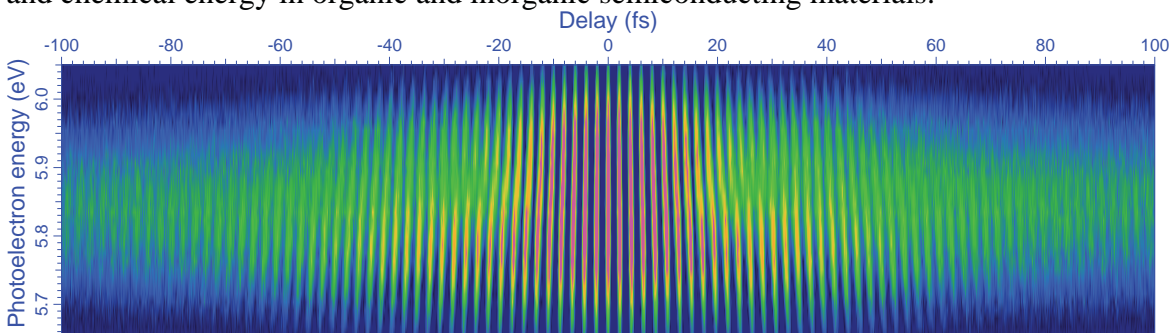


**Fig. 1.** A cross-section through a 3D movie of photoelectron counts vs. energy, momentum, and pump-probe delay time for normal emission from Ag(111) surface excited with 2.04 eV light. Fourier transform of such interferograms provides 2D spectra that correlate the induced linear and nonlinear polarization excited in the sample with specific features in the *m*PP spectra.

**CO<sub>2</sub> capture by metal-organic chains.** Efficient capture of CO<sub>2</sub> by chemical means requires a microscopic understanding of the interactions of the molecule-substrate bonding and adsorption-induced collective phenomena. By molecule-resolved imaging with scanning tunneling microscopy (STM), we investigate self-catalyzed CO<sub>2</sub> adsorption on one-dimensional (1D) substrates composed of self-assembled metal-organic chains (MOCs) supported on gold surfaces. Exposing Au(100) and Au(111) surfaces to 1,4-phenylene diisocyanide (PDI) molecules under UHV conditions leads to self-assembly of one-molecule wide chains that uniformly cover the exposed Au surfaces, with a minimum

interchain separation of  $\sim 1.4$  nm. The chains are composed of alternating 1.1 nm long units of Au adatoms forming covalent bonds to  $-\text{NC}$  functional groups of flat lying PDI molecules. The chains order into uniform grating structures even at lower coverages through long-range dipole-dipole repulsion.

Exposing MOCs to  $\text{CO}_2$  at 77 K causes their large-scale redistribution, namely they gather into close-packed structures where  $\text{CO}_2$  molecules are sandwiched in one-molecule wide ranks between the adjacent chains. We attribute the  $\text{CO}_2$  molecule-induced coalescence to a charge redistribution from the chains to the molecules, which transforms the chain interactions from repulsive to attractive. Implicit in this mechanism is charge transfer to  $\text{CO}_2$  molecules, i.e., the first step in  $\text{CO}_2$  reduction.

By mediating the interchain attraction  $\text{CO}_2$  molecules create more favorable adsorption sites for further  $\text{CO}_2$  adsorption thereby self-catalyzing their capture. The release of  $\text{CO}_2$  molecules by thermal desorption returns the MOCs to their original structure, indicating that the  $\text{CO}_2$  capture and release are reversible processes.

To understand more deeply the interactions that lead to the self-catalyzed  $\text{CO}_2$  capture, we employ low temperature scanning tunneling microscopy (LT-STM), X-ray photoelectron spectroscopy (XPS), infrared reflection absorption spectroscopy (IRAS), temperature programmed desorption (TPD), and dispersion corrected density functional theory (DFT) to characterize chemisorption and physisorption of  $\text{CO}_2$  molecules on Au surface supported Au-PDI metal-organic chains. The STM imaging reveals that Au-PDI chains activate the normally inert Au surfaces by promoting  $\text{CO}_2$  chemisorption at the Au adatom sites even at  $<20$  K. The  $\text{CO}_2^{\delta-}$  species at low coverage are imaged as single molecules attached to either or both sides of Au adatoms with a characteristic two-lobed structure (Fig. 2a). As the  $\text{CO}_2$  coverage is increased, additional molecules cluster in highly ordered two-dimensional (2D) physisorbed clusters, which grow into a full monolayer on Au crystal terraces (Fig. 2b, c). The chemisorption-induced physisorption by the “anchoring”  $\text{CO}_2^{\delta-}$  enable unprecedented imaging of single  $\text{CO}_2$  molecules from single molecules to full monolayers. The dispersion interactions with the substrates cause the monolayer films to assume a rhombic structure similar to a high-pressure  $\text{CO}_2$  crystalline solid. The IRAS, XPS, and TPD measurements support the coexistence of the chemisorbed and physisorbed  $\text{CO}_2$  molecules up to 120 K.

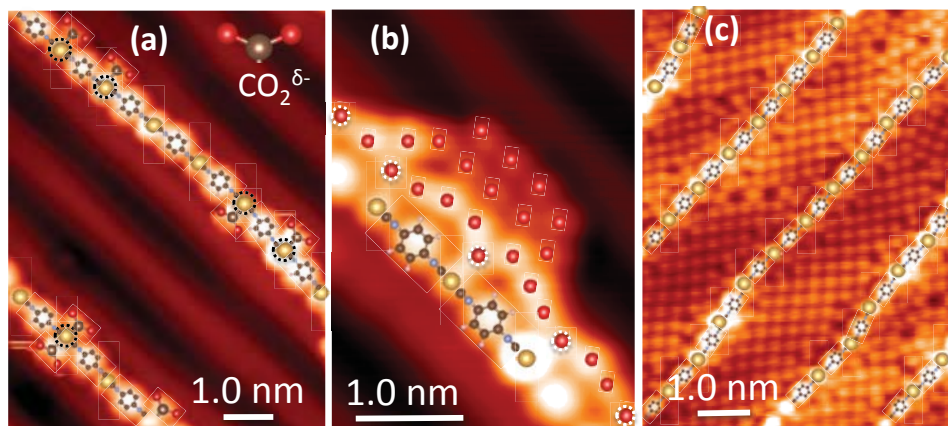


**Fig. 2.** (a) Au-PDI chains at low  $\text{CO}_2$  coverage. Single chemisorbed  $\text{CO}_2^{\delta-}$  species are found aside of Au adatoms. (b) The  $\text{CO}_2^{\delta-}$  species seed and anchor  $\text{CO}_2$  physisorption in larger cluster as the coverage is increased. (c) At full monolayer coverage  $\text{CO}_2$  molecules form a rhombic structure that is characteristic of a high-pressure  $\text{CO}_2$  phase.

The Au surface supported Au-PDI chains provide a platform for investigating the physical and chemical interactions involved in CO<sub>2</sub> capture and reduction. Au-PDI chains and Au substrates exhibit characteristics of both the homogeneous and heterogeneous catalysis, but it is not clear to what extent are the observed activity due to the Au-PDI chains, the substrate, or a cooperative interaction among them. In future experiments we plan to investigate whether similar self-assembly of metal-organic constructs occurs on other noble and transition metal substrates, and to what extent are the observed interactions enabled by the metal-organic constructs in the absence of the metallic substrate. Such metal-organic constructs are an interesting interfacial species with yet unknown chemical properties, because they appear to exist mainly on metal surfaces and not independently in other environments. Other experiments will probe the unoccupied electronic structure of Au-PDI chains by time-resolved two-photon photoemission with and without decoration of CO<sub>2</sub> molecules, to investigate the possibility of photoinduced reduction of CO<sub>2</sub>. Coadsorption with proton donating molecules may enable further reduction through proton-coupled electron transfer.

### DOE Sponsored Publications 2013-2015<sup>1-9</sup>

- <sup>1</sup> Feng, M., Shi, Y., Lin, C., Zhao, J., Liu, F., Yang, S., & Petek, H. Energy stabilization of the s-symmetry superatom molecular orbital by endohedral doping of C<sub>82</sub> fullerene with a lanthanum atom. *Phys. Rev. B* **88**, 075417 (2013).
- <sup>2</sup> Winkelmann, A., Tusche, C., Ünal, A.A., Chiang, C.-T., Kubo, A., Wang, L., & Petek, H., Ultrafast multiphoton photoemission microscopy of solid surfaces in real and reciprocal space in *Dynamics of interfacial electron and excitation transfer in solar energy conversion: theory and experiment*, edited by P. Piotrowiak (Royal Society of Chemistry, Cambridge, 2013).
- <sup>3</sup> Cui, X., Wang, C., Argondizzo, A., Garrett-Roe, S., Gumhalter, B., & Petek, H. Transient excitons at metal surfaces. *Nat Phys* **10**, 505-509 (2014).
- <sup>4</sup> Feng, M., Sun, H., Zhao, J., & Petek, H. Self-Catalyzed Carbon Dioxide Adsorption by Metal–Organic Chains on Gold Surfaces. *ACS Nano* **8**, 8644-8652 (2014).
- <sup>5</sup> Petek, H. Single-Molecule Femtochemistry: Molecular Imaging at the Space-Time Limit. *ACS Nano* **8**, 5-13 (2014).
- <sup>6</sup> Zhao, J., Feng, M., Dougherty, D.B., Sun, H., & Petek, H. Molecular Electronic Level Alignment at Weakly Coupled Organic Film/Metal Interfaces. *ACS Nano* **8**, 10988-10997 (2014).
- <sup>7</sup> Silkin, V.M., Lazić, P., Došlić, N., Petek, H., & Gumhalter, B. Ultrafast electronic response of Ag(111) and Cu(111) surfaces: From early excitonic transients to saturated image potential. *Phys. Rev. B* **92**, 155405 (2015).
- <sup>8</sup> Feng, M., Petek, H., Shi, Y., Sun, H., Zhao, J., Calaza, F., Sterrer, M., & Freund, H.-J. Cooperative Chemisorption Induced Physisorption of CO<sub>2</sub> Molecules by Metal–Organic Chains. *ACS Nano* (in press).
- <sup>9</sup> Feng, M. & Petek, H., Scrutinizing the Endohedral Space: Superatom States and Molecular Machines in *Endohedral Fullerenes: electron transfer and spin*, edited by A. Popov (Springer, in press).

## MOLECULAR STRUCTURE, BONDING AND ASSEMBLY AT NANOEMULSION AND LIPOSOME SURFACES

*PI: Geraldine Richmond, University of Oregon*

*Start date: September 1, 2015*

*Email: richmond@uoregon.edu*

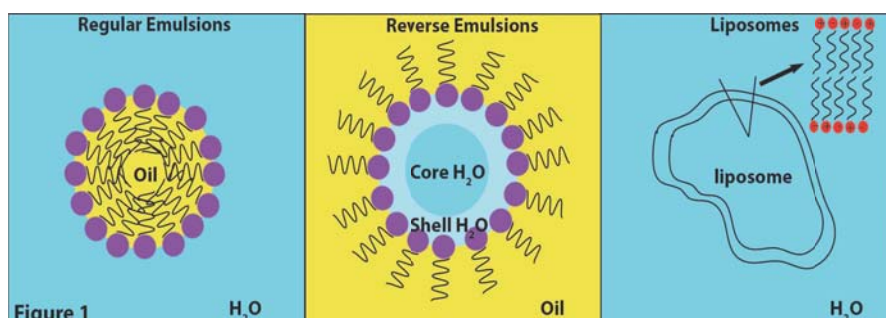
### ***Program Scope and Definition***

Nanoemulsions have attracted considerable attention in recent years due to their unique potential applications in drug delivery,<sup>2,3</sup> oil recovery,<sup>4,5</sup> and as nanoreactors for producing polymers and nanomaterials.<sup>6</sup> They are also predicted to be increasingly important commercially since significantly less emulsion stabilizing surfactant is required for their function. They are also attractive as useful dispersant of deformable nanoscale droplets with flow properties from liquid to highly solid, and optical properties ranging from opaque to nearly transparent. Relative to micelles little is known about creating and controlling nanoemulsions including the interfacial molecular processes that lead to their formation and stability. Although it may seem that nanoemulsion formation should be similar to micellar (microemulsion) systems, in fact they can behave quite differently and often for reasons that are not yet fully understood.<sup>7-10</sup> Nanoemulsions do not form spontaneously and require an external shear beyond that of ordinary procedures used to create micelles. This shear is required to overcome the effects of surface tension and create droplets in the nanoscale regime. Once formed however they can be stable for long periods of time, making them very attractive for commercial and pharmaceutical products requiring a long shelf-life. Key to advancing the utility of these and related nanoscale liposome systems is to develop the needed molecular-level understanding of the structure and bonding interactions present at the surface of these soft nanoparticles. The objective of these studies is just that: *to advance our understanding of the molecular structure, orientation and bonding of surfactants at the surface of nanoemulsions and liposomes, and the bonding characteristics of interfacial water that is either confined or surrounding the surfactant coated soft particle surfaces.* The project involves a series of carefully designed studies that explore the molecular nature of adsorption and surface interactions on regular and reverse nonemulsions created with selected cationic or anionic surfactant suspended in water and oil respectively, and liposomes suspended in water that are comprised of mixtures of these surfactants.

Our approach involves measuring the surface vibrational spectroscopy of the surfactant coated particle surfaces in-situ using vibrational sum frequency scattering spectroscopy (VSFSS),<sup>11</sup> with related complementary studies of these surfactant systems examined at the more well-defined planar oil/water interface by vibrational sum frequency spectroscopy (VSFS). Classical molecular dynamics (MD) calculations coupled with density functional theory (DFT) methods will be employed to assist in spectral assignments and understanding solvation effects. Other experimental techniques such as dynamic light scattering (DLS), zeta potential and interfacial tensiometry will also be used. These new studies launch our long-term effort to understand the molecular properties of liquid surfaces in several exciting new directions. They build on and take advantage of our leading capabilities in using both experimental techniques (e.g., VSFS, surface tensiometry, zeta potential and DLS) and computational methods (MD, DFT) to detail molecular interactions at the planar oil/water interface, and our early success in using VSFSS in preliminary studies of suspended nanoparticles. The systems chosen for study have been carefully selected with the dual goals (1) to understand how the molecular properties of these surfaces vary with such parameters as surface and solvent composition, particle size and

interfacial charge, and (2) to better define the experimental parameters involved in this relatively new VSFSS technique and its strengths and limitations as a general tool for studying suspended particle systems of importance in fields such as energy technology, environmental science, chemistry, medicine and biology.

The suspended particle systems chosen for study fall into three categories as depicted in Figure 1: (a) regular nanoemulsions, where the dispersed oil phase is encapsulated by surfactants that align with their tails in the interior of the particle suspended in the aqueous solution, (b) reverse



reverse nanoemulsions, where the dispersed aqueous phase is encapsulated by surfactants that align with their tails towards the continuous bulk oil phase, and (c) liposomes which are composed of a bilayer of surfactants that form into a spherical particle suspended in an aqueous phase.<sup>6</sup> Our target particle size for both the nanoemulsions and liposomes is in the range of 100-1000 nm.<sup>7-8</sup>

## Recent Progress

Over the past two years, we have been assembling the instrumentation for conducting the VSFSS experiments and have recently had success in our chosen model system of AOT reverse and regular nanoemulsions. These are very difficult experiments so we are delighted to be able to report success. There are several interesting preliminary results that are arising from these

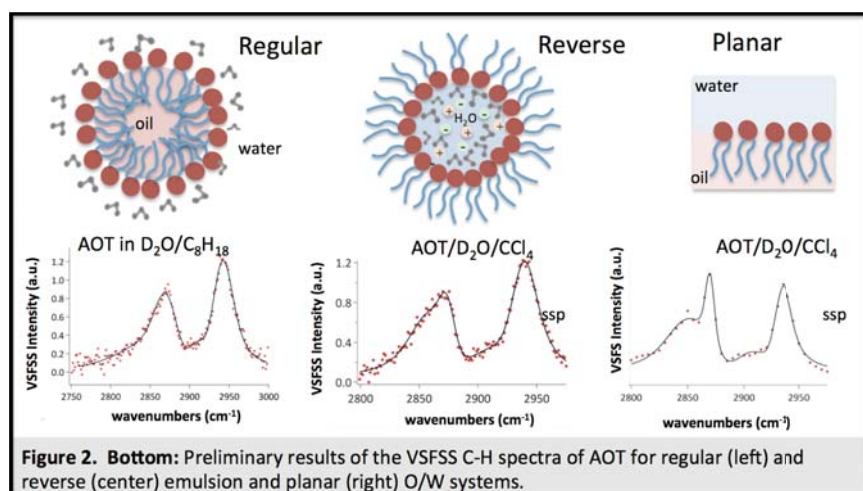
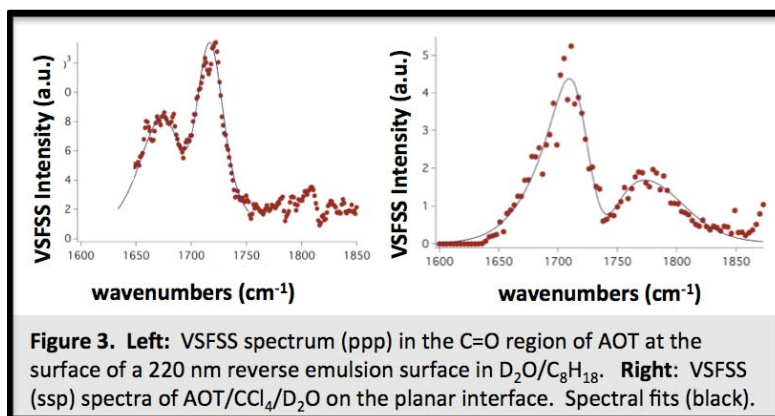


Figure 2. Bottom: Preliminary results of the VSFSS C-H spectra of AOT for regular (left) and reverse (center) emulsion and planar (right) O/W systems.

early studies that warrant further exploration and validation. Shown in Figure 2 are examples of spectra we obtain for 220 nm AOT at the reverse nanoemulsion and regular nanoemulsion surfaces, and comparative planar oil/water interface using the SSP polarization scheme. Two primary peaks appear in all spectra near  $2855(\pm 5) \text{ cm}^{-1}$  for the methylene symmetric stretch and at  $2873 \text{ cm}^{-1}$  for the methyl symmetric stretch. The response from the regular, reverse and planar surfaces are remarkably similar and indicative of similar chain disorder as the hydrocarbon tails extend into the oil phase, even though the oil phase in these preliminary studies is different for the regular nanoemulsion.

The spectra obtained thus far for the carbonyl region provide equally interesting results for the reverse nanoemulsion and planar O/W system (Figure 3). In both cases we observe the splitting of the C=O mode into two distinct peaks. However the peak positions and their relative intensities differ considerably between the reverse nanoemulsion and planar systems. Using our standard VSF spectra fitting routines to fit the spectra (black line),<sup>55</sup> several interesting peaks are determined (which appear at slightly different frequencies from simple visual inspection of the spectra due to the coherent nature of the VSF spectroscopy). The peak positions determined from the fitting are at  $1670 (\pm 5) \text{ cm}^{-1}$  and  $1720 \text{ cm}^{-1}$  for the reverse nanoemulsion. These peaks are

shifted significantly to lower energies compared to AOT vibrational modes in bulk  $\text{CCl}_4$  at  $1736 \text{ cm}^{-1}$ ,<sup>118</sup> consistent with higher degrees of water solvation of the carbonyl regions of AOT at the nanoemulsion surface. Comparing this to AOT at the  $\text{CCl}_4/\text{D}_2\text{O}$  planar interface at the same concentration yields somewhat different results. The planar spectrum (right) was fit



with three peaks. The peak around  $1730 \text{ cm}^{-1}$  for the AOT C=O mode is only slightly shifted from its single peak in  $\text{CCl}_4$ , indication of a carbonyl that is in a largely  $\text{CCl}_4$  environment. There is also a peak which is red shifted from the C=O in bulk  $\text{CCl}_4$  at about  $1660 \text{ cm}^{-1}$ , and appears as a shoulder in the VSFSS planar spectrum. We attribute this to carbonyls that align to be more solvated in the aqueous phase and near to the peak seen in the scattering experiments. Its intensity is much weaker than in the scattering experiment although similar polarizations schemes need to be employed to draw any such conclusions. There is also a small peak in the planar studies at  $1770 \text{ cm}^{-1}$  that at this point we can only speculate as being carbonyls in a hydrophobic environment created by the alkyl hydrophobic chains and  $\text{CCl}_4$ . A similar peak might be present in the reverse nanoemulsion spectrum but we need to verify this with different polarizations and improved S/N.

Although there is much more work to be done even on these preliminary studies, we are encouraged by our success in conducting these difficult experiments that have taken two years to assemble, and the clear differences and similarities in the spectra from the scattering vs. planar studies for AOT at the  $\text{CCl}_4/\text{D}_2\text{O}$  interface. The studies further highlight the value of these spectroscopic methods in understanding surface phenomena for these O/W nanoparticle systems.

### ***Future Plans***

Our plans for the coming year of funding are to verify the above preliminary results and move forward with a number of different projects. First priority in moving forward is to conduct VSFSS studies that compare the measurements of AOT regular and reverse nanoemulsions in more detail than described above including different polarization schemes. These AOT particle and planar studies will also examine the variation in interfacial behavior with surfactant concentration for both regular and reverse emulsions as we seek to understand some key issues with regards to critical micelle concentration (CMC) formation for these nanoparticle systems. Additional studies are planned to conduct similar measurements with cetyltrimethylammonium

bromide (CTAB) at both the regular and reverse nanoemulsion surface as well as the planar surface. As with AOT, concentration studies and polarization measurements will be involved. DLS, surface tension and zeta potential measurements will be performed as needed on both the AOT and CTAB systems. Central to all these initial studies is to establish experimental and sample preparation procedures for accurate VSFSS measurements of AOT and CTAB for the ~200 nm particles as a starting point with particles of varying sizes to follow as a longer term goal. Our MD and DFT computational studies described below will assist in spectral interpretation as in our previous studies.

The surface spectroscopic studies will probe AOT's behavior by studying vibrational modes such as the C-H, C=O and S-O stretch modes that appear near  $\sim 3000\text{ cm}^{-1}$ ,  $\sim 1730\text{ cm}^{-1}$  and  $\sim 1080\text{ cm}^{-1}$  respectively, along with interfacial water modes in the  $3200\text{-}3800\text{ cm}^{-1}$  region. We know from our previous work that C=O and S-O modes are sensitive to the level of hydration and nearby ions.<sup>12-13</sup> Alkyl conformational ordering will be determined through the C-H modes. For the amines the amino C-H modes of the methyl groups in the head group region, which are significantly shifted to a lower energy from the terminal methyl group, should have a strong symmetric stretch signal at  $2780\text{-}2805\text{ cm}^{-1}$  that we will monitor. Deuteration of solvents and molecules will be used where appropriate to help with spectral interferences from C-H and O-H stretching modes and absorptions. Where possible, the interfacial water will be examined through the OH stretch modes in the  $3200\text{-}3700\text{ cm}^{-1}$  region as we have in past VSF studies.<sup>14,15</sup>

## References

1. Rocca, S.; Garcia-Celma, M. J.; Caldero, G.; Pons, R.; Solans, C.; Stebe, M. J., *Langmuir* **1998**, *14* (24), 6840-6845.
2. Javadi, M.; Pitt, W. G.; Belnap, D. M.; Tsosie, N. H.; Hartley, J. M., *Langmuir* **2012**, *28* (41), 14720-14729.
3. Czarnecki, J., *Energy & Fuels* **2009**, *23* (3), 1253-1257.
4. Alvarez, G.; Jestin, J.; Argillier, J. F.; Langevin, D., *Langmuir* **2009**, *25* (7), 3985-3990.
5. Eastoe, J.; Hollamby, M. J.; Hudson, L., *Advances in Colloid and Interface Science* **2006**, *128-130*, 5-15.
6. Fayer, M. D.; Levinger, N. E., *Annu. Rev. Anal. Chem.* **2010**, *3* (1), 89-107.
7. Wilking, J.; Mason, T., *Phys. Rev. E* **2007**, *75* (4), 041407.
8. Kini, G. C.; Biswal, S. L.; Wong, M. S.; Miller, C. A., *J. Colloid Interface Sci.* **2012**, *385* (1), 111-121.
9. Mason, T. G.; Wilking, J. N.; Meleson, K.; Chang, C. B.; Graves, S. M., *J. Phys.: Condensed Matter* **2006**, *18*, 635-666.
10. Eicke, H. K.; Heinz, C., *J. Colloid Interface Sci.* **1973**, *48*, 281-290.
11. Roke, S.; Gonella, G., Nonlinear light scattering and spectroscopy of particles and droplets in liquids. *Annu. Rev. Phys. Chem.* **2012**, *63* (1), 353-378.
12. Beaman, D. K.; Robertson, E. J.; Richmond, G. L., Unique assembly of charged polymers at the oil-water interface. *Langmuir* **2011**, *27* (6), 2104-2106.
13. Beaman, D. K.; Robertson, E. J.; Richmond, G. L., From head to tail: Structure, solvation, and hydrogen bonding of carboxylate surfactants at the organic/water interface. *J. Phys. Chem. C* **2011**, *115* (25), 12508-12516.
14. McFearin, C. L.; Richmond, G. L., The role of interfacial molecular structure in the adsorption of ions at the liquid-liquid interface. *J. Phys. Chem. C* **2009**, *113* (50), 21162-21168.
15. Moore, F. G.; Richmond, G. L., Integration or segregation: How do molecules behave at oil/water interfaces? *Acc. Chem. Rev.* **2008**, *41* (6), 739-748.

## Solvation

Richard Saykally ([saykally@berkeley.edu](mailto:saykally@berkeley.edu)), Musahid Ahmed ([mahmed@lbl.gov](mailto:mahmed@lbl.gov)), Phillip L. Geissler ([plgeissler@lbl.gov](mailto:plgeissler@lbl.gov)) and Charles Harris ([cbharris@berkeley.edu](mailto:cbharris@berkeley.edu))

Lawrence Berkeley National Laboratory, Chemical Sciences Division, 1 Cyclotron Road,  
Berkeley, CA 94720

### Program Scope

It is widely recognized that the solvation properties of ions and molecules influence, or even actually determine vital phenomena and processes, like electrochemical transport, bubble formation, ion pair formation and crystallization, protein folding, corrosion, as well as chemical reactions in solutions and at interfaces. This research program addresses the development and application of novel spectroscopic and theoretical technologies to this problem.

### Recent Progress

The Geissler group performs theoretical studies of solvation at interfaces. The equilibrium distribution of small ions near an interface between air and liquid water highlights substantial shortcomings of classic theories for solvation. As first emphasized in computer simulations by Tobias and Jungwirth, such solutes can counterintuitively adsorb to the interfacial region, where they would seem to sacrifice the very favorable polarization energy underlying their high solubility. Subsequent computational work has shown that this behavior is quite general in model liquids, and has elaborated connections with a variety of supporting experimental measurements. Understanding this phenomenon in microscopic physical detail has formed a central goal of our work, both for its relevance for atmospheric and electro-chemistry and also for the basic gaps in chemical theory that it reveals. We have established key implications of capillary fluctuations for solvation near interfaces, a factor that is neglected entirely in standard calculations of dielectric continuum theory. Liquid-vapor interfaces are typically soft, permitting substantial fluctuations in topography even on molecular scales. Given the strong forces a charged solute exerts on water density, one should therefore expect surface deformations to play an important role in surface solvation of ions, as we have confirmed using simulations and theory. These effects are in fact strong even for non-attractive solutes in water (i.e., hydrophobes). Creating space for solutes to occupy is achieved in bulk by constraining and reorganizing hydrogen bonds; near a soft interface, it can emerge from surface deformations instead. A theoretical basis for describing the interplay between these mechanisms has been established by Chandler and coworkers. We implemented and improved upon that approach to construct efficient and accurate coarse-grained models for hydrophobic solvation in heterogeneous environments. They yield remarkably accurate predictions in these situations, even for detailed statistics of microscopic density fluctuations. We have also performed calculations that clarify the significance of surface potential in ion adsorption, showing that the pronounced charge asymmetry of ion adsorption does not primarily arise from the natural orientation of water molecules at the air-liquid interface.

The Saykally group seeks to explore, develop, and apply novel methodologies for atom-specific characterization of hydration in liquids, solutions and their interfaces, employing combinations of liquid microjet technology with synchrotron X-ray and nonlinear optical spectroscopy in close connection with state-of-the-art theory. As a route to clarifying the mechanism that selectively

drives ions to and away from the air/water interface, we have determined the associated entropy and enthalpy for this process from the temperature dependence of the adsorption free energy of the thiocyanate ion by UV resonant SHG spectroscopy. Another manifestation of ion solvation versus solvent-solvent interaction is ion pairing. We have recently reported the observation and characterization of "contact pairing" between positively charged guanidinium ions in aqueous solution, using the combination of synchrotron X-ray spectroscopy of liquid microjets and first principles' theory. X-ray absorption spectroscopy of solutions of LiBF<sub>4</sub> in propylene carbonate (PC), interpreted using first-principles electronic structure calculations within the eXcited electron and Core Hole (XCH) approximation, yielded new insight into the solvation structure of the Li<sup>+</sup> ion in this model electrolyte; we find a Li<sup>+</sup>-solvent interaction number of 4.5. This result suggests that computational models of lithium ion battery electrolytes need to move beyond tetrahedral coordination structures. Finally, electrokinetics technology was used to develop new ways to detect X-ray absorption spectra of weakly interacting liquids with high vapor pressures.

The Ahmed group studies clusters as a route to definitive characterization of solvation which is amenable to detailed theoretical interpretation and comparison. He has recently developed an experimental strategy for characterizing neutral versus ion-induced growth using in-source ionization of molecular beams with tunable VUV synchrotron radiation. Methanol cluster distributions at various distances between a nozzle and ionization show signatures for both ion induced and neutral nucleation. The experimental results could be explained qualitatively using Thomson's liquid drop model. The in-source ionization method has been implemented to study non-equilibrium water cluster distributions upon VUV photoionization, and study ion-molecule reaction dynamics in mixed acetylene-ethylene clusters. Computational fluid dynamics simulations of the nucleation source have been implemented and a new quadrupole mass filter incorporated into the experimental apparatus.

The Harris group focuses on electron solvation at ionic liquid(IL)/electrode interfaces relevant to a variety of electrochemical devices using Time- and Angle-Resolved Two Photon Photoemission. Our initial studies observed a temperature dependent morphological phase change in the IL film, reflected in the ultrafast solvation response of a photo-injected electron. Subsequent experiments have involved well-defined layer-by-layer coverage to discover how excess charge solvation is influenced by electrostatic screening, charge location, and photoinduced film degradation.

### **Future Plans**

Geissler plans to continue exploring correlations among multiple ions. Energy applications often involve sufficiently high ionic strength that such correlations cannot be neglected. Moreover, SHG studies by Saykally's group indicate that finite-concentration effects on adsorption appear at relatively low concentration. Building on insight from our work on this problem, we also plan to address a more general question: What reduced description of microscopic fluctuations in liquid water will allow efficient, transparent, and accurate treatment of the diverse solute chemistries pertinent to energy sciences? The perspective of Lum, Chandler, and Weeks (LCW) on hydrophobicity, which focuses exclusively on microscopic density fluctuations, provides inspiration for this effort. Charged and polar solutes are clearly sensitive to additional features of the aqueous environment, most notably the electrostatic forces generated by water molecules' strong dipole moment. We aim to identify order parameters that allow treatment of hydrophilic solvation along the lines of LCW theory. Early results indicate that these variables should

characterize both the solvent's dipole field as well as connectivity of its hydrogen bonding network.

Saykally will extend the studies described above to include temperature dependences for surface adsorption of other prototype salts, exploration of the generality of like-charge ion pairing in aqueous solution, and solvation of Li<sup>+</sup> ions in other organic carbonate battery solvents. A new project to study the hydration properties of aqueous free radicals by UV photolysis of liquid jets will be launched.

Ahmed plans to use mass spectrometry in conjunction with synchrotron radiation in an integrated approach to move seamlessly from gas phase systems to solution phase chemistry mediated via clusters. This will be achieved with Infrared spectroscopy and Rydberg ionization with new sensitive molecular beams methods to probe excited state relaxation dynamics, charge transfer and binding energetics in small clusters. We propose to substantially advance the molecular level understanding of metal ion solvation by both XAS and VUV studies by performing size selected spectroscopy experiments in a recently acquired ion trap mass spectrometer. Metal ions can bind in different ligand sites in flavin molecule – on reactive C=O sites, nitrogen lone pairs, or can form  $\pi$ -complexes with aromatic rings. Since near edge (C, N, or O) XAS is a powerful technique to probe local electronic structures and bonding, XAS would show a shift in absorption spectra as a result of complexation. Along with XAS, a complementary approach will be applied to study mass-selected (ML<sub>n</sub>)<sup>x+</sup> complexes using tunable VUV photon where information such as binding energies, coordination numbers, and solvation structures around metal ions can be obtained which in conjunction with theory can provide direct information on electrostatic and covalent bonding, and intermolecular forces.

Harris plans to investigate how ultrafast processes can be controlled by exploiting the chemically tunable nature of IL materials. Furthermore, he will aim to study IL growth and dynamics on carbon-rich electrodes in order investigate electron behavior in materials used in electrochemical devices. A new joint effort with the Saykally group will address the development of 2-dimensional SHG/SFG studies of aqueous electrolyte interfaces, which will provide much more detailed information about solvation and ion correlation at aqueous interfaces.

### Recent Publications

Vaikuntanathan, S. and Geissler, P.L., “*Putting water on a lattice: The importance of long wavelength density fluctuations in theories of hydrophobic an interfacial phenomena*” *Phys. Rev. Lett.*, 2014, 112, 020603, 1-5.

Geissler, P.L., “*Water Interfaces, Solvation, and Spectroscopy*” *Ann.. Rev. Phys. Chem.*, 2013, 64, 317-337.

Vaikuntanathan, S., Shaffer, P.R., and Geissler, P.L., “*Adsorption of solutes at liquid-vapor interface: Insights from lattice gas models*” *Faraday Discuss.*, 2013, 160, 63-74.

Otten, D. E., Saykally, R. J. "Spectroscopy and modeling of aqueous interfaces" in *Proceedings of the International School of Physics "Enrico Fermi", Course 187 "Water: Fundamentals as the Basis for Understanding the Environment and Promoting Technology,"* edited by P. G. Debenedetti, M. A. Ricci, and F. Bruni (IOS Press, Amsterdam; SIF, Bologna) 2015.

- Smith, J. W., Lam, R. K., Shih, O., Rizzuto, A. M., Prendergast, D., Saykally, R. J. "*Properties of aqueous nitrate and nitrite from x-ray absorption spectroscopy*" *J. Chem. Phys.*, **2015**, 143, 084503.
- Smith, J. W., Lam, R. K., Sheardy, A. T., Shih, O., Rizzuto, A. M., Borodin, O., Harris, S. J., Prendergast, D., Saykally, R. J., "*X-Ray absorption spectroscopy of LiBF<sub>4</sub> in propylene carbonate: a model lithium ion battery electrolyte*" *Phys. Chem. Chem. Phys.*, **2014**, 16 (23), 23496-24110
- Saykally, R. J. "*Aqua incognita: liquor aquae superficies*" in AQUA INCOGNITA: Why Ice Floats on Water and Galileo 400 years on, Pierandrea Lo Nostro & Barry W Ninham (Editors), (ISBN: 9781925138214; Connor Court, Australia; 2014).
- Lam, R. K., Shih, O., Smith, J. W., Sheardy, A. T., Rizzuto, A. M., Prendergast, D., Saykally, R. J. "*Electrokinetic detection of X-ray spectra of weakly interacting liquids: n-decane and n-nonane*" *J. Chem. Phys.*, **2014**, 140, 234202.
- B. Shih, O., England, A.H., Dallinger, G.C., Smith, J.W., Duffey, K.C., Cohen, R.C., Prendergast, D., and Saykally, R. J. "*Cation-Cation Contact Pairing in Water: Guanidinium*" *J. Chem. Phys.*, **2013**, 139, 035104.
- Kelly, D.N., Lam, R.K., Duffin, A., and Saykally, R. J. "*Characterization of Dilute Aqueous Interfaces with Liquid Microjet Electrokinetics*" *J. Phys. Chem. C.*, **2013**, 117 (24), 12702-12706.
- B. Bandyopadhyay, O. Kostko, Y. Fang, and M. Ahmed, "*Probing Methanol Cluster Growth by Vacuum Ultraviolet Ionization*," *J. Phys. Chem. A*, (2015) 119, 4083.
- M. Perera, K. M. Roenitz, R. B. Metz, O. Kostko, and M. Ahmed, "*VUV photoionization measurements and electronic structure calculations of the ionization energies of gas-phase tantalum oxides TaO<sub>x</sub> (x=3-6)*," *J. Spectrosc. Dyn.* (2014), 4, 21
- Muller, E. A., Strader, M. L., Johns, J. E., Yang, A., Caplins, B. W., Shearer, A. J., Suich, D. E., Harris, C. B., "*Femtosecond Electron Solvation at the Ionic Liquid/Metal Electrode Interface*" *J. Am. Chem. Soc.*, 2013, 135, 10646-10653.

## Molecular Theory & Modeling

*Development of Statistical Mechanical Techniques for Complex Condensed-Phase Systems*

Gregory K. Schenter  
 Physical Sciences Division  
 Pacific Northwest National Laboratory  
 902 Battelle Blvd.  
 Mail Stop K1-83  
 Richland, WA 99352  
[greg.schenter@pnnl.gov](mailto:greg.schenter@pnnl.gov)

The long-term objective of this project is to advance the development of molecular simulation techniques to better understand fundamental properties and processes of molecular and nanoscale systems in complex environments, such as condensed phases and interfaces. We have focused on complexity associated with broken symmetries corresponding to vacuum/liquid, liquid/solid, and liquid/liquid interfaces or highly concentrated electrolytes. The characterization of these systems requires a description of molecular interaction that is more robust than what is required to describe bulk, homogeneous systems. Understanding the balance between descriptions of molecular interaction and complexity will continue to be the focus of future research efforts. We will continue to develop a systematic connection between models of molecular interactions and collective behavior of molecular systems. This will lead to an improved knowledge of complex collective behavior on a macroscopic scale. It involves the investigation of representations of molecular interaction as well as statistical mechanical sampling techniques and finding the balance between efficiency and accuracy in the description of molecular interaction.

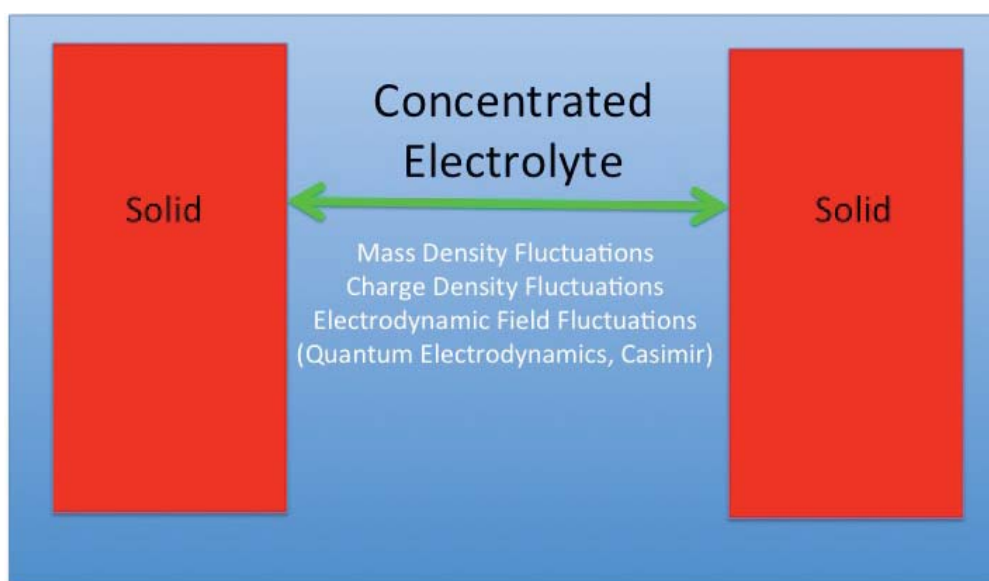


Figure 1. Forces between two solids in a concentrated electrolyte is determined from mass density, charge density and electrodynamic field fluctuations.

To better understand collective many-body phenomena we are exploring the connection between: 1) the many-body decomposition of atom based potentials, 2) the partitioning of a system into an explicit sub-system and a bath and 3) transport and fluctuations of macroscopic

mass, charge, and energy field densities, as well as electrostatic and electrodynamic fields. Each of these frameworks have a long history of development. We expect that the relation between these frameworks will need to be better understood in order to impact understanding of more complex phenomena.

Towards these ends, we have explored the influence of broken symmetry on equilibrium fluctuations. In Ref. [1], we explored how a simple hydrophobic hard sphere disrupts the hydrogen bonding structure and the resulting electric field and polarization density distributions. Future efforts will extend this work to dynamic response and perturbations that push the system beyond linear response. [see Chris Mundy's abstract] There is a dynamic consequence associated with the tuning of "frustrated charge models"[a] to recover only equilibrium fluctuations. Future work will focus on this by exploring the water exchange process about ions,[see Liem Dang's abstract] comparing and contrasting the dependence on the descriptions of molecular interaction. In our studies we search for the appropriate amount of explicit treatment of electronic structure that allows for efficient sampling of a statistical mechanical ensemble of a system of interest. We have established that a Density Functional Theory (DFT) description of molecular interaction provides a quantitative representation of the short-range interaction and structure when compared to Extended X-ray Absorption Fine Structure (EXAFS) measurements. To do this we continue to develop our MD-EXAFS approach.[4] This approach has allowed us to characterize in detail the complex equilibrium associated with the dissociation of HCl in water,[2] and gives us confidence that the short range molecular phenomena is effectively and accurately described by DFT electronic structure coupled to statistical mechanical sampling. Much of our future efforts will concentrate on characterizing fluctuations, taking advantage of effective potentials of mean force and linear response kernels from density, charge and electromagnetic fluctuations. [See Figure 1.]

In Ref. [3] we explored the consequences of solvent structure on the electrodynamic field fluctuations and consequently the Lifshitz force between the two solid surfaces. In this work we considered the water density responding to mica,  $\text{TiO}_2$ , and gold. [See Figure 2.] In Figure 3 we display a typical force versus distance curve. We find significant deviations from conventional Lifshitz theory due to water structure. Future work will involve the coupling of molecular detail to the continuum description of the phenomena.

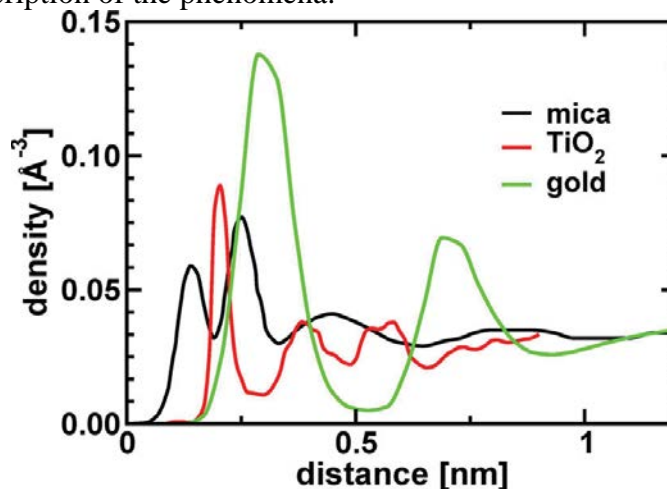


Figure 2. Water density profile.

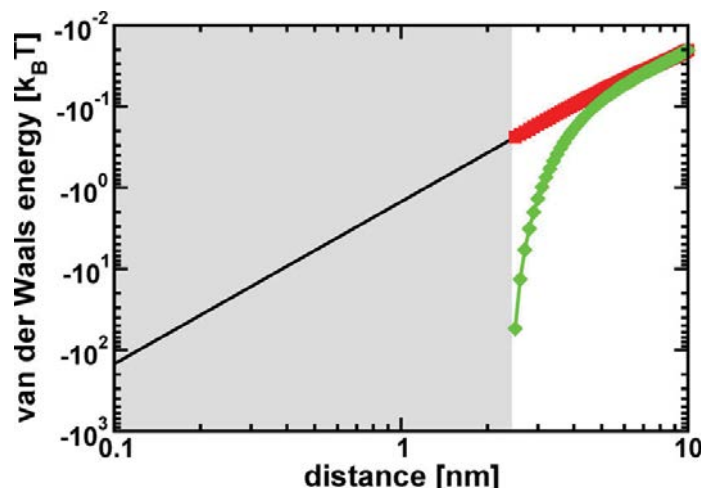


Figure 3. van der Waals interaction between  $16 \text{ nm}^2$  flat mica surfaces as a function of separation distance. Note the significant difference between the theory that takes into account the nonuniform solvent density (green diamonds), compared to the result that considers only the bulk dielectric response of water (red squares). The black solid line represents the conventional Lifshitz theory. The gray region represents a region where there is significant overlap between the nonuniform solvent distributions and molecular detail becomes more significant.

*Acknowledgements:* Direct collaborators on this project include C. J. Mundy, M. Baer and J. Fulton. Collaboration with J. Weeks and R. Remsing (U. Maryland) is significant. Valuable interactions with S. S. Xantheas, L. X. Dang and S. M. Kathmann have influenced the course of this work. Battelle operates Pacific Northwest National Laboratory for the US Department of Energy.

## References

- a. R. C. Remsing, J. M. Rodgers, and J. D. Weeks, “Desconstructing Classical Water Models at Interfaces and in Bulk,” *J. Stat. Phys.* **145**, 313 (2011).

## References to publications of CPIMS sponsored research (2014-2015)

1. R. C. Remsing, M. D. Baer, G. K. Schenter, C. J. Mundy, and J. D. Weeks, “The Role of Broken Symmetry in Solvation of a Spherical Cavity in Classical and Quantum Water Models,” *J. Phys. Chem. Lett.*, **5** (16), 2767–2774 (2014). doi:10.1021/jz501067w
2. M. D. Baer, J. L. Fulton, M. Balasubramanian, G. K. Schenter, and C. J. Mundy, “Persistent Ion Pairing in Aqueous Hydrochloric Acid,” *J. Phys. Chem. B*, **118** (26), 7211–7220 (2014). doi:10.1021/jp501091h
3. J. Chun, C. J. Mundy, and G. K. Schenter, “The Role of Solvent Heterogeneity in Determining the Dispersion Interaction Between Nanoassemblies,” *J. Phys. Chem. B* **119** (18):5873-5881 (2015). doi:10.1021/jp512550c
4. G. K. Schenter, J. L. Fulton, “Molecular Dynamics Simulations and XAFS (MD-XAFS)”, In “XAFS Techniques for Catalysts, Nanomaterials, and Surfaces”, Yasuhiro Iwasawa, Kiyotaka Asakura, and Mizuki Tada, editors, Springer, New York, 2015 in press.

## **An Atomic-scale Approach for Understanding and Controlling Chemical Reactivity and Selectivity on Metal Alloys**

E. Charles H. Sykes (charles.sykes@tufts.edu)

Department of Chemistry, Tufts University, 62 Talbot Ave, Medford, MA 02155

### **Program Scope:**

Catalytic hydrogenations are critical steps in many industries including agricultural, chemicals, foods and pharmaceuticals. In the petroleum refining industry, for instance, catalytic hydrogenations are performed to produce light, hydrogen rich products like gasoline. Hydrogen activation, uptake, and reaction are also important phenomena in fuel cells, hydrogen storage devices, materials processing, and sensing. Typical heterogeneous hydrogenation catalysts involve nanoparticles composed of expensive noble metals or alloys based on metals like Pt, Pd, and Rh. Our goal is to alloy very small amounts of these types of reactive metals with more inert and often much cheaper hosts and to understand how the local atomic geometry affects reactivity. We have focused on understanding the adsorption, diffusion, spillover and reactivity of hydrogen in a number of these types of systems. We designed well-defined Pd, Co, Au and Cu alloy surfaces that are amenable to high resolution scanning probe studies, X-ray photoelectron spectroscopy, and chemical analysis of adsorbate binding, spillover and reaction [1-10].

Continuing our work on bimetallics, by studying Co nanoparticles grown on Cu we discovered a previously unreported, but catalytically relevant, high coverage phase of hydrogen that could only be formed by virtue of Co/Cu interface sites [4, 5, 10]. We also discovered that adsorbed CO and H, the two reactants in Fischer-Tropsch Synthesis, are segregated on Co nanoparticle surfaces [6]. CO adsorbs on the Co nanoparticles via spillover from the Cu, and we found that by depositing CO onto preadsorbed H layers, the CO is able to induce a two-dimensional phase compression of H, providing the first direct visualization of this long proposed phenomenon in a catalytically relevant system.

These types of alloy systems allow us to address previously unobtainable structures, densities and phases of hydrogen due to the limitations of single crystal work in ultra-high vacuum. By understanding the energy landscape for hydrogen activation, adsorption and spillover we have been able to generate catalytically relevant high coverage hydrogen phases, design efficient and selective hydrogenation sites, and trap hydrogen on surfaces beyond its normal desorption point yielding novel catalytic intermediates.

### **Recent Progress:**

#### **Towards a Molecular Level Understanding of Fischer-Tropsch Chemistry on Cobalt Nanoparticles**

The formation of carbon-carbon bonds is one of the most important synthetic processes, as it has a wide range of pathways and applications including in Fischer-Tropsch synthesis. Furthermore, the Ullmann reaction, the coupling of two aryl halides over a Cu catalyst, is one of the oldest transition metal-catalysed reactions for forming C-C bonds between aryl groups, but it is notorious for its harsh conditions and intolerance to certain functionalities. As such, gentler more reliable pathways have been developed for forming C-C bonds that use palladium or nickel as the catalyst. These metals have found much popularity in the synthetic community and are widely used as the catalyst of choice in reactions such as the Suzuki, Stille, Heck, and Negishi cross couplings. However, while these metals can be used at the commercial scale, their cost (Pd) or toxicity (Ni) impose limitations on their use.

Following the recent interest in Co catalysts for solution-phase coupling reactions, we have used low temperature scanning tunnelling microscopy (STM), to track the reaction of both bromobenzene and benzylbromide on Co surfaces. This allows us to interrogate many fundamental aspects of forming  $sp^2$ - $sp^2$  and  $sp^3$ - $sp^3$  C-C bonds. Co nanoparticles grown on Cu(111) allow us to visualize key steps in the coupling of these molecules from intact surface-bound starting materials, through dissociated intermediates, to products on Co surfaces. Using high resolution STM we have identified the intermediates in the Co-catalysed surface coupling reactions of bromobenzene and benzylbromide (Figure 1.). The intermediate structures consist of phenyl or benzyl groups bound directly to the metallic Co surface, which is in contrast to the organometallic intermediate previously observed for the surface Ullmann coupling of bromobenzene on Cu(111). This difference suggests that Co and Cu metal catalyse the C-C coupling via different mechanisms and provides insight as to why Co catalysts do not require the same high temperatures as traditional Cu catalysts. We also report the selective low temperature formation of biphenyl from bromobenzene. Our results on well-defined metallic Co surfaces indicate that heterogeneous Co nanoparticle catalysts are interesting candidates to explore for the development of new efficient and selective C-C coupling procedures.

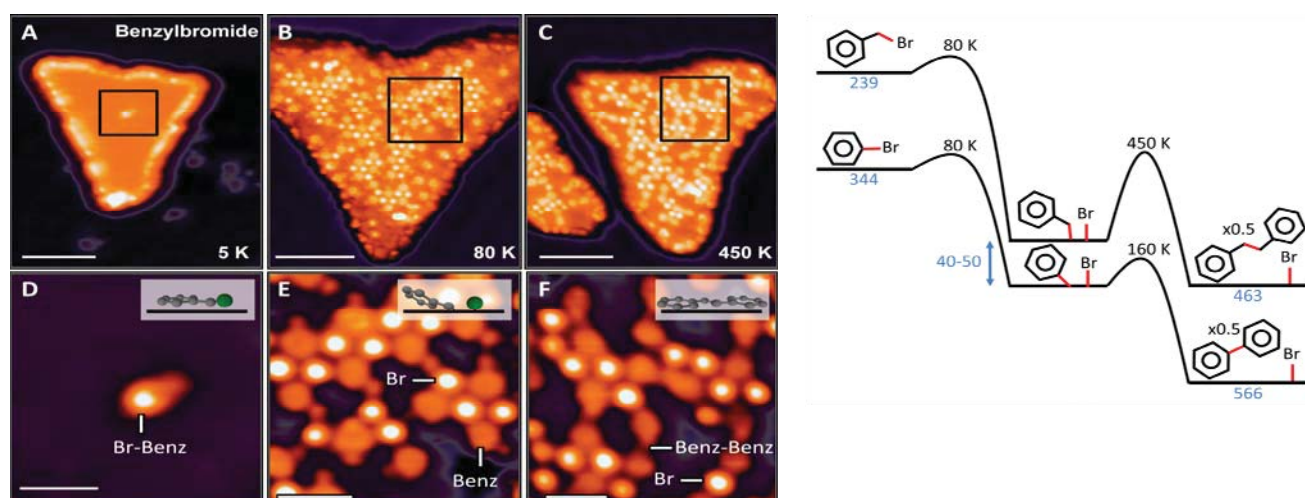


**Figure 1.** Nanoscale insight into C-C coupling on cobalt nanoparticles. STM images showing the reaction of benzylbromide on Co nanoparticles. The bottom images (Scale bars = 1 nm) are insets of the top images (Scale bars = 4 nm), as indicated by the black boxes. The schematics in the top right of D, E, and F indicate the state of the adsorbed species. A.) and D.) Images of benzylbromide as-deposited on the Co/Cu(111) surface. B.) and E.) After an 80 K anneal, the benzylbromide dissociates into Br atoms and benzyl species. C.) and F.) The molecules couple to form bibenzyl on the Co surface after a 450 K anneal. The right hand panel shows energy diagrams of the coupling of benzylbromide to bibenzyl and bromobenzene to biphenyl. BDEs (blue) are given in units of kJ/mol and refer to the bonds highlighted in red.

### Squeezing and Stretching Pd thin films: a High-resolution STM study of Pd/Au(111) and Pd/Cu(111) Bimetallics

Due to the high cost of Pd, many groups have also explored more inexpensive alternatives to pure Pd, such as bimetallic Pd alloys, ultra-thin Pd films, and single atom alloys, as that these alternatives use

smaller amounts of the active element. Many surface and near surface Pd alloys were shown to possess higher activity and selectivity than pure Pd or the supporting metals for various film thicknesses from the millimeter-scale (e.g. Pd membranes) to the nanometer-scale (e.g. clusters and isolated Pd atoms). In addition to modification of electronic states, thin films exhibit unique topographic structures, such as moiré patterns and periodic dislocation networks, which relieve strain and can organize nanostructure arrays. Both superstructures result from a mismatch between the lattice constant of the film and the underlying metal substrate, except in unique cases where dislocation networks are determined by the interface energy. In the case of a moiré pattern, the mismatch manifests as a superstructure resulting from the periodic shift in adsorption site of the surface atoms. This makes thin films interesting systems to study the deviation of lattice constants from the pure metal, the effect on the *d*-band center, and how adsorption and reaction properties are altered.

By carefully measuring moiré patterns, creating simple structural models, and examining a probe molecule's interaction with the surface, we have elucidated the structure of the Pd/Cu(111) and Pd/Au(111) layer on layer systems. The observed contraction of the Pd lattice on Cu and expansion of the Pd lattice on Au indicates that strain in thin film bimetallic alloys can be intentionally tuned via the lattice constant of the supporting metal. Our results for these systems support DFT calculated trends of *d*-band shifts which suggest that tuning the lattice constant of a metallic film via a choice in substrate metal can be a useful way to control the reactivity of the alloy's surface. We directly observe the diffusion of atomic H on these strained films and correlate diffusion barriers with compressive/expansive strain. These insights, obtained using surface science techniques, provide an important foundation for the directed design of better bimetallic thin film or nanoparticle catalysts. Furthermore, compared to Pd(111) single crystals which, even after months of UHV cleaning still contain defects and impurities, these films offer a simple, high purity system with which to study Pd surface chemistry.

### **Future Plans:**

Our approach offers the opportunity to study the atomic-scale composition and structure of active sites and relate this information to their ability to activate, spillover and react industrially relevant small molecules. We will use these guiding principles to examine catalytic metal alloys from a new perspective and discover new processes. Future work is aimed at:

- 1) Extending our single atom alloy (SAA) approach to understanding hydrogenations on PdAg and PdAu
- 2) Using the “molecular cork” effect to control the activity and selectivity of surface catalyzed hydrogenation reactions
- 3) Elucidating the optimal atomic geometry of AgCu for oxygen activation

These model systems will allow us a fundamental understanding of many important elementary steps in surface catalyzed chemistry. The atomic-scale structure of the active sites in metal alloy catalysts is hard, if not impossible, to characterize by conventional methods. Our surface science approach that includes scanning probes offers methods to characterize the structure, stoichiometry, and reactivity, and provides an atomic-scale view of local structure and adsorbate binding/diffusion. However, when working on well-defined model systems it is imperative to work with the same elements, structures and ensembles that are present in the real catalysts under working conditions. Implementation of the SAA approach to the design of real catalysts requires consideration of the effect of higher reaction

temperature and pressure, which may cause the minority active element to segregate into the bulk of the more inert host and hence cause a loss in activity. Understanding and controlling surface segregation under reaction conditions will also be crucial for the efficient use of costly elements of the alloy by keeping them in active sites on or near the surface. Promisingly, there are now many experimental and theoretical examples of metal alloys under realistic conditions in which the more active element is stabilized at the surface by adsorbates.

All our proposed systems have been chosen with these considerations in mind. Active elements will be added/alloyed into more inert Cu, Ag, and Au surfaces. The (111) facet is chosen, as it is often the most commonly exposed facet on metal nanoparticles. While minority structures like step edges or defects often dominate the reactivity of metal surfaces, the chemistry of our alloyed systems is expected to be driven at the added metal atom sites and this will be checked with control experiments of the reactivity before and after alloying.

### DOE-Sponsored Research Publications in the Last Two Years:

- 1) "Squeezing and Stretching Pd Thin Films: A High-Resolution STM Study of Pd/Au(111) and Pd/Cu(111) Bimetallics" M. E. Blecher, E. A. Lewis, A. Pronschinske, C. J. Murphy, M. F. G. Mattera, M. L. Liriano, and E. C. H. Sykes - *Surface Science* 2015 - *Accepted*
- 2) "Enhancement of Low-Energy Electron Emission in 2D Radioactive Films" A. Pronschinske, P. Pedevilla, C. J. Murphy, E. A. Lewis, F. R. Lucci, G. Brown, G. Pappas, A. Michaelides, and E. C. H. Sykes - *Nature Materials* 2015, *14*, 904-907
- 3) "Spin Modified Catalysis" R. Choudhary, P. Manchanda, A. Enders, B. Balamurugan, A. Kashyap, D. J. Sellmyer, E. C. H. Sykes, and R. Skomski - *The Journal of Applied Physics* 2015, *117*, 17D720
- 4) "Nanoscale Insight into C-C Coupling on Cobalt Nanoparticles" E. A. Lewis, C. J. Murphy, A. Pronschinske, M. L. Liriano, and E. C. H. Sykes - *Chemical Communications* 2014, *50*, 10035-10037
- 5) "Hydrogen Dissociation, Spillover, and Desorption from Cu-Supported Co Nanoparticles" E. A. Lewis, M. D. Marcinkowski, C. J. Murphy, M. L. Liriano, and E. C. H. Sykes - *The Journal of Physical Chemistry Letters* 2014, *5*, 3380-3385
- 6) "Segregation of Fischer-Tropsch Reactants on Cobalt Nanoparticle Surfaces" E. A. Lewis, D. Le, A. D. Jewell, C. J. Murphy, T. S. Rahman, and E. C. H. Sykes - *Chemical Communications* 2014, *50*, 6537-6539
- 7) "Significant Quantum Effects in Hydrogen Activation" G. Kyriakou, E. R. M. Davidson, G. Peng, L. T. Roling, S. Singh, M. B. Boucher, M. D. Marcinkowski, M. Mavrikakis, A. Michaelides, and E. C. H. Sykes - *ACS Nano* 2014, *8*, 4827-4835
- 8) "Atomic-Scale Insight into the Formation, Mobility and Reaction of Ullmann Coupling Intermediates" E. A. Lewis, C. J. Murphy, M. L. Liriano, and E. C. H. Sykes - *Chemical Communications* 2014, *50*, 1006-1008
- 9) "Controlling the Spillover Pathway with the Molecular Cork Effect" M. D. Marcinkowski, A. D. Jewell, M. Stamatakis, M. B. Boucher, E. A. Lewis, C. J. Murphy, G. Kyriakou and E. C. H. Sykes - *Nature Materials*, 2013, *12*, 523-528
- 10) "Visualization of Compression and Spillover in a Coadsorbed System: Syngas on Cobalt Nanoparticles" E. A. Lewis, D. Le, A. D. Jewell, C. J. Murphy, T. S. Rahman and E. C. H. Sykes - *ACS Nano*, 2013, *7*, 4384-4392

## Solvation Dynamics in Nanoconfined and Interfacial Liquids

Ward H. Thompson

*Department of Chemistry, University of Kansas, Lawrence, KS 66045*

*wthompson@ku.edu*

### Program Scope

There is currently significant interest in nanostructured materials that can confine liquids in nanoscale pores, due to both the appearance of new fundamental phenomena in these systems and their wide range of potential applications, including catalysis, sensing, separations, electrochemistry, and optical materials. However, the design principles are still lacking for the development of such mesoporous ( $2 \text{ nm} \leq \text{diameter} \leq 50 \text{ nm}$ ) materials for practical applications that take advantage of their large surface area-to-volume ratio and their high degree of tunability through pore size, shape, roughness, and chemical functionality. At the same time, this gap points to the need to improve our fundamental understanding of how complex liquid dynamics can arise from nanoscale confinement and vary strongly with the confining environment properties.

We are addressing some of the outstanding questions regarding these nanoconfined liquid dynamics and the implications for chemical reactions – *i.e.*, *How does a chemical reaction occur differently in a nanoconfined solvent than in a bulk solvent?* – by using solvation dynamics as a basis. Solvation dynamics is closely related to the reaction coordinate for charge transfer reactions such as electron or proton transfer reactions and is often dramatically affected by nanoconfinement.<sup>1</sup>

### Recent Progress & Future Plans

#### *Solvation Dynamics at Planar and Confining Interfaces.*

We have continued our work on solvation dynamics in confining silica frameworks and extended it to behavior at planar silica interfaces. It is by now well established that liquid layering and orientational ordering at interfaces produces an underlying free energy surface that affects the behavior of solutes, *e.g.* reactants or chromophores. We have previously proposed that this should affect chemical reactivity and spectroscopy. We have examined these effects in three ways.

First, we have carried out equilibrium simulations using replica exchange MD of the C153 dye molecule dissolved in ethanol confined within  $\sim 2.4$  diameter hydrophilic and hydrophobic amorphous silica pores.<sup>2,3</sup> This system is similar to those used in measurements by Baumann *et al.*<sup>4</sup> Our simulations for the electronic ground- and excited-states of C153 yielded a number of interesting results.<sup>5,6</sup> Foremost among these, we found that the position distribution of the molecule depends on its charge distribution (which changes upon excitation), which can also be demonstrated with a simple derivation that gives some insight into the generality of this result.<sup>6</sup> Hydrogen-bonding and non-specific solvation play competing roles, with the former dominating for the low dipole moment ground-state molecule and the latter more important for the more polar excited-state C153. In both cases, entropy shapes the position distribution but it does so in ways that are not sensitive to the solute charge distribution.

Second, we have completed non-equilibrium simulations of the time-dependent fluorescence signal of C153 initiated from the replica exchange MD sampling to ensure initial conditions representative of the ground-state distribution of positions. The results for the dynamic Stokes shift,  $S(t) = [E_{fl}(t) - E_{fl}(\infty)]/[E_{fl}(0) - E_{fl}(\infty)]$  where  $E_{fl}$  is the fluorescence energy, are shown in Fig. 1 along with a tri-exponential fit that gives the longest timescale (the one most strongly influenced by confinement) as 86 ps, in good agreement with the 102.7 ps reported by Baumann *et al.*<sup>4</sup> We are currently analyzing the nonequilibrium trajectories to develop a molecular-level picture of the origin of these slow dynamics.

Third, we are carrying out simulations of liquids at planar silica interfaces. We have developed atomistic models of amorphous silica interfaces for simulations with various liquids, particularly methanol, ethanol, and water. For testing in the initial stages, the silica slab thickness and roughness has been varied. The latter is accomplished by using different cooling rates to arrive at the solid silica structure from a high-temperature, molten silica simulation. The surface is subsequently functionalized with hydroxyl groups to model a hydrophilic surface.<sup>2,3</sup> Simulations of the methanol/silica interface are completed and being analyzed. MD simulations to investigate the orientation and second-harmonic generation spectra of the solute *p*-nitroanisole (pNA) at the methanol/silica interface<sup>8</sup> are being initiated, using a model for pNA we have developed from electronic structure calculations and existing force fields.

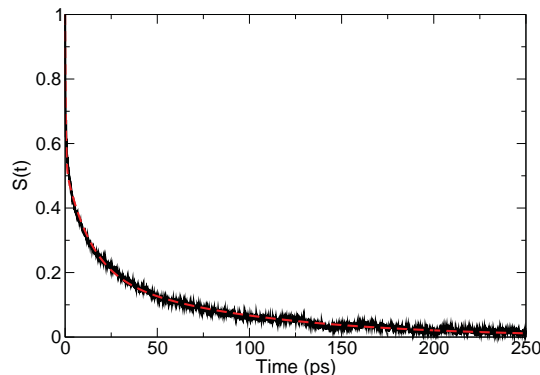


Figure 1:  $S(t)$  for C153 in ethanol confined inside a  $\sim 2.4$  nm diameter hydrophilic silica pore (black curve) from 5000 nonequilibrium trajectories along with a tri-exponential fit (dashed red line).

#### *Dynamics of Nanoconfined Water.*

In previous simulations of water confined in nanoscale silica pores we observed non-exponential (apparently power-law) dynamics in the OH reorientation.<sup>7</sup> To understand this behavior, we carried out a detailed mechanistic investigation of the hydrogen-bond (H-bond) exchanges, “jumps,” that underlie OH reorientation dynamics.<sup>9</sup> We were able to determine the site specific jump times of the interfacial water and analyze their origins. The results revealed that two entropic effects represent the dominant contributions to the site-dependent jump times: 1) volume excluded by the pore atoms prevents the approach of new H-bond acceptors required for a jump such that water molecules in small pits have considerably slowed dynamics relative to those near protrusions into the pore, and 2) the arrangement of the H-bond network near the pore surface is constrained such that breaking of some H-bonds is entropically disfavored because the H-bond extension reduces the number of ways to arrange the waters in the network. Several other factors were considered and found to be minor, including interestingly, variations in the activation energy for H-bond breaking.

We have recently simulated the vibrational (IR, Raman, and 2D-IR photon echo) spectra of water (specifically HOD in D<sub>2</sub>O) confined in a  $\sim 2.4$  nm diameter silica pore. The OH frequency is

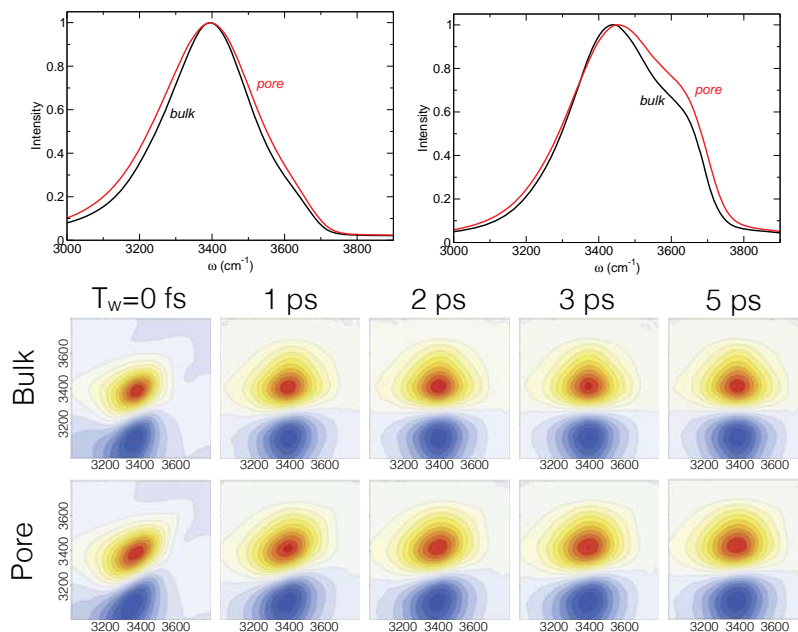


Figure 2: Simulated IR (top left), Raman (top right), and 2D-IR photon echo (bottom) spectra of HOD in  $D_2O$  in the bulk liquid and confined in a 2.4 nm silica pore.

obtained using the empirical map approach of Skinner and co-workers<sup>10</sup> Our simulations indicate that confined water exhibits an IR spectrum that is only slightly perturbed from the bulk while the Raman spectrum is principally changed by the addition of a larger shoulder at higher frequencies, as shown in Fig. 2. These results are in general agreement with the few reported vibrational spectra of water confined in silica pores.<sup>11,12</sup> The differences between the effects of confinement on the simulated IR and Raman spectra are due to weaker hydrogen-bonding near the silica interface that leads to blue-shifted OH frequencies with smaller IR but similar Raman intensities (due to the differences in non-Condon effects on the transition dipole versus the transition polarizability). The 2D-IR spectra – which, as can be seen in Fig. 2, show modest effects due to slower spectral dynamics – have not yet been reported to our knowledge and our simulations represent the first prediction of their behavior.

We have similarly studied the reorientational and H-bond dynamics along with the vibrational spectroscopy of water confined within phospholipid reverse micelles in collaboration with Prof. Damien Laage. These systems provide an interesting comparison to the more widely studied AOT reverse micelles as well as the nanoscale silica pores discussed above.

#### *Influence of Steric Bulk Arrangements on the Reorientational Dynamics of Alcohols.*

We recently completed an examination of the OH reorientation and H-bond dynamics of isomeric butanols.<sup>13</sup> The aim was to understand how the dynamics in alcohols vary with the arrangement of the steric bulk, independent of the amount of steric bulk (which we are also studying). Our analysis is in the context of the extended jump model,<sup>14</sup> which was found to describe OH reorientation in butanols very well. The analysis for OH reorientation in alcohols is challenging as multiple factors

are found to be at play. The isomeric butanols are no exception as internal energy, entropy, and dynamical effects (*e.g.*, transition state recrossing and attempt frequencies) are all found to be important. By separately calculating or estimating each of these factors we are able to reproduce the trends in the H-bond jump times and the associated activation energies. A simple model based on the liquid structure described in the O-O radial distribution functions was found to accurately describe the internal energy contributions. These results point to the need for additional work on understanding the changes in transition state recrossing factors with alcohol structure; it is not yet clear if this is a fundamental effect or evidence of the need for improved reaction coordinates and we are continuing to investigate this issue.

## References

- [1] W.H. Thompson, *Annu. Rev. Phys. Chem.* **62**, 599-619 (2011).
- [2] T.S. Gulmen and W.H. Thompson, in *Dynamics in Small Confining Systems VIII*, edited by J.T. Fourkas, P. Levitz, R. Overney, M. Urbakh (Mater. Res. Soc. Symp. Proc. **899E**, Warrendale, PA, 2005), 0899-N06-05.
- [3] T.S. Gulmen and W.H. Thompson, *Langmuir* **22**, 10919-10923 (2006).
- [4] R. Baumann, C. Ferrante, E. Kneuper, F.-W. Deeg, and C. Bräuchle, *J. Phys. Chem. A* **107**, 2422-2430 (2003).
- [5] †J.A. Harvey and W.H. Thompson, *J. Phys. Chem. B* **119**, 9150-9159 (2015). “Thermodynamic Driving Forces for Dye Molecule Position and Orientation in Nanoconfined Solvents”
- [6] †J.A. Harvey and W.H. Thompson, *J. Chem. Phys.* **143**, 044701 (2015). “Solute Location in a Nanoconfined Liquid Depends on Charge Distribution”
- [7] D. Laage and W.H. Thompson, *J. Chem. Phys.* **136**, 044513 (2012).
- [8] R.A. Siler and R.A. Walker, *J. Phys. Chem. C* **115**, 9637-9643 (2011).
- [9] †A.C. Fogarty, E. Duboué-Dijon, D. Laage, and W.H. Thompson, *J. Chem. Phys.* **141**, 18C523 (2014). “Origins of the Non-exponential Reorientation Dynamics of Nanoconfined Water”
- [10] B.M. Auer and J.L. Skinner, *J. Chem. Phys.* **128**, 224511 (2008).
- [11] R. Musat, J.P. Renault, M. Candelaresi, D.J. Palmer, D. S. Le Caër, R. Righini, and S. Pommeret, *S. Angew. Chem. Intl. Ed.* **47**, 8033-8035 (2008).
- [12] X.F. Huang, Q. Wang, X.X. Liu, S.H. Yang, C.X. Li, G. Sun, L.Q. Pan, K.Q. Lu, *J. Phys. Chem. C* **113**, 18768-18771 (2009).
- [13] †O.O. Mesele, A.A. Vartia, D. Laage, and W.H. Thompson, *J. Phys. Chem. B*, Just Accepted (2015). “Reorientation of Isomeric Butanols: Exploring the Role of Steric Bulk on Hydrogen Bond Dynamics”
- [14] D. Laage and J.T. Hynes, *Science* **311**, 832-835 (2006).

†DOE-sponsored publication in past 2 years

## Imaging Interfacial Electric Fields on Ultrafast Timescales

William A. Tisdale

Department of Chemical Engineering

Massachusetts Institute of Technology, Cambridge, MA 02139

tisdale@mit.edu

### Program Scope

The objective of this project is to explore a novel methodology for visualization of ultrafast electronic processes at interfaces. The method, which is based on optical stimulation, builds upon previous success using spontaneous second-order nonlinear optical probes to track the temporal evolution of interfacial electric fields resulting from charge separation across an interface. A goal is to speed signal acquisition by orders of magnitude so that laser scanning ultrafast microscopy becomes feasible. The ultimate aim is to generate movies of interfacial electronic phenomena occurring on femtosecond timescales and submicron length scales, thereby informing our understanding of disorder, heterogeneity, and morphology, and how these factors affect ensemble behavior in photovoltaic, electrochemical, and optoelectronic systems.

### Recent Progress I: Stimulated SHG

Second harmonic generation (SHG) is a second order nonlinear optical process in which two photons at a fundamental frequency  $\omega$  combine to form a single photon at frequency  $2\omega$ . Like any even-ordered nonlinear optical process, SHG is dipole-forbidden in the bulk of centrosymmetric media such as many crystal structures, amorphous solids, liquids, and gases; observed SHG signals in these media originate from materials' interfaces. SHG experiments selectively probe interfaces and are sensitive to the interfacial environment. SHG is an inefficient process, and high incident fundamental fluences are necessary to produce measurable signals. The incident fundamental fluence is often limited by the sample's optical damage threshold, and signals are usually very weak. Even with an optimal detection system, the signal to noise ratio (SNR) in SHG experiments is limited by the presence of shot noise. It is desirable to amplify the weak spontaneous SHG signal allowing high quality measurements to be taken in a shorter period of time. Such an advance would enable SHG measurements with time and spatial resolution, which are currently infeasible due to intractably long acquisition times resulting from spontaneous SHG's notoriously low SNR. Recently, we successfully demonstrated the amplification of weak spontaneous SHG signals by optical stimulation (Goodman & Tisdale, *Phys. Rev. Lett.* [2015]).<sup>2</sup>

To assess the feasibility of stimulated SHG, experiments were initially conducted in a model system,  $\beta$ -barium borate (BBO). Experiments with BBO revealed that stimulated SHG is well-modelled by a wave-mixing formalism first described by Armstrong *et al.* in 1962. This model describes plane waves at the fundamental and second harmonic frequencies propagating through a nonlinear medium. The fundamental field generates a

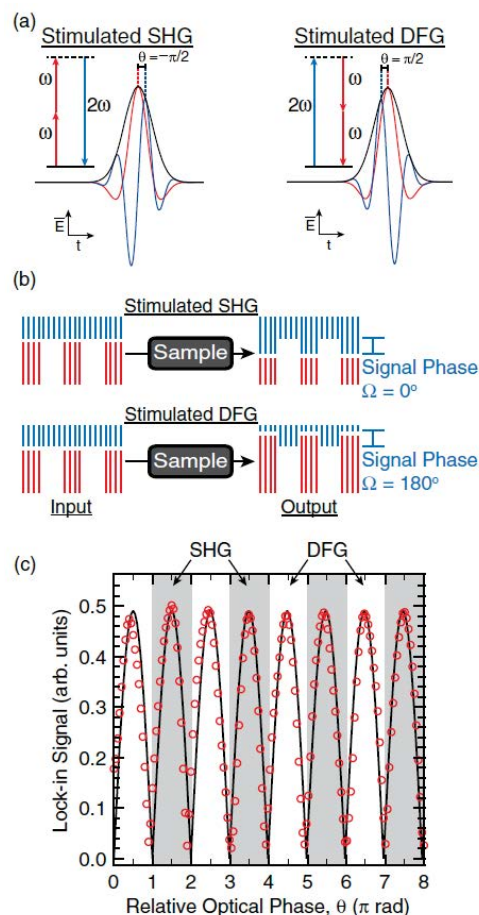


**Figure 1** Effect of optical phase on stimulated SHG processes. From Goodman & Tisdale, *Phys Rev Lett* (2015).<sup>2</sup>

nonlinear polarization that radiates the second harmonic, acting as a nonlinear source term in the wave equation for the second harmonic field. As the fields add coherently, energy is transferred between them.

In experiments where the interaction length is short, or the sample is weakly nonlinear, the generated signal is described by the derivative,  $dA_1^2/dz = 2A_1 dA_1/dz$ , which is proportional to  $A_1^2 A_2$ . The linear dependence of the signal on the second harmonic field amplitude represents the stimulating effect. In the absence of an applied stimulating field, spontaneous SHG still occurs at a low rate in the presence of nonzero vacuum occupation of the stimulating field mode. Maximum enhancement due to stimulation is obtained when two photons at the fundamental frequency are available for every photon at the second harmonic frequency.

The relative optical phase  $\theta$  determines the nature of the nonlinear conversion. The  $\theta$  dependence of the nonlinear wave mixing formalism suggests the possibility of changing the direction of energy flow between the fundamental and second harmonic fields (Fig. 1). Though the stimulated SHG and DFG signals have similar magnitudes, they have the opposite lock-in signal phase  $\Omega$  relative to the modulation of the fundamental beam, as illustrated in Fig. 1(b). A stimulated SHG signal is in phase with the reference modulation, while a stimulated DFG signal is  $180^\circ$  out of phase. The relative optical phase of the two fields and, accordingly, the direction of energy flow between the fundamental and second harmonic can be finely controlled using a piezomounted mirror, as shown in Fig. 1(c).

To demonstrate the technique's utility, stimulated SHG signals were collected from bovine collagen I. Collagen I is a naturally abundant nonlinear material that is frequently the target of bioimaging studies. SHG imaging of collagen fibrils can distinguish diseased and wild-type tissue morphologies and has recently been used to determine single fibril diameters smaller than the Abbe limit. Spontaneous and stimulated SHG signals from collagen I were recorded as a function of incident fundamental power. The results are plotted in Fig. 2. The spontaneous signal grows quadratically with incident power, while the stimulated signal increases linearly. Even at very small incident stimulating fluences ( $2.7 \text{ nJ/cm}^2$ ), the signal amplification exceeds 4 orders of magnitude.

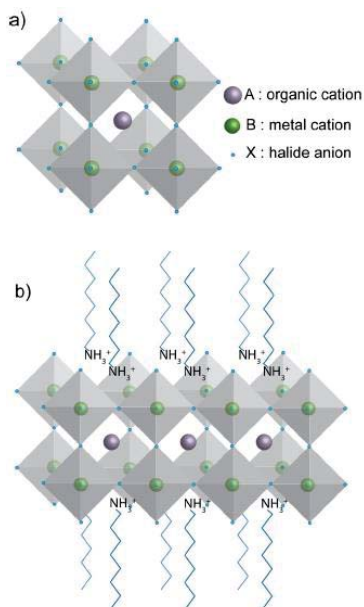


**Figure 3** Schematic illustration of (a) a perovskite unit cell and (b) 2D perovskite nanoplatelets with  $n = 1$  (one unit cell thick).

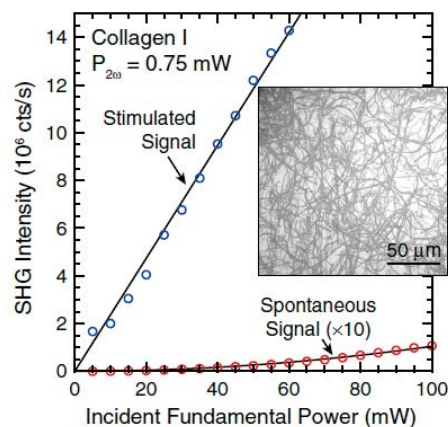


**Figure 2** Demonstration of stimulated SHG in collagen I. At low incident powers, stimulated SHG produces more than  $10^4$  times as many signal photons as spontaneous SHG. An optical micrograph of the collagen I sample is presented as an inset.

### Recent Progress II: Colloidal Organohalide Perovskite Nanoplatelets

Organometal halide perovskites are a promising platform for future photovoltaic technologies. These materials have an  $\text{ABX}_3$  structure where A is an organic cation (e.g.  $\text{CH}_3\text{NH}_3^+$ ), B is a metal cation (e.g.  $\text{Pb}^{2+}$ ) and X is a halide anion (e.g.  $\text{Cl}^-$ ,  $\text{Br}^-$ ,  $\text{I}^-$ ). The electronic and optical properties of organometal halide perovskites are strongly dependent on the nature of the constituent ions. Doping with different metal ( $\text{AB}_n\text{B}'_{1-n}\text{X}_3$ ) and halide ( $\text{ABX}_n\text{X}'_{3-n}$ ) units offers further control over their optoelectronic properties. Additionally, dimensionality may be used to tune the electronic and optical properties.

Although the effects of reduced dimensionality and quantum confinement have been extensively investigated in conventional semiconductors, the extent of theoretical and experimental studies in low-dimensional perovskite systems is comparatively limited. A family of 2D layered perovskites can be described

by  $(\text{RNH}_3)_2[\text{CH}_3\text{NH}_3\text{PbX}_3]_n\text{PbX}_4$ , where R is a long chain alkyl group (e.g. octyl, octadecyl) and  $n$  corresponds to the number of perovskite unit cells (Figure 1). For example,  $n = 1, 2$  and  $3$  correspond to layered perovskites that are one, two and three unit cells thick, respectively (Fig. 3), and  $n = \infty$  corresponds to the bulk perovskite phase.

While most work on the photovoltaic applications of organohalide perovskites has focused on thin films of three-dimensional (3D) bulk materials supported on planar and mesoporous substrates, 2D hybrid layered perovskites have recently been shown to exhibit promise for light-emitting applications, with bromide-based white-light emitters reaching photoluminescence (PL) efficiencies of up to 9%. Iodide-based 2D perovskite nanoplatelets grown *via* chemical vapor deposition showed enhanced charge carrier diffusion relative to polycrystalline films obtained by spin-coating. However, the 2D perovskite materials investigated in each of these previous studies had out-of-plane dimensions too large for quantum size effects to be observed, and were not stable in solution, thereby limiting their applicability.

Recently, we prepared colloidal nanocrystals and 2D nanoplatelets of methylammonium lead bromide ( $\text{MAPbBr}_3$ ) perovskites and identified the optical signatures of their excitonic states using a combination of optical spectroscopy and electron microscopy (Tyagi, Arveson, and Tisdale, *J Phys Chem Lett* [2015]).<sup>3</sup> We find that the excitonic features that were previously assigned to quantum-confined excitons in  $\text{MAPbBr}_3$  are in fact characteristic of bulk 3D crystals. Moreover, we find that colloidal synthesis methods can yield a mixture of perovskite nanostructures with different morphologies and optical absorption and emission spectra, including nanoscale particles and 2D nanoplatelets (Fig. 3). Upon further purification of the reaction product, we obtain single unit cell thick ( $n = 1$ ) crystalline 2D perovskite nanoplatelets exhibiting clear evidence of quantum-confinement with a sharp excitonic absorption 0.5 eV blue-shifted from that of the 3D bulk perovskite phase (Fig. 4). The thickness dependent absorption and emission spectra of these colloidal nanoplatelets closely resemble those of solid-phase layered perovskites.

#### Future Plans

*Stimulated SHG.* As in heterodyne SHG, potential signal-to-noise (SNR) gains from the larger signal amplitude are offset by the large shot noise in the stimulating field. Both the signal power and the noise power grow with the square root of the intensity of the stimulating fields. To achieve background-free stimulated enhancements and SNR gains beyond the heterodyne limit, we are pursuing a non-collinear geometry. Concurrently, we are implementing a high-frequency phase modulation scheme to overcome phase noise in the measurement. Ultimately, the goal is to implement the technique in a fast laser scanning optical microscope.

#### CPIMS-Supported Publications (2014-2015)

1. M.C. Weidman, M.E. Beck, R.S. Hoffman, F. Prins, W.A. Tisdale; "Monodisperse, Air-Stable PbS Nanocrystals *via* Precursor Stoichiometry Control," *ACS Nano* **8**, 6363-6371 (2014).
2. A.J. Goodman & W.A. Tisdale; "Enhancement of Second-Order Nonlinear-Optical Signals by Optical Stimulation," *Phys. Rev. Lett.* **114**, 183902 (2015).
3. P. Tyagi, S.M. Arveson, W.A. Tisdale; "Colloidal Organohalide Perovskite Nanoplatelets Exhibiting Quantum Confinement," *J. Phys. Chem. Lett.* **6**, 1911-1916 (2015).

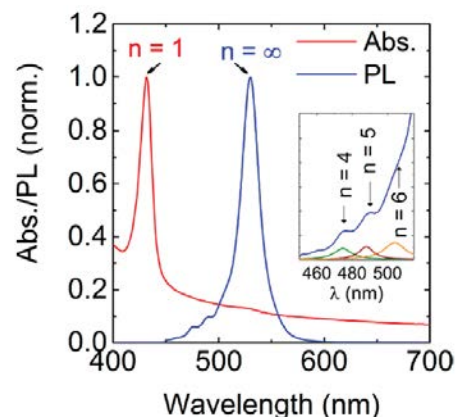


**Figure 4** Absorption (red) and PL (blue) spectra of the purified  $\text{MAPbBr}_3$  nanoplatelet solution. The inset shows an enlarged view of the blue shoulder of the emission spectrum, revealing discrete peaks corresponding to nanoplatelets with different thicknesses ( $n$ : number of layered unit cells).

## Structural Dynamics in Complex Liquids Studied with Multidimensional Vibrational Spectroscopy

Andrei Tokmakoff

*Department of Chemistry, James Franck Institute, and Institute for Biophysical Dynamics  
The University of Chicago, Chicago, IL 60637  
E-mail: tokmakoff@uchicago.edu*

The physical properties of water and aqueous solutions are inextricably linked with efforts to develop new sustainable energy sources. Energy conversion, storage, and transduction processes, particularly those that occur in biology and soft matter, make use of water for the purpose of storing and moving charge. Water's unique physical and chemical properties depend on the ability of water molecules to participate in up to four hydrogen bonds, and the rapid fluctuations and ultrafast energy dissipation of its hydrogen-bonded networks. The goal of our research is a fundamental description of the properties of water at a molecular level, and how it participates in proton transport in aqueous media. Our work over the course of the past year can be divided into four areas: (1) the generation of short pulses of broadband infrared light (BBIR) and use in two-dimensional spectroscopy (2D IR); (2) the investigation of the spectroscopy and transport of excess protons in water; and (3) the study of aqueous hydroxide to describe the interaction of the ion and water and the dynamics of proton transfer, and (4) the coupled motion of water and its hydrogen-bonding solutes.

All of the experimental studies of water and aqueous solutions that we have published during the past year have been enabled by our development of a new ultrafast infrared light source that allows unprecedented access to the study of dynamical intermolecular interactions. Our newest spectrometer uses a laser plasma source to generate coherent pulses of broadband infrared light that are shorter than 70 fs and have a spectrum spanning the entire mid-IR vibrational spectrum, from  $3800\text{ cm}^{-1}$  to  $<1000\text{ cm}^{-1}$ . This source is integrated as a probe pulse in ultrafast pump-probe and 2D IR experiments. In our 2DIR spectrometer, a pulse pair of two 45 fs pulses from a homebuilt OPA source, centered between  $3000\text{--}3500\text{ cm}^{-1}$ , vibrationally excites the system and the subsequent response is studied using the BBIR as a probe. This capability allows us to correlate the vibrational OH stretching motions in water to other molecular vibrations across the mid-IR. We have recently added an additional OPA based on difference frequency generation to provide femtosecond excitation between  $3000\text{--}1000\text{ cm}^{-1}$  in future studies. Our instrument now provides the opportunity to directly observe correlated motion of solute and solvent and energy flow throughout the vibrational infrared spectrum.

Adding strong acids to in water give rise to a continuum absorption in the mid-infrared that is largely featureless and spans over  $2000\text{ cm}^{-1}$ . This continuum is thought to be related to varying hydrogen bond configurations of the proton, ranging from a hydronium or Eigen complex to a Zundel complex. The large bandwidth of our BBIR probe pulse has afforded us the opportunity to study the dynamics of aqueous proton species that give rise to this band. Our recent 2D IR studies concentrated on describing the response from vibrational transitions within the proton continuum following O-H stretch excitation centered at  $\omega_1 = 3250\text{ cm}^{-1}$ . This pump frequency is thought to correspond to the flanking water vibrations of the Zundel species. Experiments as a function of acid concentration and waiting time allow us to identify the vibrations that arise from the excess proton. The broadband 2D IR spectra of hydrochloric acid show a highly inhomogeneous bleach of the stretch and a continuum-induced absorption that is much stronger than water. Additionally, there is strong coupling between the O-H stretch and bending motions, although the crosspeak features are more complex than for  $\text{H}_2\text{O}$ . The analysis of the bend crosspeak region between bend and stretch reveals two bleaches: one resembles the  $\text{H}_2\text{O}$  bend of bulk water and the other corresponds to the bend vibration of the Zundel complex flanking water molecules. A spectral decomposition of the

crosspeak region reveals that the proton-related bend vibration ( $1760\text{ cm}^{-1}$ ) is coupled to the strongly H-bonded O–H stretches at  $3200\text{ cm}^{-1}$ , whereas the bulk  $\text{H}_2\text{O}$  bend vibration ( $1660\text{ cm}^{-1}$ ) is coupled to the bulk water O–H stretches ( $\sim 3300\text{ cm}^{-1}$ ). The correlation of the stretch and bend frequencies of the proton crosspeak are in good agreement with the predictions for vibrational frequencies of the Zundel species.

Our analysis reveals that the Zundel stretch–bend cross peak blue-shifts along the excitation axis with increasing waiting time, asymptotically approaching the bulk water stretch excitation frequency. The shift reflects the growing probability of initially exciting the O–H stretch vibration of bulk water and detecting this excitation in the bending of a Zundel complex after waiting for a time  $\tau_2$ . A fit to the Zundel peak frequency in  $\omega_1$  as a function of  $\tau_2$  reveals that this shift occurs on a timescale of 480 fs. The spectral shifting could originate either from proton transport or vibrational excitation transfer. In the former case, the initially excited  $\text{H}_2\text{O}$  accepts a proton, becoming a Zundel complex, while in the latter, only vibrational energy is transferred between the two species as a result of strong vibrational coupling between bulk water and the Zundel bend. Since both processes can contribute, the 480 fs timescale sets a lower bound for the exchange time between bulk water molecules and the Zundel complex. Our ongoing experimental work is aimed at studying spectral regions associated with Eigen complexes, improving vibrational assignments to features within the continuum, and using excitation and probing throughout the IR to follow the ultrafast exchange of proton structures.

The interpretation of our data is tied to accurate assignments of the vibrational spectral features for different proton complexes. We are collaborating with Prof. Greg Voth (Univ. of Chicago) to assist in clarifying the relationships between atomic structures and IR spectra, drawing from his development of multi-state empirical valence bond (MS-EVB) models of proton transport in water for modeling vibrational spectra. These efforts are proceeding in three directions: (1) development of a new MS-EVB model that improves the treatment of OH stretching anharmonicity; (2) mixed quantum-classical modeling of the infrared spectrum of a fluctuating OH bond vibration participating in proton transfer; and (3) spectral calculations for clusters derived from snapshots of MS-EVB simulations.

Proton transport in aqueous alkali hydroxide solutions has been described in terms of proton transfer from water to hydroxide resulting in shifting of the  $\text{OH}^-$  unit in space combined with the interconversion between different solvated structures of the ion. As with excess protons, the linear IR spectra of aqueous hydroxides show a broad continuum absorption feature across the mid-IR region with a handful of distinguishable features. We have performed BB 2D IR experiments to probe the entire continuum absorption upon exciting OH stretching motion. Our first effort was to draw conclusions as to the origin of the continuum absorption and assign peaks in the spectrum to aqueous hydroxide complexes. Our analysis of 2D IR spectra using normal mode analysis of hydroxide clusters from an EVB simulation concludes that a peak at  $2850\text{ cm}^{-1}$  originates from the asymmetric ( $E$ ) vibration of the OH bonds of the water molecules solvating the ion, whereas a hidden band at  $3250\text{ cm}^{-1}$  comes from symmetric ( $A_1$ ) vibrations. A third band observed at  $2000\text{ cm}^{-1}$  remains unassigned, but likely involves bending vibrations of the complex. Our studies of the vibrational dynamics of these complexes following excitation of the O–H stretching vibrations of ion-bound water reveals vibrational energy dissipation into intermolecular motions of the liquid in  $< 1\text{ ps}$ . We have proposed a model for vibrationally non-adiabatic energy dissipation to describe this energy flow that occurs as fast as the liquid can move.

**DOE Supported Publications (2013-2015)**

1. “Experimental Evidence of Fermi Resonances in Isotopically Dilute Water from Ultrafast Broadband IR Spectroscopy,” Luigi De Marco, Krupa Ramasesha, and Andrei Tokmakoff, *Journal of Physical Chemistry B*, **117** (2013) 15319–15327.
2. “Water Vibrations have Strongly Mixed Intra- and Inter-Molecular Character,” Krupa Ramasesha, Luigi De Marco, Aritra Mandal, and Andrei Tokmakoff, *Nature Chemistry*, (2013) **5** (2013) 935–940.
3. “Local and Collective Reaction Coordinates in the Transport of the Aqueous Hydroxide Ion,” Sean T. Roberts, Aritra Mandal, and Andrei Tokmakoff, *Journal of Physical Chemistry B*, **118** (2014) 8062–8069.
4. “Collective Vibrations of Water-Solvated Hydroxide Ions Investigated with Broadband 2D IR Spectroscopy,” Aritra Mandal, Krupa Ramasesha, Luigi De Marco, and Andrei Tokmakoff, *Journal of Chemical Physics*, **140** (2014) 204508.
5. “Direct Observation of Intermolecular Interactions Mediated by Hydrogen Bonding,” Luigi De Marco, Martin Thämer, Mike Reppert, and Andrei Tokmakoff, *Journal of Chemical Physics*, **141** (2014) 034502.
6. “2D IR Spectroscopy of the excess proton in liquid water,” Martin Thämer, Luigi De Marco, Krupa Ramasesha, Aritra Mandal, Andrei Tokmakoff, *Science*, **350** (2015) 78-82.
7. “Vibrational Dynamics of Aqueous Hydroxide Solutions Probed using Broadband 2DIR Spectroscopy,” Aritra Mandal and Andrei Tokmakoff, *Journal of Chemical Physics*, in press.

## **The Role of Electronic Excitations on Chemical Reaction Dynamics at Metal, Semiconductor and Nanoparticle Surfaces**

John C. Tully

*Department of Chemistry, Yale University, 225 Prospect Street,*

*P. O. Box 208107, New Haven, CT, 06520-8107 USA*

john.tully@yale.edu

### **Program Scope**

Achieving enhanced control of the rates and molecular pathways of chemical reactions at the surfaces of metals, semiconductors and nanoparticles will have impact in many fields of science and engineering, including heterogeneous catalysis, photocatalysis, materials processing, corrosion, solar energy conversion and nanoscience. However, our current atomic-level understanding of chemical reactions at surfaces is incomplete and flawed. Conventional theories of chemical dynamics are based on the Born-Oppenheimer separation of electronic and nuclear motion. Even when describing dynamics at metal surfaces where it has long been recognized that the Born-Oppenheimer approximation is not valid, the conventional approach is still used, perhaps patched up by introducing friction to account for electron-hole pair excitations or curve crossings to account for electron transfer. There is growing experimental evidence that this is not adequate. We are examining the influence of electronic transitions on chemical reaction dynamics at metal and semiconductor surfaces. Our program includes the development of new theoretical and computational methods for nonadiabatic dynamics at surfaces, as well as the application of these methods to specific chemical systems of experimental attention. Our objective is not only to advance our ability to simulate experiments quantitatively, but also to construct the theoretical framework for understanding the underlying factors that govern molecular motion at surfaces and to aid in the conception of new experiments that most directly probe the critical issues.

### **Recent Progress**

#### ***Exact Potential Energy Surfaces for Nonadiabatic Dynamics***

An underlying goal of our research program is to develop a theoretical framework for simulating molecular dynamics subject to motion on multiple potential energy surfaces, i.e., nonadiabatic molecular dynamics. Of particular importance is practicality; for applications to large molecules, surfaces and condensed phases, it is critical that methods emerge that are not only accurate and predictive, but for which computational effort scales acceptably with the size of the system. This has motivated us in the past to develop mixed quantum-classical approaches such as Surface Hopping in which nuclear motion is treated by classical mechanics, but with forces that respond to nonadiabatic electronic transitions. Surface Hopping is quite practical and very widely used, but it has well-documented shortcomings that somewhat limit its applicability. Many workers have proposed extensions to Surface Hopping that address some of the limitations. An important example is the development, funded under this grant, of the Independent Electron Surface Hopping method that allows treatment of systems that exhibit a continuum of excited electronic states such as metal and semiconductor surfaces.

Over the past two years, we have embarked on a new approach to nonadiabatic dynamics that is fundamentally different from surface hopping. The starting point for the new approach is an Exact Factorization of the total wavefunction into electronic and nuclear factors (in contrast to

the approximate Born-Oppenheimer factorization). As shown by several workers, it is easy to demonstrate that this can be accomplished. Moreover, this results in a Schrödinger equation for nuclear motion that is governed by a single “exact” potential energy surface, an appealing property compared to the need to deal with multiple potential energy surfaces as with Surface Hopping. There are major challenges that must be overcome, however, before this approach can be turned into a useful method. Most obvious is associated with the complexity of the Schrödinger equations for the nuclear and electronic degrees of freedom, which are coupled and must somehow be solved together. Of equal importance, accurate solution of these equations must ultimately be equivalent to quantum mechanical evolution on multiple states, and will thereby be impractical for all but very small systems. Therefore approximate methods of solution must be sought, most likely addressing nuclear motion using classical mechanics.

Addressing these challenges will require a better understanding of the Exact Factorization approach, especially the exact potential energy surface that governs nuclear motion. We have pursued this by computing the exact potential energy curves for very simple model systems: two coupled electronic states and one nuclear degree of freedom. These models can be solved exactly by conventional multi-state quantum mechanical methods, and the exact potential energy curve can be extracted from the results. Our calculations verify that the Exact Factorization method does indeed reproduce the exact results. However, the exact potential energy curves that emerge often display severe energy, spatial and time dependences. It does not appear to be very easy to extract the kinds of insights that will be needed to suggest practical approximations.

In order to make progress, we have recently examined a simple model of nonadiabatic tunneling: two crossing diabatic potential curves with off-diagonal coupling. It has been observed previously for such a model that the transmission (tunneling) probability through the barrier is significantly lower than would be calculated for the same barrier within the adiabatic approximation, even for energies well below the energy of the adiabatic excited state. This can be relevant to proton transfer and proton coupled electron transfer processes. We have found that examination of the exact potential energy curve for this model sheds new light on this puzzling behavior, and reveals properties of the Exact Factorization scheme that are difficult to extract from previous applications. A key to our progress was to address the model within a time independent scattering formulation, thereby removing the time dependence of the exact potential energy curve. To summarize our results, at energies well below the barrier height, most of the incoming wave is reflected before it reaches the region of significant nonadiabatic coupling near the peak of the barrier. Nevertheless, the small fraction of the wavefunction that does tunnel must traverse the nonadiabatic region which provides an additional repulsive force, as exhibited by an increase in the barrier height in the exact potential energy curve. This increase results from the fact that the transition between the two diabatic states in this region lags, so the exact potential diverges slightly from the adiabatic potential. This divergence is sufficient to more than compensate for a decrease that occurs in the second derivative nonadiabatic coupling correction to the Born-Oppenheimer potential. Although the exact potential energy curve exhibits some high energy spikes that occur at approximate nodes of the nuclear wavefunction, these spikes have very little effect on the quantum mechanical scattering. They would be disastrous for classical mechanical motion, however, so procedures must be developed to remove them if we are to make progress toward a practical, classical-based dynamics approach.

### ***The Influence of Phase Transitions on Chemical Reaction Rates***

As we reported in our 2014 CPIMS Abstract, the experimental group of Elsa C. Y. Yan

(Yale University) measured the thermal rate of isomerization of the 11-cis retinyl chromophore in the visual pigment rhodopsin, in the absence of light. The motivation for this study was to put limits on the dark noise, i.e., the background signal that limits vision in dim light. In the course of this study they made a remarkable discovery: at temperatures between 52.0 and 64.6°C, the measured rate constants fit well to an Arrhenius straight line with, however, an unexpectedly large activation energy of  $114 \pm 8$  kcal/mol, much larger than the 60 kcal/mol photoactivation energy at 500 nm. Moreover, they obtained an unprecedentedly large prefactor of  $10^{72 \pm 5} \text{ s}^{-1}$ , about 45 orders of magnitude larger than any previously reported prefactor for a unimolecular reaction and 60 orders of magnitude larger than typical frequencies of molecular motions! At lower temperatures the measured Arrhenius parameters were found to be more normal:  $E_a = 22 \pm 2$  kcal/mol and  $A_{pref} = 10^{9 \pm 1} \text{ s}^{-1}$  in the range 37.0 – 44.5°C. These initial results were published in PNAS in 2014, with theoretical contributions supported by this grant. The key hypothesis presented in the first paper, supported by QM/MM calculations by the group of Victor Batista (Yale University), is that the reaction barrier is somewhat lower when the protein is melted than when the chromophore is more constrained in the folded state. This barrier lowering produces a driving force to lower the melting temperature when the system is constrained at the transition state. If the initial state is ordered and the transition state is partially or completely melted, according to transition state theory, there will be huge increases in both the enthalpy and entropy of activation. At lower temperatures where both the initial and transition states are ordered, the activation energy and entropy will be more normal, producing a distinct “elbow” in the Arrhenius plot, as observed.

Since this initial report, we have made advances both in experiment and theory, the latter supported by this DOE grant. In order to confirm the hypothesis that the high activation energy and prefactor arise from a partial or complete melting transition, rate measurements were carried out on two rhodopsin mutants that were selected because they exhibit some disruption of the hydrogen bonding network, resulting in a lowering of the temperature of melting. Our main theoretical contribution was to develop a two-state (ordered and disordered) model to predict the striking non-Arrhenius behavior, including the dramatic elbow and unprecedented prefactor observed at higher temperatures. In its simplest form, the model requires only 4 parameters, the enthalpy and entropy of melting, the barrier to reaction when ordered, and the barrier to reaction when melted. Using experimentally determined values for these parameters, the model qualitatively reproduces all of the major observations, including the observed trends between wild type and mutant proteins. While quantitative discrepancies remain, this work represents a conclusive demonstration of the phase transition origin of these remarkable results. This behavior may well prove to be quite general, not only in biological reactions, but also in condensed phase and surface reactions carried out at temperatures and pressures close to 2D or 3D phase transitions.

## Future Plans

### *Electronic Friction at Metal Surfaces*

The Independent Electron Surface Hopping (IESH) theory developed previously under this grant has been shown to successfully predict the rates and pathways of energy flow of molecules interacting with metal surfaces, even in the presence of distinct electron transfer processes. Extension to interactions of electronically and/or vibrationally excited molecules at

semiconductor surfaces is in progress. However, in many cases where electron transfer events are unimportant, a simpler theory appears to be adequate, in which energy exchanged to metal electron-hole-pair excitations are treated by Langevin dynamics. There are two different formulations for computing the frictions and fluctuating forces that appear in the Langevin equation, a free electron gas local density (FEGLD) approximation and an ab initio perturbation theory (AIPT) approach. The latter method is more rigorously founded and, unlike FEGLD, can be utilized to compute the full friction tensor. However, AIPT has suffered from spurious dependences on basis sets, incomplete convergence, and uncertainties in mapping discrete results onto a continuum of electronic levels. Our current work largely eliminates these problems. We now have a robust AIPT method that we are implementing in a number of ab initio codes, allowing ab initio molecular dynamics with electronic friction. We are now testing the validity of the FEGLD against the more accurate AIPT method, with focus on the directionality of the friction, an aspect that FEGLD cannot address. We will apply this new capability to compute vibrational lifetimes and lineshapes of molecules on metal surfaces relevant to solar energy, as well as explore the influence of electronic excitations on chemical reactions at metal surfaces.

### ***The Influence of Phase Transitions on Chemical Reaction Rates***

While the two-state model developed to account for the striking non-Arrhenius behavior observed for the temperature dependent rates of isomerization of rhodopsin has proved to be very successful at a qualitative level, it is too simplified to expect quantitatively accurate predictions. A number of possible factors are missing from the model, including partial disorder rather than complete melting, recrossing corrections and/or Kramer's friction at the transition state, etc. We are developing a mean-field-based quantitative model to place this phenomenon on a more solid and more quantitative footing. The mean field theory will be augmented by molecular dynamics simulations, with appropriately designed non-Boltzmann sampling methods, to compute the huge changes in activation enthalpy and entropy that occur at the transition state, to monitor the nature and degree of disorder in the isomerizing protein, and to compute the effect of this disorder on the reaction barrier.

### **References to Publications of DOE-Sponsored Research in last two years:**

Unusual Kinetics of Thermal Decay of Dim-Light Photoreceptors in Vertebrate Vision, Y. Guo, S. Sekharan, J. Liu, V. S. Batista, J. C. Tully\*, E. C. Y. Yan\*, *PNAS* **111**, 10438-10443, (2014).

Photoinduced Water Oxidation at the Aqueous GaN (10(1)over-bar0) Interface: Deprotonation Kinetics of the First Proton-Coupled Electron-Transfer Step, M. Z. Ertem, N. Kharche, V. S. Batista, M. S. Hybertsen, J. C. Tully and J. T. Muckerman, *ACS Catalysis*, **5**, 2317-2323 (2015)

NO Vibrational Energy Transfer on a Metal Surface: Still a Challenge to First-Principles Theory, B. C. Krueger, N. Bartels, C. Bartels, A. Kandrasenka, J. C. Tully, A. M. Wodtke and T. Schafer, *J. Phys. Chem.* **119**, 3268-3272 (2015)

## Reactive Processes in Aqueous Environment

Marat Valiev

<sup>1</sup>Environmental Molecular Sciences Laboratory and  
Pacific Northwest National Laboratory

902 Battelle Blvd.

Mail Stop K9-90

Richland, WA 99352

[marat.valiev@pnl.gov](mailto:marat.valiev@pnl.gov)

Our research is focused on providing molecular level understanding of solute-solvent interactions. We take a comprehensive approach that integrates gas phase analysis of solute electronic structure with solvation studies performed at the various length scales (from small clusters to bulk). The important objective is to understand how specific features of the solute (geometry, charge distribution, etc.) are influencing the solvation process and its evolution to the bulk limit. At the same time we are also interested to know how the presence of solvent impacts the electronic structure of the solute. The latter has an added importance of providing connection to the experimental efforts, which is important aspect of our research.

Our investigation of bulk solvation processes relies on combined quantum mechanical molecular mechanics approach (QM/MM). This is approach that we are using in our current investigation of excited state properties green fluorescent protein (GFP) chromophore in aqueous solution.

Experimental measurements indicate that excited state spectrum of GFP shows great variation with respect to pH levels, which is the phenomenon that we are investigating using computational modeling. Under acidic condition GFP is likely to be in the cationic form (see Fig 1A) with protonation presumably

on an N atom of the imidazolinone ring. Our calculated excitation energy of 3.12 eV for this configuration agrees well with the experimental maximum absorption at 396 nm (3.13 eV). Basic conditions should lead to the appearance of anionic form of GFP (see Fig. 1B). Again our calculated excitation energy 2.91 eV is good agreement

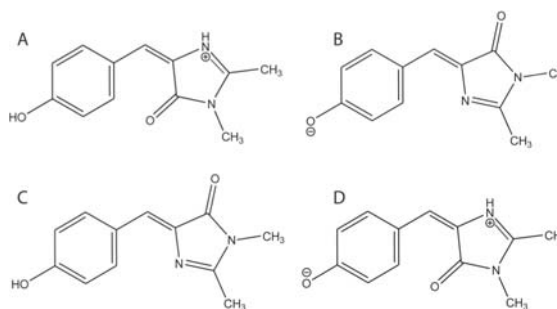


**Figure 1:** Protonation states of GFP chromophore

with the experimental data, which shows maximum absorption spectrum at 426 nm (2.91 eV). For the neutral pH conditions we find that that experimental data (370 nm) is best reproduced by cis-conformer of neutral GFP. The other potential zwitterionic form was found to give excited state energy 2.65 eV (468 nm), which is in a disagreement with experiment. Future investigations of this system will be focused on the cluster solvation environment in conjunction with photoelectron spectroscopy measurements.

In addition to bulk aqueous environment we are also interested in solvation processes at the cluster level. The absence of the bulk solvent environment amplifies effects of solute solvent interactions exposing level of detail that may not be possible to resolve in bulk observations. This is the approach we have recently applied to analyze solvation properties negatively charged  $\text{SCN}^-$ , which is a well-known chaotrope. There is a growing consensus that the key to kosmotropic/chaotropic behaviors lies in the local solvent region, but the exact microscopic basis for such differentiation is not well understood. Combining experimental photoelectron spectroscopy measurements (Xue-Bin Wang, PNNL) with theoretical modeling we examine evolution of solvation structure up to eight waters. We observe that  $\text{SCN}^-$  indeed fits the description of weakly hydrated ion and its solvation is heavily driven by stabilization of water-water interaction network. However, the impact on water structure is more subtle than that associated with “structure breaker”. In particular, we observe that the solvation

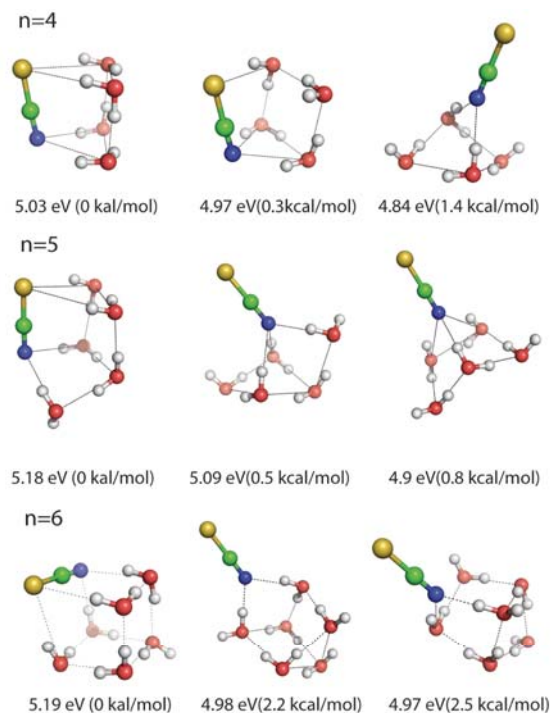


**Figure 2:** Optimized structures of the lowest energy isomers for the n=4-6 SCN water clusters. Calculated VDEs (eV) for each structure and relative energy (kcal/mol) are indicated.

structure of SCN<sup>-</sup> preserves the “packing” structure of the water network but changes local directionality of hydrogen bonds in the local solvent region. The resulting effect closer to that of “structure weakener”, where solute can be readily accommodated into the native water network, at the cost of compromising its stability due to constraints on hydrogen bonding directionality. Future studies of SCN<sup>-</sup> solvation will involve progressively larger clusters (up to 50 water molecules).

#### Acknowledgments:

Direct collaborators on this project include Xue-Bin Wang (PNNL), S. Lymar (BNL), K. Kowalski (EMSL), and J. H. Weare (UCSD). Discussions with S. S. Xantheas, L. X. Dang, C. J. Mundy, G. K. Schenter, and S. K. Kathmann have influenced the course of this work. Battelle operates Pacific Northwest National Laboratory for the US Department of Energy.

#### Publications (2014-2015):

Deng, S. H. M.; Hou, G.-L.; Kong, X.-Y.; Valiev, M.; Wang, X.-B.: Examining the Amine Functionalization in Dicarboxylates: Photoelectron Spectroscopy and Theoretical Studies of Aspartate and Glutamate. *The Journal of Physical Chemistry A* **2014**.

Shaikh, N.; Valiev, M.; Lymar, S. V., Decomposition of amino diazeniumdiolates (NONOates): Molecular mechanisms. *J Inorg Biochem* **2014**, *141*, 28-35.

Valiev, M.; Deng, S. H. M.; Wang, X.-B., How Anion Chaotrope Changes the Local Structure of Water: Insights from Photoelectron Spectroscopy and Theoretical Modeling of SCN<sup>-</sup> Water Clusters. *The Journal of Physical Chemistry B* **2015**, in press

## Chemical Kinetics and Dynamics at Interfaces

### *Cluster Model Investigation of Condensed Phase Phenomena*

**Xue-Bin Wang**

Physical Sciences Division, Pacific Northwest National Laboratory, P.O. Box 999, MS K8-88, Richland,  
WA 99352. E-mail: [xuebin.wang@pnnl.gov](mailto:xuebin.wang@pnnl.gov)

#### Program Scope

We aim at obtaining a microscopic understanding of solution chemistry and condensed phase phenomena using gas phase clusters as model systems. Clusters occupy an intermediate region between gas phase molecules and the condensed states of matter and play an important role in heterogeneous catalysis, aerosol chemistry, and biological processes. We use electrospray ionization (ESI) to generate a wide variety of molecular and ionic clusters to simulate key species involved in the condensed phase reactions and transformations, and characterize them using low temperature, and temperature-controlled negative ion photoelectron spectroscopy (NIPES). Inter- and intra-molecular interactions and their variation as function of size and composition, important to understand complex chemical reactions and nucleation processes in condensed and interfacial phases can be directly obtained. Experiments and *ab initio* calculations are synergistically combined to (1) probe solute anisotropic effects in hydrated anion and neutral clusters; (2) obtain a molecular-level understanding of the solvation and stabilization of complex singly- and multiply-charged anions important in condensed phases; (3) quantify thermodynamic driving forces resulted from hydrogen-bonded networks formed in aerosol nucleation processes and enzymatic catalytic reactions; (4) study temperature-dependent conformation changes and isomer populations of complex solvated clusters; (5) investigate intrinsic electronic structures of environmentally and catalytically important species and reactive diradicals; and (6) understand the molecular processes and initial steps of dissolution of salt molecules in polar solvents. The central theme of this research program lies at obtaining a fundamental understanding of environmental materials and solution chemistry important to many primary DOE missions (waste storage, subsurface and atmospheric contaminant transport, catalysis, etc.), and enhances scientific synergies between experimental and theoretical studies towards achieving such goals.

#### Recent Progress

***Probing the early stages of salt nucleation:*** Due to the fast solvent evaporation in electrospray ionization (ESI), the concentration of initially dilute electrolyte solutions rapidly increases to afford the formation of supersaturated droplets and generation of various pristine anhydrous salt clusters in the gas phase. The size, composition, and charge distributions of these clusters, in principle, witness the nucleation evolution in solutions. We reported a microscopic study on the initial stage of nucleation and crystallization of sodium/potassium thiocyanate salt solutions simulated in the ESI process. Singly charged  $M_x(\text{SCN})_{x+1}^-$ , doubly charged  $M_y(\text{SCN})_{y+2}^{2-}$ , ( $M = \text{Na}, \text{K}$ ), and triply charged  $K_z(\text{SCN})_{z+3}^{3-}$  anion clusters ( $x$ ,  $y$ , and  $z$  stand for the number of alkali atoms in the singly-, doubly-, and triply-charged clusters, respectively) were produced via electrospray of the corresponding salt solutions, and were characterized by negative ion photoelectron spectroscopy (NIPES). The vertical detachment energies (VDEs) of these sodium/potassium thiocyanate cluster anions were obtained, and theoretical calculations were carried out for the sodium thiocyanate clusters in assisting spectral identification. The measured VDEs of singly charged anions  $M_x(\text{SCN})_{x+1}^-$  ( $M = \text{Na}$  and  $\text{K}$ ) demonstrate that they are superhalogen anions. The existence of doubly charged anions  $M_y(\text{SCN})_{y+2}^{2-}$  ( $y = 2x$ ,  $x \geq 4$  and  $3$  for  $M = \text{Na}$  and  $\text{K}$ , respectively) and triply charged anions  $K_z(\text{SCN})_{z+3}^{3-}$  ( $z = 3x$ ,  $x \geq 6$ ) were initially discovered from the photoelectron spectra for those singly charged anions of  $M_x(\text{SCN})_{x+1}^-$  with the same mass-to-charge ratio ( $m/z$ ), and later independently confirmed by the observation of their distinct mass spectral distributions and by taking their NIPE spectra for those pure multiply charged anions with their  $m/z$  different from the singly charged species. For large clusters, multiply charged clusters were found to become preferred, but at

higher temperatures, those multiply charged clusters were suppressed. The series of anion clusters investigated here range from molecular-like  $M_1(\text{SCN})_2^-$  to nano-sized  $K_{22}(\text{SCN})_{25}^{3-}$ , providing a vivid molecular-level growth pattern reflecting the initial salt nucleation process (SHM Deng, XY Kong, and XB Wang, *J. Chem. Phys.* **2015**, *142*, 024313).

**Cluster model study of kosmotrope and chaotrope anion specificities in solutions:** Specific ion effects are ubiquitous in solutions and play important roles in biological processes and functions. Collaborating with PNNL theoreticians, Drs. Valiev and Kathmann, we provided compelling experimental and theoretical evidence that the anisotropic nature of complex polyoxyanion solutes can have a critical influence on the solvation process. Combined photoelectron spectroscopy and theoretical modeling results show that the electron binding energy of  $\text{IO}_3^-(\text{H}_2\text{O})_n$  ( $n = 0 - 12$ ) clusters is characterized by an anomalous drop at  $n = 10$ . Such behavior is unprecedented for rigid solute molecules, and is related to the anisotropy of the neutral iodate radical that displays a strong selectivity to solvent configurations generated by the charged anion complex. As a *kosmotrope* anion,  $\text{IO}_3^-$  shows that it can organize solvent water molecules via a cyclic water-network around it and hence a ‘*structure maker*’ (Wen, Hou, Kathmann, Valiev, and Wang, **2013**, *J. Chem. Phys.* *138*, 031101). As a comparison, we also carried out a cluster model study on *chaotrope*  $\text{SCN}^-$  anion solvation. We found distinctly different solvation motif of  $\text{SCN}^-$  relative to  $\text{IO}_3^-$ , and  $\text{SCN}^-$  can readily integrate into native water-networks by replacing a single water molecule in the corner or by substituting a water-dimer on the edge. In this regard, the *chaotrope*  $\text{SCN}^-$  anion can be better called ‘*structure weakener*’ instead of ‘*structure breaker*’ (M Valiev, SHM Deng, and XB Wang, submitted).

**Hilltop spectroscopy via negative ion photodetachment:** Negative Ion Photoelectron (NIPE) spectra of the radical anion of cyclopropane-1,2,3-trione,  $(\text{CO})_3^{\bullet-}$ , have been obtained at 20 K, using both 355 and 266 nm lasers for electron photodetachment. The spectra show broadened bands, due to the short lifetimes of both the singlet and triplet states of neutral  $(\text{CO})_3$  and, to a lesser extent, to the vibrational progressions that accompany the photodetachment process. The smaller intensity of the band with the lower electron binding energy suggests that the singlet is the ground state of  $(\text{CO})_3$ . From the NIPE spectra, the electron affinity (EA) and the singlet-triplet energy gap of  $(\text{CO})_3$  are estimated to be, respectively,  $EA = 3.1 \pm 0.1$  eV and  $\Delta E_{\text{ST}} = -14 \pm 3$  kcal/mol. High-level, (U)CCSD(T)/aug-cc-pVQZ// (U)CCSD(T)/aug-cc-pVTZ, calculations give  $EA = 3.04$  eV for the  $^1\text{A}_1'$  ground state of  $(\text{CO})_3$  and  $\Delta E_{\text{ST}} = -13.8$  kcal/mol for the energy gap between the  $^1\text{A}_1'$  and  $^3\text{A}_2$  states, in excellent agreement with values from the NIPE spectra. In addition, simulations of the vibrational structures for formation of these states of  $(\text{CO})_3$  from the  $^2\text{A}_2''$  state of  $(\text{CO})_3^{\bullet-}$  provide a good fit to the shapes of broad bands in the 266 nm NIPE spectrum. The NIPE spectrum of  $(\text{CO})_3^{\bullet-}$  and the analysis of the spectrum by high-quality electronic structure calculations demonstrate that NIPES can not only access and provide information about transition structures, but NIPES can also access and provide information about hilltops on potential energy surfaces (B Chen, DA Hrovat, R West, SHM Deng, XB Wang, and WT Borden, *J. Am. Chem. Soc.* **2014**, *136*, 12345).

**Examining the critical roles of protons in facilitating oxidation of chloride ions by permanganates—a cluster model study:** The oxidation power of permanganates ( $\text{MnO}_4^-$ ) is known to be strongly dependent on pH values, and is greatly enhanced in acidic solutions, in which, for example,  $\text{MnO}_4^-$  can even oxidize  $\text{Cl}^-$  ions to produce  $\text{Cl}_2$  molecules. Although such dependence has been ascribed due to the different reduced states of Mn affordable in different pH media, a molecular level understanding and characterization of initial redox pair complexes available in different pH solutions is very limited. We reported a comparative study of  $[\text{MnO}_4]^-$  and  $[\text{MnO}_4 \bullet \text{Sol}]^-$  (Sol =  $\text{H}_2\text{O}$ , KCl, and HCl) anion clusters by negative ion photoelectron spectroscopy (NIPES) and theoretical computations to probe chemical bonding and electronic structures of  $[\text{MnO}_4 \bullet \text{Sol}]^-$  clusters, aimed to obtain a microscopic understanding of how  $\text{MnO}_4^-$  interacts with surrounding molecules. Our study shows that  $\text{H}_2\text{O}$  behaves as a solvent molecule, KCl is a spectator bound by pure electrostatic interactions, both of which do not influence the  $\text{MnO}_4^-$  identity in their respective clusters. In contrast, in  $[\text{MnO}_4 \bullet \text{HCl}]^-$ , the proton is found to interact with both  $\text{MnO}_4^-$  and  $\text{Cl}^-$  with appreciable covalent characters, and the frontier MOs of the cluster are

comprised of contributions from both  $\text{MnO}_4^-$  and  $\text{Cl}^-$  moieties. Therefore the proton serves as a chemical bridge, bringing two negatively charged redox species together to form an intimate redox pair. By adding more  $\text{H}^+$  to  $\text{MnO}_4^-$ , the oxygen atom can be taken away in the form of a water molecule, leaving  $\text{MnO}_4^-$  as an electron deficient  $\text{MnO}_3^+$  species, which can subsequently oxidize  $\text{Cl}^-$  ions (J Zhang, ZR Sun, and XB Wang, *J. Phys. Chem. A* **2015**, *119*, 6244).

### Future Directions

The main thrust of our BES program will continue to be on cluster model studies of condensed phase phenomena in the gas phase. The experimental capabilities that we have developed give us the opportunity to attack a broad range of fundamental chemical physics problems pertinent to ionic solvation, solution chemistry, homogeneous / heterogeneous catalysis, aerosol chemistry, biological processes, and material synthesis. The ability to cool and control ion temperature enables us to study different isomer populations and conformation changes of environmentally important hydrated clusters. Another major direction is to use gaseous clusters to model ion-specific interactions in solutions, ion transport and ion-receptor interactions in biological systems, and initial nucleation processes relevant to atmospheric aerosol formation.

### References to Publications of DOE CPIMS Sponsored Research (2013 - present)

1. H Wen, GL Hou, SM Kathmann, M Valiev, and XB Wang, "Solute Anisotropy Effects in Hydrated Anion and Neutral Clusters", *J. Chem. Phys.* *138*, 031101-1-4 (2013).
2. X Bao, DA Hrovat, WT Borden, and XB Wang, "Negative Ion Photoelectron Spectroscopy Confirms the Prediction that  $(\text{CO})_5$  and  $(\text{CO})_6$  Each Has a Singlet Ground State", *J. Am. Chem. Soc.* *135*, 4291-4298 (2013).
3. GL Hou, W Lin, SH Deng, J Zhang, W Zheng, F Paesani, and XB Wang, "Negative Ion Photoelectron Spectroscopy Reveals Thermodynamic Advantage of Organic Acids in Facilitating Formation of Bisulfate Ion Clusters: Atmospheric Implications", *J. Phys. Chem. Lett.* *4*, 779-785 (2013).
4. IV Kuvychko, KP Castro, SH Deng, XB Wang, SH Strauss, and OV Boltalina, "Taming Hot  $\text{CF}_3$  Radicals: Incrementally Tuned Families of Polyarene Electron Acceptors for Air-Stable Molecular Optoelectronics", *Angew. Chem. Int. Ed.* *52*, 4871-4874 (2013).
5. EF van der Eide, GL Hou, SH Deng, H Wen, P Yang, RM Bullock, and XB Wang, "Metal-Centered 17-Electron Radicals  $\text{CpM}(\text{CO})_3^*$  ( $\text{M} = \text{Cr}, \text{Mo}, \text{W}$ ): A Combined Negative Ion Photoelectron Spectroscopic and Theoretical Study", *Organometallics* *32*, 2084-2091 (2013).
6. IV Kuvychko, C Dubceac, SH Deng, XB Wang, AA Granovsky, AA Popov, MA Petrukhina, SH Strauss, and OV Boltalina, " $\text{C}_{20}\text{H}_4(\text{C}_4\text{F}_8)_3$ : A Fluorine-Containing Annulated Corannulene that Is a Better Electron Acceptor Than  $\text{C}_{60}$ ", *Angew. Chem. Int. Ed.* *52*, 7505-7508 (2013).
7. A Shokri, XB Wang, and SR Kass, "Electron-Withdrawing Trifluoromethyl Groups in Combination with Hydrogen Bonds in Polyols: Brønsted Acids, Hydrogen-Bond Catalysts, and Anion Receptors", *J. Am. Chem. Soc.* *135*, 9525-9530 (2013).
8. BW Larson, JB Whitaker, XB Wang, AA Popov, G Rumbles, N Kopidakis, SH Strauss, and OV Boltalina, "Electron Affinity of Phenyl- $\text{C}_{61}$ -Butyric Acid Methyl Ester (PCBM)", *J. Phys. Chem. C* *117*, 14958-14964 (2013).
9. GL Hou, MM Wu, H Wen, Q Sun, XB Wang, WJ Zheng, "Photoelectron spectroscopy and theoretical study of  $\text{M}(\text{IO}_3)_2^-$  ( $\text{M} = \text{H}, \text{Li}, \text{Na}, \text{K}$ ): Structural evolution, optical isomers, and hyperhalogen behavior", *J. Chem. Phys.* *139*, 044312-1-7 (2013).
10. J Zhang, DA Hrovat, ZR Sun, X Bao, WT Borden, and XB Wang, "The Ground State of  $(\text{CS})_4$  Is Different from that of  $(\text{CO})_4$ : An Experimental Test of a Computational Prediction by Negative Ion Photoelectron Spectroscopy", *J. Phys. Chem. A* *117*, 7841-7846 (2013).
11. TT Clikeman, SHM Deng, S Avdoshenko, XB Wang, AA Popov, SH Strauss, and OV Boltalina, "Fullerene "Superhalogen" Radicals: the Substituent Effect on Electronic Properties of 1,7,11,24,27- $\text{C}_{60}\text{X}_5$ ", *Chemistry – A European Journal* *19*, 15404-15409 (2013).

12. A Shokri, Y Wang, GA O'Doherty, XB Wang, and SR Kass, "Hydrogen-Bond Networks: Strengths of Different Types of Hydrogen Bonds and An Alternative to the Low Barrier Hydrogen-Bond Proposal", *J. Am. Chem. Soc.* 135, 17919-17924 (2013).
13. J Zhang, P Yang, ZR Sun, and XB Wang, "Covalently Bound Tetracoordinated Organoborons as Superhalogens: A Combined Negative Ion Photoelectron Spectroscopy and Theoretical Study", *J. Phys. Chem. A* (ASAP) (dx.doi.org/10.1021/jp410009a) (2014).
14. A Shokri, SHM Deng, XB Wang, and SR Kass, "Molecular Recognition: Preparation and Characterization of Two Tripodal Anion Receptors", *Organic Chemistry Frontiers* 1, 54-61 (2014).
15. B Chen, DA Hrovat, SHM Deng, J Zhang, XB Wang, and WT Borden, "The negative ion photoelectron spectrum of meta-benzoquinone radical anion (MBQ<sup>•-</sup>): A joint experimental and computational study", *J. Am. Chem. Soc.* 136, 3589-3596 (2014).
16. TT Clikeman, EV Bukovsky, IV Kuvychko, LK San, SH M Deng, XB Wang, YS Chen, SH Strauss, and OV Boltalina, "Poly(trifluoromethyl)azulenes: structures and acceptor Properties" *Chem. Comm.* 50, 6263-6266 (2014).
17. SHM Deng, XY Kong, GX Zhang, Y Yang, WJ Zheng, ZR Sun, DQ Zhang, and XB Wang, "Vibrationally Resolved Photoelectron Spectroscopy of the Model GFP Chromophore Anion Revealing the Photoexcited S<sub>1</sub> State Being Both Vertically and Adiabatically Bound against the Photodetached D<sub>0</sub> Continuum" *J. Phys. Chem. Lett.* 5, 2155-2159 (2014).
18. SHM Deng, GL Hou, XY Kong, M Valiev, and XB Wang, "Examining the Amine Functionalization in Dicarboxylates: Photoelectron Spectroscopy and Theoretical Studies of Aspartate and Glutamate" *J. Phys. Chem. A* 118, 5256-5262 (2014).
19. M Samet, XB Wang, and SR Kass, "A Preorganized Hydrogen Bond Network and Its Effect on Anion Stability" *J. Phys. Chem. A* 118, 5989-5993 (2014).
20. B Chen, DA Hrovat, R West, SHM Deng, XB Wang, and WT Borden, "The Negative Ion Photoelectron Spectrum of Cyclopropane-1,2,3-Trione Radical Anion, (CO)<sub>3</sub><sup>•-</sup> – A Joint Experimental and Computational Study" *J. Am. Chem. Soc.* 136, 12345-12354 (2014).
21. XB Wang and Steven R. Kass, "Anion A<sup>-</sup> • HX Clusters with Reduced Electron Binding Energies: Proton vs Hydrogen Atom Relocation upon Electron Detachment", *J. Am. Chem. Soc.* 136, 17332-17336 (2014).
22. TT Clikeman, SHM Deng, AA Popov, XB Wang, SH Strauss and OV Boltalina. "Fullerene cyanation does not always increase electron affinity: an experimental and theoretical study". *Phys. Chem. Chem. Phys.* 17, 551-556 (2015).
23. J Zhang, B Zhou, ZR Sun, and XB Wang. "Photoelectron Spectroscopy and Theoretical Studies of Anion- $\pi$  Interactions: Binding Strength and Anion Specificity". *Phys. Chem. Chem. Phys.* 17, 3131-3141 (2015).
24. LK San, EV Bukovsky, BW Larson, JB Whitaker, SHM Deng, N Kopidakis, G Rumbles, AA Popov, YS Chen, XB Wang, OV Boltalina and SH Strauss. "A faux hawk fullerene with PCBM-like properties" *Chem. Sci.* 6, 1801-1815 (2015).
25. SHM Deng, XY Kong, and XB Wang. "Probing the early stages of salt nucleation--experimental and theoretical investigations of sodium/potassium thiocyanate cluster anions", *J. Chem. Phys.* 142, 024313-1-9 (2015).
26. J Zhang, ZR Sun, and XB Wang. "Examining the Critical Roles of Protons in Facilitating Oxidation of Chloride Ions by Permanganates: A Cluster Model Study", *J. Phys. Chem. A* 119, 6244-6251 (2015).
27. DA Hrovat, GL Hou, XB Wang, and WT Borden. "Negative Ion Photoelectron Spectroscopy Confirms the Prediction that 1,2,4,5-Tetraoxatetramethylenebenzene Has a Single Groud", *J. Am. Chem. Soc.* 137, 9094-9099 (2015).
28. A Sen, GL Hou, XB Wang, C Dessent. "Electron Detachment as a Probe of Intrinsic Nucleobase Dynamics in Dianion-Nucleobase Clusters: Photoelectron Spectroscopy of the Platinum II Cyanide Dianion Bound to Uracil, Thymine, Cytosine and Adenine", *J. Phys. Chem. B* (ASAP) (DOI: 10.1021/acs.jpcc.5b07108).
29. TT Clikeman, EV Bukovsky, XB Wang, YS Chen, G Rumbles, SH Strauss, OV Boltalina. "Core Perylene Diimide Designs via Direct Bay and Ortho (Poly)trifluoromethylation: Synthesis, Isolation, X-ray Structures, Optical and Electronic Properties", *Eur. J. Org. Chem.* (accepted) (DOI: 10.1002/ejoc.201501024).

## Free Radical Reactions of Hydrocarbons at Aqueous Interfaces

Principal Investigator: Kevin R. Wilson

Lawrence Berkeley National Laboratory, 1 Cyclotron Road, MS 6R2100, Berkeley, CA 94720

Email: [krwilson@lbl.gov](mailto:krwilson@lbl.gov)

**Program Scope and Long Term Objectives:** This project will probe the surface chemistry of hydrocarbon molecules residing on nanometer and micron-sized droplets exposed to gas phase hydroxyl radicals using atmospheric pressure surface sensitive mass spectrometry and ambient pressure photoelectron spectroscopy. This program aims to:

(1) *Quantify the link between molecular structure and surface reactivity at an aqueous, viscous and solid interfaces using model hydrocarbon architectures (e.g. isomers)*

(2) *Determine how the presence and distribution of interfacial ions control the surface reactivity of a hydrocarbon at an aqueous interface.*

This work broadly supports the Department of Energy's Basic Energy Sciences program to better assess, mitigate and control the efficiency, utilization, and environmental impacts of energy use. This work seeks a rigorous molecular understanding of how heterogeneous reaction pathways lead to either bulk solvation of a surface active organic molecule or its removal from the interface through decomposition into gas phase products.

**Recent Progress:** During the last funding period, we have sought to understand how thermodynamic phase (solid, glass, and aqueous phases) control the heterogeneous hydroxyl radical (OH) oxidation pathways of organic molecules. The heterogeneous reactions were investigated using an aerosol flow tube reactor. The molecular and elemental transformation of the particles is quantified using Direct Analysis in Real Time (DART), a soft atmospheric pressure ionization source, coupled to a high resolution mass spectrometer.

Water plays an important role in controlling the physicochemical dynamics of aerosols in the atmosphere. Using citric acid as a model system, the reactive uptake kinetics of hydroxyl radicals are measured over a large range of relative humidity. By comparing the kinetics measured by probing the outer surface layers of the aerosol with measurements of the entire particle composition, the effective OH reaction probability, measured via the reactive decay of citric acid, is found to be a complex and non-linear function of the liquid water content of the particle. At a relative humidity between 20 and 50%, the decay of citric acid with OH exposure is controlled by the viscosity of the particle. Using an accessible volume model of the reaction kinetics, it is found that the depletion of citric acid and the formation of reaction products occurs over a narrow region near the particle interface. The radial width of this reaction zone scales as the square root of the estimated citric acid diffusion coefficient and is on the order of ~8 nm at 20% RH. At RH = 50% the reaction zone increases to ~50 nm and encompasses most of the particle's volume. At RH > 50%, the aerosol becomes aqueous and well-mixed on the timescale of the heterogeneous reaction. As RH is increased beyond 50% the reaction probability is observed to decrease and depend upon

both the fraction of citric acid and the liquid water in the aerosol. The formation and dissipation of chemical gradients at interfaces have important implications for understanding gas-particle partitioning and chemical mechanisms (i.e. bulk vs. interface) of viscous and semisolid interfaces, which we observe to be governed by complex feedbacks between the size of the interfacial reaction zone, viscosity, particle size and RH.

Previously we conducted sensitive measurements of the droplet size, using phase Doppler interferometry, at a relative humidity (RH~99.9%), on submicron particles containing an ammonium sulfate core and an organic layer of a model compound of varying thickness. New measurements were recently made on the same series of model compounds but under supersaturated conditions (RH > 100%). These measurements were designed to test key assumption often used in Köhler Theory to describe the mechanism of cloud droplet formation in the atmosphere. We found, quite unexpectedly that for all of the model systems, except pure ammonium sulfate and sucrose, the droplet sizes measured at activation are 40-60% larger than predicted by theory assuming that the organic material is dissolved inside the droplet bulk. Instead, analysis of the data using a compressed film monolayer model, shows that the droplet size at activation is controlled by interfacial organic molecules that rapidly accumulate at the surface as the droplet forms and grows. These results show the importance of surface chemistry in controlling environmental phenomena such as cloud formation.

In another study, we have focused on understanding systems whose chemical evolution involves the coupling of surface and gas-phase chemical reactions. Traditional descriptions of gas-particle partitioning of aerosol particles rely solely on thermodynamic properties (e.g., volatility). Under realistic conditions where phase partitioning is dynamic rather than static, the transformation of a particle involves the interplay of multiphase partitioning and chemical reactions. A key challenge remains in quantifying the fundamental timescales for evaporation and oxidation of semi-volatile particle constituents. Isomer-resolved product measurements of a series of normal-alkanes (C<sub>18</sub>, C<sub>20</sub>, C<sub>22</sub>, and C<sub>24</sub>) are used to distinguish between gas-phase and heterogeneous oxidation reactions formed by the reaction of these species with hydroxyl radicals (OH). The product isomer distributions when combined with kinetics measurements of evaporation and oxidation enable a quantitative description of the multiphase timescales to be simulated using a kinetic model. Multiphase partitioning and oxidative transformation of semi-volatile normal-alkanes under laboratory conditions is largely controlled by the particle phase state, since the timescales of heterogeneous oxidation and evaporation are found to occur on competing timescales (on the order of 10<sup>-1</sup> hours). This is in contrast to atmospheric conditions where heterogeneous oxidation timescales are much longer (on the order of 10<sup>2</sup> hours), with gas-phase oxidation being the dominant process regardless of the evaporation kinetics. These results demonstrate the dynamic nature of multiphase partitioning and surface chemistry and reveal the fundamental timescales of these processes.

We have also made substantial progress on building a droplet reactor. This reactor is designed to measure surface reactions on 20-80 micron diameter aqueous droplets. This reactor is designed

for use in our atmospheric pressure mass spectrometer and in the ambient pressure X-ray photoelectron spectrometer at the Molecular Environmental Science Beamline. Single droplet mass spectra and XPS spectra will be recorded during a surface reaction with OH. The mass spectrometry measurements will elucidate reaction mechanisms and kinetics by providing a molecular probe of the droplet composition. These measurements will be combined with XPS interface measurements of elemental composition (e.g. depth profiling).

**Future Plans:** A key question that has emerged in our ongoing studies is: how does the gas phase reactivity of OH depend upon the characteristics of the interface (e.g. viscosity, water content, and organic surface coverage). Previous measurements in our lab have quantified the heterogeneous reaction by measuring the decay of an organic molecule in the particle phase. The reactive decay depends upon both the OH reaction probability as well as secondary radical reactions that can also consume the organic fraction (i.e. radical chain cycling). We plan to construct an instrument to measure directly the heterogeneous OH decay kinetics using laser induced fluorescence. These measurements will be compared with those which monitor the decay kinetics of the organic molecule in the particle itself in order to quantify the degree of radical chain cycling. Furthermore, these fundamental measurements of the OH reaction probability will enable deeper insight into the governing factors (e.g. hydrogen bonding) that control the reactive uptake of free radicals on complex aqueous, glassy and solid surfaces.

In the next year, we will also continue to focus on understanding how C-C bond scission reactions produced by surface reactions of OH radicals depend upon molecular structure (i.e. carbon chain length), interfacial orientation, and particle viscosity. As we observed previously, there is emerging evidence that the degree of branching on the hydrocarbon skeleton controls the formation of smaller molecular weight reaction products. By measuring the heterogeneous reaction of OH with a series of compounds that differ only in the number and location of methyl substituents should quantify the relationship between the number of tertiary carbon reaction sites and C-C bond scission propensity. As our new ion mobility mass spectrometer comes online, we expect to be able to measure surface reactions with isomer specificity.

Finally, we will use a new laser tweezers setup to probe the surface chemistry of individual micron sized droplets over long reaction times (hours to days). Here we will use Raman scattering for chemical composition determination and the droplet's whispering gallery modes for high precision droplet sizing (~1 nm) to elucidate changes in single droplet chemistry as a function of reaction time to OH. We will also design a novel interface to our mass spectrometer to obtain single droplet mass spectra as a function of reaction time.

**Publications Acknowledging the Office of Science Early Career Award:**

1. J.F. Davies and K.R. Wilson, "*Nanoscale Interfacial Gradients Formed by the Reactive Uptake of OH Radicals onto Viscous Aerosol Surfaces,*" Chem. Sci., DOI: 10.1039/C5SC02326B, (2015)

2. C. T. Cheng, M. N. Chan, and K. R. Wilson, "*The Role of Alkoxy Radicals in the Heterogeneous Reaction of Two Structural Isomers of Dimethylsuccinic Acid*," Phys. Chem. Chem. Phys., DOI: 10.1039/C5CP03791C (2015)
3. H. Zhang, D. R. Worton, S. Shen, T. Nah, G. Isaacman-VanWertz, K. R. Wilson, and A. H. Goldstein, "*Fundamental Timescales Governing Organic Aerosol Multiphase Partitioning and Oxidative Aging*," Environ. Sci. Technol., DOI: 10.1021/acs.est.5b02115 (2015)
4. F. A. Houle, W. D. Hinsberg, and K. R. Wilson, "*Oxidation of a model alkane aerosol by OH radical: the emergent nature of reactive uptake*," Phys. Chem. Chem. Phys., **17**, 4412, DOI: 10.1039/C4CP05093B (2015).
5. A. A. Wiegel, K. R. Wilson, W. D. Hinsberg, and F. A. Houle, "*Stochastic methods for aerosol chemistry: a compact molecular description of functionalization and fragmentation in the heterogeneous oxidation of squalane aerosol by OH radicals*," Phys. Chem. Chem. Phys., **17**, 4398, DOI: 10.1039/C4CP04927F (2015).
6. C. Ruehl and K.R. Wilson, "*Surface organic monolayers control the hygroscopic growth of submicron particles at high relative humidity*," J. Phys. Chem. A, DOI: 10.1021/jp502844g (2014)
7. M.N. Chan, H. Zhang, A. H. Goldstein, and K. R. Wilson, "*The Role of Water and Phase in the Heterogeneous Oxidation of Solid and Aqueous Succinic Acid Aerosol by Hydroxyl Radicals*," J. Phys. Chem. C, DOI: 10.1021/jp5012022 (2014).
8. H. Zhang, C. Ruehl, A. Chan, T. Nah, D. Worton, G. Isaacman, A. Goldstein, and K. R. Wilson, "*OH Initiated Heterogeneous Oxidation of Cholestane: A Model System for Understanding the Photochemical Aging of Cyclic Alkane Aerosols*," J. Phys. Chem. A. **117**, 12449 (2013).
9. T. Nah, M.N. Chan, S. R. Leone, and K. R. Wilson, "*Real Time in Situ Chemical Characterization of Sub-micrometer Organic Particles Using Direct Analysis in Real Time-Mass Spectrometry*," Anal. Chem., **85**, 2087 (2013).
10. M.N. Chan, T. Nah, and K. R. Wilson, "*In-Situ Chemical Detection of Sub-micron Organic Aerosols using Direct Analysis in Real Time Mass Spectrometry (DART-MS): The Effect of Aerosol Size and Volatility*," Analyst, **138**, 3749-3757 (2013).
11. C. R. Ruehl, T. Nah, G. Isaacman, D. R. Worton, A. W. H. Chan, K. R. Kolesar, C. D. Cappa, A. H. Goldstein, and K. R. Wilson, "*The influence of molecular structure and aerosol phase on the heterogeneous oxidation of normal and branched alkanes by OH*," J. Phys. Chem. A., **117**, 3990 (2013)
12. C. W. Harmon, C. R. Ruehl, C. D. Cappa, and K. R. Wilson, "*A Statistical Description of the Evolution of Cloud Condensation Nuclei Activity during the Heterogeneous Oxidation of Squalane and Bis (2-ethylhexyl) Sebacate Aerosol by Hydroxyl Radicals*," Phys. Chem. Chem. Phys., **15**, 9679 (2013).

## Ionic Liquids: Radiation Chemistry, Solvation Dynamics and Reactivity Patterns

James F. Wishart

Chemistry Department, Brookhaven National Laboratory, Upton, NY 11973-5000

wishart@bnl.gov

### Program Definition

Ionic liquids (ILs) are a rapidly expanding family of condensed-phase media with important applications in energy production, storage and consumption, including advanced devices and processes and nuclear fuel and waste processing. ILs generally have low volatilities and are combustion-resistant, highly conductive, recyclable and capable of dissolving a wide variety of materials. They are finding new uses in dye-sensitized solar cells, chemical synthesis, catalysis, separations chemistry, batteries, supercapacitors and other areas. Ionic liquids have dramatically different properties compared to conventional molecular solvents, and they provide a new and unusual environment to test our theoretical understanding of primary radiation chemistry, charge transfer and other reactions. We are interested in how IL properties influence physical and dynamical processes that determine the stability and lifetimes of reactive intermediates and thereby affect the courses of reactions and product distributions. We study these issues by characterization of primary radiolysis products and measurements of their yields and reactivity, quantification of electron solvation dynamics and scavenging of electrons in different states of solvation. From this knowledge we wish to learn how to predict radiolytic mechanisms and control them or mitigate their effects on the properties of materials used in nuclear fuel processing, for example, and to apply IL radiation chemistry to answer questions about general chemical reactivity in ionic liquids that will aid in the development of applications listed above.

Soon after our radiolysis studies began it became evident that the slow solvation dynamics of the excess electron in ILs (which vary over a wide viscosity range) increase the importance of pre-solvated electron reactivity and consequently alter product distributions and subsequent chemistry. This difference from conventional solvents has profound effects on predicting and controlling radiolytic yields, which need to be quantified for the successful use under radiolytic conditions. Electron solvation dynamics in ILs are measured directly when possible and estimated using proxies (e.g. coumarin-153 dynamic emission Stokes shifts or benzophenone anion solvation) in other cases. Electron reactivity is measured using ultrafast kinetics techniques for comparison with the solvation process.

A second important aspect of our interest in ionic liquids is how their unusual sets of properties affect charge transfer and charge transport processes. This is important because of the many applications of ionic liquids in devices that operate on the basis of charge transport. While interest in understanding these processes in ionic liquids is growing, the field is still in an early stage of development. We are using donor-bridge-acceptor systems to study electron transfer reactions across variable distances in a series of ionic liquids with a range of structural motifs and whose dynamical time scales vary from moderately fast to extremely slow, and to compare them with conventional solvents.

**Methods.** Picosecond pulse radiolysis studies at BNL's Laser-Electron Accelerator Facility (LEAF) are used to identify reactive species in ionic liquids and measure their solvation and reaction rates. This work is aided greatly by the development of Optical Fiber Single-Shot (OFSS) detection at LEAF by A. Cook (DOI: 10.1063/1.3156048) and its present extension into the NIR regime. LEAF's new capability in mid-infrared transient absorption detection<sup>1</sup> allows precise identification of radiolytic intermediates and their reaction kinetics. IL solvation and rotational dynamics, and electron transfer reactions, are measured by TCSPC in the laboratory of E. W. Castner, Jr. at Rutgers Univ. Picosecond transient absorption measurements of excited state dynamics and electron transfer reactions are done in our lab at BNL. Diffusion rates of anions, cations and solutes are obtained by PGSE NMR in the S. Suarez and S.

Greenbaum labs at CUNY and by Castner's group at Rutgers. We have extensive collaborations with other major groups in ionic liquid synthesis, physical chemistry, simulations and radiation chemistry.

**Ionic liquid synthesis and characterization.** Our work often involves novel ILs that we design to the requirements of our radiolysis and solvation dynamics studies and are not commercially available. We have developed robust in-house capabilities and long-standing collaborations (particularly with S. Lall-Ramnarine of Queensborough CC and R. Engel of Queens College) to design, prepare and characterize ILs in support of our research objectives. Cation synthesis is done by several methods, including a CEM microwave reactor, resulting in higher yields of purer products in much shorter time than traditional methods. We have a diverse instrumentation cluster including DSC, TGA, viscometry, AC conductivity, Karl Fischer moisture determination, ion chromatography and ESI-mass spec (for purity analysis and radiolytic product identification). The cluster serves as a resource for a widespread network of collaborations. Our efforts are substantially augmented by student internships from the BNL Office of Educational Programs, particularly the VFP (formerly FaST) program, which brings collaborative faculty members and their students into the lab for ten weeks each summer. Since 2003, a total of 46 undergrads, three graduate students, one pre-service teacher, two high school students and four junior faculty have worked on IL projects in our lab, many of them for more than one summer.

## Recent Progress

### *Effects of ionic liquids on intramolecular ET processes.*<sup>2</sup>

Photoinduced intramolecular electron transfer from a *N,N*-dimethyl-*p*-phenylenediamine donor to a coumarin 343 acceptor across a diproline bridge was studied by time-resolved fluorescence in three ILs, and acetonitrile was used as a control. The ILs were selected to vary their viscosities and polar/nonpolar domain structures. The results were compared to our previous work using a single proline spacer. The second bridging proline permits multiple energetically accessible conformations that have significant variations in donor-acceptor electronic coupling, leading to dynamics that include both adiabatic and nonadiabatic contributions. Conformational energies and donor-acceptor electronic coupling  $H_{DA}$  values were calculated. Electron transfer kinetics was quantified using probability distributions (Figure 1). One of the ILs ( $P_{1,10}$  NTf<sub>2</sub>) has distinct polar/nonpolar structural segregation while the others do not, as shown by SAXS studies and MD simulations.<sup>48-50</sup>  $P_{1,10}$  NTf<sub>2</sub> showed a larger ET reorganization energy  $\lambda$  compared to the other ILs, as well as a lower activation energy due to the fact that this ET reaction is in the Marcus inverted regime.

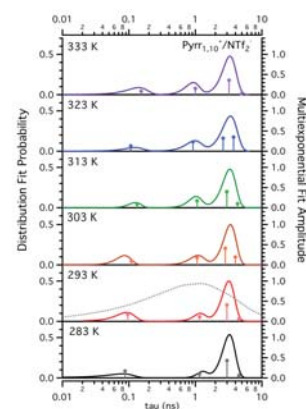


**Figure 1.** Kinetic distributions and multi-exponential fitting of emission decay of the two-proline D-B-A complex in  $P_{1,10}$  NTf<sub>2</sub>.

**Radiation chemistry of fluoroethylene carbonate.**<sup>3</sup> It was known that addition of fluoroethylene carbonate (FEC) to conventional electrolytes yields a robust solid electrolyte interphase (SEI) on the (Li)<sub>x</sub>(Si)<sub>y</sub> alloy surface in rechargeable Li-ion batteries, but the mechanism for this was unknown. We used pulse radiolysis, EPR and other techniques to establish the redox chemistry of FEC. While the oxidation chemistry is similar to that of other carbonates, the reduction chemistry is strikingly different. Specifically, one-electron reduction of FEC causes the fission of two (instead of one) C-O bonds, resulting in concerted defluorination and decarboxylation, as shown by radiolysis studies at LEAF (Figure 2). This reaction yields the vinoxyl radical that can abstract an H atom from FEC, initiating both the chain reaction

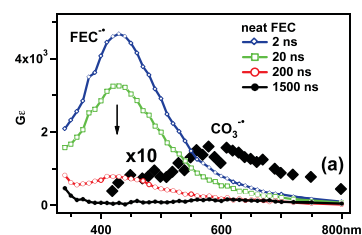


**Figure 2.** Decay of the FEC<sup>•-</sup> radical anion produces carbonate radical CO<sub>3</sub><sup>•-</sup> by fission of two C-O bonds.

causing FEC decomposition and radical polymerization involving the reaction products. The resulting polymer can further defluorinate, yielding interior radicals that migrate and recombine to produce a highly cross-linked network. Our results suggest that the outer SEI resulting from FEC addition has elastomeric properties, which account for its cohesion during expansion and contraction of silicon particles in the course of Li alloying/dealloying cycling.

## Future Plans

**Scavenging and solvation processes of pre-solvated electrons in ionic liquids.** Our early work in the reactivity of excess electrons in ionic liquids demonstrated the importance of pre-solvated electron scavenging in trying to understand and predict the distributions of early radiolysis products and radiolytic damage accumulation. It was also clear that the slower relaxation dynamics of ILs made them excellent media for the general study of fundamental radiolysis processes without the need to use cryogenic techniques, in combination with the advanced instrumentation of the LEAF Facility. We recently connected our observed electron solvation dynamics to the kinetics of electron scavenging. In other preliminary work we have observed that selected scavengers (e.g., nitrate, benzophenone) in ILs show different reaction profiles towards the various precursor states to the solvated electron. Different scavenger reactivities towards pre-solvated and solvated electrons have been known empirically for many years and cryogenic kinetic work by Jonah and Lewis showed specific mechanistic differences between scavengers similar to what we have seen in ILs. However, the combination of extended IL dynamical time scales and the time resolution of the LEAF OFSS detection system, coupled with the fact that it uses only small amounts of samples that do not have to be flowed, as well as the ability of ILs to dissolve polar and nonpolar scavengers, provides a unique opportunity to characterize the fundamental reactivity of pre-solvated electron species and understand how the properties of scavengers control their reaction profiles. The extension of the LEAF OFSS detection capability to the NIR (900-1700 nm) greatly facilitates the study of dynamical and electron solvation processes in our ILs. This knowledge will permit the design of better systems to control radiation-induced reactivity, for example in the processing of radioactive materials (whether in ionic liquids or not), in systems for radiation processing and sterilization, and during long-term exposure to space, for example. (with A. Cook, BNL)

## Publications

1. *Development of nanosecond time-resolved infrared detection at the LEAF pulse radiolysis facility* D. C. Grills, J. A. Farrington, B. H. Layne, J. M. Preses, H. J. Bernstein, J. F. Wishart, *Rev. Sci. Instrum.* **86**, 044102 (2015) DOI: 10.1063/1.4918728
2. *Distributed Electron Transfer Dynamics for a Donor-Bridge-Acceptor Complex in Ionic Liquids*, J. A. Devine, M. Labib, M. E. Harries, R. Abdel Malak Rached, J. Issa, J. F. Wishart, E. W. Castner, Jr., *J. Phys. Chem. B* **119**, 11336–11345 (2015). DOI: 10.1021/acs.jpcc.5b03320
3. *What Makes Fluoroethylene Carbonate Different?* I. A. Shkrob, J. F. Wishart, D. P. Abraham, *J. Phys. Chem. C* **119**, 14954-14964 (2015). DOI: 10.1021/acs.jpcc.5b03591
4. *Ultrafast Transient Absorption Spectrum of the Room Temperature Ionic Liquid 1-Hexyl-3-Methylimidazolium Bromide: Confounding Effects of Photo-degradation* R. M. Musat, R. A. Crowell, D. E. Polyanskiy, M. F. Thomas, J. F. Wishart, Y. Katsumura, K. Takahashi, *Radiat. Phys. Chem.*, **117**, 78-82 (2015). DOI: 10.1016/j.radphyschem.2015.07.015
5. *A comparison of the  $\gamma$ -radiolysis of TODGA and T(EH)DGA using UHPLC-ESI-MS analysis* C. A. Zarzana, G. S. Groenewold, B. J. Mincher, S. P. Mezyk, A. Wilden, H. Schmidt, G. Modolo, J. F. Wishart and A. R. Cook, *Solv. Extr. Ion Exch.*, **33**, 431-447 (2015). DOI: 10.1080/07366299.2015.1012885

6. *Mechanism of the Formation of a Mn-Based CO<sub>2</sub> Reduction Catalyst Revealed by Pulse Radiolysis with Time-Resolved Infrared Detection* D. C. Grills, J. A. Farrington, B. H. Layne, S. V. Lyman, B. A. Mello, J. M. Preses, J. F. Wishart, *J. Am. Chem. Soc.*, **136**, 5563-5566 (2014). DOI: 10.1021/ja501051s
7. *Binary Ionic Liquid Mixtures for Supercapacitor Applications* S. I. Lall-Ramnarine, S. N. Suarez, N. V. Zmich, D. Ewko, S. Ramati, D. Cuffari, M. Sahin, Y. Adam, E. Rosario, D. Paterno and J. F. Wishart, *ECS Transactions* **64**, 57-69 (2014). DOI: 10.1149/06404.0057ecst

## Intermolecular interactions in the gas and condensed phases

Sotiris S. Xantheas

Physical Sciences Division, Pacific Northwest National Laboratory  
902 Battelle Blvd., Mail Stop K1-83, Richland, WA 99352

[sotiris.xantheas@pnl.gov](mailto:sotiris.xantheas@pnl.gov)

**Program Scope:** The objective of this research effort aims at developing a comprehensive, molecular-level understanding of the collective phenomena associated with intermolecular interactions occurring in the gas phase, in guest/host molecular systems and in aqueous environments. The motivation of the present work stems from the desire to establish the key elements that describe the structural and associated spectral features of solutes in a variety of hydrogen bonded environments such as bulk water, aqueous interfaces and aqueous hydrates. Simple model systems including small molecules of complex electronic structure as well as aqueous clusters offer a starting point in this process by providing the test bed for validating new approaches for analyzing the electronic structure as well as the nature of interactions and the magnitude of collective phenomena at the molecular level. For instance, high level first-principles calculations of the structures, energetics, and vibrational spectra of aqueous neutral and ionic clusters provide useful information needed to assess the accuracy of reduced representations of intermolecular interactions, such as classical potentials used to model the macroscopic structural and thermodynamic properties of those systems. The database of accurate cluster structures, binding energies, and vibrational spectra can, furthermore, aid in the development of new density functionals, which are appropriate for studying the underlying interactions. Representative applications include the development of novel descriptions of the electronic structure of simple molecules, the modeling of liquid water and ice, the quantitative description of aqueous ion solvation, the structure of clathrate hydrates and the interaction of host molecules with those guest networks. The detailed molecular-scale account of aqueous systems provided by these studies is relevant to Department of Energy programs in contaminant fate and transport and waste processing as well as hydrogen storage.

**Recent progress:** Although the interaction between monatomic negative and positive (such as halide and alkali metal) ions and water has been exhaustively studied, this is not the case for monatomic multivalent ions, for which the electronic structure is more complex. Several of those ions (such as  $\text{Ca}^{2+}$  and  $\text{Mg}^{2+}$ ) play an important role in many biological processes, whereas other metal trivalent ions have been shown to optimize catalytic processes. The complexity arises from the fact that the second ionization potential (IP) of most metals is above the IP of water ( $12.6206 \pm 0.0020$  eV). Metal atoms typically have second and higher IPs that are larger than the IP of water, resulting in the Coulombic explosion of the first few  $[\text{M}(\text{H}_2\text{O})_n]^{+q}$  ( $q \geq 2$ ) gas phase clusters as the  $\text{M}^{+(q-1)} + (\text{H}_2\text{O})_n^+$  or

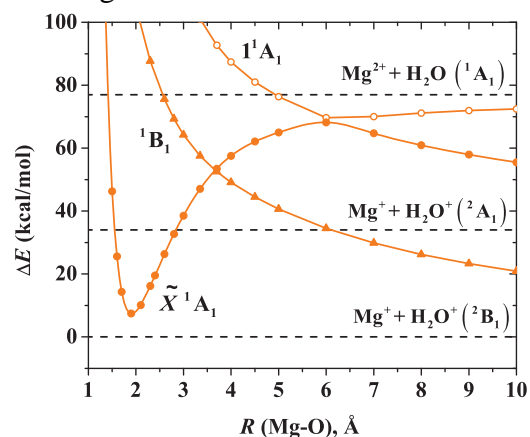


**Figure 1.** MCSCF potential energy curves for the various states of  $[\text{Mg}(\text{H}_2\text{O})]^{2+}$  and their asymptotic correlation. Filled (open) symbols trace the ground (first excited)

$\text{MOH}^{+(q-1)} + \text{H}_3\text{O}^+(\text{H}_2\text{O})_n$  energy levels are energetically more stable than the  $\text{M}^{q+} + (\text{H}_2\text{O})_n$  ones for small  $n$  (cf. Figure 1). The theoretical analysis of the various electronic states arising from the sequential hydration of the  $\text{Ca}^{2+}$ ,  $\text{Mg}^{2+}$  and  $\text{Al}^{3+}$  cations with up to six water molecules offer insight into the shifting of electronic states and dissociation asymptotes with the degree of solvation, identify their complex interaction with other states arising from different dissociation

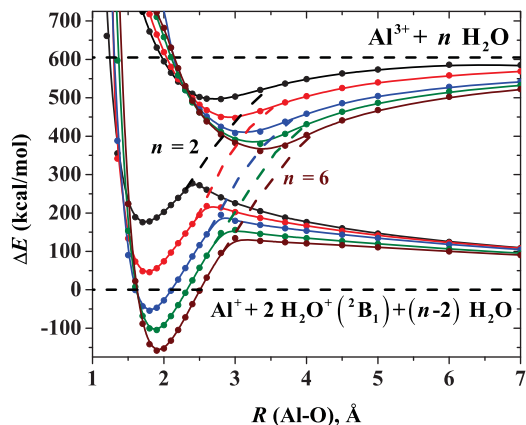


**Figure 2.** MCSCF potential energy curves for the  $[\text{Al}(\text{H}_2\text{O})_n]^{3+}$  system showing the energetic stabilization of the  $\text{Al}^{3+}(\text{H}_2\text{O})_n$  cluster with respect to the lowest energy asymptote for  $n \geq 4$ .

channels and shed light on the mechanism behind the energetic stabilization of the multi-charged hydrated  $\text{M}^{+q}(\text{H}_2\text{O})_n$  moieties observed in solution with respect to the water ionization products. The stabilization of the  $\text{M}^{+k}(\text{H}_2\text{O})_n$  gas phase metal complexes is mainly facilitated by the maximization of the binding between the metal ion center and water aided by the simultaneous minimization of the Coulombic repulsion between the ligands. In order to create a stable (with respect to the lowest asymptote)  $\text{M}^{+k}(\text{H}_2\text{O})_n$  complex, a critical number of water molecules is necessary. For Mg this number is at least two, while for Al at least four water molecules are required as for that cluster size the  $\text{Al}^{3+}(\text{H}_2\text{O})_n$  ( $n \geq 4$ ) clusters become energetically more stable with respect to the asymptote that involves ionization of water (cf. Figure 2). Equivalently, one could argue that there is an effective ionization potential of the  $(\text{H}_2\text{O})_n$  cluster, which increases with  $n$  and eventually becomes larger than the corresponding ionization potential of the metal, thus facilitating the formation of the metal cation-water complex.

A more complex system deals with the ground and low lying electronically excited states of the  $[\text{Fe}(\text{H}_2\text{O})_6]^{2+}$  and  $[\text{Fe}(\text{H}_2\text{O})_6]^{3+}$  clusters as well as their aggregate. Due to the fact that both the second and third ionization potentials of iron are larger than the one for water, the ground state products asymptotically correlate with dissociation channels that are repulsive in nature at large separations as they contain at least one  $\text{H}_2\text{O}^+$  fragment and a singly positively charged metal center ( $\text{Fe}^+$ ). The most stable equilibrium structures emanate – via intersections and/or avoided crossings – from the channels consisting of the lowest electronic states of  $\text{Fe}^{2+}({}^5\text{D}; 3d^6)$  or  $\text{Fe}^{3+}({}^6\text{S}; 3d^5)$  and six neutral water molecules. Upon hydration, the ground state of  $\text{Fe}^{2+}(\text{H}_2\text{O})_6$  is a triply ( ${}^5\text{T}_g$ ) degenerate one with the doubly ( ${}^5\text{E}_g$ ) degenerate state lying  $\sim 20$  kcal/mol higher in energy. Similarly, the  $\text{Fe}^{3+}(\text{H}_2\text{O})_6$  cluster has a ground state of  ${}^6\text{A}_g$  symmetry under  $\text{T}_h$  symmetry, which is well separated from the first excited state. Focusing on the ground and the first few excited states of the  $[\text{Fe}(\text{H}_2\text{O})_6]^{2+}$  and  $[\text{Fe}(\text{H}_2\text{O})_6]^{3+}$  clusters, we also studied their mutual interaction in the gas phase. We obtained the optimal geometries of the  $\text{Fe}^{2+}(\text{H}_2\text{O})_6 - \text{Fe}^{3+}(\text{H}_2\text{O})_6$  gas phase complex for different Fe–Fe distances. For distances

channels and shed light on the mechanism behind the energetic stabilization of the multi-charged hydrated  $\text{M}^{+q}(\text{H}_2\text{O})_n$  moieties observed in solution with respect to the water ionization products. The stabilization of the  $\text{M}^{+k}(\text{H}_2\text{O})_n$  gas phase metal complexes is mainly facilitated by the maximization of the binding between the metal ion center and water aided by the simultaneous minimization of the Coulombic repulsion between the ligands. In order to create a stable (with respect to the lowest asymptote)  $\text{M}^{+k}(\text{H}_2\text{O})_n$  complex, a critical number of water molecules is necessary. For Mg this number is at least two, while for Al at least four water molecules are required as for that cluster size the  $\text{Al}^{3+}(\text{H}_2\text{O})_n$  ( $n \geq 4$ ) clusters become energetically more stable with respect to the asymptote that involves ionization of water (cf. Figure 2). Equivalently, one could argue that there is

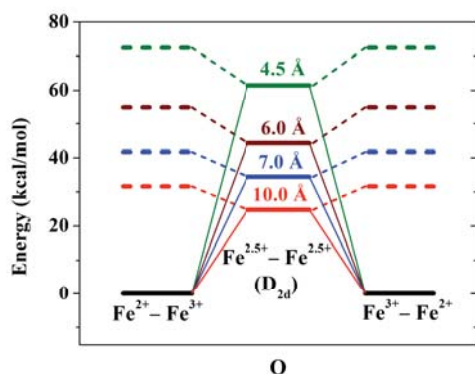


**Figure 3.** Energy diagram along one possible  $\text{Fe}^{2+}(\text{H}_2\text{O})_6$  (left) –  $\text{Fe}^{3+}(\text{H}_2\text{O})_6$  (right) to  $\text{Fe}^{3+}(\text{H}_2\text{O})_6$  (left) –  $\text{Fe}^{2+}(\text{H}_2\text{O})_6$  (right) conversion pathway (Q) via the  $\text{D}_{2d}$  configuration for different Fe – Fe distances (4.5, 6.0, 7.0, and 10.0 Å). The solid/dashed curves trace the ground/excited states.

shorter than 6.0 Å, the water molecules in the respective first solvation shells located between the two metal centers were found to interact via weak hydrogen bonds. We examined a total of ten electronic states for this complex, including those corresponding to the electron transfer (ET) from the ferrous to the ferric ion; a possible path via a quasi-symmetric transition state is suggested (cf. Figure 3).

**Future Plans:** The electronic states that are associated with the hydrolysis channels producing the metal hydroxide complexes will be examined. We will also examine the possibility of different electronic / charge states for metals with low coordination of ligands (i.e. at interfaces) when compared to the ones of the fully coordinated complexes. Such a finding can have severe implications in the development of both classical potentials and low level electronic structure methods, which, by design, cannot simultaneously describe both the low and high coordinated complexes that are associated with different charged states. We will also seek to identify a molecular level description of the ET process in terms of the electronic states involved for the  $\text{Fe}(\text{H}_2\text{O})_6]^{2+} - [\text{Fe}(\text{H}_2\text{O})_6]^{3+}$  system in an aqueous solution. This will be facilitated via a combined QM/MM approach, in which the important electronic states of the complex (identified from the cluster calculations) will be included.

**Acknowledgments:** This research used the resources of the National Energy Research Scientific Computing Center (NERSC), which is supported by the Office of Science of the U.S. Department of Energy under Contract No. DE-AC02-05CH11231, under a NERSC Initiative for Scientific Exploration (NISE) Award and the Molecular Science Computing Facility (MSCF) in EMSL, a national scientific user facility sponsored by the Department of Energy's Office of Biological and Environmental Research located at PNNL. Battelle operates Pacific Northwest National Laboratory for the US Department of Energy.

#### References to publications of DOE sponsored research (2014 - 2015)

1. E. Miliordos and S. S. Xantheas, "Unimolecular and hydrolysis channels for the detachment of water from microsolvated alkaline earth dication ( $\text{Mg}^{2+}$ ,  $\text{Ca}^{2+}$ ,  $\text{Sr}^{2+}$ ,  $\text{Ba}^{2+}$ ) clusters", Thom H. Dunning Jr. Special Issue (invited), *Theoretical Chemistry Accounts* **133**, 1450 (2014)
2. E. Miliordos and S. S. Xantheas, "On the bonding nature of ozone ( $\text{O}_3$ ) and its sulfur-substituted analogues,  $\text{SO}_2$ ,  $\text{OS}_2$ , and  $\text{S}_3$ : Correlation between their biradical character and molecular properties", *Journal of the American Chemical Society* **136**, 2808 (2014)
3. E. Miliordos and S. S. Xantheas, "Elucidating the mechanism behind the stabilization of multi-charged metal cations in water: A case study of the electronic states of microhydrated  $\text{Mg}^{2+}$ ,  $\text{Ca}^{2+}$  and  $\text{Al}^{3+}$ ". Highlighted in DOE's Pulse (Science and Technology Highlights from the DOE National Laboratories), #417, 7 July 2014 <http://web.ornl.gov/info/news/pulse/no417/story1.shtml>. Hot article for the week Oct 22, 2013, <http://blogs.rsc.org/cp/2013/10/22/this-weeks-hot-articles-11/>. Highlighted in NERSC's web page, June 2014, <http://www.nersc.gov/news-publications/news/science-news/2014/thirsty-metals-key-to-longer-battery-lifetimes/>. Reported in Science Springs, July 7 2014 <http://sciencesprings.wordpress.com/2014/07/07/from-doe-pulse-satisfying-metals-thirst-vital-for-high-capacity-batteries/>, Communication to the Editor, *Physical Chemistry Chemical Physics* **16**, 6886 (2014). Journal cover
4. A. E. Vasdekis, M. J. Wilkins, J. W. Grate, R. T. Kelly, A. Konopka, S. S. Xantheas, T.-M. Chang "Solvent Immersion Imprint Lithography", *Lab on a Chip* **14**, 2072 (2014)

5. T. Yoshida, W. A. Farone and S. S. Xantheas, “Isomers and conformational barriers of gas phase nicotine, nornicotine and their protonated forms”, James L. Skinner special issue (invited), *Journal of Physical Chemistry B* **118**, 8273 (2014)
6. S. S. Xantheas and J. C. Werhahn, “Universal Scaling of Potential Energy Functions describing Intermolecular Interactions: I. Foundations and scalable forms for new generalized Lennard-Jones, Mie, Morse and Buckingham exponential-6 potentials”, *Journal of Chemical Physics* **141**, 064117 (2014)
7. J. C. Werhahn, D. Akase and S. S. Xantheas, “Universal Scaling of Potential Energy Functions describing Intermolecular Interactions: II. The halide- and alkali metal-water interactions”, *Journal of Chemical Physics* **141**, 064118 (2014)
8. E. Miliordos, E. Aprà and S. S. Xantheas, “A benchmark theoretical study of the  $\pi$ - $\pi$  interaction energy in the benzene dimer”, Kenneth D. Jordan special issue (invited), *Journal of Physical Chemistry A* **118**, 7568 (2014)
9. N. Sahu, S. R. Gadre, P. Bandyopadhyay, E. Miliordos and S. S. Xantheas, “Low energy isomers of  $(\text{H}_2\text{O})_{25}$  from a hierarchical method based on Monte Carlo Temperature Basin Paving and Molecular Tailoring Approaches benchmarked by full MP2 calculations”, *Journal of Chemical Physics* **141**, 164304 (2014)
10. C. C. Pradzynski, C. W. Dierking, F. Zurheide, R. M. Forck, U. Buck, T. Zeuch and S. S. Xantheas, “Infrared detection of  $(\text{H}_2\text{O})_{20}$  isomers of exceptional stability: a drop-like and a face-sharing pentagonal prism cluster” Communication to the Editor, *Physical Chemistry Chemical Physics* **16**, 26691 (2014)
11. J. C. Werhahn, E. Miliordos and S. S. Xantheas, “A new variation of the Buckingham exponential-6 potential with a tunable, singularity-free short-range repulsion and an adjustable long-range attraction”, *Chemical Physics Letters* **619**, 133 (2015)
12. E. Miliordos and S. S. Xantheas, “On the validity of the basis set superposition error and complete basis set limit extrapolations for the binding energy of the formic acid dimer”, *Journal of Chemical Physics* **142**, 094311 (2015)
13. E. Miliordos and S. S. Xantheas, “Ground and excited states of the  $[\text{Fe}(\text{H}_2\text{O})_6]^{2+}$  and  $[\text{Fe}(\text{H}_2\text{O})_6]^{3+}$  clusters: Insights into the electronic structure of the  $[\text{Fe}(\text{H}_2\text{O})_6]^{2+}$  –  $[\text{Fe}(\text{H}_2\text{O})_6]^{3+}$  complex”, *Journal of Chemical Theory and Computation* **11**, 1549 (2015)
14. E. Miliordos and S. S. Xantheas, “An accurate and efficient computational protocol for obtaining the Complete Basis Set (CBS) limits of the binding energies of water clusters at the MP2 and CCSD(T) levels of theory: Application to  $(\text{H}_2\text{O})_m$ ,  $m = 2 - 6, 8, 11, 16$  and  $17$ ”, *Journal of Chemical Physics* **142**, 234303 (2015)
15. S. Imoto, S. S. Xantheas and S. Saito, “Ultrafast dynamics of liquid water: Energy relaxation and transfer processes of the OH stretch and the HOH bend”, B. Bagchi Special issue (invited), *Journal of Physical Chemistry B* **119**, 11068 (2015)
16. J. A. Fournier, C. T. Wolke, and M. A. Johnson, T. T. Odbadrakh and K. D. Jordan, S. M. Kathmann and S. S. Xantheas, “Snapshots of Proton Accommodation at a Microscopic Water Surface: Vibrational Spectral Signatures of the Charge Defect in Cryogenically Cooled  $\text{H}^+(\text{H}_2\text{O})_{n=2-28}$  Clusters”, Feature Article (invited), *Journal of Physical Chemistry A* **119**, 9425 (2015). Journal cover
17. K. R. Brorsen, S. Y. Willow, S. S. Xantheas, and M. S. Gordon, “The melting temperature of liquid water with the effective fragment potential”, *Journal of Physical Chemistry Letters* **6**, 3555 (2015)

## Room Temperature Single-Molecule Detection and Imaging by Stimulated Raman Scattering Microscopy

Principal Investigator: X. Sunney Xie

Dept. of Chemistry and Chemical Biology, Harvard University  
12 Oxford Street, Cambridge, MA 02138, Cambridge, MA 02138  
xie@chemistry.harvard.edu

### PROGRAM SCOPE

The scope of this program is to push the detection sensitivity limit of stimulated Raman scattering (SRS) imaging to single molecule. Raman provides specific vibrational signatures of chemical bonds, which enables new modes of chemical imaging without labels. Unlike fluorescence, which has a large cross-section, single molecule Raman detection without surface enhancement has long been a major technical challenge. We attempt to tackle this challenge with our newly developed SRS imaging technique and study long chain conjugated molecules and use near-resonance enhancement.

### RECENT PROGRESS

In order to detect single molecules with SRS, we had to continue to push its detection limit. First of all, to identify specific chemicals at very low concentration, a multi-color spectral imaging became necessary. By measuring the spectrum of the three most common chemicals of a cell (DNA, proteins and lipids), we can now detect DNA molecules in a single cell, as well as its protein and lipid components (Fig. 1A). Using multicolor SRS, we are able to reconstruct the chemical distribution of these three chemicals in a label-free manner in a cell (Fig. 1B). Imaging DNA at high wavenumber region offers higher sensitivity than imaging DNA at finger print region.

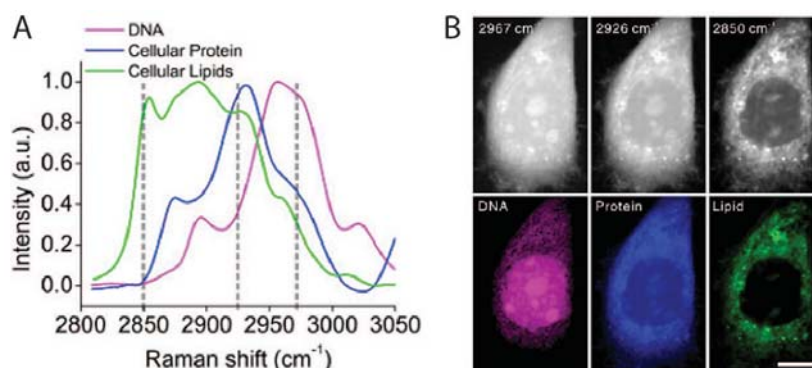


**Figure 1.** A) The Raman spectrum of DNA, protein and lipid in cells. B) Reconstruction of chemical mapping of a cell with multi-color SRS images at their Raman shifts, giving the distributions of DNA (pink), protein (blue) and lipid (green).

In addition, we have developed a robust fiber laser source for SRS (Fig. 2A). The solid state laser has strict environmental requirements, such as mechanical vibration, temperature and humidity, that need to be well controlled in order for the system to work normally. Fiber laser is less bulky and offers the advantage that doesn't have such environmental requirements (Fig. 2B). However, the laser noise at higher frequency causes low signal-to-noise ratio in SRS. Therefore, we developed a noise cancellation electronics that allow us to achieve high-speed SRS imaging

with the robust fiber laser source (Fig. 2C). We hope that this new source will improve the stability and sensitivity of the imaging system.

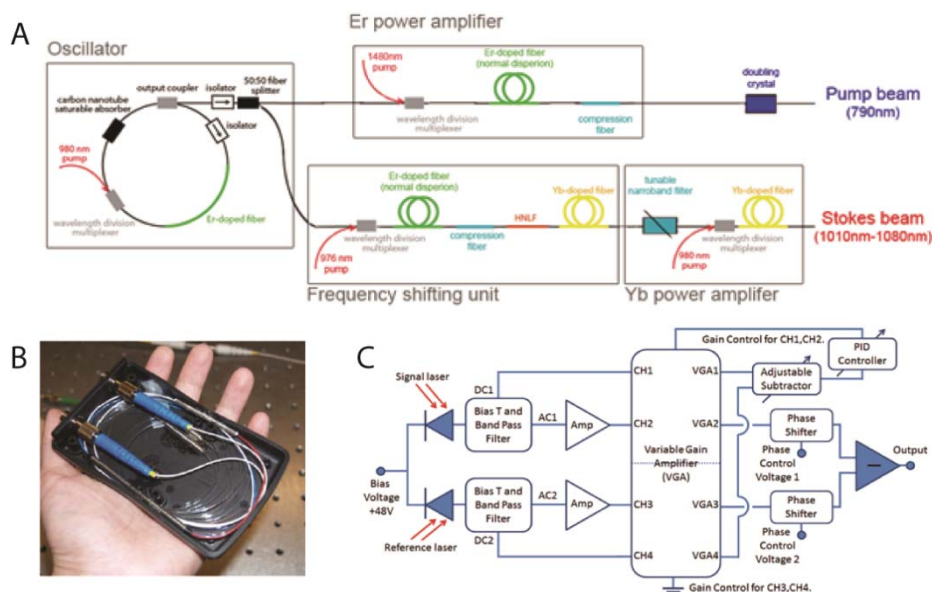


**Figure 2.** A) New fiber laser source for SRS. B) Oscillator for our fiber laser source providing pump and Stokes beams for SRS. C) Schematic for noise cancellation electronics for SRS detection in order to circumvent the high frequency noise of the fiber laser.

## FUTURE PLANS

To further improve the sensitivity of SRS, we are developing a simultaneous four-color SRS imaging technique. Current SRS multi-color imaging techniques require taking images for each color in serial order. Due to sample movement and photo-bleaching effect, conventional multi-color SRS cannot effectively produce chemical mapping for low concentration chemicals. We propose to generate three new Stokes wavelengths from the original Stokes laser in high non-linear fiber and amplify them with fiber amplifiers. By modulating these Stokes beams at different frequencies and demodulate them digitally, we can achieve simultaneous four-color SRS. We expect this technique to solve the issues mentioned above and continue our quest for single molecule SRS.

## PUBLICATIONS OF DOE SPONSORED RESEARCH (2013-2015)

1. Fu, Dan; Holtom, Gary; Freudiger, Christian; Zhang, Xu; Xie, X. Sunney. "Hyperspectral Imaging with Stimulated Raman Scattering by Chirped Femtosecond Lasers," *J Phys. Chem. B* 117, 4634-4640 (2013).
2. Fu, Dan; Xie, X. Sunney, Reliable Cell Segmentation Based on Spectral Phasor Analysis of Hyperspectral Stimulated Raman Scattering Imaging Data. *Anal. Chem.* 86 (9), 4115-4119 (2014).
3. Fa-Ke Lu, Srinjan Basu, Vivien Igras, Mai P. Hoang, Minbiao Ji, Dan Fu, Gary R. Holtom, Victor A. Neel, Christian W. Freudiger, David E. Fisher, X. Sunney Xie, "Label-free DNA imaging in vivo with stimulated Ramanscattering microscopy". *Proc. Natl. Acad. Sci. U.S.A.* 112, 11624-11628 (2015).

An aerial photograph of a green field, possibly a golf course or sports field, with a grid of red and black markers. The text "List of Participants" is overlaid in the center.

## *List of Participants*

## LIST OF PARTICIPANTS

Dr. Musahid Ahmed  
Lawrence Berkeley National Laboratory  
<https://sites.google.com/site/musaswebcorner/home>

Professor L. Robert Baker  
Ohio State University  
<https://research.cbc.osu.edu/baker.2364/>

Dr. David Bartels  
Notre Dame Radiation Laboratory  
<http://rad.nd.edu/people/faculty/david-m-bartels/>

Dr. Ali Belkacem  
Lawrence Berkeley National Laboratory  
<http://ultrafast.lbl.gov/amos/dr-ali-belkacem/>

Dr. Hendrik Bluhm  
Lawrence Berkeley National Laboratory  
<https://sites.google.com/a/lbl.gov/hendrik-bluhm/>

Dr. Nicholas Camillone  
Brookhaven National Laboratory  
<http://www.bnl.gov/chemistry/bio/Camillone%20Nicholas.asp>

Professor Ian Carmichael  
Notre Dame Radiation Laboratory  
<http://rad.nd.edu/people/faculty/ian-carmichael/>

Dr. Andrew Cook  
Brookhaven National Laboratory  
<https://www.bnl.gov/chemistry/bio/CookAndrew.asp>

Professor Tanja Cuk  
Lawrence Berkeley National Laboratory  
<http://www.cchem.berkeley.edu/tkgrp/>

Dr. Liem Dang  
Pacific Northwest National Laboratory  
[http://www.pnl.gov/science/staff/staff\\_info.asp?staff\\_num=5604](http://www.pnl.gov/science/staff/staff_info.asp?staff_num=5604)

Professor Michael Duncan  
University of Georgia  
<http://research.franklin.uga.edu/maduncan/>

Professor Michael Fayer  
Stanford University  
<http://www.stanford.edu/group/fayer/>

Dr. Gregory Fiechtner  
DOE/Basic Energy Sciences  
<http://science.energy.gov/bes/csgb/about/staff/dr-gregory-i-fiechtner/>

Mr. John L. Fulton  
Pacific Northwest National Laboratory  
[http://www.pnl.gov/science/staff/staff\\_info.asp?staff\\_num=5587](http://www.pnl.gov/science/staff/staff_info.asp?staff_num=5587)

Professor Etienne Garand  
University of Wisconsin  
<http://garand.chem.wisc.edu/>

Dr. Bruce Garrett  
Pacific Northwest National Laboratory  
[http://www.pnl.gov/science/staff/staff\\_info.asp?staff\\_num=5496](http://www.pnl.gov/science/staff/staff_info.asp?staff_num=5496)

Professor Phillip Geissler  
Lawrence Berkeley National Laboratory  
<http://www.cchem.berkeley.edu/plggrp/index.html>

Dr. Mary K. Gilles  
Lawrence Berkeley National Laboratory  
<https://commons.lbl.gov/display/csd/Mary+K.+Gilles>

Dr. Niranjana Govind  
Pacific Northwest National Laboratory  
[http://www.pnl.gov/science/staff/staff\\_info.asp?staff\\_num=8375](http://www.pnl.gov/science/staff/staff_info.asp?staff_num=8375)

Dr. Alexander Harris  
Brookhaven National Laboratory  
<http://www.bnl.gov/chemistry/bio/HarrisAlex.asp>

Professor Teresa Head-Gordon  
Lawrence Berkeley National Laboratory  
<http://thglab.berkeley.edu/>

Dr. Wayne Hess  
Pacific Northwest National Laboratory  
[http://www.pnl.gov/science/staff/staff\\_info.asp?staff\\_num=5505](http://www.pnl.gov/science/staff/staff_info.asp?staff_num=5505)

Professor Wilson Ho  
University of California, Irvine  
<http://www.physics.uci.edu/~wilsonho/whoghp.htm>

Professor Bret Jackson  
University of Massachusetts Amherst  
<http://www.chem.umass.edu/faculty/jackson.html>

Dr. Ireneusz Janik  
Notre Dame Radiation Laboratory  
<http://rad.nd.edu/people/faculty/ireneusz-janik/>

Professor Caroline Chick Jarrold  
Indiana University  
<http://mypage.iu.edu/~cjarrold/index.htm>

Professor Mark Johnson  
Yale University  
<http://ilab.chem.yale.edu/>

Professor Kenneth Jordan  
University of Pittsburgh  
<http://www.pitt.edu/~jordan/>

Dr. Shawn Kathmann  
Pacific Northwest National Laboratory  
[http://www.pnl.gov/science/staff/staff\\_info.asp?staff\\_num=5601](http://www.pnl.gov/science/staff/staff_info.asp?staff_num=5601)

Professor Munira Khalil  
University of Washington  
<https://sites.google.com/a/uw.edu/khalilgroup/>

Dr. Bruce Kay  
Pacific Northwest National Laboratory  
[http://www.pnl.gov/science/staff/staff\\_info.asp?staff\\_num=5530](http://www.pnl.gov/science/staff/staff_info.asp?staff_num=5530)

Dr. Greg Kimmel  
Pacific Northwest National Laboratory  
[http://www.pnl.gov/science/staff/staff\\_info.asp?staff\\_num=5527](http://www.pnl.gov/science/staff/staff_info.asp?staff_num=5527)

Dr. Jeffrey L. Krause  
DOE/Basic Energy Sciences  
<http://science.energy.gov/bes/csgb/about/staff/dr-jeffrey-l-krause/>

Dr. Jay LaVerne  
Notre Dame Radiation Laboratory  
<http://rad.nd.edu/people/faculty/jay-a-laverne/>

Professor H. Peter Lu  
Bowling Green State University  
<https://www.bgsu.edu/arts-and-sciences/chemistry/faculty/peter-lu.html>

Dr. Sergei Lyamar  
Brookhaven National Laboratory  
<https://www.bnl.gov/chemistry/bio/LymarSergei.asp>

Diane Marceau  
DOE/Basic Energy Sciences  
<http://science.energy.gov/bes/csgb/about/staff/>

Dr. Kranthi K. Mandadapu  
University of California, Berkeley  
<http://www.cchem.berkeley.edu/kranthi/>

Professor Thomas Markland  
Stanford University  
<http://web.stanford.edu/group/markland/>

Dr. Christopher Mundy  
Pacific Northwest National Laboratory  
[http://www.pnl.gov/science/staff/staff\\_info.asp?staff\\_num=5981](http://www.pnl.gov/science/staff/staff_info.asp?staff_num=5981)

Professor Richard Osgood  
Columbia University  
<http://cumsl.msl.columbia.edu/>

Dr. Mark Pederson  
DOE/Basic Energy Sciences  
<http://science.energy.gov/bes/csgb/about/staff/dr-mark-r-pederson/>

Professor Hrvoje Petek  
University of Pittsburgh  
<http://www.ultrafast.phyast.pitt.edu/Home.html>

Dr. Tanja Pietraß  
DOE/Basic Energy Sciences  
<http://science.energy.gov/bes/csgb/about/staff/dr-tanja-pietrass/>

Professor Sylwia Ptasinska  
University of Notre Dame  
<http://www3.nd.edu/~sptasins/>

Professor Krishnan Raghavachari  
Indiana University  
<http://php.indiana.edu/~krgroup/>

Professor Geraldine L. Richmond  
University of Oregon  
<http://richmondscience.uoregon.edu/>

Professor Richard Saykally  
Lawrence Berkeley National Laboratory  
<http://www.cchem.berkeley.edu/rjsgrp/>

Dr. Gregory Schenter  
Pacific Northwest National Laboratory  
[http://www.pnl.gov/science/staff/staff\\_info.asp?staff\\_num=5615](http://www.pnl.gov/science/staff/staff_info.asp?staff_num=5615)

Dr. David K. Shuh  
Lawrence Berkeley National Laboratory  
<http://actinide.lbl.gov/gtsc/Staff/dkshuh/>

Professor Charles Sykes  
Tufts University  
<http://ase.tufts.edu/chemistry/sykes/Sykes%20Lab%20Research%20Group.html>

Professor Ward Thompson  
University of Kansas  
<http://thompsongroup.ku.edu/>

Professor William A. Tisdale  
Massachusetts Institute of Technology  
<http://web.mit.edu/tisdalelab>

Professor Andrei Tokmakoff  
University of Chicago  
<http://tokmakofflab.uchicago.edu/>

Professor John Tully  
Yale University  
<http://www.chem.yale.edu/~tully/>

Dr. Marat Valiev  
Pacific Northwest National Laboratory  
[http://www.pnl.gov/science/staff/staff\\_info.asp?staff\\_num=8349](http://www.pnl.gov/science/staff/staff_info.asp?staff_num=8349)

Dr. Xue-Bin Wang  
Pacific Northwest National Laboratory  
[http://www.pnl.gov/science/staff/staff\\_info.asp?staff\\_num=7753](http://www.pnl.gov/science/staff/staff_info.asp?staff_num=7753)

Professor Michael White  
Brookhaven National Laboratory  
<http://www.bnl.gov/chemistry/bio/WhiteMichael.asp>

Dr. Kevin R. Wilson  
Lawrence Berkeley National Laboratory  
<http://wilsonresearchgroup.lbl.gov/home>

Dr. James Wishart  
Brookhaven National Laboratory  
<http://www.chemistry.bnl.gov/SciandTech/PRC/wishart/wishart.html>

Dr. Sotiris Xantheas  
Pacific Northwest National Laboratory  
[http://www.pnl.gov/science/staff/staff\\_info.asp?staff\\_num=5610](http://www.pnl.gov/science/staff/staff_info.asp?staff_num=5610)